Optimization of Standard Depth Control Systems to Improve Row-Crop Planter Performance in the Southeast US

by

Aurelie Poncet

A dissertation submitted to the Graduate Faculty of
Auburn University
in partial fulfillment of the
requirements for the Degree of
Doctor of Philosophy

Auburn, Alabama
December 10, 2016

Keywords: Downforce, Planting Technology, Precision Agriculture, Seeding Depth, Uniformity

Approved by

Timothy McDonald, Chair, Professor of Biosystems Engineering
John Fulton, Associate Professor of Food, Agricultural, and Biological Engineering, Ohio State University
Kipling Balkcom, Research Agronomist at the National Soil Dynamics Laboratory, USDA and Affiliate Associate Professor of Crop, Soil and Environmental Sciences
Thorsten Knappenberger, Assistant Professor of Crop, Soil, and Environmental Sciences
Joey Shaw, Professor of Crop, Soil, and Environmental Sciences
Steven Taylor, Professor of Biosystems Engineering and Associate Dean of Research, College of Engineering.

Abstract

Modern row-crop planters are designed to place individual seeds in the ground at a proper and predetermined depth to promote immediate germination and uniform emergence of seedlings. Seeding depth is manually adjusted by the operator prior to planting operation by selecting a row-unit depth and a row-unit downforce. Once set, row-unit depth and downforce are not adjusted again for a field though soil conditions may vary, and optimum planting performance requires adjusting planter settings selection to these changing soil conditions. However, limited technology is available today to manage in-field seeding depth variability, and research must be conducted to gain a better understanding of seeding depth and crop response to row-unit depth and downforce adjustments and field spatial variability. The objective of this study was to characterize seeding depth response to changing soil conditions within fields and determine protocol to use active seeding depth by downforce planting technologies to manage in-field seeding variability in the Southeast US.

This study was conducted in 2014 and 2015 in Central Alabama for non-irrigated corn (*Zea mays L*) and cotton (*Gossypium hirsutum L*). Planting operation was performed using a 6-row John Deere MaxEmerge Plus planter equipped with mechanical heavy duty downforce springs. Three row-unit depths were used along with three row-unit downforce for each crop. Two fields exhibiting typical Coastal Plain features but characterized by different soil properties and terrain attributes were also selected for this study. The experiment was a split-plot design. Soil electrical conductivity (EC) and soil water content at planting were used to describe field spatial variability. Gauge-wheel load was measured in real-time during planting operation at a sampling frequency of 20 Hz. Seeding depth was measured after emergence. Data were analyzed using mixed-effect analyses of variance, linear and polynomial regressions, and spatial methods.

Corn and cotton seeding depth increased with row-unit depth and downforce. Row-unit downforce adjustments affected measured seeding depth by as much as 1.1 cm. Corn and cotton seeding depth was significantly affected by changing soil conditions between fields and growing seasons. Shallower seeding depths were achieved in clayier and wetter soil conditions. Measured gauge-wheel load increased with increasing row-unit downforce and reduced with increasing row-unit depth. Significant site-specific seeding depth variability was identified within individual corn trials, and within 1 of 4 cotton trials. Corn seeding depth was not significantly correlated to soil water content within fields. Corn seeding depth was significantly correlated to in-field changes in soil EC. Seeding depth relationship to soil EC explained in-field variations in seeding depth ranging from 0.3 cm to 1.6 cm across individual corn trials. Corn seeding depth was also significantly affected by gauge-wheel load at planting. Corn emergence and yields were primarily affected by changing conditions between fields and growing seasons. Warmer soil temperatures and less clayey soils provided better field conditions for corn emergence resulting in higher final live populations, increased seedling vigor, and quicker and more uniform emergence. Corn emergence was also significantly affected by measured seeding depth and measured gauge-wheel load. Optimum seeding depths and gauge-wheel load optimizing corn emergence were identified for individual field trials. Optimum seeding depths maximizing corn yields were also indentified within 3 of 4 field trials. Improved emergence was correlated to higher yields at harvest. Seeding depth correlation to soil EC within individual field trials enabled to generate prescription maps which could be use to implement prescription-based seeding depth by downforce planting technologies. Equations were developped to describe in-field row-unit depth and downforce adjustments between management zones. Furthermore, results demonstrated the possibility of computing local gauge-wheel load predictions and equations were also developped to describe in-field row-unit depth and downforce adjustments using real-time gauge-wheel load data. Therefore, there is a potential for using site-specific planting technologies to improve seeding depth performance of standard row-crop planters. These technologies could operate based

on prescription maps for seeding depth or real-time monitoring of row-unit performance, and more particularly gauge-wheel operation. Most seeding depth adjustments could be provided by dynamic downforce systems, but optimum row-crop planter performance requires joined row-unit depth by downforce adjustments.

Acknowledgments

First and foremost, I would like to express my sincere gratitude and appreciation to my advisors Dr. Fulton and Dr. McDonald for their infinite support, advice, patience, and guidance throughout my work. Their high standards, constructive criticism, and dedication pushed me to think outside of the box and challenged me to become a better researcher and scientist.

Next, I would also like to express my gratitude and appreciation to all my committee members, Drs. Balkcom, Shaw, Knappenberger, and Taylor for their advice, insightful comments, and support throughout this project. Thank you also to Dr. Russ Muntifering for accepting to serve as university reader for my dissertation.

Moreover, I would like to give special thanks to Greg Pate at the E.V. Smith Research for his availability and the invaluable help, support, and assistance he provided throughout my work. Thank you also to all the staff working at the E.V. Smith Research Center for their participation in my research, support, and kindness.

Furthermore, I would like to thank the whole department of Biosystems Engineering who provided me with funding, advice, support, and assistance throughout this research. Special thanks goes to Simerjeet Virk, and my colleagues Rees Bridges, Chennan Kevin Xue, and Pengmin Pan whose efforts, help, and advice made my research a success. Thank you to all the graduate and undergraduate students who helped and participated with data collection.

Finally, I would like to thank my family and friends for their unconditional love, support, and encouragements when nothing seemed to work. Particular thanks go to my mother, my father, my brother, my grand-parents, Sue Ann Balch, Sarah Richard, Amirah Hill, Khalida Harun, and Michael Minkler who have been pillars of strength throughout these years.

Table of Contents

Abstract ii

Acknowledgments v

List of Figures ix

List of Tables xix

Nomenclature xxii

1 Introduction and Research Objectives 1

1.1 Problem Statement 1

1.2 Goals 4

1.3 Hypotheses 5

1.4 Research Objectives 5

1.5 Dissertation Outline 6

2 Literature Review 7

2.1 Row-Crop Planters 7

2.1.1 Standard Design and Functioning 7

2.1.2 Standard Seeding Depth Control Systems 11

2.1.3 Recent Planting Advancements 14

2.2 Performance Criteria 18

2.2.1 Targeted Seeding Rate 18

2.2.2 Seed Spacing 19

2.2.3 Adequate and Uniform Seeding Depth 21

2.3 The Soil Interface 21

2.3.1 Soil-Planter Interactions 22

2.3.2 Soils, Seeding Depth, and Crop Requirements 24

2.3.3 Measuring Spatial Variability for Precision Planting Applications . . 25
2.4 Summary . . . 26
3 Material and Methods . . . 27
3.1 Row-Crop Planter . . . 27
3.2 Experimental Design . . . 30
3.3 Site Overview and Management . . . 31
3.4 Data Collection . . . 32
3.4.1 Row-Unit Monitoring . . . 32
3.4.2 Overall Soil Conditions . . . 34
3.4.3 Field Spatial Variability . . . 40
3.4.4 Measured Seeding Depth . . . 43
3.4.5 Daily Emergence (Corn Only) . . . 44
3.4.6 Final Yields (Corn Only) . . . 45
3.5 Data Analysis . . . 46
3.5.1 Chapter 4 . . . 46
3.5.2 Chapter 5 . . . 47
3.5.3 Chapter 6 . . . 47
3.5.4 Chapter 7 . . . 49
4 Planting Response to Row-Unit Depth and Downforce Adjustments within Coastal Plain Soils . . . 50
4.1 Measured Seeding Depth . . . 50
4.2 Seeding Depth Variability . . . 61
4.3 Seeding Depth Precision . . . 61
4.4 Measured Gauge-Wheel Load . . . 66
4.5 Gauge-Wheel Load Variability . . . 73
4.6 Discussion . . . 74
4.7 Summary . . . 75

5 Site-Specific Seeding Depth Variability 77
5.1 Identification of Site-Specific Seeding Depth Variability 77
5.2 Explanation of Site-Specific Seeding Depth Variability 80
5.2.1 Seeding Depth Relationship to Soil EC and Soil Water Content . . . 80
5.2.2 Seeding Depth Relationship to Measured Gauge-Wheel Load 84
5.3 Discussion 85
5.4 Summary 85
6 Corn Emergence and Yield Response to Seeding Depth, Gauge-Wheel Load and Varying Field Conditions in the Southeast US . . 87
6.1 Final Corn Population 87
6.2 Emergence Timeliness 94
6.3 Uniformity of Emergence 97
6.4 Seedling Vigor 102
6.5 Final Yields 105
6.6 Discussion 110
6.7 Summary 110
7 Implementation of Prescription-Based Implied Technologies to Manage In-Field Seeding Depth Variability in the Southeast US. 112
7.1 Prescription-Based Seeding Depth Management 112
7.1.1 Allowable Seeding Depth Variability 113
7.1.2 Management Zones Delineation 114
7.1.3 Determination of Proper Depth and Downforce Settings 116
7.1.4 Evaluation of Benefits 118
7.2 Real-Time Seeding Depth Management 119
7.2.1 Real-Time Adjustments of Row-Unit Depth and Downforce Settings . 120
7.2.2 Computation of Local Gauge-Wheel Load Predictions 120
7.3 Discussion 121

7.4 Summary . . . 122
8 Conclusions . . . 123
8.1 Research Conclusions . . . 123
8.2 Practical Implications . . . 124
8.3 Future Research . . . 125
Appendices . . . 135
A Suppplementary Information for Individual Field Trials . . . 136
A.1 Tillage - Planting Date - Seed Variety . . . 136
A.2 Plots and Sampling Layouts . . . 136
A.3 Additional Field Trial . . . 149
B Statistical Results . . . 150
B.1 Complement to Chapter 4 . . . 151
B.2 Complement to Chapter 5 . . . 155
B.3 Complement to Chapter 6 . . . 161
B.4 Complement to Chapter 7 . . . 171
C Experimental Equipment Specifications . . . 175
C.1 John Deere Model 8130 Tractor . . . 176
C.2 John Deere Model 1700 Integral MaxEmerge® Plus Planter . . . 177
C.3 Veris 3100 . . . 178
C.4 Field Scout TDE 300 Soil Moisture Meter . . . 179
C.5 Trimble GeoXH Handheld . . . 180
C.6 DICKEY-John Grain Moisture Meter . . . 181
D Instrumentation and Data Acquisition . . . 182
D.1 National Instrument NI USB-6225 Data Acquisition Module . . . 183
D.2 Analog Device 5B38 Signal Conditioning Module . . . 184
D.3 CUI PYB20-Q24-D12-U DC-DC Converter . . . 185
D.4 CUI PYB15-Q24-S5-U DC-DC Converter . . . 186

D.5 Vishay Precision Transducers Model No 3810 187
D.6 Automation Direct TRD-GK3600-RZD Heavy Duty Encoder 188
D.7 LabVIEW Program 189

List of Figures

1.1 Optimum planting performance maximize crop yield potential at the beginning of the growing season. 2

1.2 Modern row-crop planters are constituted of individual row-units designed to place seeds in the ground at a proper and predetermined depth. Seeding depth is controlled through the use of two gauge-wheels mounted on individual planter row-unit. 3

1.3 Example of spatial variability in corn development within a field. 3

2.1 Row-crop planters are designed to simultaneously open a soil furrow of controlled depth, place metered and singulated seeds in the opened furrow, cover the furrow, and firm the soil within the seedbed to ensure proper seed to soil contact. . . . 7

2.2 Illustration of the vacuum-disk metering system. 8

2.3 Mechanism for seeding rate establishment on standard vacuum row-crop planters. 9

2.4 Common soil furrow opener designs for row-crop planters (Srivastava, Goering, Rohrbach, & Buckmaster, 2006). 10

2.5 Example of furrow covering devices for row-crop planters (Dawn, 2014). 10

2.6 Row-unit components that can be used on standard row-crop planters. 11

2.7 Standard row-unit depth and downforce setup on row-crop planters (example of a John Deere MaxEmerge Plus row-unit.) 12

2.8 Row-unit depth adjustment on standard row-crop planters. ***1:*** *Depth T-Handle,* ***2:*** *Handle Assembly,* ***3:*** *Rocker, and* ***4:*** *Gauge-Wheel Arm.* 13

2.9 Row-unit downforce adjustment on standard row-crop planters (example of MaxEmerge Plus row-unit). ***1:*** *Coil Springs,* ***2:*** *Adjustment Handle, and* ***3:*** *Application Arm.* 13

2.10 Adoption of automatic section control on row-crop planters limits skips and overlaps in areas that have been already planted, at headland turns, and/or point rows. (Runge, Fulton, Griffin, Virk, & Brooke, 2014) 16

2.11 Variable-rate seeding precision technology for row-crop planters. 17

2.12 Turn compensation (left) and Raven OmniRow® (right) precision technologies for row-crop planters. 17

2.13 Optimum plant population maximizes yield potential of individual plants. . . . 19

2.14 Non-uniform versus uniform seed spacing and associated benefits. 20

2.15 Non-uniform versus uniform plant emergence along with associated benefits. . . 21

2.16 Force diagram providing an inventory of the different forces acting on individual planter row-unit at planting. Example of a John Deere MaxEmerge Plus row-unit. 23

3.1 Image of the 6-row John Deere planter equipped with MaxEmerge Plus Row-Units used in this research. 27

3.2 Row-unit depth adjustment on the MaxEmerge Plus row-unit. 29

3.3 Illustration of the procedure used to check the depth setting increments for individual planter row-units. 29

3.4 Standard row-unit downforce system on the MaxEmerge Plus row-unit. 30

3.5 Aerial image of the two fields selected for this study and division into field trials. *Google Earth Image. Imagery Date: 12/18/2015 (Field A) and 2/26/2015 (Field B)* 32

3.6 Data acquisition system mounted on the planter to monitor row-crop planter performance at planting. **1:** Data Acquisition System, **2:** GPS Receiver, **3:** LabVIEW™ Program running on a tablet, **4:** Shaft Encoder, **5:** Load Pins, and **6:** Precision Ag. Controller Trimble Field-IQ. 33

3.7 Soil survey map provided by the USDA Web Soil Survey for field A. 35

3.8 NRCS order 1 soil survey for field B (Terra et al., 2004). 36

3.9 Average daily soil temperatures recorded at the E.V. Smith Research Center during the 2014 and 2015 corn growing season. 37

3.10 Average daily atmoshperic temperatures recorded at the E.V. Smith Research Center during the 2014 and 2015 corn growing season and computed cumulative corn growing degree days. 38

3.11 Average daily precipitations recorded at the E.V. Smith Research Center during the 2014 and 2015 corn growing season and cumulative distribution of precipitations. 38

3.12 Average daily soil temperatures recorded at the E.V. Smith Research Center during the 2014 and 2015 cotton growing season. 39

3.13 Average daily atmoshperic temperatures recorded at the E.V. Smith Research Center during the 2014 and 2015 cotton growing season and computed cumulative corn growing degree days. 39

3.14 Average daily precipitations recorded at the E.V. Smith Research Center during the 2014 and 2015 cotton growing season and cumulative distribution of precipitations. 40

3.15 Spatial variability in soil EC measured within field A. 42

3.16 Spatial variability in soil EC measured within field B. 43

3.17 Protocol for measuring (a) corn and (b) cotton seeding depth. 44

3.18 Classification of corn seedling emergence. 45

3.19 Weight wagon used to calibrate yield monitor data at every plot, and collection of grain sample to adjust final yields at 15.5% moisture content. 45

4.1 Summary of corn measured seeding depth. Whiskers length represents 1.5 times the inter-quartile range. Data beyond the whiskers were plotted as points. . . . 51

4.2 Summary of cotton measured seeding depth. Whiskers length represents 1.5 times the inter-quartile range. Data beyond the whiskers were plotted as points. . . . 51

4.3 Corn seeding depth response to row-unit depth adjustments by field and growing season. 56

4.4 Cotton seeding depth response to row-unit depth adjustments by field and growing season. 56

4.5 Row-unit parallel linkage configuration and downforce system performance for selected corn row-unit depths. 57

4.6 Summary of corn seeding depth standard deviation. Whiskers length was defined by 1.5 times the inter-quartile range. Data beyond the whiskers were plotted as points. 64

4.7 Summary of measured gauge-wheel load for corn. Whiskers length was defined by 1.5 times the inter-quartile range. Data beyong the whiskers were plotted as points. 68

4.8 Summary of measured gauge-wheel load for cotton. Whiskers length was defined by 1.5 times the inter-quartile range. Data beyong the whiskers were plotted as points. 68

4.9 Illustration of how row-unit depth and downforce adjustments and soil conditions influence seeding depth. 76

5.1 Site-specific seeding depth relationship to standardized soil EC within the 2014-A corn trial. 82

5.2 Site-specific seeding depth relationship to standardized soil EC within the 2014-B corn trial. 82

5.3 Site-specific seeding depth relationship to standardized soil EC within the 2015-A corn trial. 83

5.4 Site-specific seeding depth relationship to standardized soil EC within the 2015-A corn trial. 83

6.1 Determination of optimum seeding depth to maximize final population of corn within individual 2014 field trials – SD: row-unit depth adjustment. 93

6.2 Determination of optimum seeding depth to maximize final population of corn within individual 2014 field trials – SD: row-unit depth adjustment. 93

6.3 Determination of optimum seeding depth to maximize final yield of corn within individual field trials – SD: row-unit depth adjustment. 109

7.1 Management zones delineated for site-specific row-unit depth and downforce modifications within the 2014-A corn trial. 114

7.2 Management zones delineated for site-specific row-unit depth and downforce modifications within the 2014-B corn trial 115

7.3 Management zones delineated for site-specific row-unit depth and downforce modifications within the 2015-A corn trial. 115

7.4 Management zones delineated for site-specific row-unit depth and downforce modifications within the 2015-B corn trial 116

7.5 Row-unit depth and downforce combinations permitting to achieve 5.1 cm targeted depth within the 2014-B corn trial in zones A and B. 118

A.1 Plot layouts for 2014-A and 2014-B corn trials. 137

A.2 Plot layouts for 2015-A and 2015-B corn trials. 138

A.3 Plot layouts for 2015-A and 20015-B cotton trials. 139

A.4 Plot layouts for 2014-A and 2014-B cotton trials. 140

A.5 Sampling sites layout for 2014-A corn trial. 141

A.6 Sampling sites layout for 2014-B corn trial. 142

A.7 Sampling sites layout for 2014-A cotton trial. 143

A.8 Sampling sites layout for 2014-B cotton trial. 144

A.9 Sampling sites layout for 2015-A corn trial. 145

A.10 Sampling sites layout for 2015-B corn trial. 146

A.11 Sampling sites layout for 2015-A cotton trial. 147

A.12 Sampling sites layout for 2015-B cotton trial. 148

B.1 (a) Residual plot and (b) Quantile-Quantile plot used to validate the assumptions of linear mixed-effect analysis conducted for measured planting depth of corn. . 151

B.2 (a) Residual plot and (b) Quantile-Quantile plot used to validate the assumptions of linear mixed-effect analysis conducted for measured planting depth of cotton. 151

B.3 (a) Residual plot and (b) Quantile-Quantile plot used to validate the assumptions of linear mixed-effect analysis conducted for corn planting depth standard deviation at a given location. 152

B.4 (a) Residual plot and (b) Quantile-Quantile plot used to validate the assumptions of linear mixed-effect analysis conducted on measured gauge-wheel load data for corn. 152

B.5 (a) Residual plot and (b) Quantile-Quantile plot used to validate the assumptions of linear mixed-effect analysis conducted on measured gauge-wheel load data for cotton. 153

B.6 (a) Residual plot and (b) Residuals Quantile-Quantile plot for linear regression analysis conducted to evaluate corn planting depth response to row-unit depth and downforce adjustments by field and growing season. 155

B.7 (a) Residual plot and (b) Residuals Quantile-Quantile plot for linear regression analysis conducted to evaluate cotton planting depth response to row-unit depth and downforce adjustments by field and growing season. 155

B.8 (a) Residual plot and (b) Residuals Quantile-Quantile plot for Ordinary Least Square Regression conducted to evaluate planting depth response to planter seeding depth, row-unit downforce, and standardized soil EC within the 2014-A corn trial. 156

B.9 (a) Residual plot and (b) Residuals Quantile-Quantile plot for Geographically Weighted Regression conducted to evaluate planting depth response to planter seeding depth, row-unit downforce, and standardized soil EC within the 2014-B corn trial. 156

B.10 (a) Residual plot and (b) Residuals Quantile-Quantile plot for Geographically Weighted Regression conducted to evaluate planting depth response to planter seeding depth, row-unit downforce, and standardized soil EC within the 2015-A corn trial. 157

B.11 (a) Residual plot and (b) Residuals Quantile-Quantile plot for Geographically Weighted Regression conducted to evaluate planting depth response to planter seeding depth, row-unit downforce, and standardized soil EC within the 2015-B corn trial. 157

B.12 (a) Residual plot and (b) Residuals Quantile-Quantile plot for linear regression conducted to evaluate planting depth response to planter seeding depth, row-unit downforce, and measured gauge-wheel load within the 2014-A corn trial. 159

B.13 (a) Residual plot and (b) Residuals Quantile-Quantile plot for linear regression conducted to evaluate planting depth response to planter seeding depth, row-unit downforce, and measured gauge-wheel load within the 2014-B corn trial. 159

B.14 (a) Residual plot and (b) Residuals Quantile-Quantile plot for linear regression conducted to evaluate planting depth response to planter seeding depth, row-unit downforce, and measured gauge-wheel load within the 2015-A corn trial. 160

B.15 (a) Residual plot and (b) Residuals Quantile-Quantile plot for linear regression conducted to evaluate planting depth response to planter seeding depth, row-unit downforce, and measured gauge-wheel load within the 2015-B corn trial. 160

B.16 Corn daily live population by field, seeding depth, and row-unit downforce during 2014 growing season (summary of row data). 161

B.17 Corn daily live population by field, seeding depth, and row-unit downforce during 2015 growing season (summary of row data). 161

B.18 (a) Residual plot and (b) Quantile-Quantile plot computed to validate the assumptions of linear mixed-effect analysis conducted for final maize population during 2014 growing season. 162

B.19 (a) Residual plot and (b) Quantile-Quantile plot computed to validate the assumptions of linear mixed-effect analysis conducted for final maize population during 2015 growing season. 162

B.20 (a) Residual plot and (b) Quantile-Quantile plot computed to validate the assumptions of linear mixed-effect analysis conducted for maize emergence duration within 2014 field trials. 164

B.21 Uniformity of seedling growth by seeding depth and row-unit downforce within the 2014-A field trial (summary of row data). 165

B.22 Uniformity of seedling growth by seeding depth and row-unit downforce within the 2014-B field trial (summary of row data). 165

B.23 Uniformity of maize seedlings growth by seeding depth and row-unit downforce within 2015-A field trial. 166

B.24 Uniformity of maize seedlings growth by seeding depth and row-unit downforce within 2015-B field trial (summary of row data). 166

B.25 (a) Residual plot and (b) Quantile-Quantile plot computed to validate the assumptions of linear mixed-effect analysis conducted to characterize 2014 maize emergence uniformity. 167

B.26 (a) Residual plot and (b) Quantile-Quantile plot computed to validate the assumptions of linear mixed-effect analysis conducted to characterize 2015 maize emergence uniformity. 167

B.27 (a) Residual plot and (b) Quantile-Quantile plot computed to validate the assumptions of linear mixed-effect analysis conducted for Emergence Rate Index to describe 2014 maize seedling vigor. 169

B.28 (a) Residual plot and (b) Quantile-Quantile plot computed to validate the assumptions of linear mixed-effect analysis conducted for final maize yield. 170

B.29 Estimation of (a) auto-covariance and (b) partial auto-covariance for smoothed gauge-wheel load data in 2014-A corn trial. 171

B.30 Estimation of (a) auto-covariance and (b) partial auto-covariance for smoothed gauge-wheel load data in 2014-B corn trial. 171

B.31 Estimation of (a) auto-covariance and (b) partial auto-covariance for smoothed gauge-wheel load data in 2015-A corn trial. 172

B.32 Estimation of (a) auto-covariance and (b) partial auto-covariance for smoothed gauge-wheel load data in 2015-B corn trial. 172

B.33 Estimation of (a) auto-covariance and (b) partial auto-covariance among residuals from ARIMA model established to compute local gauge-wheel load predictions within the 2014-A corn trials. 173

B.34 Estimation of (a) auto-covariance and (b) partial auto-covariance among residuals from ARIMA model established to compute local gauge-wheel load predictions within the 2014-B corn trials. 173

B.35 Estimation of (a) auto-covariance and (b) partial auto-covariance among residuals from ARIMA model established to compute local gauge-wheel load predictions within the 2015-A corn trials. 174

B.36 Estimation of (a) auto-covariance and (b) partial auto-covariance among residuals from ARIMA model established to compute local gauge-wheel load predictions within the 2015-B corn trials. 174

D.1 LabVIEW program used to collect data with the data acquisition system. . . . 189

D.2 User interface for LabVIEW program. 190

List of Tables

3.1 Row-unit depth calibration for 6-row planter used in this study. 28

3.2 Targeted seeding depths for corn and cotton and associated T-handle settings. . 31

3.3 Comparison of overall soil characteristics in field A and B 35

3.4 Comparison of precipitation intensity during the 2014 and 2015 corn growing season. 37

3.5 Comparison of precipitation intensity during the 2014 and 2015 cotton growing season. 37

3.6 Summarized soil water content data by crop, growing season, and field 41

3.7 Summarized soil electrical conductivity data at 0 to 30 cm depth and evaluation of interpolation models accuracy for individual fields and growing seasons. . . . 42

4.1 Mixed-effect analysis of variance conducted for corn measured seeding depth data. 52

4.2 Mixed-effect analysis of variance conducted for cotton measured seeding depth data. 53

4.3 Mean seeding depth [cm] of corn by row-unit depth, row-unit downforce, field, and growing season. 54

4.4 Mean seeding depth [cm] of cotton by row-unit depth, row-unit downforce, field, and growing season. 55

4.5 Analysis of covariance conducted to model field-scale corn seeding depth response to row-unit downforce by field, growing season, and row-unit depth. 58

4.6 Analysis of covariance conducted to model field-scale cotton seeding depth response to row-unit downforce by field, growing season, and row-unit depth. . . . 59

4.7 Generalized linear mixed-effect analysis of variance conducted for planter ability to place cotton seeds within the soil furrow. 60

4.8 In-field standard deviation in corn seeding depth [cm] by row-unit depth, row-unit downforce, field and growing season. 62

4.9 In-field standard deviation in cotton measured seeding depth [cm] by row-unit depth, row-unit downforce, field and growing season. 62

4.10 Coefficient of variation [%] for corn measured seeding depth by row-unit depth, row-unit downforce, field and growing season. 63

4.11 Coefficient of variation [%] for cotton measured seeding depth by row-unit depth, row-unit downforce, field and growing season. 63

4.12 Results of mixed-effect analysis of variance conducted for corn seeding depth standard deviation data. 65

4.13 Mean corn seeding depth standard deviation by row-unit depth, field, and growing season (all row-unit downforce confounded). 66

4.14 Evaluation of corn seeding depth precision by row-unit depth, field, and growing season (all row-unit downforce confounded). 66

4.15 Results of mixed-effect analysis of variance conducted for corn measured gauge-wheel load data. 69

4.16 Results of mixed-effect analysis of variance conducted for cotton measured gauge-wheel load data. 70

4.17 Analysis of covariance conducted to model field-scale corn gauge-wheel load response to row-unit downforce by field, growing season, and row-unit depth. . . . 71

4.18 Analysis of covariance conducted to model field-scale cotton gauge-wheel load response to row-unit downforce by field, growing season, and row-unit depth. . . 72

4.20 In-field standard deviation in measured gauge-wheel load [kN] for corn by row-unit depth, row-unit downforce, field, and growing season. 73

4.21 In-field standard deviation in measured gauge-wheel load [kN] for cotton by row-unit depth, row-unit downforce, field, and growing season. 74

5.1 Analysis of covariance conducted to model field-scale corn seeding depth response to row-unit depth and downforce adjustments by field and growing season. . . . 78

5.2 Analysis of covariance conducted to model field-scale cotton seeding depth response to row-unit depth and downforce adjustments by field and growing season. 79

5.3 Evaluation of spatial auto-correlations among residuals from ANCOVA models characterizing site-specific seeding depth variability within individual corn trials. 80

5.4 Evaluation of spatial auto-correlations among residuals from ANCOVA models characterizing site-specific seeding depth variability within individual cotton trials. 80

5.5 Corn seeding depth relationship to row-unit depth, row-unit downforce, and standardized soil EC by field and growing season. 81

5.6 Evaluation of spatial auto-correlations among residuals from regression models characterizing seeding depth relationship to standardized soil EC within individual corn trials. 81

5.7 Corn seeding depth relationship to row-unit depth, row-unit downforce, and measured gauge-wheel load by field and growing season. 84

5.8 Evaluation of spatial auto-correlations among regression model residuals characterizing seeding depth response to measured gauge-wheel load within individual corn trials. 84

6.1 Mixed-effect analysis of variance conducted for corn final population data during the 2014 growing season. 89

6.2 Mixed-effect analysis of variance conducted for corn final population data during the 2015 growing season. 90

6.3 Analysis of covariance (ANCOVA) conducted to model 2014 field-scale final corn population response to measured seeding depth and gauge-wheel load. 91

6.4 Analysis of covariance (ANCOVA) conducted to model 2015 field-scale final corn population response to measured seeding depth and gauge-wheel load. 92

6.5 Corn emergence window for the 2014 growing season. 94

6.6 Mixed-effect analysis of variance conducted for 2014 corn emergence duration data. 95

6.7 Analysis of covariance (ANCOVA) conducted to model 2014 field-scale corn emergence duration response to measured seeding depth and gauge-wheel load. . . . 96

6.8 Mixed-effect analysis of variance conducted for uniformity of corn emergence during the 2014 growing season. 98

6.9 Mixed-effect analysis of variance conducted for uniformity of corn emergence during the 2015 growing season. 99

6.10 Analysis of covariance (ANCOVA) conducted to model field-scale measured seeding depth and gauge-wheel load effects on uniformity of 2014 corn emergence. . 100

6.11 Analysis of covariance (ANCOVA) conducted to model field-scale measured seeding depth and gauge-wheel load effects on uniformity of 2015 corn emergence. . 101

6.12 Mixed-effect analysis of variance conducted for Emergence Rate Index (ERI) data computed to quantify corn seedling vigor during the 2014 growing season. . . . 103

6.13 Analysis of covariance (ANCOVA) conducted to model field-scale measured seeding depth and gauge-wheel load effects on corn seedling vigor during the 2014 growing season. 104

6.14 Mean corn yield by row-unit depth, row-unit downforce, field, and growing season. 106

6.15 Mixed-effect analysis of variance conducted for corn final yield data. 107

6.16 Analysis of covariance (ANCOVA) conducted to model field-scale corn final yield response to measured seeding depth and gauge-wheel load. 108

6.17 Spearman's correlations to characterize relationships between corn final yields and corn emergence metrics within all field trials. 109

7.1 ARIMA models describing spatial auto-correlations among gauge-wheel load data within individual field trials. 121

A.1 Supplementary information provided for individual field trials conducted in this study – strip-tillage date, planting date, seed variety. 136

A.2 Mean seeding depth of corn and seeding depth standard deviation by row-unit depth and downforce within the 2014 field trial conducted at the Tennessee Valley Research Center. 149

B.1 Mean corn planting depth standard deviation at a given sampling site by seeding depth, row-unit downforce, field and growing season. 153

B.2 Mean measured gauge-wheel load for corn by seeding depth, row-unit downforce, field and growing season. 154

B.3 Mean measured gauge-wheel load for cotton by seeding depth, row-unit downforce, field and growing season. 154

B.4 Corn planting depth response to measured gauge-wheel load by planter seeding depth, field, and growing season. 158

B.5 Final maize population by seeding depth, row-unit downforce, and field during 2014 growing season. 163

B.6 Final maize population by seeding depth, row-unit downforce, and field during 2015 growing season. 163

B.7 Gibb's Index to describe 2014 maize emergence uniformity by seeding depth, row-unit downforce, and field (summary of row data). 168

B.8 Gibb's Index to describe 2015 maize emergence uniformity by seeding depth, row-unit downforce, and field (summary of row data). 168

B.9 Emergence Rate Index (ERI) to describe 2014 maize seedling vigor by seeding depth, row-unit downforce, and field. 169

B.10 Maize final yield by seeding depth, row-unit downforce, field, and growing season. 170

Nomenclature

Applied Downforce: Supplementary weight applied by the downforce system onto individual row-unit.

Field Spatial Variability: In-field changes in soil physical properties – including texture, water content, structure, friability, porosity, mineralogy, chemistry.

Gauge-Wheel Load: Soil reaction force onto the planter gauge-wheels at planting.

Row-Unit Depth: Row-unit depth T-handle adjustment. Controls the vertical distance between the bottom of the furrow opener and the bottom of the gauge-wheels operating on the soil surface.

Row-unit Downforce: Row-unit downforce spring adjustment. Controls the amount of downforce applied onto individual row-units.

Seeding Depth: Achieved depth in the field (soil on top of seeds).

Target Depth: Corn and cotton seeding depths aimed at planting – 2.5, 5.1, and 7.6 cm for corn, and 0.6, 1.3, and 2.5 cm for cotton. Targeted depths were used to selected row-unit depth treatments for corn and cotton.

Chapter 1

Introduction and Research Objectives

1.1 Problem Statement

Agriculture is like other industries in that it must continuously adjust with changing demographic demand, global economy, and research innovations. A prime example would be the modernization of agricultural practices initiated at the beginning of the 20^{th} century. Then, worldwide development of emerging technologies such as mechanization of farm equipment, development of irrigation, and production of high-yielding grain crops, synthetic fertilizers and pesticides enabled intensification of crop production which addressed population needs of that time (Kush, 1999). Since, the world population has continued to increase and the USDA predicts an additional population growth of about 14% by 2030 (USDA, 2016). Such an increase in population would result in an additional 1.0 billion people on the Earth and generate considerable demand for agricultural production of food, fiber, and energy, therefore requiring farmers to increase crop yields per unit area.

Seeds that are produced today can be optimized for specific conditions (Fernandez-Cornejo, 2004). However, continued advances in technology along with the rarefaction of non-renewable resources generates significant increase in prices for agricultural inputs and energy (USDA, 2006) and each seed has become more valuable. Therefore, each seed should be managed to maximize yield potential whereas standard management strategies limit accounting for field spatial variability. Standard management strategies have become inadequate to continue to support higher crop yield productions (Evans and Fischer, 1999) and modern farmers are required to adopt more efficient management strategies including site-specific practices through advancement of precision agriculture (Auernhammer, 2001; Auernhammer and Schueller, 1999)

Precision technologies increase machine automation (Heraud and Lange, 2009) and permit adjustments of equipment performance to field spatial variability. They also provide operators and researchers with valuable feedback on field operation, therefore permitting improvement of farm management strategies (Winstead et al., 2010). Adoption of precision technologies can be beneficial at every stage of the growing season, and recent focus has been with planting that represents a critical field operation. Indeed, maximum yield potential of a crop is established at planting, and mistakes at this stage can negatively affect crop growth and reduce final yields, as well as farm profitability (Figure 1.1). Furthermore, seeds cost continuously increases due to improving seed technology (Schnitkey, 2015), and optimizing row-crop planter performance become even more fundamental to maximize farm profitability.

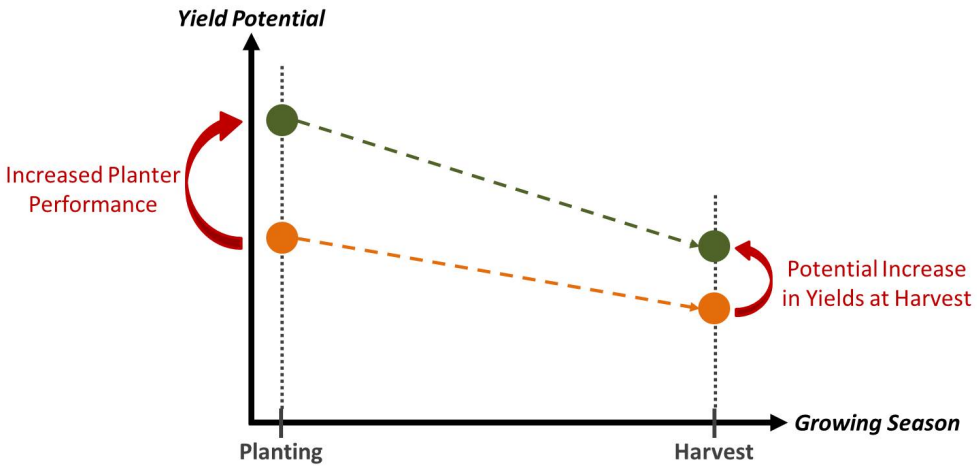

Figure 1.1: Optimum planting performance maximize crop yield potential at the beginning of the growing season.

Modern row-crop planters (Figure 1.2) are designed to place seeds in the ground at a proper and predetermined depth, while providing adequate seed to soil contact to maximize the likelihood of emergence uniformity and early growth among seedlings (Schneider and Gupta, 1985). Indeed, uniform stand establishment is desirable as it limits plant competition for water, nutrients and sunlight (Martin et al., 2005) and can contribute to increase

crop yields by as much as 5% to 10% (Carter et al., 1990) . Most U.S. row-crop planters control seeding depth through a pair of gauge-wheels mounted on individual row-units. Seeding depth is manually adjusted by changing a row-unit depth, followed by the adjustment of a row-unit downforce. Row-unit downforce is adjusted manually to determine the amount of load transferred from the planter toolbar onto individual row-units to maintain preferred seeding depth. Typically, row-unit depth and downforce are adjusted prior to the planting operation. Once set, the same settings are then used throughout the field though soil properties may vary. Optimization of planter performance requires developing technologies that permit adjustment of row-unit depth and downforce settings to changing field conditions (Knappenberger and Köller, 2011).

Figure 1.2: Modern row-crop planters are constituted of individual row-units designed to place seeds in the ground at a proper and predetermined depth. Seeding depth is controlled through the use of two gauge-wheels mounted on individual planter row-unit.

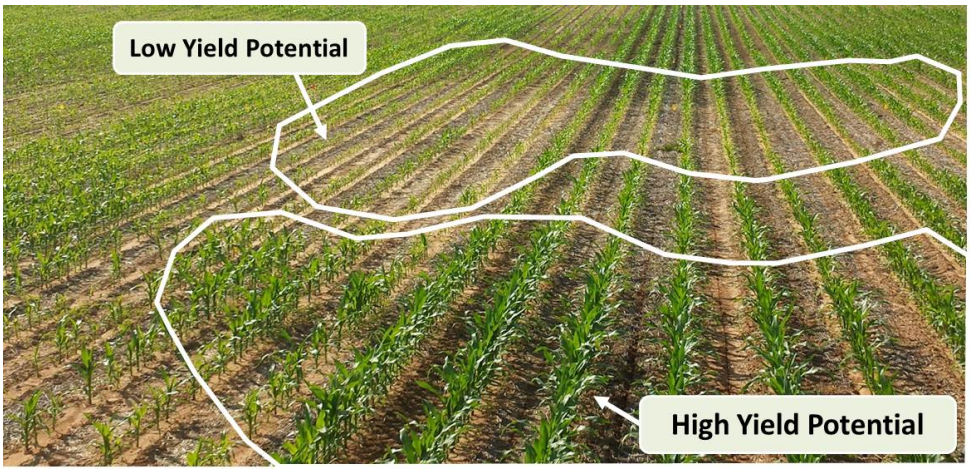

Figure 1.3: Example of spatial variability in corn development within a field.

Recent precision agriculture advances provided producers with several technologies to improve row-crop planter performance. Typically, these technologies enable control of product application (automatic section control, variable seeding rate, accurate placement of genetic traits); monitor row-unit performance (singulation and population feedback, downforce monitoring); and visualize data (in-cab displays). However, minimal modern technology is available to adjust row-unit depth and downforce planter settings to field spatial variability, and most recent research efforts are focused on the development of planting technologies with such capabilities. These technologies would enable producers to control row-unit depth and/or downforce to match soil conditions within fields (Burce et al., 2009; Guarido et al., 2013). These technologies would operate using either prescription maps for seeding depth, real-time monitoring of row-unit behavior, and/or real-time sensing of key soil properties such as soil water content and/or soil electrical conductivity. Traditional row-unit downforce systems can now be replaced with pneumatic or hydraulic actuators permitting in-field adjustments of row-unit downforce during planting. However, these technologies constitute only a first step toward the development of more complex technologies expected to provide active control of both row-unit depth and downforce planter settings. Developing planting technologies with such capabilities is challenging, and success requires establishment of a unified control algorithm to properly adjust row-unit depth and downforce settings to changing soil conditions.

1.2 Goals

Long term goals for this research are as follow:

1. Understand planter and crop response to row-unit depth adjustment, row-unit downforce, and changing field conditions to identify farmers' needs and develop planting technologies that address them.

2. Identify constraints to which the technology must be subjected, including technology response time and applied downforce requirements.

3. Provide farmers with specifications to ensure proper use of the technology in any field conditions to maximize benefits.

1.3 Hypotheses

Based on the above review and current knowledge on row-crop planters, the following hypotheses were formulated for this research:

1. Seeding depth is significantly affected by row-unit depth and downforce adjustments, changing soil conditions between fields and growing seasons, and field spatial variability.

2. Crop development is significantly affected by seeding depth, gauge-wheel load, changing soil conditions between fields and growing seasons, and field spatial variability.

3. Prescription-based or real-time technologies to manage in-field seeding depth variability will improve standard row-crop planter performance.

1.4 Research Objectives

This study was conducted for corn and cotton, which constitute two major row-crops cultivated in Alabama and in the Southeastern United States. The objectives for this research were to:

1. Characterize the influence of planter setup and field variables on corn and cotton seeding depth within Coastal Plain soils,

2. Evaluate corn emergence and yield response to seeding depth, gauge-wheel load, and field conditions in Coastal Plain soils, and

3. Describe prescription-based and real-time planting technologies to manage in-field seeding depth variability in the Southeast US.

1.5 Dissertation Outline

This dissertation was divided into eight chapters. Chapter 1 provides background information to justify this research leading to the definition of the overall research objectives. Chapter 2 covers a review of literature, providing information related to row-crop planters, planting technologies, planting performance, and soils. Chapter 3 describes material and methodologies used for this study, including equipment and calibration procedures, experimental design, data collection and data analysis. Chapter 4 through 7 provide results and discussion related to the research objectives. Chapter 4 discusses field-scale corn and cotton planting response to row-unit depth and downforce adjustments. Chapter 5 examines corn and cotton site-specific seeding depth response to field spatial variability. Chapter 6 models corn emergence and final yield response to seeding depth, gauge-wheel load, and field conditions. Chapter 7 discusses implementation of prescription-based and real-time planting technologies to manage seeding depth variability at planting. Finally, chapter 8 provides a summary of research findings and practical applications, and discusses ideas and suggestions for future research work.

Chapter 2

Literature Review

2.1 Row-Crop Planters

2.1.1 Standard Design and Functioning

Row-crop – or precision – planters are constituted of individual row-units designed to simultaneously open a soil furrow of controlled depth; meter seeds at proper rate; place seeds in the opened furrow at equal distance intervals; cover the furrow; and firm the soil within the seedbed to provide adequate seed-to-soil contact for germination (Morrison, 1989; Figure 2.1). Individual row-units are attached to the planter main toolbar by means of parallel linkages (Hudspeth and Wanjura, 1970), and each row-unit includes at least a metering device to meter and singulate seeds, a furrow opener, and a furrow closing system.

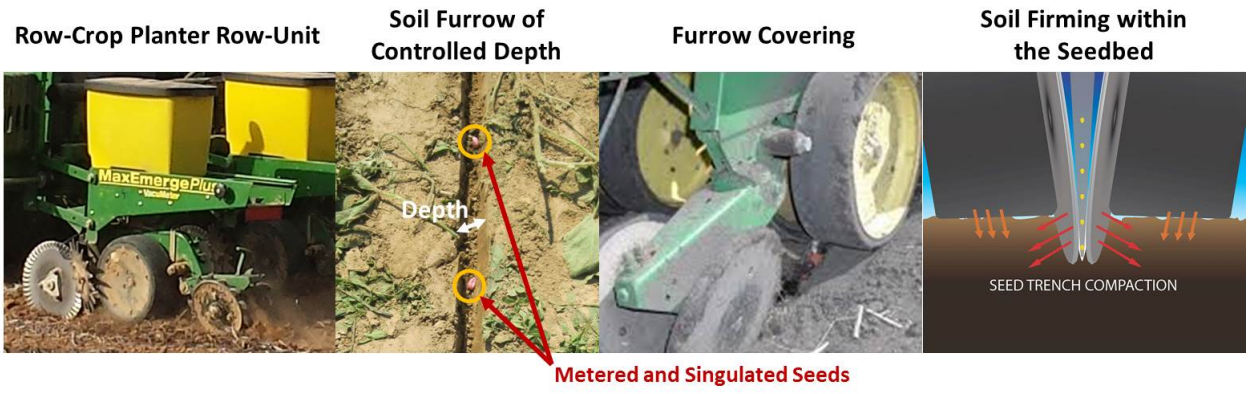

Figure 2.1: Row-crop planters are designed to simultaneously open a soil furrow of controlled depth, place metered and singulated seeds in the opened furrow, cover the furrow, and firm the soil within the seedbed to ensure proper seed to soil contact.

- ***Metering Device***

The metering device meters and singulates seeds (Srivastava et al., 2006). Several metering solutions have been developed and used over time to improve planter metering and singulation performances, but focus was given to Vacuum-Disk Metering systems due to their dominance in the present market (Figure 2.2). Seeds are first delivered to a seed reservoir located on the bottom part of the metering device. The seed reservoir is separated by a vertical seed plate in rotation. The side of the vertical plate in contact with the seed reservoir includes seed cells perforated in their center and specifically designed to hold one and only one seed of given size. The other side of the plate is maintained under vacuum to draw individual seeds from the seed reservoir and hold them within the perforated seed cells as the plate rotates. The vacuum is physically broken at the entrance of the seed delivery system allowing seeds to be released from the plate. A system of brushes is usually placed at the entrance of the seed delivery system to ensure proper vacuum break and effective seed release.

Figure 2.2: Illustration of the vacuum-disk metering system.

Individual row-unit metering devices are typically linked by a system of gears and chains to a single shaft controlling the rotation speed of all metering devices simultaneously (Figure 2.3). Seeding rate is established based on the rotation speed of the main shaft, the number of planter row-units, row-unit width, and the number of seed cells located on individual plates.

Different plates varying in size, shape, and number of seed cells are commercially available to match any seed size, shape and seeding rate requirements. Plates can be easily exchanged, prior to planting.

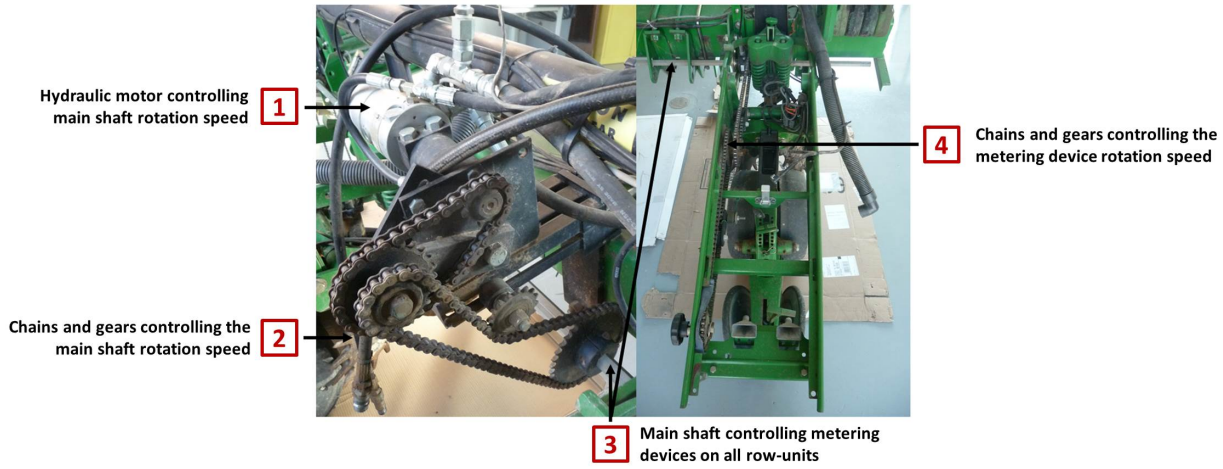

Figure 2.3: Mechanism for seeding rate establishment on standard vacuum row-crop planters.

- ***Soil Furrow Opener***

The soil furrow opener creates a well-defined trench to place individual seeds at a predetermined depth (Murray et al., 2006). Common soil furrow opener designs include single and double disks, staggered double-disks, runners, and hoes (Figure 2.4). Double disc openers are most widely used today to improve row-unit ability to cut through soil surface residues and provide better depth uniformity (Dickey and Jasa, 1983). Double disc openers can be used alone or in combination with a runner type to obtain cleaner soil furrows.

- ***Soil Furrow Closing System***

The furrow closer covers individual seeds placed within the opened furrow to ensure optimum seed-to-soil contact for germination (Dickey and Jasa, 1983). Furrow covering devices typically consist of two closing wheels, existing in different sizes and shapes (Figure

2.5). For instance, curved teeth closing wheels can be used to break side-wall compaction. Rubber – smooth – closing wheels are most adapted in drier and less clayey soil conditions. Intermediate shapes between curved teeth and smooth surface closing wheels are usually beneficial with conventional tillage to avoid soil crusting, and for shallower seeding depths. Two closing wheels of different shapes can also be installed on the same row-unit to improve furrow closing performance. Closing wheels are usually used in association with a pair of gauge-wheels and/or rear-press wheels that firm the soil within the seedbed.

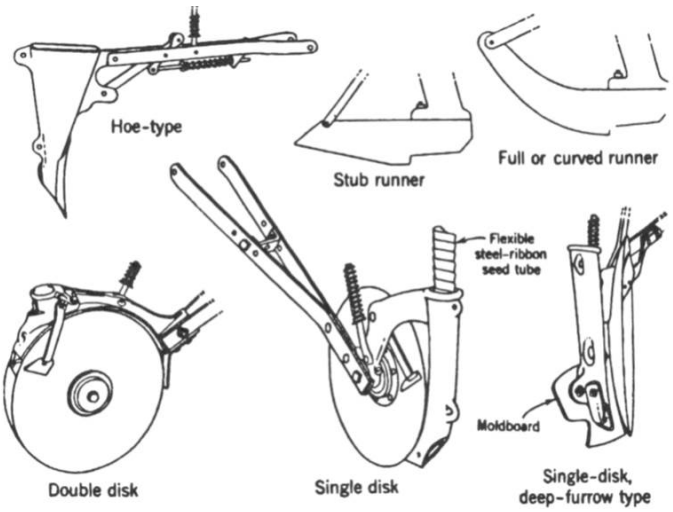

Figure 2.4: Common soil furrow opener designs for row-crop planters (Srivastava et al., 2006).

Figure 2.5: Example of furrow covering devices for row-crop planters (Dawn, 2014).

- ***Other Row-Unit Components***

Furthermore, planter row-units can be equipped with a coulter to cut more abundant and unevenly distributed residues on the soil surface (Dickey and Jasa, 1983). Common coulter designs include smooth, rippled, fluted, and rippled with smooth edge (Figure 2.6). Wider ripples or flutes enhance coulters ability to cut soil residues, but also increase weight requirements for proper performance. Rippled coulters usually allow higher planting speeds than fluted coulters. Coulters must operate shallower than the furrow opener. Finally, planter row-units can also be equipped with row cleaners – trash wheels – to remove residues and clods from the soil surface, and seed firmers to limit in-furrow seed bounces and furrow closure disturbances (Staggenborg et al., 2004).

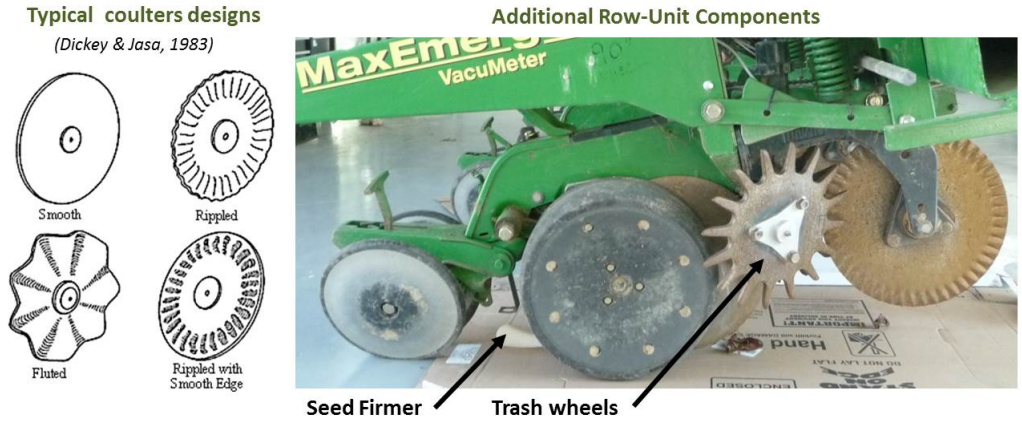

Figure 2.6: Row-unit components that can be used on standard row-crop planters.

2.1.2 Standard Seeding Depth Control Systems

For most U.S. row-crop planters, depth is controlled through a pair of gauge-wheels mounted on individual row-units. Seeding depth is selected prior to the planting operation by manually adjusting a row-unit depth and a row-unit downforce (Figure 2.7). Row-unit depth is usually adjusted by means of a spring-loaded depth T-handle (Figure 2.8), which

can be positioned in a series of holes causing the handle assembly to rotate (Bridges, 2016). The lower hand of the handle assembly forms a rocker providing a upper hard stop to both gauge-wheel arms. As the T-handle is positioned further down, wider gauge-wheel arm rotation is allowed, which effectively increases seeding depth. Row-unit downforce is adjusted by means of a downforce system controlling the amount of additional weight – applied downforce – transferred from the planter toolbar onto individual row-units. Row-unit downforce establishes the load exerted by the gauge-wheels – and more generally the depth control mechanism – onto the soil around the seed furrow (Morrison, 1988). Standard downforce systems consist of two coil springs, an adjustment handle, and a rotating force application arm (Figure 2.9). Activation angle and spring compression rate of the system are determined by the location of the adjustment handle attachment to the lever on the force arm, and changing handle position on the lever produces different downforce settings (Bridges, 2016).

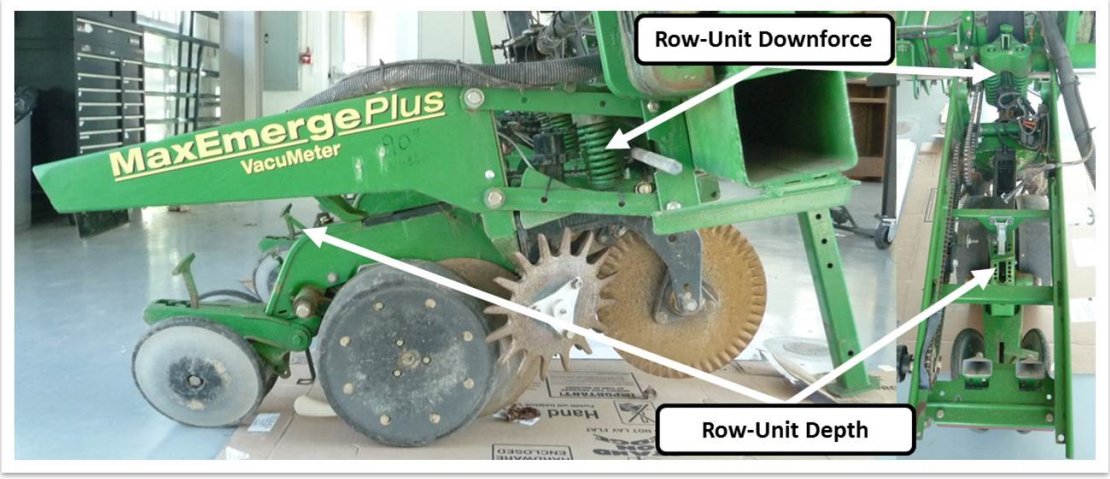

Figure 2.7: Standard row-unit depth and downforce setup on row-crop planters (example of a John Deere MaxEmerge Plus row-unit.)

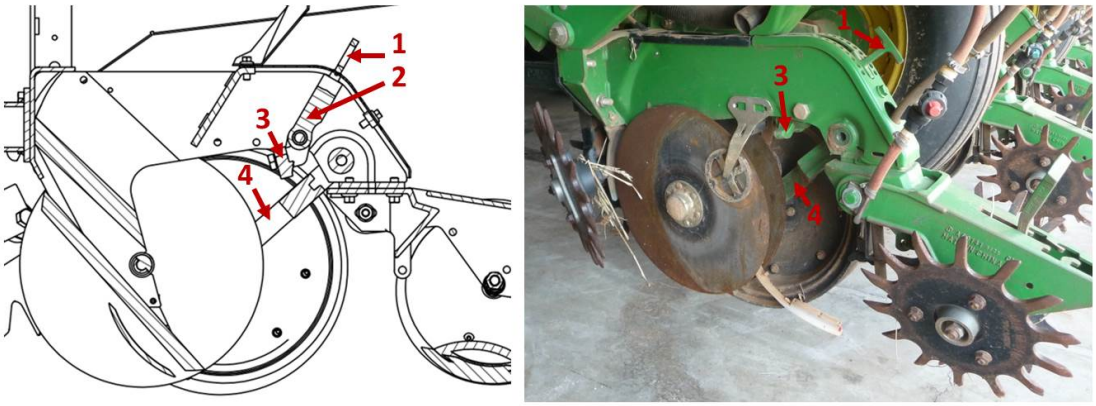

Figure 2.8: Row-unit depth adjustment on standard row-crop planters. ***1:*** *Depth T-Handle,* ***2:*** *Handle Assembly,* ***3:*** *Rocker, and* ***4:*** *Gauge-Wheel Arm.*

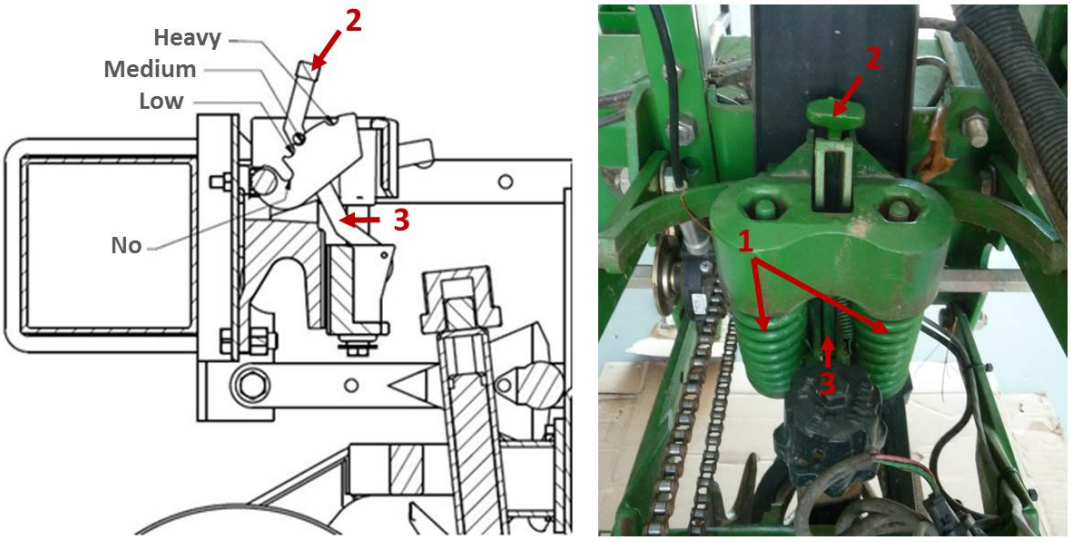

Figure 2.9: Row-unit downforce adjustment on standard row-crop planters (example of Max-Emerge Plus row-unit). ***1:*** *Coil Springs,* ***2:*** *Adjustment Handle, and* ***3:*** *Application Arm.*

2.1.3 Recent Planting Advancements

Row-crop planters commercialized by John Deere, Case IH, Kinze, White, and other manufacturers includes 4 to 48 rows, with 6 to 18 rows being commonly used in Southeastern US. Traditionally, all row-units operate as a single unit but such systems are not efficient enough to support higher crop yield production. Development of new planting equipment and technologies is then required to improve row-crop planter performance, and a summary of recent planting advancements is presented below.

- ***Real-Time Row-Unit Performance Monitoring***

Optimum row-crop planter performance requires real-time assessment of individual row-unit performance during planting operation, and several technologies are available today to provide per-row feedback to the operator (Morrison, 2010). These technologies usually allow real-time monitoring of plant population, seed singulation, applied downforce, ride quality, gauge-wheel load margin and variety among other parameters. Existing technology includes John Deere SeedStar^{TM}, Precision Planting 20/20 SeedSense, and Case IH Accu-Stat sytems.

- ***Improving Planting Equipment***

One solution to improve row-crop planter performance is to optimize planting equipment itself, and a first strategy consists of reducing row-unit width to promote more uniform plant distribution and therefore more efficient use of soil resources (Abendroth and Elmore, 2006; Pioneer, 2014). This lead to the development of 38 cm, 51 cm, and 56 cm spacing row-crop planters, split planters and twin-row planters. A second strategy consists in developing planter mechanisms allowing faster planting speeds to increase acreage capacity, field efficiency and operation timeliness (Scott, 2015). Existing high speed planting solutions include John Deere ExactEmerge^{TM} row-unit, and Precision Planting Speed Tube. Adoption of centralized seed distribution systems such as the ones provided with John Deere Integral

planters and Kinze Bulk Fill Hoppers also contributes to improve field efficiency and operation timeliness. Multi-hybrid planters provide growers with the capability of adjusting hybrid placement to field spatial variability. Finally, row-crop planter performance can be improved through optimization of seed metering systems performance (Miller et al., 2012) which lead to the development of Precision Planting eSet, eSetPro, vSet and John Deere VacuMeter™ seed metering devices.

- ***Optimizing Row-Pattern Management***

The next solution to improve row-crop planter performance consists of optimizing row-pattern management at planting by adopting auto-guidance and automatic section control precision technologies. Auto-guidance represents entry-level technology for adoption of precision agriculture and uses satellite-based positioning to automatically steer the vehicle based on a pre-determined path planning strategy. Auto-guidance systems are often associated with a Real-Time Kinematic (RTK) correction signal to achieve sub-centimeter position accuracy. Adoption of auto-guidance contributes to improve operation efficiency and timeliness throughout the growing season by limiting skips and overlaps (estimated close to 10% of implement width without guidance (Price, 2011)), reducing operator fatigue, and providing the possibility to perform field operations in poor visible conditions. Automatic section control enables one to turn OFF individual row-units or planter sections to limit skips and overlaps in areas that have been already planted, at headland turns, and/or at point rows (Figure 2.10) (NDSU, 2010; Mullenix et al., 2008). Automatic section control relies on the use of hydraulic, electronic, or pneumatic row clutches, and existing systems include Ag Leader® sectional control and Raven AccuRow™. Adoption of such technology can contribute to decrease the number of seeds planted in a field by up to 30% depending on size and shape (Luck et al., 2011).

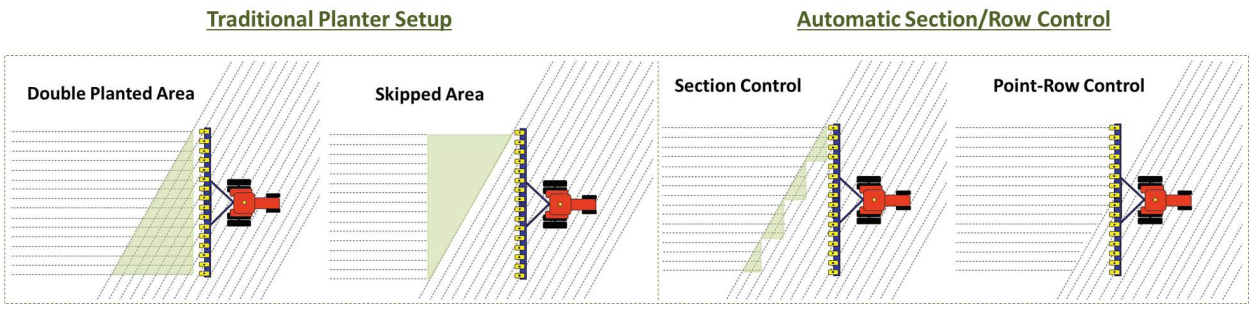

Figure 2.10: Adoption of automatic section control on row-crop planters limits skips and overlaps in areas that have been already planted, at headland turns, and/or point rows. (Runge et al., 2014)

- ***Increasing Field Productivity***

The next solution to improve row-crop planter performance consists of increasing field productivity by adopting Variable-Rate Seeding (VRS) and turn compensation precision technologies. Row-crop response to plant population is environment-dependent, and VRS can contribute to increase field productivity by permitting in-field adjustments of seeding rate at planting (Figure 2.11). Successful implementation of VRS planting technology requires proper identification of management zones within a field, and VRS prescription maps are often created based on soil data from the field, yield and cropping history, grower's knowledge of the general productivity of field areas, and other information such as landscape, topography, slope, drainage, soil electrical conductivity, and/or remote imagery (Jeschke et al., 2012; Dekalb®, 2015). For fields exhibiting average spatial variability, corn seeding rates are typically set to vary by 12,350 to 14,800 seeds ha^{-1}. Existing VRS systems include Precision Planting RowFlow and AgLeader SeedCommand™. Economic benefits from VRS are difficult to evaluate with results in literature suggesting low return on investment for this technology (Hest, 2011) .

Furthermore, metering devices on standard row-crop planters are driven by a central hydraulic motor causing metering plates on individual row-units to rotate at the same speed (section 2.1.1). When the planter is performing on straight passes, planter performance

is optimum and seeds are delivered uniformly across individual row-units. However, when performing in curved passes a speed differential is created across the planter and adoption of turn compensation precision technology can be beneficial to permit by-section or by-row seeding rate control (Figure 2.12). Existing turn compensation solutions include Precision Planting vDrive System®, and Raven OmniRow® planting technologies.

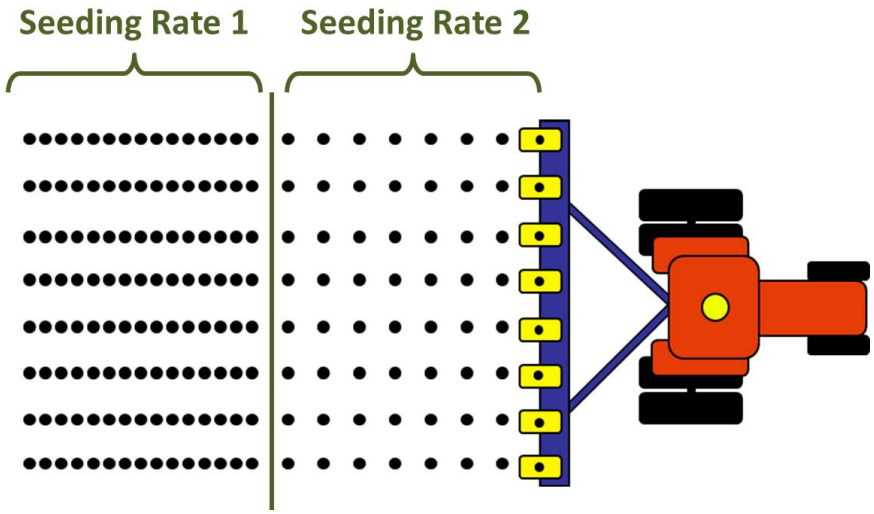

Figure 2.11: Variable-rate seeding precision technology for row-crop planters.

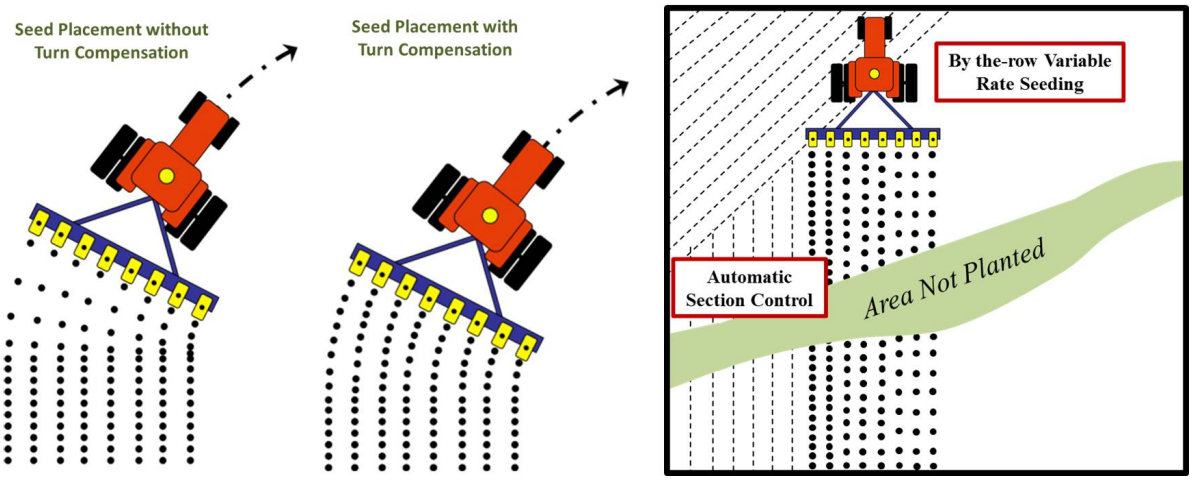

Figure 2.12: Turn compensation (left) and Raven OmniRow® (right) precision technologies for row-crop planters.

- ***Controlling Seeding Depth***

Finally, standard depth control system performance is often affected by changing soil conditions within a field, (Bowen, 1966) and another strategy to improve row-crop planter performance consists of optimizing standard depth control systems to manage field spatial variability (Weatherly and Bowers, 1997; Rene-Laforest et al., 2014). This lead to the development of active downpressure systems replacing traditional mechanical springs (section 2.1.2) by pneumatic or hydraulic actuators to control row-unit downforce in real-time during field operation. Current dynamic downforce solutions include John Deere Active Pneumatic Downforce System, Precision Planting Airforce® and DeltaForce® systems, and AgLeader® Hydraulic Downforce system. Hydraulic downforce systems are usually characterized by quicker response times than pneumatic systems. Existing systems typically control row-unit downforce simultaneously across the whole planter, by section, or by row. Existing technology can also account for changes in hopper weight during planting.

2.2 Performance Criteria

Optimum planting performance requires placing individual seeds within adequate soil conditions to promote uniform emergence and growth of seedlings which limits plant-to-plant variability and minimizes plant competition for water, nutrients, and sunlight (Carter et. al, 1990). Mistakes at planting often negatively impact crop growth and yield, and peak planter performance remains key to maximize yield potential and profitability (Karayel and Ozmerzi, 2008). Typically, planter performance is evaluated based on planter's ability to achieve targeted seeding rate, uniform seed spacing, and adequate and uniform seeding depth.

2.2.1 Targeted Seeding Rate

Row-crops demonstrate an optimal response to plant population (Zhang et al., 2006; Yao and Shaw, 1964). Whereas insufficient plant populations promote the allocation of more

resources toward crop vegetative development rather than toward the organs contributing to yield, excessive plant populations increase competition for available resources therefore increasing crop sensitivity to drought stress and pathogens. Therefore, optimum seeding rate maximizes yield potential of individual plants, and targeted seeding rate is usually determined based on crop, variety, soil fertility, targeted yield, field management strategy, and expected seed mortality. Typical seeding rate recommendations range from 74,000 to 98,500 seeds ha^{-1} for corn (Butzen, 2003), and from 86,500 to 136,000 seeds ha^{-1} for cotton (Deltapine®, 2012). Most current planters are able to accurately meter seeds and reach targeted seeding rates under recommended planting speeds.

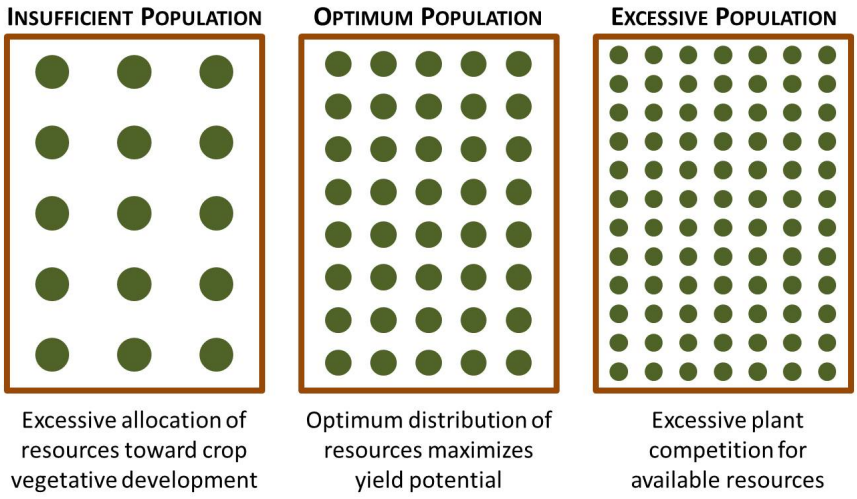

Figure 2.13: Optimum plant population maximizes yield potential of individual plants.

2.2.2 Seed Spacing

Seed spacing describes the horizontal distribution of seeds within the soil furrow, and uniform seed spacing maximizes crop yield potential allowing for a better distribution of available soil moisture, nutrients, and sunlight between plants, improving water use efficiency, facilitating gas movement within the soil, and optimizing mutual shading between plants (Figure 2.14). Expected average seed spacing can be calculated from planter seeding rate

and row-unit width. Non-uniform spacing typically result from non-ideal metering device performance – zero (skip) or multiple seeds placed at a single location – , and/or important in-furrow seed bounces and furrow closure disturbance. Uneven seed placement can reduce crop yields by as much as 5% to 10% (Searle et al., 2008). Spacing is typically measured between consecutive seeds, seedlings, or plants and characterized through computation of the following parameters: mean spacing, spacing standard deviation, miss index, multiple index, quality of feed, and precision index (Yazgi and Degirmencioglu, 2007). Mean spacing corresponds to the average spacing distance observed between consecutive seeds, seedlings, or plants. Spacing standard deviation characterizes spacing variability between consecutive seeds, seedlings, or plants. The miss and multiple indices evalulates the proportion of seeds which were not properly singulated. The miss index also accounts for seed mortality when spacing is measured between seedlings or plants. On the other hand, the quality of feed index determines the proportion of seeds that were properly singulated before being placed within the soil furrow. Finally, the precision index evaluates the spacing variability between seeds, seedlings, or plants that were properly singulated. Spacing standard deviation of 2.5 to 5.1 cm is usually considered as providing acceptable spacing variability and modern vacuum planters are able to achieve uniform seed spacing under recommended planting speed with proper equipment maintenance (Kocher et al., 2011; Staggenborg et al;, 2004).

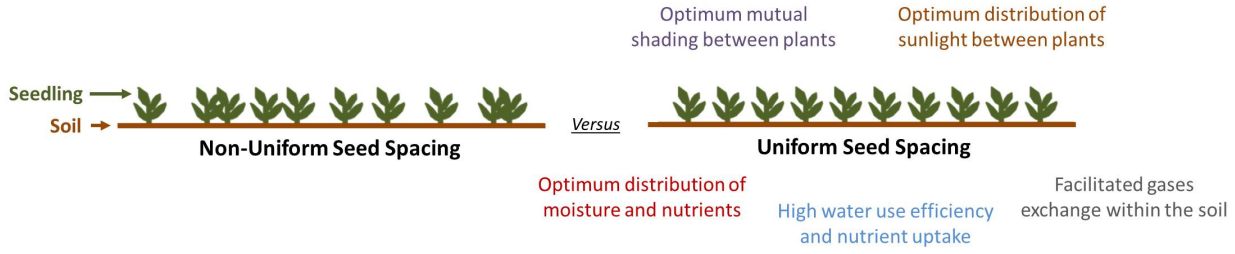

Figure 2.14: Non-uniform versus uniform seed spacing and associated benefits.

2.2.3 Adequate and Uniform Seeding Depth

Targeted seeding depth is selected prior to planting operation based on crop, variety, soil morphology, climatic conditions, and field management strategy. Standard seeding depth recommendations are 4.4 to 6.3 cm for corn (Thomison et al., 2013), and 1.2 to 1.9 cm for cotton (Deltapine®, 2015). Adequate seeding depth provides individual seeds with necessary soil water, temperature, and aeration to promote uniform emergence and minimal seed loss (Figure 2.15) therefore limiting seedling competition for water, nutrient, and sunlight. Uniform emergence can contribute to increase crop yields by as much as 5% to 10% (Carter et al., 1990; Nafzinger et al., 1991; Wanjura, 1982) although non-uniform emergence is often observed within fields. Non-uniform emergence typically results from planter failure in achieving uniform depth across the field as standard depth control systems cannot adjust for field spatial variability.

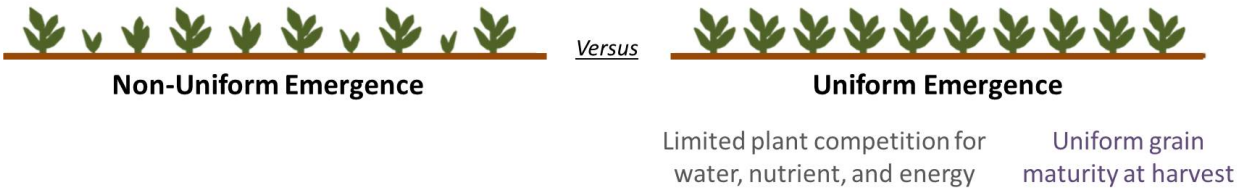

Figure 2.15: Non-uniform versus uniform plant emergence along with associated benefits.

2.3 The Soil Interface

Soil conditions at planting can impact row-crop planter seeding depth performance whereas they often vary within fields, and optimum planter performance requires developing precision technologies permitting to adjust row-unit depth and downforce settings to these changing soil conditions (Rene-Laforest et al., 2014). These technologies would operate based on the use of prescription maps for seeding depth, real-time monitoring of row-unit performance, and/or real-time sensing of key soil properties. Specifications should

be established based on a thorough understanding of soil-planter interactions at planting and existing knowledge about crop requirements for germination and growth. Nonetheless, development of such technologies remains challenging as too little information is presently availabe to model site-specific soil-planter interactions, and a summary of existing literature is presented below.

2.3.1 Soil-Planter Interactions

Seeding depth response to row-unit depth and downforce adjustments and soil conditions at planting is determined by how individual planter row-units interact with their environment. The following forces are typically in play at planting (Figure 2.16):

- $\vec{W}$, $\vec{F_{\mathbf{S}}}$: Frame weight, hopper and seed weight. Respectively applied at the center of gravity of the row-unit frame, and at the center of gravity of the filled hopper.
- $\vec{F_{\mathbf{DF}}}$, θ: Additional weight applied by the downforce system onto planter row-unit, four-link angle. $\vec{F_{\mathrm{DF}}}$ = *f(Downforce Adjustment, θ)*,
- $\vec{F_{\mathbf{PW}y}}$: Press-wheel load. Applied at the center of gravity of the press-wheel assembly. Depends on press-wheel position in comparison to the rest of the row-unit, seeding depth, total row-unit weight, ...
- $\vec{F_{\mathbf{R1}}}$, $\vec{F_{\mathbf{R2}}}$, $\vec{F_{\mathbf{R3}}}$, $\vec{F_{\mathbf{R4}}}$, $\vec{F_{\mathbf{R5}}}$: Vertical soil resistance - applied onto the coulter, soil furrow opener, gauge-wheels, closing wheels, and trashwheels, respectively.
- $\vec{F_{\mathrm{T}}}$: Horizontal traction - resultant force. Exerted by the tractor.
- $\vec{F_{\mathrm{R}x}}$: Horizontal soil resistance - resultant force.
- $\vec{F_{\mathrm{D}}}$: Horizontal draft force - resultant force.

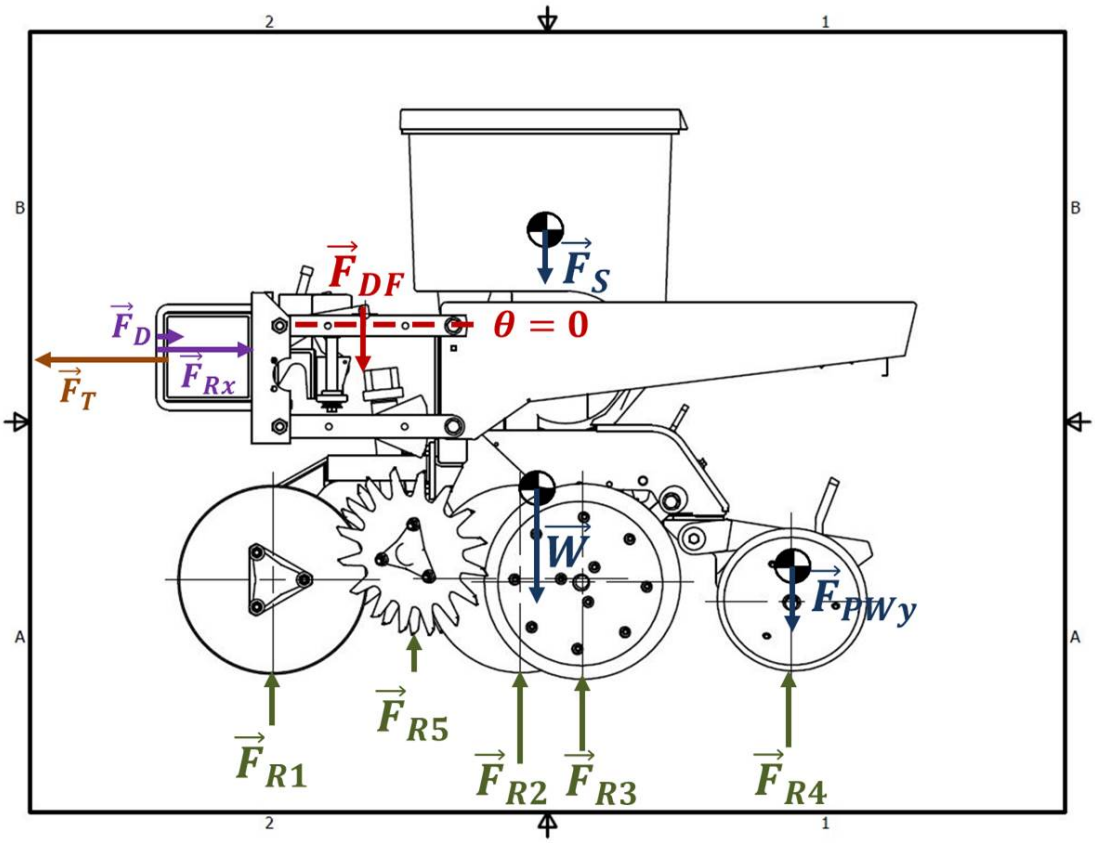

Figure 2.16: Force diagram providing an inventory of the different forces acting on individual planter row-unit at planting. Example of a John Deere MaxEmerge Plus row-unit.

Seeding depth is established based on 1) the resultant between vertical forces applied onto the soil and vertical forces required for furrow opening and covering, and 2) row-unit geometry which varies with row-unit depth adjustment (Morrison, 1988; Hanna et al., 2010). Excess vertical forces applied onto the soil but not required for furrow opening and covering are supported by the planter gauge-wheel loads or more generally by the depth control mechanism. Assuming a state of equilibrium, equations 2.1 to 2.3 are verified. As soil conditions vary within fields, the state of equilibrium is shifted and the planter fails to perform at uniform seeding depth.

$\sum \vec{F}_{\mathrm{y}} = \vec{0}$, and:

$$\vec{W} + \vec{F_S} + \vec{F_{DF}} = \vec{F_{R1}} + \vec{F_{R2}} + \vec{F_{R3}} + \vec{F_{R5}} \tag{2.1}$$

$$\vec{F_{PWy}} = \vec{F_{R4}} \tag{2.2}$$

$\sum \vec{F}_{\mathrm{x}} = \vec{0}$, and:

$$\vec{F_T} = \vec{F_{Rx}} + \vec{F_D} \tag{2.3}$$

2.3.2 Soils, Seeding Depth, and Crop Requirements

Seed germination requires sufficient water and temperature to rupture the seed coat and trigger the development of the seed embryonic tissues (Hunter and Erickson, 1952; Martin and Thraikill, 1993). Optimum seeding depth provides individual seeds with adequate soil conditions to ensure immediate and uniform germination throughout the field (Morrison Jr and Gerik, 198). Water is absorbed from the soil in direct contact with the seed, and corn and cotton seeds require a minimum soil matric potential of – 33 kPa (field capacity) to germinate. Higher soil matric potentials result in quicker imbibition rate and therefore quicker germination. Corn seeds typically imbibe 30% of their weight in water within 24 to 48 hours after planting. Soil temperatures ranging from 20°C to 30°C, and from 28°C to 34°C are required for optimum corn and cotton germination, respectively (Schneider and Gupta, 1985; Holekamp et al., 1966). Seed germination also requires adequate soil aeration to allow seed respiration and circulation of gases within the soil. Available water to the seed, soil temperature, and aeration are typically affected by several parameters including climate conditions, soil texture, soil water content, soil friability, and soil compaction within the seedbed. Available soil water and soil temperature patterns also vary within the soil profile,

and deeper seeding depths often exhibit more homogeneous soil water content throughout the field as well as reduced temporal fluctuations in soil temperature (Knappenberger and Köller, 2011). Beyond germination, corn development requires the establishment of a strong nodal root system that will provide structural support to the plant and incease crop resistance to drought stress. Therefore, corn is very sensitive to shallow seeding depths and corn seeds should never be planted shallower than 3.1 to 3.8 cm. On the other hand, cotton is very sensitive to deep seeding depths which provide excessive soil resistance to seedling emergence, and cotton should never be planted deeper than 2.5 cm. Research demonstrated that seeding depth should be maintained within a variation of +/- 0.3 cm to ensure optimum crop establishment (Bowen, 1966).

2.3.3 Measuring Spatial Variability for Precision Planting Applications

Implementation of active depth by downforce planting technologies requires proper characterization of field spatial variability, which can be accomplished using several different methods. First, field spatial variability can be evaluated using soil data from the field. Data would be sampled based on a pre-determined strategy and used to generate prescription maps for seeding depth. Soil samples typically provide information concerning soil physical properties, including texture, soil chemistry, and soil fertility across the field. Soil data from the field could also be combined with other information, such as cropping and yield history for better management zone delimitation. Field spatial variability could then be measured by sensing different soil properties such as soil water content or soil electrical-conductivity (EC). Several studies have been conducted to investigate the possibility of using real-time soil water content to drive seeding depth at planting (Weatherly and Bowers, 1997), and results were divided as soil water content exhibits strong local spatial variability. Soil EC measures soil salinity, and soil EC measurements correlate to several soil properties including soil texture, soil water content, soil temperature, and soil chemical properties (White et al., 2012). Soil EC is already widely used in precision agriculture to provide high resolution

description of spatial variability within fields, and soil EC could represent a key soil property to dictate seeding depth at planting. Eventually, field spatial variability could also be measured using remote sensing and aerial imagery.

2.4 Summary

With increasing seed costs and demand for more efficient management strategies, individual seeds have become more valuable and should be placed in the soil to maximize yield potential. Several advanced planting technologies have been developed to optimize row-crop planter performance. Planting performance is typically defined as the ability of the planter to achieve targeted seeding rate, uniform seed spacing, and uniform seeding depth throughout the field. Current planters are able to achieve proper seeding rate and spacing under recommended planting speeds and proper equipment maintenance. However, most row-crop planters fail to achieve uniform seeding depth as standard depth control systems do not adjust row-unit depth and downforce settings to field spatial variability. Non-uniform seeding depth within fields often results in suboptimal emergence rates and non-uniform emergence, which significantly impacts crop growth and yields. Therefore, optimum planter performance requires developing precision technologies for in-field adjustments of row-unit depth and downforce planter settings to provide producers with the capability of managing field spatial variability at planting. Such technologies would operate based on the use of prescription maps for seeding depth, real-time monitoring of row-unit performance, and/or real-time sensing of key soil properties. However, development of such technologies remains challenging with little knowledge available to model soil-planter interactions. Research is needed to better understand crop and planter response to row-unit depth and downforce adjustments and field spatial variability to further improve current planting technologies.

Chapter 3

Material and Methods

3.1 Row-Crop Planter

A standard 91-cm (36-in) row-spacing, 6-row John Deere planter with MaxEmerge Plus row-units (John Deere, Moline, IL USA) retrofitted with Precision Planting (Tremont, IL USA) eSet meter adds-ons was used in this research (Figure 3.1). Individual row-units were equipped with a Dawn ripple coulter assembly containing two 36-cm (14-in) trashwheels to clean soil residues, a double disc opener, two gauge-wheels, a seed firmer behind the opening discs to limit seed bounce within the soil furrow, and two rubber closing wheels for furrow closing.

Figure 3.1: Image of the 6-row John Deere planter equipped with MaxEmerge Plus Row-Units used in this research.

Row-unit depth and downforce settings were adjusted manually on the planter. Row-unit depth was selected by changing the position of a T-handle on each row-unit (see section 2.1.2), with 17 possible settings (Figure 3.2). Row-unit depth was doubled-checked in the lab for individual planter row-unit and depth setting using the following procedure (Figure 3.3). The planter was raised, and row-unit depth was adjusted by changing the depth T-handle position. Manually graduated (1.3-cm graduation interval) 5.1-cm x 15.2-cm pine structural beams were then placed below the planter gauge-wheels, and planter height was lowered until total row-unit weight was carried by the gauge-wheels (other row-unit components were not in contact with the soil or the beams). Seeding depth corresponding to the selected T-handle setting was then measured as the vertical distance between the bottom of the opening discs and the bottom of the gauge-wheels in contact with the beams. Calibrated depths were identical for individual row-units (Table 3.1). Row-unit downforce was controlled by standard, mechanical heavy duty springs (Figure 3.4), with 4 possible settings: none, low, medium, and heavy. Individual downforce settings provided an addition of (applied downforce) 0 kN, 0.57 kN, 1.13 kN, and 1.81 kN onto individual row-units based on manufacturer's specifications (John Deere, 2004).

Table 3.1: Row-unit depth calibration for 6-row planter used in this study.

T-Handle Setting		Seeding Depth [cm]	T-Handle Setting		Seeding Depth [cm]
1	-	-	5	5-5	5.7
1	1-1	0.6	6	6-5	6.4
2	2-1	1.3	6	6-6	7.0
2	2-2	1.9	7	7-6	7.6
3	3-2	2.5	7	7-7	8.3
3	3-3	3.2	8	8-7	8.9
4	4-3	3.8	8	8-8	9.5
4	4-4	4.4	9	9-8	10.2
5	5-4	5.1	9	9-9	10.8

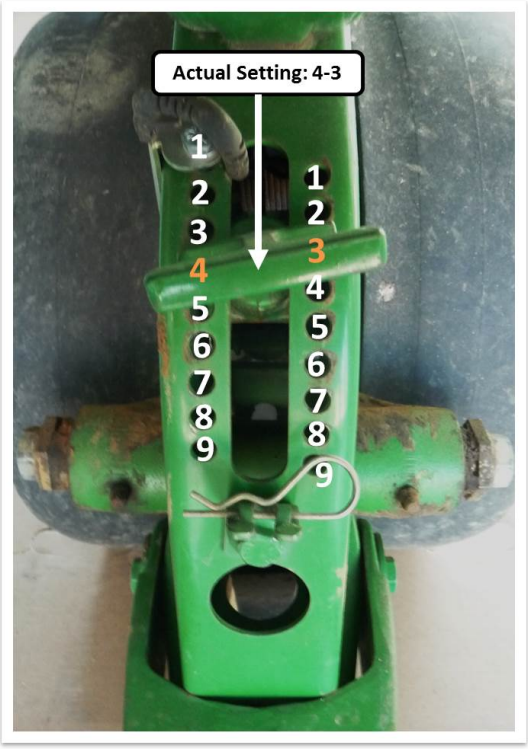

Figure 3.2: Row-unit depth adjustment on the MaxEmerge Plus row-unit.

Figure 3.3: Illustration of the procedure used to check the depth setting increments for individual planter row-units.

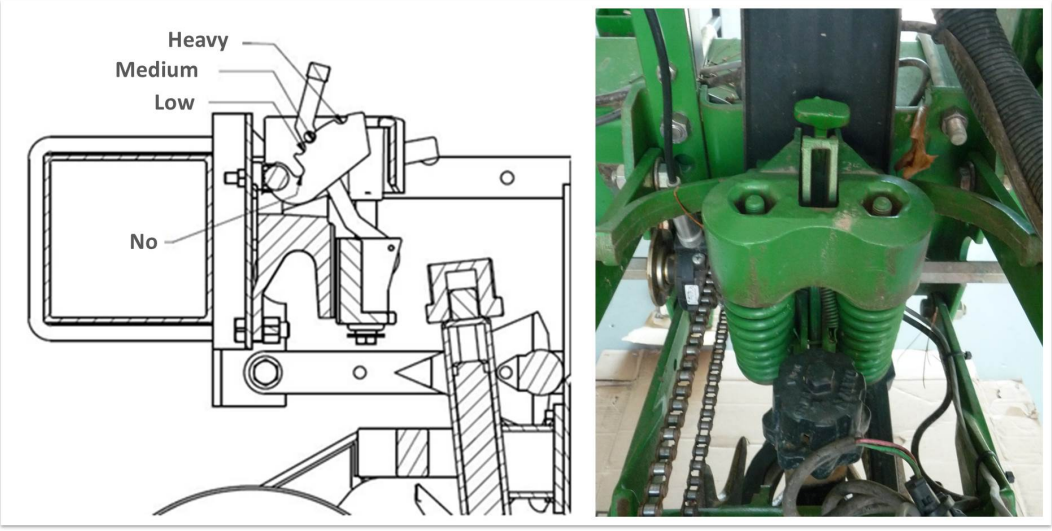

Figure 3.4: Standard row-unit downforce system on the MaxEmerge Plus row-unit.

3.2 Experimental Design

The study was conducted at the E.V. Smith Research Center (Shorter, AL USA; 32.441762 N, 85.897455 W) on non-irrigated maize (*Zea mays L*) and cotton (*Gossypium hirsutum L*). Three row-unit depths were selected for each crop to represent common planting practices in central Alabama (and more generally in the Southeast US Coastal Plains). Corn is typically planted between 4.4 and 6.3 cm (1.75 and 2.5 in), and 2.5 cm, 5.1 cm, and 7.6 cm (1, 2 and 3 in) were selected as targeted seeding depths for corn. On the other hand, cotton is usually planted between 1.2 and 1.9 cm (0.5 and 0.75 in), and 0.6 cm, 1.3 cm, and 2.5 cm (0.25, 0.5 and 1 in) were selected as targeted seeding depths for cotton. Targeted depths were associated to their corresponding T-handle setting. Row-unit depth was re-adjusted in the field at the beginning of the study to account for soil compaction below the gauge-wheels. The same row-unit depths were used throughout the study (Table 3.2). None [+0.0 kN], medium [+1.1 kN] and heavy [+1.8 kN] row-unit downforce were selected for both corn and cotton. Two fields (defined as A and B) exhibiting typical Coastal Plain soil features but characterized by different soil conditions and terrain attributes were also selected for this study.

Table 3.2: Targeted seeding depths for corn and cotton and associated T-handle settings.

Crop	Seeding Depth [cm]	T-handle Setting
Cotton	0.6	2-2
	1.3	3-3
	2.5	4-4
Corn	2.5	4-4
	5.1	6-6
	7.6	8-8

Fields A and B were split in half, with each half planted to one of the two crops (Figure 3.5). The experiment was arranged as a split-plot design. Half fields constituted the whole plot, while row-unit depth and downforce combinations represented the subplot. Treatment arrangement within each half field was based on a randomized complete block design, with 4 blocks in field A, and 3 blocks in field B. Therefore, by design and due to smaller available width in field B, treatment combinations were replicated 4 times in field A, and 3 times in field B. The trial was conducted in strips, with one planter pass corresponding to one treatment combination (plot). Individual plot dimensions were 5.5 m width (planter width), and 110 m or 180 m length in field A and B, respectively. The experiment was replicated during 2014 and 2015, with crops rotated within individuals fields each year.

3.3 Site Overview and Management

Corn and cotton were planted at 65,480 seeds ha^{-1} (26,500 seeds ac^{-1}) and 128,495 seeds ha^{-1} (52,000 seeds ac^{-1}), respectively. Fields were strip-tilled at 30 cm depth (12 in) prior to planting, using a 6-row Remlinger Precision Strip Till unit (Remlinger Mfg, Kalida, OH USA). Both fields were stripped-tilled for the first time during 2014 growing season, following corn. In 2015, corn and cotton trials were planted directly after 2014 cotton and corn trials, respectively. Soil surface residue coverage after planting was 30% to 50%. Corn trials were planted on April 13, 2014 and April 9, 2015. Cotton trials were planted on May 5, 2014 and May 5, 2015. Planting operation was performed at 8 $km.h^{-1}$ (5 mph). Corn trials

were harvested on September 8, 2014 and August 31, 2015. Cotton trials were harvested on Septamber 30, 2014 and October 30, 2015.

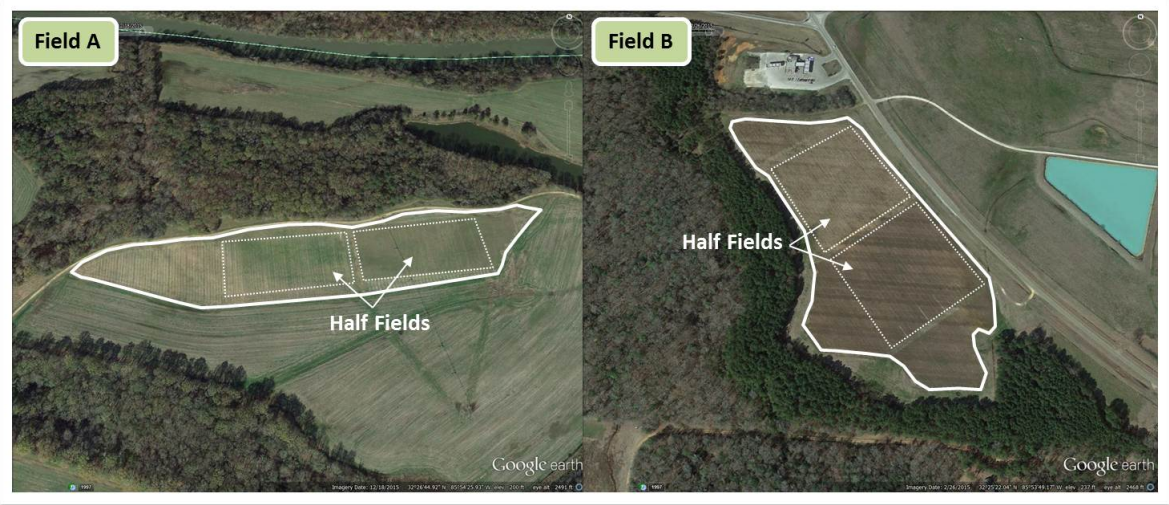

Figure 3.5: Aerial image of the two fields selected for this study and division into field trials. *Google Earth Image. Imagery Date: 12/18/2015 (Field A) and 2/26/2015 (Field B)*

3.4 Data Collection

3.4.1 Row-Unit Monitoring

A data acquisition system was built for this research and mounted on the planter to monitor real-time planting performance (Figure 3.6). The system was run using LabVIEW© software (National Instrument Corporation, Austin, TX USA) and consisted of a National Instrument© USB-6225 data acquisition module, two Analog Devices, Inc© 5B38 load cell signal conditioners, one 12 VDC voltage regulator, and one 5 VDC voltage regulator. All components were assembled inside a waterproof enclosure with power and I/O signals passed using bulkhead Deutsch DT and DTM series connectors. The system also included two load pins (Model No. 3810, Vishay Precision Group, India) measuring real-time gauge-wheel

loading on rows 2 and 5, and a shaft encoder (Model No. TRD-GK3600-RZD, AutomationDirect.com, GA USA) measuring main shaft rotation speed (RS) for seeding rate determination. The system was also connected to a GPS receiver installed on the planter and to a Precision Ag. controller to obtain real-time GPS positioning data (associated with RTK correction) and tractor ground speed. Manufacturer specifications for the load pins ensured accuracy for measurements up to 5.3 kN. Lab calibration was performed to convert load cell output voltages into measured load. Calibration curves were developed for individual row-unit depths; accounting for geometry variations between the load cell and gauge-wheel arm as T-handle settings changed. Data were collected during planting along individual plots at sampling frequencies of 10 Hz for GPS positioning and ground speed data, and 20 Hz for measured gauge-wheel load and main shaft rotation speed. Measured gauge-wheel load was characterized as the average load measured by the two load cells. Real-time seeding rate (SR) was computed using equation 3.1.

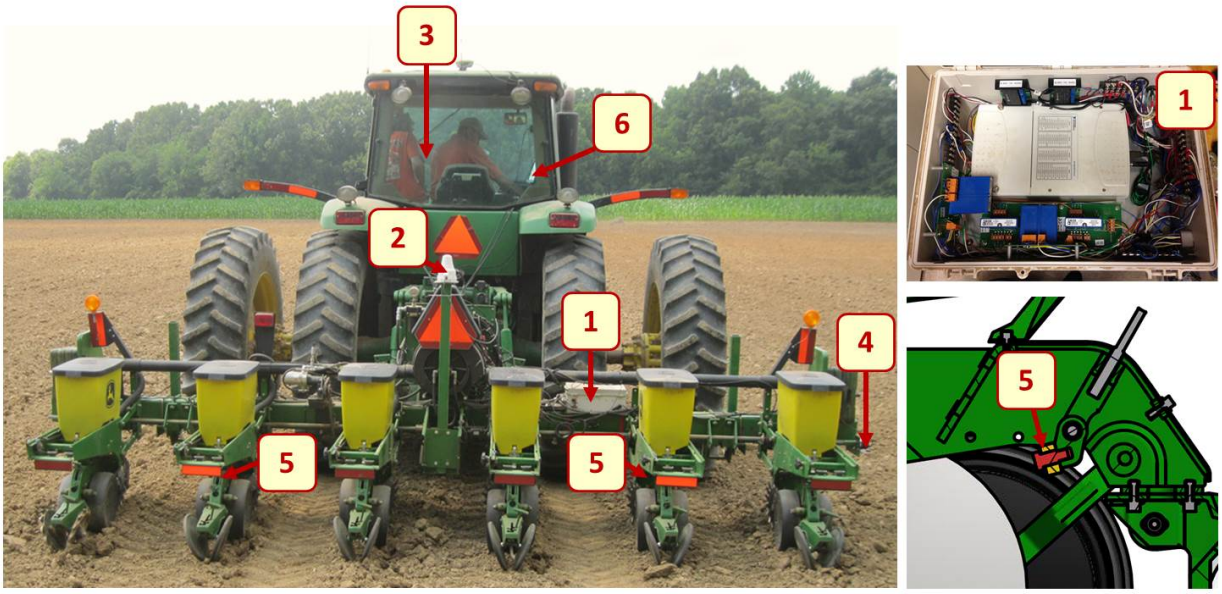

Figure 3.6: Data acquisition system mounted on the planter to monitor row-crop planter performance at planting. **1:** Data Acquisition System, **2:** GPS Receiver, **3:** LabVIEW™ Program running on a tablet, **4:** Shaft Encoder, **5:** Load Pins, and **6:** Precision Ag. Controller Trimble Field-IQ.

$$SR = \frac{RS \times SC \times 43,560 \times 1.609 \times 60 \times 2.47}{RW \times GS \times 5280} = \frac{RS \times SC \times 1967}{RW \times GS} \tag{3.1}$$

With: **SR:** seeding rate [seeds.ha^{-1}], **RS:** main shaft rotation speed [rpm], **SC:** number of seeds cells on the vertical seed plate, **RW:** row-unit width [0.9 m = 3 ft], and **GS:** ground speed [km.h^{-1}].

3.4.2 Overall Soil Conditions

The USDA Web Soil Survey in association with field observations and information provided in literature were used to evaluate and compare overall field characteristics, including terrain, soil morphology, and water movement through the soil (Figures 3.7 and 3.8, Table 3.3). Daily soil temperature, atmosphere temperature, and precipitation data were obtained for each growing season from the Alabama Mesonet Weather Database (AWIS Weather Services, Figures 3.9 through 3.14, Tables 3.4 and 3.5). Average soil temperature was computed as the average between maximum and minimum soil temperatures. Similarly, average atmospheric temperature was computed as the average between maximum and minimum atmospheric temperatures. Corn and cotton growing degree days [^oC] were computed using equation 3.2 (Sutherland, 2012). All temperatures are expressed in degree Celsius [^oC]. Maximum daily air temperature was capped at the crop upper temperature threshold: 30 ^oC for corn, 37.8 ^oC for cotton. Base temperature was 10 ^oC for corn, and 15.6 ^oC for cotton. Negative degree-day values were set to zero.

Surface soils in field A were clayier than surface soils in field B, and soils in field A were characterized by higher water holding capacity and slower drainage than soils in field B. The 2015 growing season was characterized by overall cooler soil temperatures than the 2014 growing season, except during corn planting and emergence. The 2015 growing season was also characterized by overall warmer atmospheric temperatures than the 2014 growing season, resulting in a quicker accumulation of corn and cotton growing days in 2015 versus 2014. Furthermore, the 2015 growing season was characterized by more rainfall than the

2014 growing season, with higher total cumulative precipitations. Rainfall was also better distributed in 2015 versus 2014, with a higher number of precipitation events and reduced average precipitations during an event.

$$\text{Degree-Days} = \sum_{Planting}^{Harvest} \frac{\text{Max. Daily Air Temp} + \text{Min. Daily Air Temp}}{2} - \text{Base Temp} \quad (3.2)$$

Table 3.3: Comparison of overall soil characteristics in field A and B

	Field A	**Field B**
Soil Classification	Fine-loamy, mixed, semiactive, thermic Aquic Hapludults	Fine, mixed, semiactive, thermic Typic Hapludults
Soil Series	Altavista Silt Loam or similar	Luverne Sandy Loam or similar
Hillslope Component	Intermediate Fluvial Terrace	Upland
Slope	0% to 2%	1% to 5%
Drainage	Slower	Faster
Water Table	Shallower	Deeper

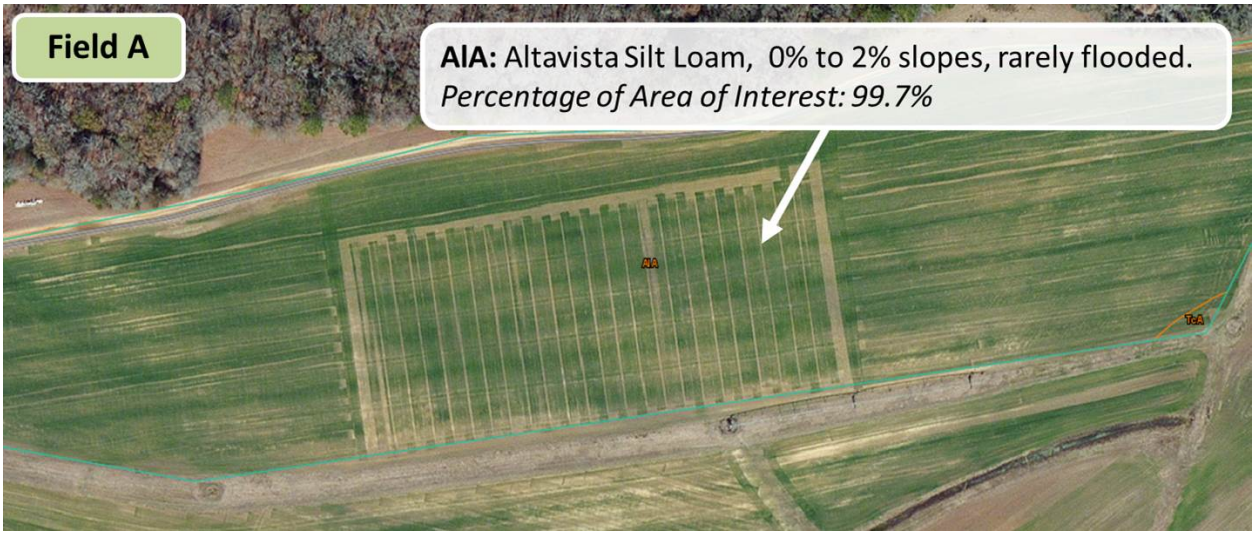

Figure 3.7: Soil survey map provided by the USDA Web Soil Survey for field A.

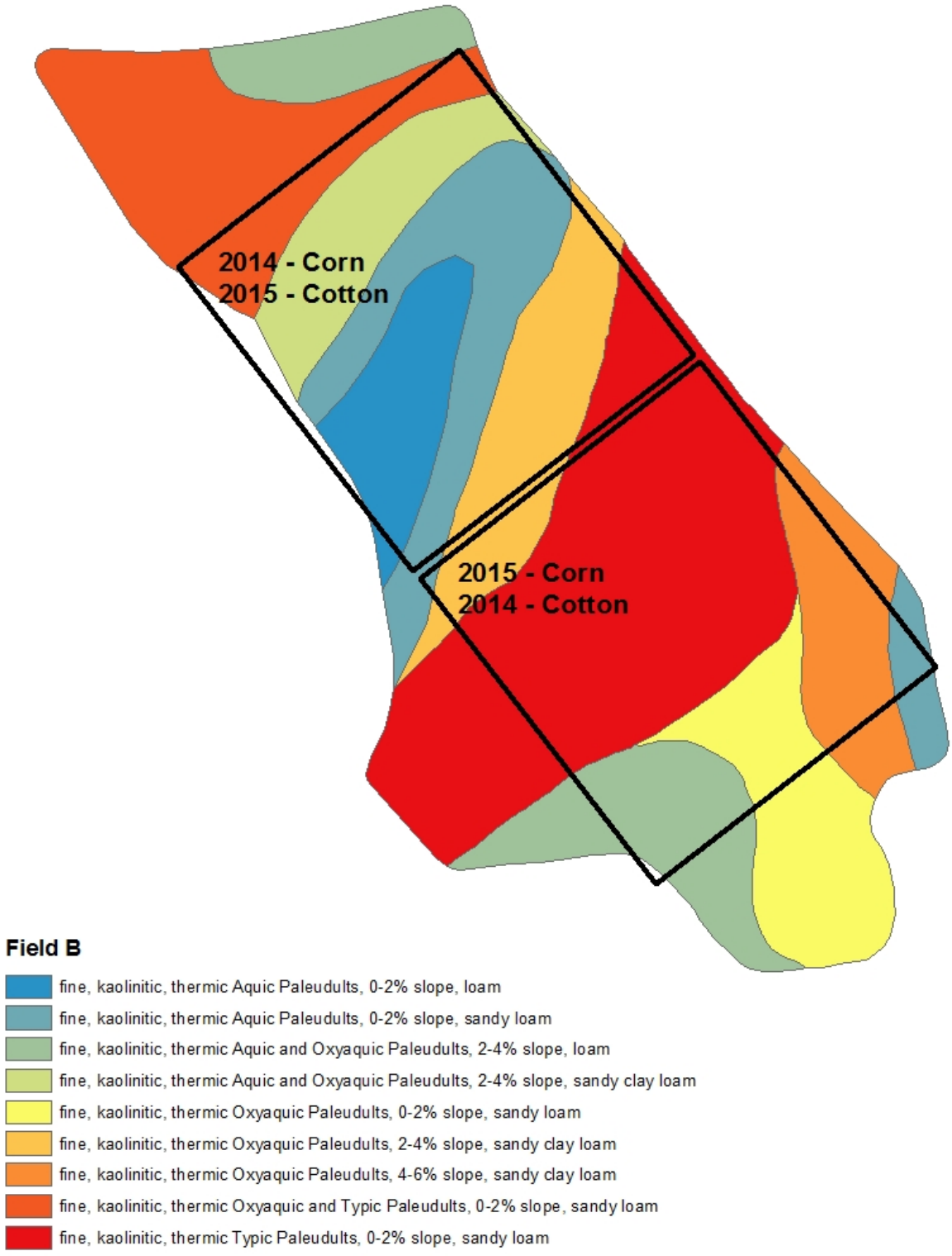

Figure 3.8: NRCS order 1 soil survey for field B (Terra et al., 2004).

Table 3.4: Comparison of precipitation intensity during the 2014 and 2015 corn growing season.

	2014	2015
Length of Growing Season [days]	149	145
Number of Precipiration Events [days]	44	59
Average Precipitations during an Event [mm]	12.4 [se = 0.3]	10.2 [se = 0.2]
Total Precipitations during the Growing Season [mm]	545.1	601.5

Table 3.5: Comparison of precipitation intensity during the 2014 and 2015 cotton growing season.

	2014	2015
Length of Growing Season [days]	149	179
Number of Precipiration Events [days]	40	64
Average Precipitations during an Event [mm]	10.9 [se = 0.3]	8.6 [se = 0.2]
Total Precipitations during the Growing Season [mm]	434.9	551.7

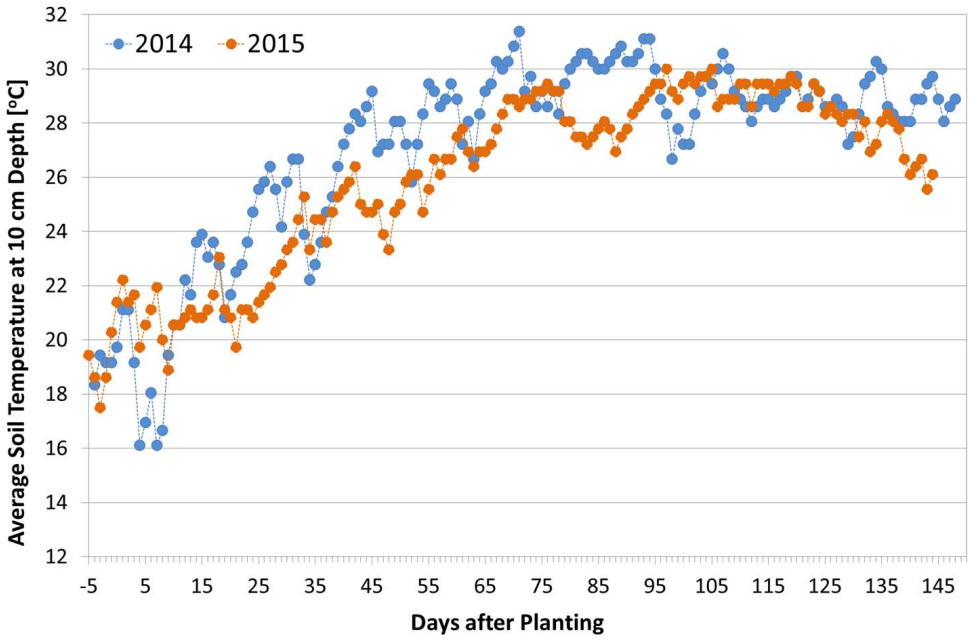

Figure 3.9: Average daily soil temperatures recorded at the E.V. Smith Research Center during the 2014 and 2015 corn growing season.

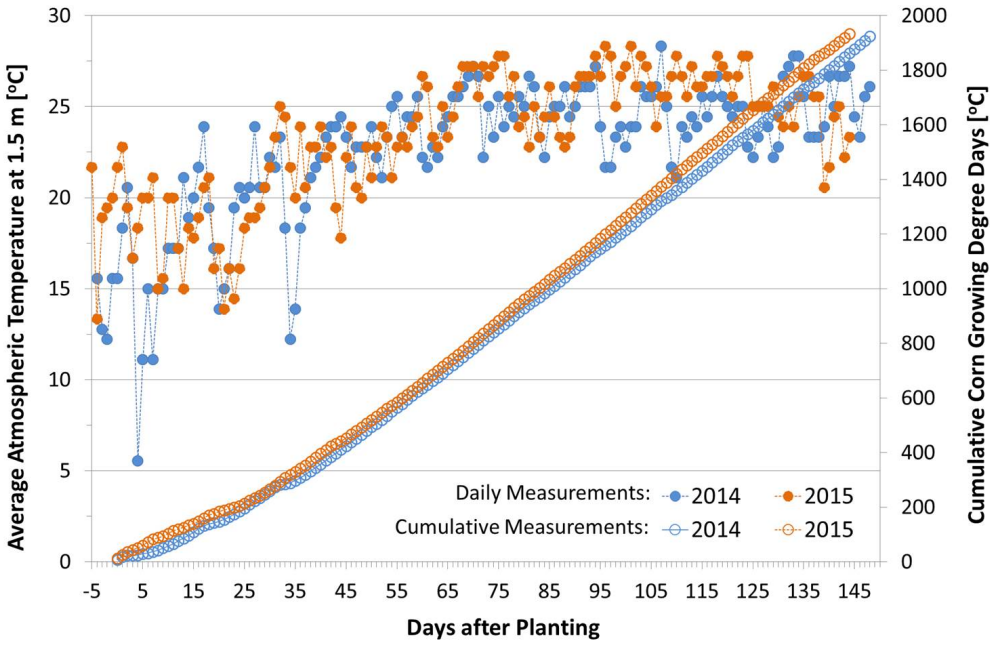

Figure 3.10: Average daily atmoshperic temperatures recorded at the E.V. Smith Research Center during the 2014 and 2015 corn growing season and computed cumulative corn growing degree days.

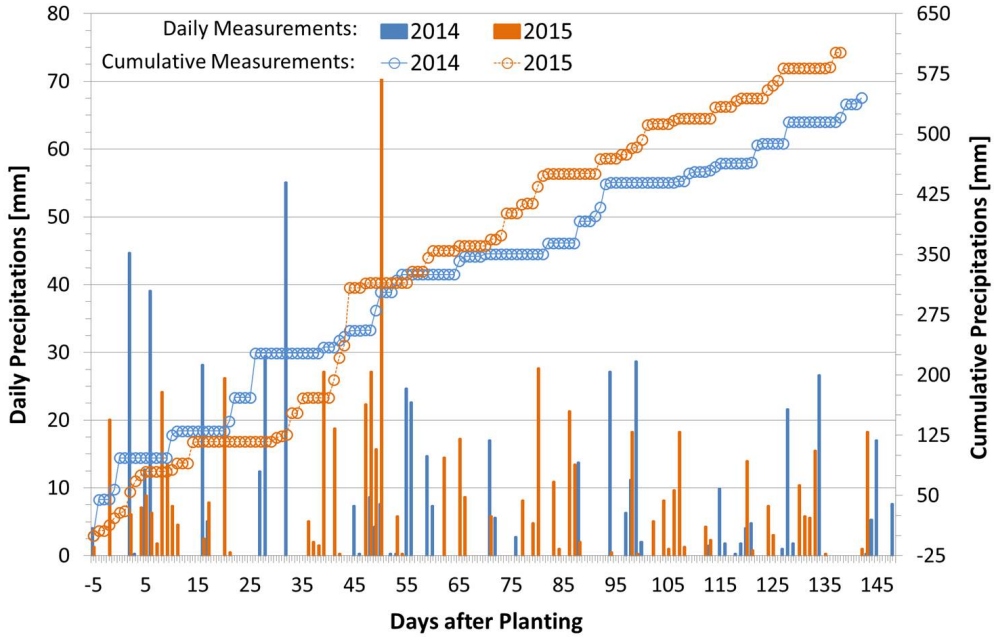

Figure 3.11: Average daily precipitations recorded at the E.V. Smith Research Center during the 2014 and 2015 corn growing season and cumulative distribution of precipitations.

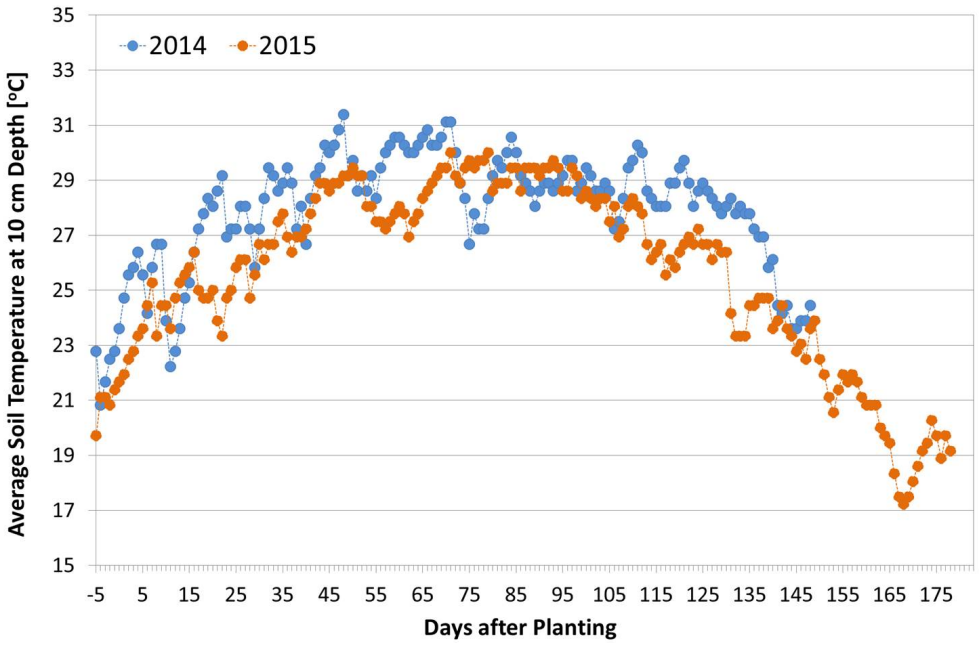

Figure 3.12: Average daily soil temperatures recorded at the E.V. Smith Research Center during the 2014 and 2015 cotton growing season.

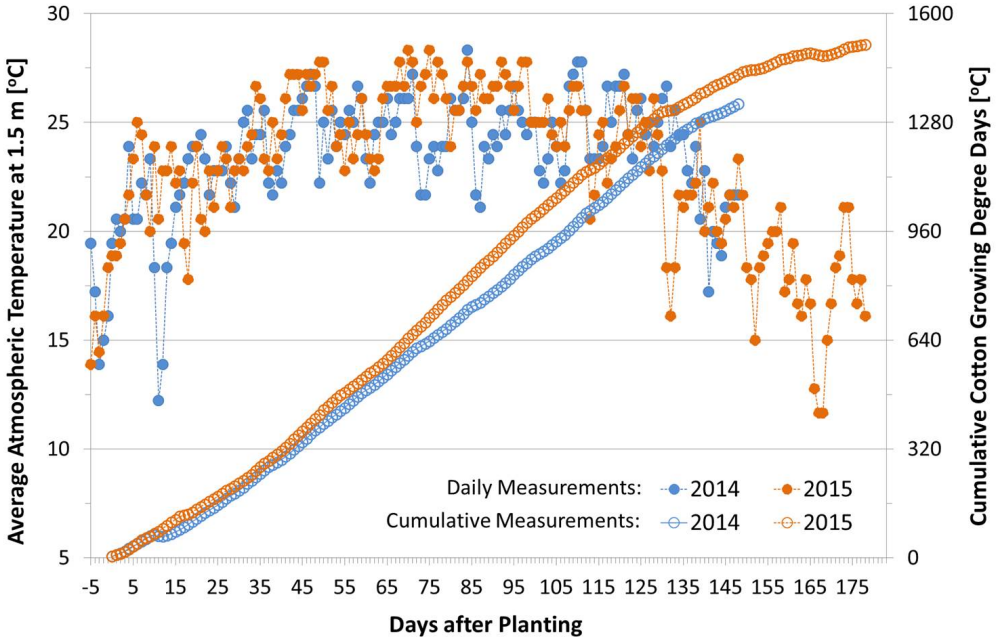

Figure 3.13: Average daily atmoshperic temperatures recorded at the E.V. Smith Research Center during the 2014 and 2015 cotton growing season and computed cumulative corn growing degree days.

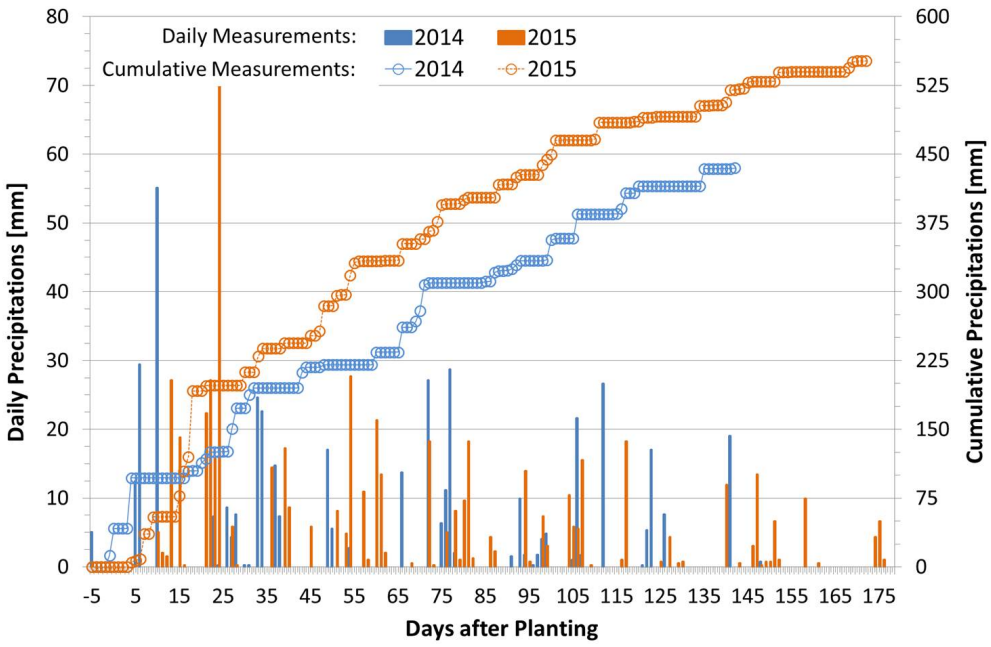

Figure 3.14: Average daily precipitations recorded at the E.V. Smith Research Center during the 2014 and 2015 cotton growing season and cumulative distribution of precipitations.

3.4.3 Field Spatial Variability

Field spatial variability was evaluated using volumetric soil water content and apparent soil electrical conductivity (EC) data. Soil water content was measured at planting. Soil EC was measured earlier in the spring at higher average water content to ensure proper contact between the soil and coulter electrodes. Volumetric soil water content data were collected at 3.8 cm (1.5 in) depth using a soil water content probe (Spectrum Technologies, FieldScout TDR 300 Soil Moisture Meter, Aurora, IL USA), and based on the following sampling strategy. Data were collected in a grid (systematic sampling) at the intersection between individual plots, and 5 or 8 equidistant transects across fields A and B, respectively. Data were also collected at additional sampling sites placed at random between the first and last transects delimited for grid sampling. Ultimately, data were collected at 6 or 9 sampling sites within each plot for field A and B, respectively. Soil water content data were summarized by field, growing season, and crop (Table 3.6).

Table 3.6: Summarized soil water content data by crop, growing season, and field

Crop	Season	Field	Volumetric Soil Water Content	
			Average [vol vol^{-1}]	Standard Error [vol vol^{-1}]
Corn	2014	A	29.2	0.36
		B	21.2	0.27
	2015	A	27.6	0.37
		B	24.3	0.24
Cotton	2014	A	26.6	0.31
		B	14.7	0.31
	2015	A	16.7	0.22
		B	16.8	0.28

Apparent soil EC was measured for the top 30 cm of the soil profile using a Veris 3100 (Veris technologies, Inc., Salina, KS USA). Data were collected at 1 Hz sampling frequency and at 7 to 15 km.h^{-1} ground speed. Measured soil EC data were then interpolated using Kriging methodology, and results served to extrapolate EC values at individual sampling sites used to measure soil water content. Interpolations were computed using R software (R Core Team, 2016), and the "automap" package (Hiemstra et al., 2008) which provided an automatic routine to optimize semi-variogram fitting. Five percent of the original data sets were selected at random and set aside for model validation, while computations were performed on the remaining 95% of the data. Interpolated data were then used to estimate soil EC at the points previously selected for model validation, and residuals root-mean-squared-error (RMSE) was computed using equation 3.3. Accuracy of the interpolation models was assessed based on computed RMSE values and RMSE / average soil EC ratio. Summarized soil EC data by field and growing season and interpolated maps are presented in Table 3.7 and in Figures 3.15 to 3.16.

$$RMSE = \sqrt{MSE} = \sqrt{\frac{1}{n}\sum_{i=1}^{n}(\hat{Y}_i - Y_i)^2} \tag{3.3}$$

Table 3.7: Summarized soil electrical conductivity data at 0 to 30 cm depth and evaluation of interpolation models accuracy for individual fields and growing seasons.

	Growing Season x Field			
	2014-A	**2014-B**	**2015-A**	**2015-B**
Average Soil EC [mS.m^{-1}]	21.2	6.7	18.4	6.4
Soil EC Std. Deviation [mS.m^{-1}]	3.7	1.3	3.6	1.0
Variogram Model	Matern	Matern	Matern *Stein's P.*	Matern *Stein's P.*
Residuals RMSE [mS.m^{-1}]	1.5	1.1	1.3	1.5
Residuals RMSE / Average [%]	7.1	16.4	7.1	23.4

Higher in-field spatial variability was observed in field A than in field B due to the relative abundance of clay in field A and poorer drainage. Interpolated soil EC data provided an accurate estimation of soil EC with small RMSE and RMSE to average soil EC ratios. Increased RMSE to average soil EC ratios in field B was explained by smaller soil EC values measured in this field. Terra et al. (2006) and Terra et al. (2004) demonstrated that soil EC in Coastal Plain soils was mainly related to soil properties resulting from historical erosion. Their results demonstrated that in the particular case of field B, soil EC was correlated to slope and clay content, with correlation coefficients equal to 0.66 and 0.43, respectively. Higher soil EC was observed in more eroded areas characterized with higher clay content.

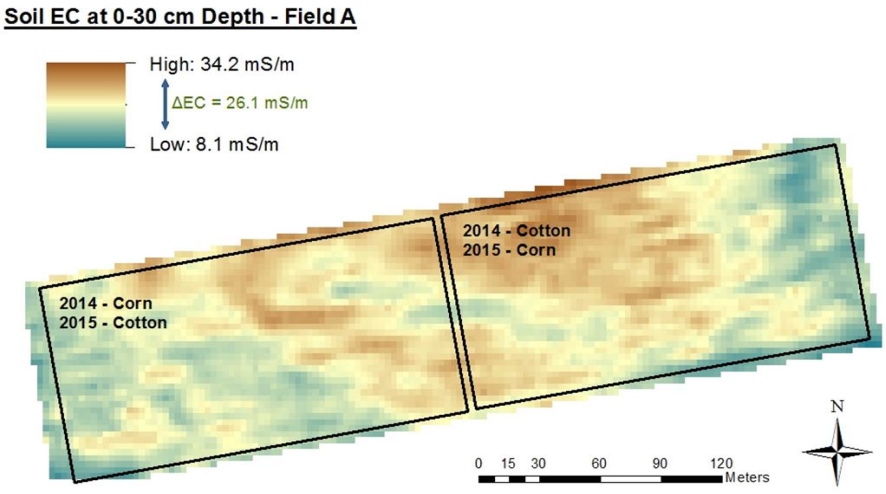

Figure 3.15: Spatial variability in soil EC measured within field A.

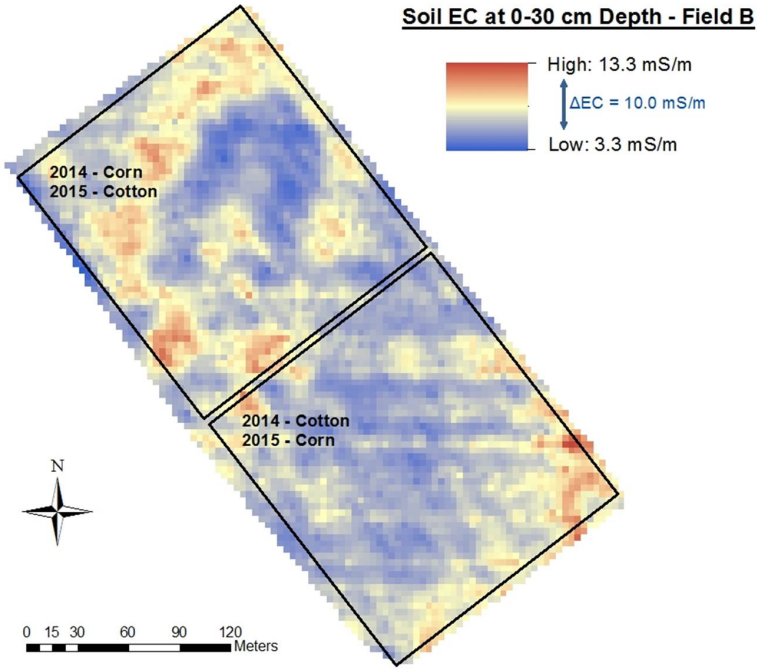

Figure 3.16: Spatial variability in soil EC measured within field B.

3.4.4 Measured Seeding Depth

Corn seeding depth was measured by excavating an emerged plant and measuring the distance between the soil surface and visible seed (Figure 3.17). Corn seeding depth was measured at each sampling site previously defined to collect soil water content data (see section 3.5.3), and measured seeding depth at any given site was computed as the average between 4 measurements collected on each one of the 4 middle rows of the planter. Cotton seeding depth was measured by extracting two weeks old emerged seedlings and measuring the distance between the soil surface and the seed source – characterized by the point where the hypocotyl and radicle meets (Figure 3.17). Cotton seeding depth was measured at every other sampling site previously defined to collect soil water content data, and measured seeding depth for cotton was computed as the average between 2×4 measurements collected

across the four middle rows of the planter. Standard deviation between the 4 and 8 measurements characterizing corn and cotton seeding depth was used to evaluate seeding depth precision.

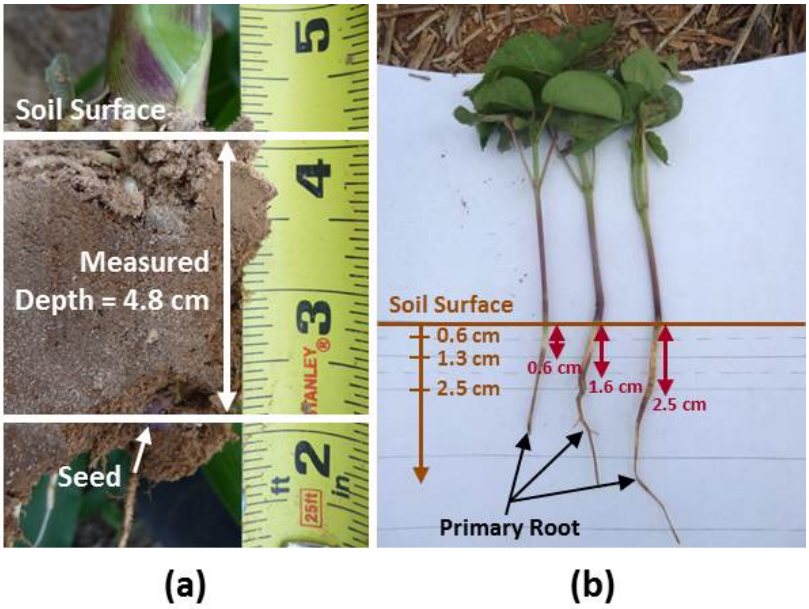

Figure 3.17: Protocol for measuring (a) corn and (b) cotton seeding depth.

3.4.5 Daily Emergence (Corn Only)

Emergence data were collected to describe the uniformity of corn emergence. Seedlings were classified based on the following categories: "spike", "through surface", "first leaf opened", "second leaf visible", and "two leaves opened" (Figure 3.18). Any corn plant was considered emerged if taller than 0.3 cm. Seedlings were counted on a daily basis from the beginning of emergence to when all seedlings reached the "two leaves opened" stage. Population counts were carried out on three of the four middle rows of the planter over a 1.5 m distance.

Figure 3.18: Classification of corn seedling emergence.

3.4.6 Final Yields (Corn Only)

Corn final yield was measured at harvest using a yield monitor installed on the combine. Field trials were squared off prior to harvest to ensure equal plot length. Individual plots were harvested separately, and harvested grain was weighted using a weight wagon (Figure 3.19) to calibrate the yield monitor data. Grain samples were also collected for each plot to determine their moisture content. Final yield data were adjusted at 15.5% moisture content.

Figure 3.19: Weight wagon used to calibrate yield monitor data at every plot, and collection of grain sample to adjust final yields at 15.5% moisture content.

3.5 Data Analysis

3.5.1 Chapter 4

Measured seeding depth, seeding depth standard deviation, and gauge-wheel load data were averaged out by plot to ensure independence between observations. Analyses of variance (ANOVA) using mixed-effect models were computed to characterize treatment effects on field-scale planter performance. Estimated means were computed using the Restricted Maximum Likelihood (REML) method, and then used to characterize treatment effects. 95% confidence intervals for estimated means were computed using Fisher's least significant difference method, with results used to evaluate the significance of differences between individual treatment levels and combinations (Piepho et al., 2003). Mixed-effect analyses of variance were computed using R software and the "lme4" package (Bates et al., 2015). Mixed-effect analyses were then associated with linear analyses of covariance to better characterize interactions effects among treatments.

Field observations indicated that a non-negligible percentage of cotton seeds were not planted in the soil furrow, but rather ended up on the soil surface. Most of these seeds did not germinate due to insufficient moisture, and therefore were not accounted for while measuring cotton seeding depth. The amount of cotton seeds not placed in the soil furrow was quantified at individual sampling sites previously delimited, and the data followed a binomial distribution. Consequently, data were analyzed using a generalized linear mixed-effect model. Analysis was computed using the "blme" (Chung et al., 2013) package in R. Treatment effects were calculated from the logistic outputs of the model using equation 3.4, with $S_{\text{Treatment}}$ corresponding to the estimated treatment effect on the percentage of cotton seeds not being placed within the soil furrow.

$$S_{Treatment} = \frac{e^{logit}}{1 + e^{logit}} \tag{3.4}$$

In-field seeding depth standard deviation was calculated as the standard deviation between all seeding depth measurements collected within a given treatment combination. Coefficients of variation for measured seeding depth were computed for individual treatment combinations as the ratio between in-field seeding depth standard deviation, and seeding depth estimates obtained from mixed-effect analysis of variance. In-field gauge-wheel load standard deviation was calculated as the standard deviation between the average gauge-wheel load measured within individual plots corresponding to a given treatment combination.

3.5.2 Chapter 5

Measured seeding depth data were analyzed at the sampling site resolution using the following procedure. Analyses of covariance were computed to characterize corn and cotton field-scale seeding depth response to row-unit depth and downforce adjustments. Global Moran's I index were computed on model residuals to evaluate spatial relationships between observations. Ordinary Least Square (OLS) and Geographically Weighted (GW) regressions were then computed to evaluate seeding depth relationships to changing soil EC and soil water content within individual field trials exhibiting significant site-specific seeding depth variability. OLS regressions only were computed to evaluate seeding depth relationship to measured gauge-wheel load within individual field trials exhibiting significant site-specific seeding depth variability. Maps illustrating site-specific seeding depth correlation to soil EC were computed using natural neighbor interpolation – original points data at individual sampling sites. Data analysis for chapter 5 was computed using ArcGIS ® software.

3.5.3 Chapter 6

Daily emergence data were summarized to characterize daily changes in live population within each plot – all growing stages confounded. Summarized data were modeled using equation 3.5 which permitted estimation of the following parameters: final live population,

emergence window, emergence rate index, and uniformity index. Final population was estimated by c (equation 3.5) and expressed as a percentage of achieved seeding rate. Beginning of emergence was estimated by d. Full emergence was achieved when emergence rate was lower than 2.5%, and the end of emergence was determined using equation 3.6. Emergence rate index was computed using equation 3.7 (Hanna et al., 2010). Uniformity of emergence was evaluated using standardized Gibbs' Index and based on equation 3.8.

$$E_t = c\left(1 - exp\left(-\frac{t-d}{\tau}\right)\right) \tag{3.5}$$

$$t_{end} = d - \tau \times ln\left(\frac{2.5 \times \tau}{c}\right) \tag{3.6}$$

$$ERI = \sum_{n=d}^{t_{end}} \frac{\%n - \%(n-1)}{n} \tag{3.7}$$

$$UI = 1 - \frac{K}{K-1} \times \left(1 - \sum_{i=1}^{K} p_i^2\right) \tag{3.8}$$

E_t: *daily live population [% of achieved seeding rate],* ***c,*** *τ:* *model parameters,* ***t:*** *number of days after planting,* ***d:*** *beginning of emergence,* ***t_{end}:*** *end of emergence, and* ***%n, %(n-1):*** *percentage of plants emerged on day n and n-1.*

Mixed-effect analyses of variances were then computed to characterize treatment effects on individual emergence metrics and final yields. Estimated means were computed using the REML method, and used to characterize treatment effects. 95% confidence intervals for estimated means were computed using Fisher's least significant difference method, and results were used to evaluate the significance of differences among treatment combinations. Measured gauge-wheel load data were smoothed at 1 Hz sampling frequency to remove high frequency noise. Smoothed data were then rasterized and used to extrapolate gauge-wheel

load values at individual sampling sites used to measure corn and cotton seeding depth (section 3.3.3). Linear regression analyses were then computed to characterize individual emergence metrics and final yield response to measured seeding depth and gauge-wheel load. Relationships among individual emergence metrics and final yields were evaluated through computation of Spearman's correlation coefficients.

3.5.4 Chapter 7

Prescription maps were created based on the maps produced in Chapter 5 to illustrate site-specific seeding depth correlations to in-field changes in soil EC. Prescription maps were generated using ArcGIS ® software. Smoothed gauge-wheel load data – 1 Hz frequency – were standardized by removing mean row-unit depth and downforce effects within individual field trials. Auto-Regressive Integrated Moving Average (ARIMA) models were computed to evaluate spatial dependency among standardized gauge-wheel load data within individual field trials. ARIMA models were computed in R using the "forecast" package (Hyndman and Khandakar, 2008).

Chapter 4

Planting Response to Row-Unit Depth and Downforce Adjustments within Coastal Plain Soils

Chapter 4 investigates corn and cotton field-scale planting response to row-unit depth and downforce adjustments, and varying field conditions in Coastal Plain soils. Results and discussion address objective 1. Measured seeding depth characterized planter ability to achieve targeted depths, hence describing seeding depth accuracy. In-field seeding depth standard deviation and seeding depth coefficient of variation measured seeding depth variability within individual field trials. Seeding depth standard deviation at a given location described seeding depth precision. Measured gauge-wheel load evaluated row-unit response to treatments. Gauge-wheel load standard deviation measured gauge-wheel load variability within individual field trials. This chapter is presented within six sections outlining univariate field-scale planting response to treatment combinations and including discussion of the results. Complementary results to Chapter 4 are presented in appendix B.1.

4.1 Measured Seeding Depth

Corn and cotton measured seeding depth data by row-unit depth, row-unit downforce, and field trial are presented in Figures 4.1 and 4.2. Measured seeding depth data were analyzed using mixed-effect analyses of variance, with results summarized in Tables 4.1 and 4.2. Corn seeding depth was significantly affected by growing season, field, row-unit depth, row-unit downforce, and the following interaction effects: row-unit depth x row-unit downforce, growing season x row-unit depth, field x row-unit depth, growing season x row-unit downforce, and growing seasons x field x row-unit depth. Cotton seeding depth

was significantly affected by growing season, row-unit depth, row-unit downforce, and the following interaction effects: growing season x field, growing season x row-unit depth, growing season x row-unit downforce, and growing season x field x row-unit depth. Computed linear mixed-effect models explained 88.3% and 84.7% of the variability exhibited by corn and cotton measured seeding depth data, respectively. Row-unit depth was most influential and explained 75.3% and 69.8% of the variability exhibited by corn and cotton measured seeding depth data, respectively.

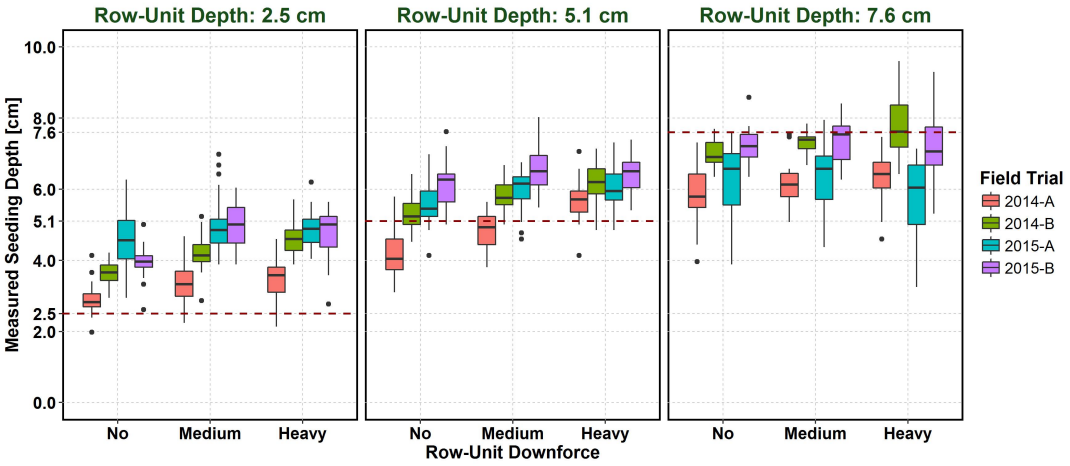

Figure 4.1: Summary of corn measured seeding depth. Whiskers length represents 1.5 times the inter-quartile range. Data beyond the whiskers were plotted as points.

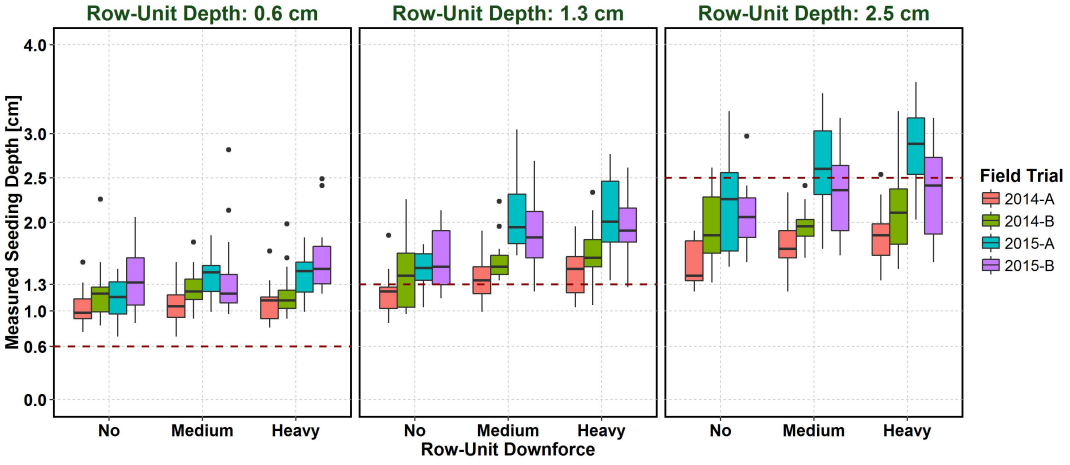

Figure 4.2: Summary of cotton measured seeding depth. Whiskers length represents 1.5 times the inter-quartile range. Data beyond the whiskers were plotted as points.

Table 4.1: Mixed-effect analysis of variance conducted for corn measured seeding depth data.

Mixed-Effect Model Equation:

$$MD = \mu + Y_i + F_j + (Y:F)_{ij} + SD_k + DF_l + (SD:DF)_{kl} + (Y:SD)_{ik} + (F:SD)_{jk} + (Y:DF)_{il} + (F:DF)_{jl} + (Y:F:SD)_{ijk} + (Y:F:DF)_{ijl} + (Y:SD:DF)_{ikl} + (F:SD:DF)_{jkl} + (Y:F:SD:DF)_{ijkl} + \tau_r + \epsilon_{ijkl}$$

Scaled Residuals [cm]:

Min	1Q	Median	3Q	Max
-3.1	-0.3	0.0	0.4	2.2

Random Effects:

Groups	Variance [cm^2]	Std. Dev. [cm]
Whole Plot Error	0.07	0.27
Sub Plot Error	0.17	0.41

Fixed Effects - ANOVA Table:

Model Parameters	Df	Sum Sq.	Mean Sq.	F-Value	Sum Sq. [%]
Y	1	2.49	2.49	14.23 **	1.6
F	1	3.75	3.75	21.47 **	2.4
Y:F	1	0.46	0.46	2.62	0.3
SD	2	125.49	62.74	358.93 ***	79.1
DF	2	6.43	3.22	18.4 ***	4.1
SD:DF	4	2.04	0.51	2.92 *	1.3
Y:SD	2	7.68	3.84	21.96 ***	4.8
F:SD	2	4.10	2.05	11.72 ***	2.6
Y:DF	2	2.68	1.34	7.68 ***	1.7
F:DF	2	0.18	0.09	0.51	0.1
Y:F:SD	2	1.68	0.84	4.79 *	1.1
Y:F:DF	2	0.06	0.03	0.17	0.0
Y:SD:DF	4	0.46	0.11	0.66	0.3
F:SD:DF	4	0.92	0.23	1.31	0.6
Y:F:SD:DF	4	0.16	0.04	0.24	0.1

*Significance: ***: P = 0.001; **: P = 0.01; *: P = 0.05; .: P = 0.1*

*With: **MD**: Measured Seeding Depth; **I**: Model Intercept; $\boldsymbol{Y_i}$, $\boldsymbol{F_j}$, $\boldsymbol{SD_k}$, $\boldsymbol{DF_l}$: Year, Field, Row-Unit Depth, and Row-Unit Downforce main effects; $\boldsymbol{i} \ni \{2014, 2015\}$, $\boldsymbol{j} \ni \{A, B\}$, $\boldsymbol{k} \ni \{2.5, 5.1, 7.6\}$, $\boldsymbol{l} \ni \{No, Medium, Heavy\}$; $\boldsymbol{\tau_r}$: **Random Effect** – defined as a replication within a field and growing season; $\boldsymbol{r} \in \{1, 2, ..., 14\}$; $\boldsymbol{\epsilon_{ijkl}}$: **Random Error**; **":"** denotes interaction between two or more main effects.*

Table 4.2: Mixed-effect analysis of variance conducted for cotton measured seeding depth data.

Mixed-Effect Model Equation:

$$MD = \mu + Y_i + F_j + (Y:F)_{ij} + SD_k + DF_l + (SD:DF)_{kl} + (Y:SD)_{ik} + (F:SD)_{jk} + (Y:DF)_{il} + (F:DF)_{jl} + (Y:F:SD)_{ijk} + (Y:F:DF)_{ijl} + (Y:SD:DF)_{ikl} + (F:SD:DF)_{jkl} + (Y:F:SD:DF)_{ijkl} + \tau_r + \epsilon_{ijkl}$$

Scaled Residuals [cm]:

Min	1Q	Median	3Q	Max
-2.9	-0.5	-0.1	0.4	3.1

Random Effects:

Groups	Variance [cm^2]	Std. Dev. [cm]
Whole Plot Error	0.00	0.08
Sub Plot Error	0.03	0.18

Fixed Effects - ANOVA Table:

Model Parameters	Df	Sum Sq.	Mean Sq.	F-Value	Sum Sq. [%]
Y	1	2.04	2.04	64.68 ***	8.9
F	1	0.04	0.04	1.17	0.2
Y:F	1	0.24	0.24	7.77	1.1 *
SD	2	16.31	8.15	258.17 ***	71.0
DF	2	1.96	0.98	31.06 ***	8.5
SD:DF	4	0.31	0.08	2.42 .	1.3
Y:SD	2	0.73	0.36	11.50 ***	3.2
F:SD	2	0.12	0.06	1.88	0.5
Y:DF	2	0.31	0.16	4.95 *	1.4
F:DF	2	0.16	0.08	2.57 .	0.7
Y:F:SD	2	0.51	0.25	8.07 ***	2.2
Y:F:DF	2	0.05	0.02	0.74	0.2
Y:SD:DF	4	0.05	0.01	0.39	0.2
F:SD:DF	4	0.04	0.01	0.30	0.2
Y:F:SD:DF	4	0.10	0.03	0.81	0.4

*Significance: ***: P = 0.001; **: P = 0.01; *: P = 0.05; .: P = 0.1*

*With: **MD**: Measured Seeding Depth; **I**: Model Intercept; $\boldsymbol{Y_i}$, $\boldsymbol{F_j}$, $\boldsymbol{SD_k}$, $\boldsymbol{DF_l}$: Year, Field, Row-Unit Depth, and Row-Unit Downforce main effects; $\boldsymbol{i} \ni \{2014, 2015\}$, $\boldsymbol{j} \ni \{A, B\}$, $\boldsymbol{k} \ni \{0.6, 1.3, 2.5\}$, $\boldsymbol{l} \ni \{No, Medium, Heavy\}$; $\boldsymbol{\tau_r}$: **Random Effect** – defined as a replication within a field and growing season; $\boldsymbol{r} \in \{1, 2, ..., 14\}$; $\boldsymbol{\epsilon_{ijkl}}$: **Random Error**; **":"** denotes interaction between two or more main effects.*

As expected, increasing row-unit depth significantly increased corn and cotton seeding depth (Tables 4.3 and 4.4). Increasing row-unit downforce significantly increased corn and cotton seeding depth due to heavier load applied onto the soil, and similar row-unit downforce effect has been described in literature by Hanna et al. (2010). Corn and cotton seeding depth response to row-unit depth and downforce adjustments varied with field and growing season. Corn seeding depth was 10% to 30% deeper in field B than in field A suggesting that clayier soils in field A augmented soil resistance to furrow opening therefore producing shallower seeding depths. Corn seeding depth in field A was 10% to 50% deeper in 2015 than in 2014. The 2015 corn planting season was characterized by wetter soil conditions than the 2014 corn planting season due to moderate to intense [20 mm] precipitations recorded 2 days prior to 2015 corn planting (Figure 3.10). Therefore, wetter soil conditions in field A also contributed to increase soil resistance to furrow opening producing even shallower seeding depths. At the 7.6 cm row-unit depth in field A, the planter did not provide sufficient reaction force to oppose soil resistance to furrow opening and failed to achieve the targeted depth.

Table 4.3: Mean seeding depth [cm] of corn by row-unit depth, row-unit downforce, field, and growing season.

Row-Unit Depth	**Row-Unit Downforce**	**Field A**		**Field B**	
		– 2014 –	**– 2015 –**	**– 2014 –**	**– 2015 –**
2.5 cm	**No**	2.9 ^{s}	4.6 ^{nopq}	3.7 ^{qrs}	4.0 ^{pqr}
	Medium	3.4 ^{rs}	5.0 ^{jklmnop}	4.3 ^{opqr}	5.1 ^{ijklmnop}
	Heavy	3.5 ^{rs}	4.9 ^{lmnop}	4.7 ^{mnopq}	4.9 ^{klmnop}
5.1 cm	**No**	4.2 ^{pqr}	5.5 ^{hijklmn}	5.4 ^{hijklmno}	6.2 ^{efgh}
	Medium	4.8 ^{mnop}	6.0 ^{ghij}	5.9 ^{ghijkl}	6.6 ^{bcdefg}
	Heavy	5.8 ^{ghijklm}	6.0 ^{fghi}	6.3 ^{cdefgh}	6.5 ^{bcdefgh}
7.6 cm	**No**	5.9 ^{ghijk}	6.2 ^{efgh}	7.1 ^{abcdef}	7.3 ^{abcd}
	Medium	6.2 ^{fgh}	6.4 ^{cdefgh}	7.4 ^{abc}	7.4 ^{ab}
	Heavy	6.3 ^{defgh}	5.7 ^{ghijklm}	7.8 ^{a}	7.2 ^{abcde}

$^{a,\cdots,s}$ *: Least significant difference between treatments at a 95% confidence interval.*

Table 4.4: Mean seeding depth [cm] of cotton by row-unit depth, row-unit downforce, field, and growing season.

Row-Unit Depth	Row-Unit Downforce	Field A		Field B	
		– 2014 –	– 2015 –	– 2014 –	– 2015 –
0.6 cm	**No**	1.0 ^{l}	1.1 ^{jkl}	1.2 ^{hijkl}	1.4 ^{ghijkl}
	Medium	1.1 ^{kl}	1.4 ^{ghijkl}	1.2 ^{hijkl}	1.4 ^{ghijkl}
	Heavy	1.1 ^{jkl}	1.4 ^{ghijkl}	1.2 ^{hijkl}	1.6 ^{efghi}
1.3 cm	**No**	1.2 ^{ijkl}	1.5 ^{ghij}	1.4 ^{ghijkl}	1.6 ^{efghi}
	Medium	1.4 ^{ghijkl}	2.1 ^{cd}	1.6 ^{efghi}	1.9 ^{cdef}
	Heavy	1.5 ^{ghijk}	2.1 ^{cd}	1.6 ^{efgh}	1.9 ^{cde}
2.5 cm	**No**	1.5 ^{fghi}	2.2 ^{bc}	1.9 ^{cdef}	2.1 ^{cd}
	Medium	1.7 ^{defg}	2.6 ^{ab}	1.9 ^{cde}	2.3 ^{bc}
	Heavy	1.9 ^{def}	2.9 ^{a}	2.1 ^{cd}	2.3 ^{bc}

$^{a,\ldots,l}$ *: Least significant difference between treatments at a 95% confidence interval.*

Summary of corn and cotton seeding depth response to row-unit depth by field and growing season is presented in Figures 4.3 and 4.4. Comparable seeding depth response to row-unit depth was observed within the 2014-A, 2014-B, and 2015-B corn trials with 1 cm increase in row-unit depth resulting in a 0.6 cm increase in corn seeding depth. Smaller seeding depth response to row-unit depth was observed within the 2015-A corn trial, with 1 cm increase in row-unit depth resulting in a 0.3 increase in corn seeding depth. Such results suggested that clayier and wetter soil conditions observed in 2015-A corn trial reduced soil bearing capacity at planting therefore limiting planter ability to provide optimum response to row-unit depth adjustment. For cotton, 1 cm increase in row-unit depth resulted in a 0.3 to 0.6 cm increase in cotton seeding depth within individual field trials. Computed regression models provided good estimation of seeding depth response to row-unit depth across selected row-unit depths. Non-zero intercepts along with larger slope values obtained for corn versus cotton suggested that seeding depth response to row-unit depth adjustment could be non-linear across a wider range of row-unit depths.

Seeding depth response to row-unit downforce was stronger for corn than cotton (Tables 4.5 and 4.5). Simply, cotton was planted shallower than corn. Therefore, smaller force was required to achieve cotton targeted depths and smaller proportion of applied downforce was

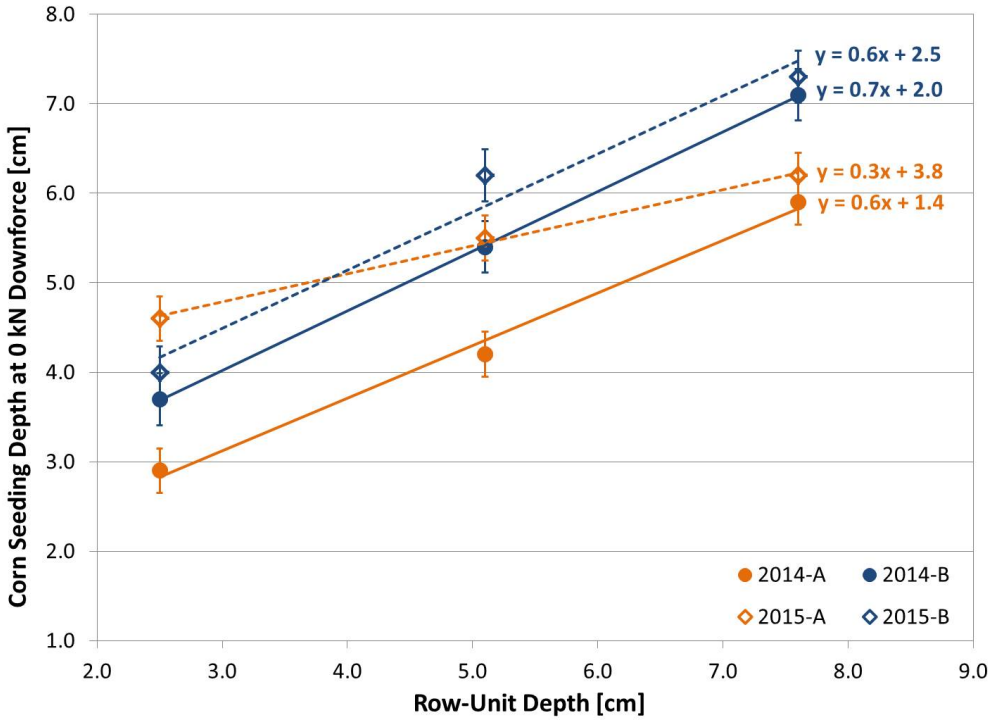

Figure 4.3: Corn seeding depth response to row-unit depth adjustments by field and growing season.

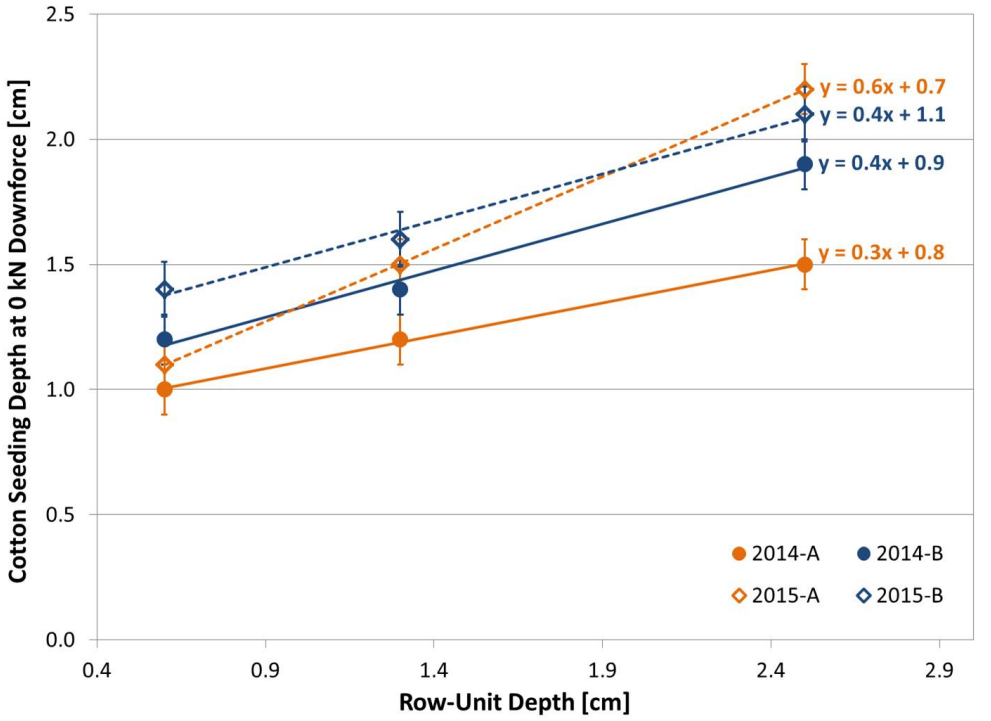

Figure 4.4: Cotton seeding depth response to row-unit depth adjustments by field and growing season.

directed toward the planter components actively involved with furrow opening and closing. Cotton seeding depth response to row-unit downforce ranged from 0.10 to 0.23 cm.kN^{-1} and was fairly consistent between row-unit depths, fields, and growing seasons. Corn seeding depth response to row-unit downforce was stronger at the 5.1 and 2.5 cm row-unit depths than at the 7.6 cm row-unit depth. This result was consistent with field observations (Figure 4.5) showing that row-unit operation permitted proper performance of the downforce system at 2.5 and 5.1 cm row-unit depth but not at the 7.6 cm row-unit depth.

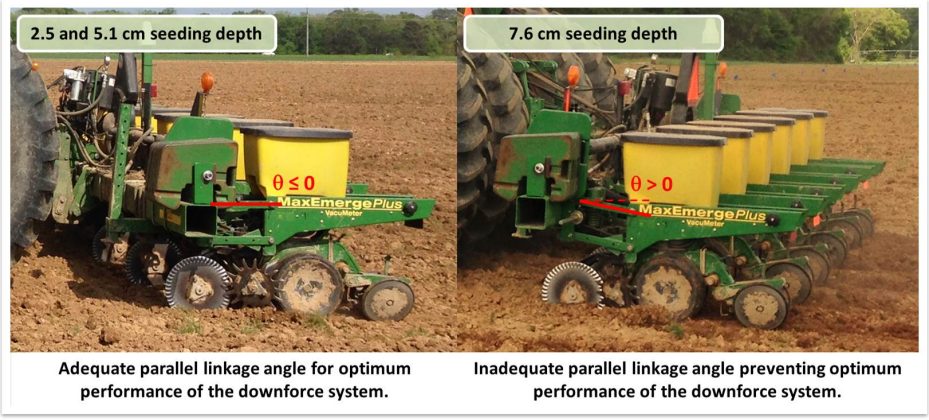

Figure 4.5: Row-unit parallel linkage configuration and downforce system performance for selected corn row-unit depths.

For the particular case of cotton (section 3.6.1), results from statistical analysis demonstrated that row-unit depth, row-unit downforce, and the two-way interaction between field and growing season significantly affected the percentage of cotton seeds that failed to be placed within the soil furrow (Table 4.7). Increasing row-unit depth and downforce improved the planter ability to place cotton seeds within the soil furrow through improved contact between the soil and planter components. Cotton seed placement in field A was better in 2014 than in 2015 as wetter soil conditions reduced soil roughness therefore limiting soil furrow closure. Planter ability to place seeds within the soil furrow in field B was consistent between growing seasons.

Table 4.5: Analysis of covariance conducted to model field-scale corn seeding depth response to row-unit downforce by field, growing season, and row-unit depth.

Optimized Linear Regression Model Equation:

$$MD = I + Y_i + F_j + (Y:F)_{ij} + SD_k + DF + SD_k:DF + (Y:SD)_{ik} + (F:SD)_{jk} + Y_i:DF + (Y:F:SD)_{ijk} + \epsilon_{ij}$$

Overall Model Statistics:	
Adjusted R^2 :	85.9%
F-Statistic :	51.52
Model p-value :	< 0.001

Residuals [cm]:

Min	**1Q**	**Median**	**3Q**	**Max**
-2.1	-0.2	0.0	0.3	1.2

Regression Coefficients:

Model Parameters	**Estimate**	**SE**	**t-value**
Intercept	2.74	0.18	15.27 ***
$\mathbf{Y_{2015}}$	1.90	0.23	8.35 ***
$\mathbf{F_B}$	0.91	0.21	4.25 ***
$\mathbf{(Y:F)_{2015,B}}$	-1.16	0.30	-3.85 ***
$\mathbf{SD_{5.1}}$	1.52	0.24	6.30 ***
$\mathbf{SD_{7.6}}$	3.15	0.24	13.10 ***
DF	0.54	0.12	4.62 ***
$\mathbf{SD_{5.1}}$**:DF**	0.08	0.14	0.55
$\mathbf{SD_{7.6}}$**:DF**	-0.30	0.14	-2.12 *
$\mathbf{(Y:SD)_{2015,5.1}}$	-0.61	0.28	-2.16 *
$\mathbf{(Y:SD)_{2015,7.6}}$	-1.63	0.28	-5.83 ***
$\mathbf{(F:SD)_{B,5.1}}$	0.02	0.30	0.05
$\mathbf{(F:SD)_{B,7.6}}$	0.34	0.30	1.12
$\mathbf{Y_{2015}}$**:DF**	-0.33	0.12	-2.80 **
$\mathbf{(Y:F:SD)_{2015,B,5.1}}$	0.78	0.43	1.82 .
$\mathbf{(Y:F:SD)_{2015,B,7.6}}$	1.11	0.43	2.60 *

Significance: ***: *P = 0.001;* **: *P = 0.01;* *: *P = 0.05;* .: *P = 0.1*

Derived Linear Equations for Individual Field Trials:

Season	**Field**	**— SD = 2.5 cm —**	**— SD = 5.1 cm —**	**— SD = 7.6 cm —**
2014	**A**	$MD = 2.74 + 0.54 \cdot DF$	$MD = 4.26 + 0.62 \cdot DF$	$MD = 5.89 + 0.24 \cdot DF$
2014	**B**	$MD = 3.65 + 0.54 \cdot DF$	$MD = 5.19 + 0.62 \cdot DF$	$MD = 7.14 + 0.24 \cdot DF$
2015	**A**	$MD = 4.64 + 0.21 \cdot DF$	$MD = 5.55 + 0.29 \cdot DF$	$MD = 6.16 - 0.09 \cdot DF$
2015	**B**	$MD = 4.39 + 0.21 \cdot DF$	$MD = 6.10 + 0.29 \cdot DF$	$MD = 7.36 - 0.09 \cdot DF$

With: ***MD****: Measured Seeding Depth [cm];* ***I****: Model Intercept;* $\boldsymbol{Y_i}$, $\boldsymbol{F_j}$, $\boldsymbol{SD_k}$*: Year, Field, and Row-Unit Depth effects – categorical variables;* $\boldsymbol{i} \ni \{2014, 2015\}$, $\boldsymbol{j} \ni \{A, B\}$, $\boldsymbol{k} \ni \{2.5, 5.1, 7.6\}$*;* ***DF****: Row-Unit Downforce [kN] – continuous variable;* $\boldsymbol{\epsilon_{ij}}$*: Random Error [cm];* ***":"*** *denotes interaction between main effects.*

Table 4.6: Analysis of covariance conducted to model field-scale cotton seeding depth response to row-unit downforce by field, growing season, and row-unit depth.

Optimized Linear Regression Model Equation:

$$MD = I + Y_i + SD_k + DF + (Y:F)_{ij} + (Y:SD)_{ik} + Y_i:DF + (Y:F:SD)_{ijk} + \epsilon_{ij}$$

Overall Model Statistics:

Adjusted R^2 :	84.6%
F-Statistic :	54.0
Model p-value :	< 0.001

Residuals [cm]:

Min	1Q	Median	3Q	Max
-0.7	-0.1	0.0	0.1	0.6

Regression Coefficients:

Model Parameters	Estimate	SE	t-value
Intercept	0.99	0.06	15.39 ***
$\mathbf{Y_{2015}}$	0.10	0.09	1.15
$\mathbf{SD_{1.3}}$	0.26	0.08	3.28 **
$\mathbf{SD_{2.5}}$	0.62	0.08	7.92 ***
DF	0.10	0.03	3.19 **
$\mathbf{(Y:F)_{2014,B}}$	0.13	0.08	1.55
$\mathbf{(Y:F)_{2015,B}}$	0.13	0.08	1.59
$\mathbf{(Y:SD)_{2015,1.3}}$	0.31	0.11	2.82 **
$\mathbf{(Y:SD)_{2015,2.5}}$	0.64	0.11	5.75 ***
$\mathbf{Y_{2015}}$**:DF**	0.12	0.05	2.68 **
$\mathbf{(Y:F:SD)_{2014,B,1.3}}$	0.05	0.12	0.42
$\mathbf{(Y:F:SD)_{2015,B,1.3}}$	-0.21	0.12	-1.73 .
$\mathbf{(Y:F:SD)_{2014,B,2.5}}$	0.16	0.12	1.34
$\mathbf{(Y:F:SD)_{2015,B,2.5}}$	-0.46	0.12	-3.87 ***

*Significance: ***: P = 0.001; **: P = 0.01; *: P = 0.05; .: P = 0.1*

Derived Linear Equations for Individual Field Trials:

Season	Field	—— SD = 0.6 cm ——	—— SD = 1.3 cm ——	—— SD = 2.5 cm ——
2014	**A**	$MD = 0.99 + 0.10 \cdot DF$	$MD = 1.24 + 0.10 \cdot DF$	$MD = 1.61 + 0.10 \cdot DF$
2014	**B**	$MD = 1.12 + 0.10 \cdot DF$	$MD = 1.43 + 0.10 \cdot DF$	$MD = 1.90 + 0.10 \cdot DF$
2015	**A**	$MD = 1.09 + 0.23 \cdot DF$	$MD = 1.66 + 0.23 \cdot DF$	$MD = 2.35 + 0.23 \cdot DF$
2015	**B**	$MD = 1.23 + 0.23 \cdot DF$	$MD = 1.59 + 0.23 \cdot DF$	$MD = 2.02 + 0.23 \cdot DF$

*With: **MD**: Measured Seeding Depth [cm]; **I**: Model Intercept; $\boldsymbol{Y_i}$, $\boldsymbol{F_j}$: Year, Field, and Row-Unit Depth effects – categorical variables; $\boldsymbol{i} \ni \{2014, 2015\}$, $\boldsymbol{j} \ni \{A, B\}$, $\boldsymbol{k} \ni \{0.6, 1.3, 2.5\}$; **DF**: Row-Unit Downforce [kN] – continuous variable; $\boldsymbol{\epsilon_{ij}}$: Random Error [cm]; **":"** denotes interaction between main effects.*

Table 4.7: Generalized linear mixed-effect analysis of variance conducted for planter ability to place cotton seeds within the soil furrow.

Generalized Linear Mixed-Effect Model Equation:

$$Y_{ijkl} = 1/\Big(1 + exp(-(I + (Y:F)_{ij} + SD_k + DF_l + \tau_r + \epsilon_{ijkl})\Big)$$

Scaled Residuals (ϵ_{ijkl}):

Min	1Q	Median	3Q	Max
-1.64	-0.47	-0.26	0.30	7.15

Random Effects:

Groups	Variance [cm^2]	Std. Dev. [cm]
τ_r	0.01	0.08

Fixed Effects - ANOVA Table:

Model Parameters	Estimate	Std. Error	Z Value
Intercept	-1.76	0.14	-12.56 ***
SD$_{1.3}$	-2.08	0.12	-17.37 ***
SD$_{1.5}$	-5.11	0.45	-11.32 ***
DF$_{Medium}$	0.28	0.13	2.15 *
DF$_{No}$	1.35	0.12	11.23 ***
(Y:F)$_{2014,A}$	-1.25	0.18	-7.11 ***
(Y:F)$_{2014,B}$	0.13	0.15	0.87
(Y:F)$_{2015,A}$	0.59	0.14	4.26 ***

*Significance: ***: P = 0.001; **: P = 0.01; *: P = 0.05; .: P = 0.1*

Estimated Response to Treatments (Y_{ijkl}):

Seeding Depth [cm]	Row-Unit Downforce	Seeds on Surface [%]			
		2014-A	2014-B	2015-A	2015-B
0.6	**No**	50.0	43.0	54.4	39.8
	Medium	6.1	20.7	29.2	18.6
	Heavy	4.7	16.4	23.7	14.7
1.3	**No**	2.3	8.6	12.9	7.6
	Medium	0.8	3.1	4.9	2.8
	Heavy	0.6	2.4	3.7	2.1
2.5	**No**	0.1	0.5	0.7	0.4
	Medium	0.0	0.2	0.2	0.1
	Heavy	0.0	0.1	0.2	0.1

*With: $\boldsymbol{Y_{ijkl}}$: Percentage of cotton seeds that failed to be placed within the soil furrow [%]; $\boldsymbol{I}$: Model Intercept; $\boldsymbol{Y_i}$, $\boldsymbol{F_j}$, $\boldsymbol{SD_k}$, $\boldsymbol{DF_l}$: Year, Field, Row-Unit Depth, and Row-Unit Downforce main effects; $\boldsymbol{i} \ni \{2014, 2015\}$, $\boldsymbol{j} \ni \{A, B\}$, $\boldsymbol{k} \ni \{0.6, 1.3, 2.5\}$, $\boldsymbol{l} \ni \{No, Medium, Heavy\}$; $\boldsymbol{\tau_r}$: **Random Effect** – defined as a replication within a field and growing season; $\boldsymbol{r} \in \{1, 2, ..., 14\}$; $\boldsymbol{\epsilon_{ijkl}}$: **Random Error**; **":"** denotes interaction between two or more main effects.*

4.2 Seeding Depth Variability

In-field seeding depth standard deviation data for corn ranged from 0.3 to 1.2 cm (Table 4.8), and assuming normality approximately 68% of corn seeds were placed within a seeding depth interval of 0.6 to 2.4 cm. Similarly, in-field seeding depth standard deviation data for cotton ranged from 0.2 to 0.6 cm (Table 4.9), and assuming normality approximately 68% of cotton seeds were placed within a seeding depth interval of 0.4 to 1.2 cm. Bowen (1966) demonstrated that seeding depth should be maintained within a variation of +/- 0.3 cm to ensure optimum crop establishment, and achieved seeding depth performance were not optimum. In-field corn seeding depth standard deviation was higher in 2015 than in 2014 suggesting that wetter soil conditions during 2015 planting season increased planter response to field spatial variability. In-field corn seeding depth standard deviation also increased with increasing row-unit depth due to increasing contact between the soil and planter components involved with furrow opening and covering. In-field cotton seeding depth standard deviation was fairly consistent among treatments as shallower seeding depths resulted in limited soil-planter interactions. Coefficients of variation for measured seeding depth ranged from 4.0% to 20.9% for corn, and from 10.5% to 35.7% for cotton (Tables 4.10 and 4.11). Measured seeding depth strongly varied within fields. Additional analysis was required to characterize site-specific seeding depth variability.

4.3 Seeding Depth Precision

Shallow cotton seeding depths resulted in a significant percentage of cotton seeds ending up on the soil surface rather than within the soil furrow (section 4.1). Hence, the shallower limit of cotton seeding depth distribution was bounded by the distance to the soil surface, which did not permit accurate determination of cotton seeding depth standard deviation. Cotton seeding depth standard deviation data were irrelevant, and results and discussion presented in this section focus on corn only. Corn seeding depth standard deviation data

Table 4.8: In-field standard deviation in corn seeding depth [cm] by row-unit depth, row-unit downforce, field and growing season.

Row-Unit Depth [cm]	Row-Unit Downforce	Field A		Field B	
		– 2014 –	– 2015 –	– 2014 –	– 2015 –
2.5	**No**	0.4	0.9	0.3	0.4
	Medium	0.6	0.8	0.5	0.6
	Heavy	0.5	0.5	0.5	0.7
5.1	**No**	0.6	0.6	0.5	0.6
	Medium	0.6	0.6	0.4	0.6
	Heavy	0.7	0.5	0.5	0.5
7.6	**No**	0.8	1.1	0.4	0.5
	Medium	0.6	0.9	0.3	0.6
	Heavy	0.7	1.2	0.9	1.0

Table 4.9: In-field standard deviation in cotton measured seeding depth [cm] by row-unit depth, row-unit downforce, field and growing season.

Row-Unit Depth [cm]	Row-Unit Downforce	Field A		Field B	
		– 2014 –	– 2015 –	– 2014 –	– 2015 –
2.5	**No**	0.2	0.2	0.4	0.4
	Medium	0.2	0.2	0.2	0.5
	Heavy	0.2	0.2	0.3	0.4
5.1	**No**	0.2	0.2	0.4	0.3
	Medium	0.2	0.5	0.2	0.5
	Heavy	0.3	0.4	0.3	0.4
7.6	**No**	0.2	0.6	0.4	0.4
	Medium	0.3	0.5	0.2	0.5
	Heavy	0.3	0.4	0.5	0.6

Table 4.10: Coefficient of variation [%] for corn measured seeding depth by row-unit depth, row-unit downforce, field and growing season.

Row-Unit Depth [cm]	Row-Unit Downforce	Field A		Field B	
		– 2014 –	– 2015 –	– 2014 –	– 2015 –
2.5	No	15.4	18.9	9.0	11.3
	Medium	16.5	16.1	11.5	11.5
	Heavy	15.5	10.2	9.7	14.3
5.1	No	14.8	11.7	9.3	9.7
	Medium	12.2	9.3	6.7	9.0
	Heavy	11.4	9.1	8.2	8.2
7.6	No	13.7	17.4	5.5	6.3
	Medium	9.4	14.3	4.0	8.1
	Heavy	11.5	20.9	11.1	13.8

Table 4.11: Coefficient of variation [%] for cotton measured seeding depth by row-unit depth, row-unit downforce, field and growing season.

Row-Unit Depth [cm]	Row-Unit Downforce	Field A		Field B	
		– 2014 –	– 2015 –	– 2014 –	– 2015 –
2.5	No	20.0	18.2	33.3	28.6
	Medium	18.2	14.3	16.7	35.7
	Heavy	18.2	14.3	25.0	25.0
5.1	No	16.7	13.3	28.6	18.8
	Medium	14.3	23.8	12.5	26.3
	Heavy	20.0	19.0	18.8	21.1
7.6	No	13.3	27.3	21.1	19.0
	Medium	17.6	19.2	10.5	21.7
	Heavy	15.8	13.8	23.8	26.1

are presented by row-unit depth, row-unit downforce, and field trial in Figure 4.6. Corn seeding depth standard deviation was significantly affected by row-unit depth and growing season (Tables 4.12 and 4.13). Computed linear mixed-effect model explained 7.1% of corn seeding depth standard deviation and most of the variability exhibited by corn seeding depth standard deviation data was not explained by treatment effects. One explanation to low goodness of fit of the model was that seeding depth standard deviation data provided a confounded estimate of several factors including vertical seed placement error but also seeding depth differences between row-units, human errors – estimated close to 0.25 cm –, and random errors.

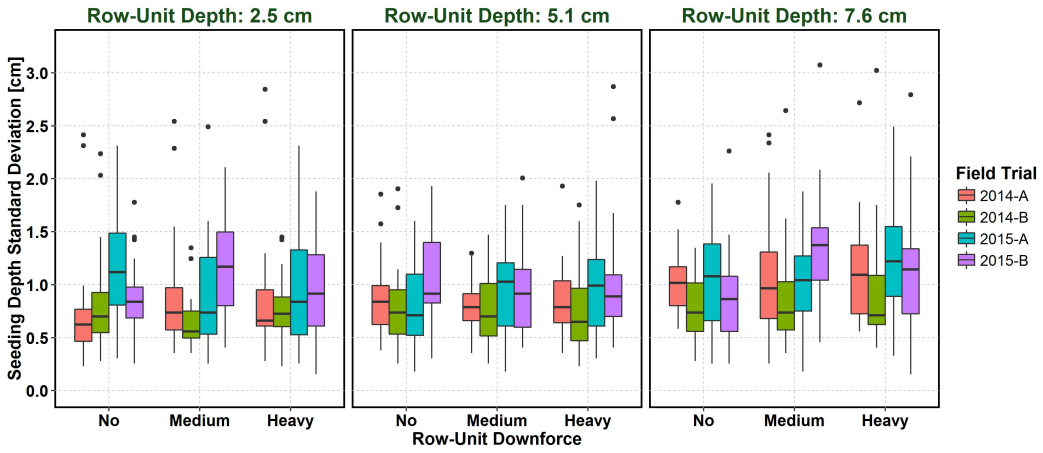

Figure 4.6: Summary of corn seeding depth standard deviation. Whiskers length was defined by 1.5 times the inter-quartile range. Data beyond the whiskers were plotted as points.

Corn seeding depth standard deviation was higher in 2015 versus 2014. One explanation was that the 2015 growing season provided cloddier soil conditions than the 2014 growing season, therefore increasing the amount of random noise imputed by the soil onto the planter system and limiting planter ability to perform at a precise seeding depth. Complementary analysis was then computed to evaluate planter ability to achieve precise seeding depth. By design, minimum seeding depth adjustment on the planter was 0.6 cm, and seeding depth precision was arbitrarily defined as the ability of the planter to achieve smaller standard deviation than the difference in measured seeding depth between two consecutive depth

Table 4.12: Results of mixed-effect analysis of variance conducted for corn seeding depth standard deviation data.

Mixed-Effect Model Equation:

$$DSD = \mu + Y_i + F_j + (Y:F)_{ij} + SD_k + DF_l + (SD:DF)_{kl} + (Y:SD)_{ik} + (F:SD)_{jk} + (Y:DF)_{il} + (F:DF)_{jl} + (Y:F:SD)_{ijk} + (Y:F:DF)_{ijl} + (Y:SD:DF)_{ikl} + (F:SD:DF)_{jkl} + (Y:F:SD:DF)_{ijkl} + \tau_r + \epsilon_{ijk}$$

Model Fit:

REML Criterion at Convergence: 33.4

Scaled Residuals [cm]:

Min	1Q	Median	3Q	Max
-2.4	-0.5	-0.1	0.5	2.9

Random Effects:

Groups	Variance [cm^2]	Std. Dev. [cm]
Whole Plot Error	0.00	0.06
Sub Plot Error	0.05	0.22

Fixed Effects - ANOVA Table:

Model Parameters	Df	Sum Sq.	Mean Sq.	F-Value	Sum Sq. [%]
Y	1	0.53	0.53	10.87 **	19.6
F	1	0.05	0.05	1.04	1.9
Y:F	1	0.15	0.15	2.98	5.4
SD	2	0.70	0.35	7.19 **	25.9
DF	2	0.09	0.04	0.93	3.4
SD:DF	4	0.19	0.05	0.97	7.0
Y:SD	2	0.07	0.03	0.70	2.5
F:SD	2	0.07	0.03	0.71	2.6
Y:DF	2	0.02	0.01	0.22	0.8
F:DF	2	0.08	0.04	0.80	2.9
Y:F:SD	2	0.06	0.03	0.59	2.1
Y:F:DF	2	0.17	0.09	1.78	6.4
Y:SD:DF	4	0.08	0.02	0.39	2.8
F:SD:DF	4	0.12	0.03	0.63	4.6
Y:F:SD:DF	4	0.33	0.08	1.68	12.1

With: ***DSD****: Depth Standard Deviation;* $\boldsymbol{Y_i}$*,* $\boldsymbol{F_j}$*,* $\boldsymbol{SD_k}$*,* $\boldsymbol{DF_l}$*: Year, Field, Row-Unit Depth, and Row-Unit Downforce main effects;* $\boldsymbol{i} \ni \{2014, 2015\}$*,* $\boldsymbol{j} \ni \{A, B\}$*,* $\boldsymbol{k} \ni \{2.5, 5.1, 7.6\}$*,* $\boldsymbol{l} \ni \{No, Medium, Heavy\}$*;* $\boldsymbol{\tau_r}$*:* ***Random Effect*** *– defined as a replication within a field and growing season;* $\boldsymbol{r} \in \{1, 2, ..., 14\}$*;* $\boldsymbol{\epsilon_{ijkl}}$*:* ***Random Error****; ":" denotes interaction between two or more main effects.*

settings. Changes in measured seeding depth between consecutive settings were computed using results presented section 4.1. Comparisons to mean corn seeding depth standard deviation indicated that the planter was not performing precisely (Tables 4.14).

Table 4.13: Mean corn seeding depth standard deviation by row-unit depth, field, and growing season (all row-unit downforce confounded).

		2014		2015	
Row-Unit Depth [cm]	**Field**	**Estimated Depth Std. Dev. [cm]**	**Confidence Interval [cm]**	**Estimated Depth Std. Dev. [cm]**	**Confidence Interval [cm]**
2.5		0.8 ^{bc}	[0.7-1.0]	1.0 ^{abc}	[0.9-1.2]
5.1	**A**	0.9 ^{abc}	[0.7-1.0]	0.9 ^{abc}	[0.8-1.0]
7.6		1.1 ^{ab}	[0.9-1.2]	1.1 ^{a}	[1.0-1.2]
2.5		0.7 ^{c}	[0.6-0.9]	1.0 ^{abc}	[0.8-1.2]
5.1	**B**	0.8 ^{c}	[0.6-0.9]	1.0 ^{abc}	[0.8-1.2]
7.6		0.8 ^{abc}	[0.7-1.0]	1.1 ^{a}	[1.0-1.3]

$^{a,\ldots,l}$ *: Least significant difference between treatments at a 95% confidence interval.*

Table 4.14: Evaluation of corn seeding depth precision by row-unit depth, field, and growing season (all row-unit downforce confounded).

		2014		2015	
Row-Unit Depth [cm]	**Field**	**Threshold Std. Deviation [cm]**	**Estimated Std. Deviation [cm]**	**Threshold Std. Deviation [cm]**	**Estimated Std. Deviation [cm]**
2.5			0.8 [NP]		1.0 [NP]
5.1	**A**	0.3	0.9 [NP]	0.2	0.9 [NP]
7.6			1.1 [NP]		1.1 [NP]
2.5			0.7 [NP]		1.0 [NP]
5.1	**B**	0.4	0.8 [NP]	0.3	1.0 [NP]
7.6			0.8 [NP]		1.1 [NP]

[P]: *Precise* [NP]: *Non-Precise*

4.4 Measured Gauge-Wheel Load

Corn and cotton measured gauge-wheel load by row-unit depth, row-unit downforce, and field trial are presented in Figures 4.7 and 4.8. Measured gauge-wheel load of corn was significantly affected by growing season, row-unit depth, row-unit downforce, and the following interaction effects: growing season x field, field x row-unit depth, growing season x row-unit downforce, field x row-unit downforce, row-unit depth x row-unit downforce, and

growing season x field x row-unit depth x row-unit downforce (Table 4.15). Cotton measured gauge-wheel load of cotton was significantly affected by growing season, field, row-unit depth, row-unit downforce, and the following interaction effects: growing season x row-unit depth, growing season x row-unit downforce, field x row-unit downforce, row-unit depth x row-unit downforce, growing season x field x row-unit depth, year x field x row-unit downforce, field x row-unit depth x row-unit downforce, and growing season x field x row-unit depth x row-unit downforce (4.16). Computed linear mixed-effect models explained 95.5% and 94.9% of the variability exhibited by corn and cotton gauge-wheel load data, respectively. Row-unit downforce was most influential and explained 42.7% and 76.7% of the variability exhibited by corn and cotton measured gauge-wheel load data, respectively.

Increasing row-unit downforce significantly increased gauge-wheel load because increasing row-unit weight increases vertical forces applied onto the soil. Corn and cotton gauge-wheel load response to row-unit downforce was affected by field, growing season, and row-unit depth and linear regression analyses were computed to characterize these effects (Tables 4.17 and 4.18). Intercepts and slope estimates reduced with increasing row-unit depth, and measured gauge-wheel load as well as gauge-wheel load response to row-unit downforce reduced with increasing row-unit depth. Planter gauge-wheels are designed to carry the difference between vertical forces applied onto the soil (row-unit weight) and vertical forces required to open and close the soil furrow (see section 2.3.1). Therefore, assuming proper downforce system performance results demonstrated that increasing row-unit depth increased the proportion of applied downforce that was directed toward furrow opening and covering. Computed slopes were higher in 2015 versus 2014, and 2015 growing season was characterized by stronger gauge-wheel load response to row-unit downforce. Such results were consistent with previous findings indicating less resistance to furrow opening and therefore deeper seeding depths within 2015 versus 2014 corn and cotton trials.

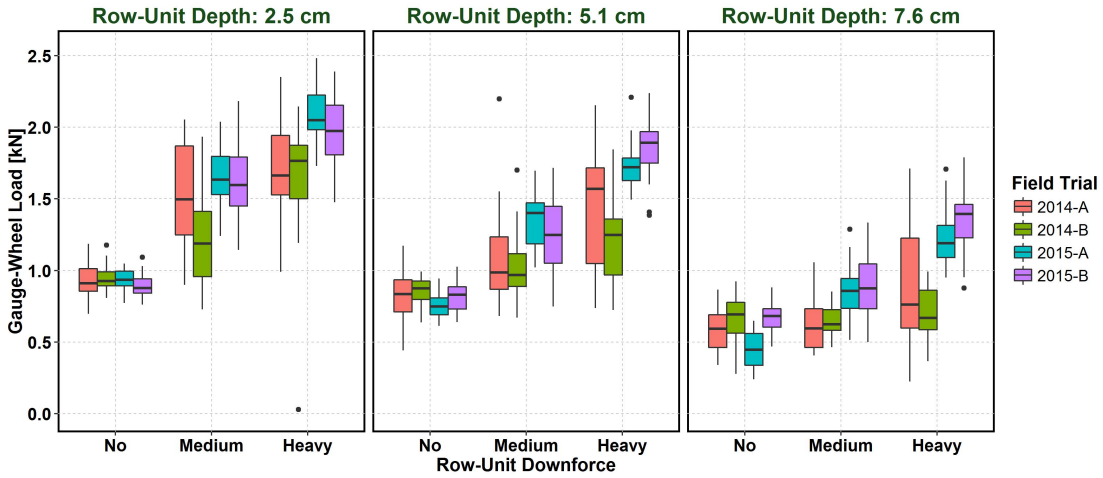

Figure 4.7: Summary of measured gauge-wheel load for corn. Whiskers length was defined by 1.5 times the inter-quartile range. Data beyong the whiskers were plotted as points.

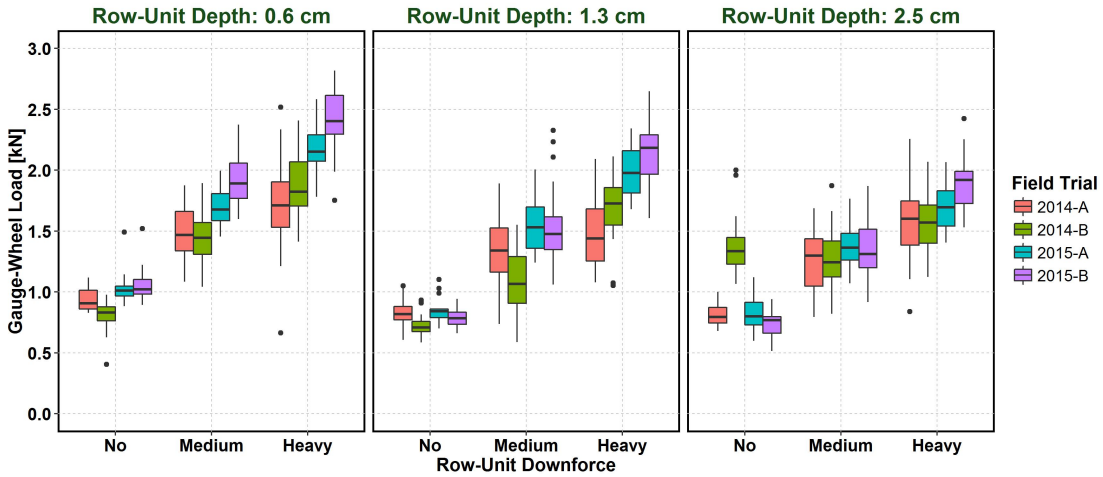

Figure 4.8: Summary of measured gauge-wheel load for cotton. Whiskers length was defined by 1.5 times the inter-quartile range. Data beyong the whiskers were plotted as points.

Table 4.15: Results of mixed-effect analysis of variance conducted for corn measured gauge-wheel load data.

Mixed-Effect Model Equation:

$$GWL = \mu + Y_i + F_j + (Y:F)_{ij} + SD_k + DF_l + (SD:DF)_{kl} + (Y:SD)_{ik} + (F:SD)_{jk} + (Y:DF)_{il} + (F:DF)_{jl} + (Y:F:SD)_{ijk} + (Y:F:DF)_{ijl} + (Y:SD:DF)_{ikl} + (F:SD:DF)_{jkl} + (Y:F:SD:DF)_{ijkl} + \tau_r + \epsilon_{ijk}$$

Model Fit:

REML Criterion at Convergence: -117

Scaled Residuals [kN]:

Min	1Q	Median	3Q	Max
-2.3	-0.5	-0.1	0.5	2.2

Random Effects:

Groups	Variance [cm^2]	Std. Dev. [cm]
Whole Plot Error	0.00	0.02
Sub Plot Error	0.01	0.09

Fixed Effects - ANOVA Table:

Model Parameters	Df	Sum Sq.	Mean Sq.	F-Value	Sum Sq. [%]
Y	1	0.77	0.77	87.93 ***	3.5
F	1	0.01	0.01	0.99	0.0
Y:F	1	0.05	0.05	6.16 *	0.2
SD	2	8.58	4.29	490.45 ***	38.7
DF	2	10.24	5.12	585.59 ***	46.2
SD:DF	4	0.92	0.23	26.42 ***	4.2
Y:SD	2	0.00	0.00	0.08	0.0
F:SD	2	0.09	0.04	4.97 **	0.4
Y:DF	2	1.18	0.59	67.24 ***	5.3
F:DF	2	0.12	0.06	6.66 **	0.5
Y:F:SD	2	0.01	0.01	0.73	0.1
Y:F:DF	2	0.05	0.02	2.60 .	0.2
Y:SD:DF	4	0.02	0.00	0.56	0.1
F:SD:DF	4	0.03	0.01	0.79	0.1
Y:F:SD:DF	4	0.12	0.03	3.49 *	0.6

With: ***GWL****: Measured Gauge-Wheel Load;* $\boldsymbol{Y_i}$, $\boldsymbol{F_j}$, $\boldsymbol{SD_k}$, $\boldsymbol{DF_l}$*: Year, Field, Row-Unit Depth, and Row-Unit Downforce main effects;* $\boldsymbol{i} \ni \{2014, 2015\}$, $\boldsymbol{j} \ni \{A, B\}$, $\boldsymbol{k} \ni \{2.5, 5.1, 7.6\}$, $\boldsymbol{l} \ni \{No, Medium, Heavy\}$; $\boldsymbol{\tau_r}$*:* ***Random Effect*** *– defined as a replication within a field and growing season;* $\boldsymbol{r} \in \{1, 2, ..., 14\}$; $\boldsymbol{\epsilon_{ijkl}}$*:* ***Random Error****; ":" denotes interaction between two or more main effects.*

Table 4.16: Results of mixed-effect analysis of variance conducted for cotton measured gauge-wheel load data.

Mixed-Effect Model Equation:

$$GWL = \mu + Y_i + F_j + (Y:F)_{ij} + SD_k + DF_l + (SD:DF)_{kl} + (Y:SD)_{ik} + (F:SD)_{jk} + (Y:DF)_{il} + (F:DF)_{jl} + (Y:F:SD)_{ijk} + (Y:F:DF)_{ijl} + (Y:SD:DF)_{ikl} + (F:SD:DF)_{jkl} + (Y:F:SD:DF)_{ijkl} + \tau_r + \epsilon_{ijk}$$

Model Fit:

REML Criterion at Convergence: -94.6

Scaled Residuals [kN]:

Min	1Q	Median	3Q	Max
-2.37	-0.5	0.0	0.5	2.1

Random Effects:

Groups	Variance [cm^2]	Std. Dev. [cm]
Whole Plot Error	0.00	0.02
Sub Plot Error	0.01	0.10

Fixed Effects - ANOVA Table:

Model Parameters	Df	Sum Sq.	Mean Sq.	F-Value	Sum Sq. [%]
Y	1	1.37	1.37	128.14 ***	5.9
F	1	0.17	0.17	15.94 **	0.7
Y:F	1	0.01	0.01	0.99	0.0
SD	2	1.91	0.95	89.15 ***	8.3
DF	2	16.81	8.40	785.58 ***	72.9
SD:DF	4	0.41	0.10	9.60 ***	1.8
Y:SD	2	0.68	0.34	31.60 ***	2.9
F:SD	2	0.07	0.03	3.14 .	0.3
Y:DF	2	0.75	0.38	35.25 ***	3.3
F:DF	2	0.13	0.07	6.29 **	0.6
Y:F:SD	2	0.15	0.08	7.24 **	0.7
Y:F:DF	2	0.12	0.06	5.66 *	0.5
Y:SD:DF	4	0.06	0.02	1.46	0.3
F:SD:DF	4	0.20	0.05	4.78 **	0.9
Y:F:SD:DF	4	0.21	0.05	5.02 **	0.9

*With: **GWL**: Measured Gauge-Wheel Load; $\boldsymbol{Y_i}$, $\boldsymbol{F_j}$, $\boldsymbol{SD_k}$, $\boldsymbol{DF_l}$: Year, Field, Row-Unit Depth, and Row-Unit Downforce main effects; $\boldsymbol{i} \ni \{2014, 2015\}$, $\boldsymbol{j} \ni \{A, B\}$, $\boldsymbol{k} \ni \{0.6, 1.3, 2.5\}$, $\boldsymbol{l} \ni \{No, Medium, Heavy\}$; $\boldsymbol{\tau_r}$: **Random Effect** – defined as a replication within a field and growing season; $\boldsymbol{r} \in \{1, 2, ..., 14\}$; $\boldsymbol{\epsilon_{ijkl}}$: **Random Error**; **":"** denotes interaction between two or more main effects.*

Table 4.17: Analysis of covariance conducted to model field-scale corn gauge-wheel load response to row-unit downforce by field, growing season, and row-unit depth.

Optimized Linear Regression Model Equation:

$$GWL = I + Y_i + (Y:F)_{ij} + SD_k + DF + SD_k:DF + (F:SD)_{jk} + Y_i:DF + F_j:DF + \epsilon_{ij}$$

Overall Model Statistics:	
Adjusted R^2 :	94.2%
F-Statistic :	165.9
textbfModel p-value :	< 0.001

Residuals [kN]:

Min	**1Q**	**Median**	**3Q**	**Max**
-0.33	-0.05	0.01	0.06	0.27

Regression Coefficients:

Model Parameters	**Estimate**	**SE**	**t-value**
Intercept	0.98	0.04	26.63 ***
Y_{2015}	-0.09	0.03	-2.52 *
$SD_{5.1}$	-0.16	0.04	-3.76 ***
$SD_{7.6}$	-0.43	0.04	-100.10 ***
DF	0.42	0.03	14.94 ***
$(Y:F)_{2014,B}$	-0.06	0.05	-1.32
$(Y:F)_{2015,B}$	0.04	0.05	0.94
$(F:SD)_{B,5.1}$	0.04	0.05	0.85
$(F:SD)_{B,7.6}$	0.13	0.05	2.74 **
Y_{2015}:DF	0.26	0.03	10.19 ***
F_B:DF	-0.07	0.03	-2.80 **
$SD_{5.1}$:DF	-0.12	0.03	-3.65 ***
$SD_{7.6}$:DF	-0.27	0.03	-8.72 ***

*Significance: ***: P = 0.001; **: P = 0.01; *: P = 0.05; .: P = 0.1*

Derived Linear Equations for Individual Field Trials:

Season	**Field**	**— SD = 2.5 cm —**	**— SD = 5.1 cm —**	**— SD = 7.6 cm —**
2014	**A**	$GWL = 0.98 + 0.82 \cdot DF$	$GWL = 0.82 + 0.30 \cdot DF$	$GWL = 0.54 + 0.15 \cdot DF$
2014	**B**	$GWL = 0.92 + 0.34 \cdot DF$	$GWL = 0.80 + 0.23 \cdot DF$	$GWL = 0.61 + 0.07 \cdot DF$
2015	**A**	$GWL = 0.89 + 0.68 \cdot DF$	$GWL = 0.73 + 0.56 \cdot DF$	$GWL = 0.46 + 0.41 \cdot DF$
2015	**B**	$GWL = 0.93 + 0.61 \cdot DF$	$GWL = 0.81 + 0.49 \cdot DF$	$GWL = 0.63 + 0.34 \cdot DF$

*With: **GWL**: Measured Gauge-Wheel Load [kN]; **I**: Model Intercept; $\boldsymbol{Y_i}$, $\boldsymbol{F_j}$, $\boldsymbol{SD_k}$: Year, Field, and Row-Unit Depth effects – categorical variables; $\boldsymbol{i} \ni \{2014, 2015\}$, $\boldsymbol{j} \ni \{A, B\}$, $\boldsymbol{k} \ni \{2.5, 5.1, 7.6\}$; **DF**: Row-Unit Downforce [kN] – continuous variable; $\boldsymbol{\epsilon_{ij}}$: Random Error [cm]; **":"** denotes interaction between main effects.*

Table 4.18: Analysis of covariance conducted to model field-scale cotton gauge-wheel load response to row-unit downforce by field, growing season, and row-unit depth.

Optimized Linear Regression Model Equation:

$$GWL = I + Y_i + F_j + SD_k + DF + (Y:SD)_{ik} + (F:SD)_{jk} + Y_i:DF + F_j:DF + SD_k:DF + (Y:F:SD)_{ijk} + (Y:F)_{ij}:DF + (F:SD)_{jk}:DF + (Y:F:SD)_{ijk}:DF + \epsilon_{ij}$$

Overall Model Statistics:

Adjusted R^2 :	94.2%
F-Statistic :	82.8
textbfModel p-value :	< 0.001

Residuals [kN]:

Min	1Q	Median	3Q	Max
-0.30	-0.06	0.00	0.05	0.26

Regression Coefficients:

Model Parameters	Estimate	SE	t-value
Intercept	0.97	0.07	13.57 ***
Y_{2015}	0.07	0.09	0.74
F_B	-0.16	0.09	-1.74 ;
$SD_{1.3}$	-0.12	0.09	1.31
$SD_{2.5}$	-0.16	0.09	-1.84 .
DF	0.42	0.05	8.10 ***
$(Y:SD)_{2015,1.3}$	-0.07	0.12	-0.57
$(Y:SD)_{2015,2.5}$	-0.06	0.12	-0.48
$(F:SD)_{B,1.3}$	-0.01	0.13	-0.06
$(F:SD)_{B,2.5}$	0.8	0.12	5.54 ***
Y_{2015}:DF	0.19	0.07	2.69 **
F_B:DF	0.16	0.07	2.23 *
$SD_{1.3}$:DF	-0.04	0.07	-0.58
$SD_{2.5}$:DF	-0.00	0.07	-0.03
$(Y:F:SD)_{2015,B,0.6}$	0.19	0.13	1.43
$(Y:F:SD)_{2015,B,1.3}$	0.09	0.12	0.73
$(Y:F:SD)_{2015,B,2.5}$	-0.62	0.11	-5.52 ***
$(Y:F)_{2015,B}$:DF	-0.02	0.10	-0.16
$(F:SD)_{B,1.3}$:DF	-0.02	0.10	-0.22
$(F:SD)_{B,2.5}$:DF	-0.49	0.10	-5.03 ***
$(Y:F:SD)_{2015,A,1.3}$:DF	0.06	0.10	0.59
$(Y:F:SD)_{2015,B,1.3}$:DF	0.05	0.10	0.50
$(Y:F:SD)_{2015,A,2.5}$:DF	-0.12	0.09	-1.30
$(Y:F:SD)_{2015,B,2.5}$:DF	0.37	0.10	3.59 ***

*Significance: ***: P = 0.001; **: P = 0.01; *: P = 0.05; .: P = 0.1*

Derived Linear Equations for Individual Field Trials:

Season	Field	— SD = 2.5 cm —	— SD = 5.1 cm —	— SD = 7.6 cm —
2014	**A**	$GWL = 0.97 + 0.43 \cdot DF$	$GWL = 0.85 + 0.38 \cdot DF$	$GWL = 0.81 + 0.42 \cdot DF$
2014	**B**	$GWL = 0.81 + 0.59 \cdot DF$	$GWL = 0.68 + 0.52 \cdot DF$	$GWL = 1.32 + 0.10 \cdot DF$
2015	**A**	$GWL = 1.04 + 0.61 \cdot DF$	$GWL = 0.84 + 0.63 \cdot DF$	$GWL = 0.82 + 0.49 \cdot DF$
2015	**B**	$GWL = 1.06 + 0.76 \cdot DF$	$GWL = 0.76 + 0.74 \cdot DF$	$GWL = 0.71 + 0.63 \cdot DF$

*With: **GWL**: Measured Gauge-Wheel Load [kN]; **I**: Model Intercept; $\boldsymbol{Y_i}$, $\boldsymbol{F_j}$, $\boldsymbol{SD_k}$: Year, Field, and Row-Unit Depth effects – categorical variables; $\boldsymbol{i} \ni \{2014, 2015\}$, $\boldsymbol{j} \ni \{A, B\}$, $\boldsymbol{k} \ni \{2.5, 5.1, 7.6\}$; **DF**: Row-Unit Downforce [kN] – continuous variable; $\boldsymbol{\epsilon_{ij}}$: Random Error [cm]; ":" denotes interaction between main effects.*

4.5 Gauge-Wheel Load Variability

In-field standard deviation in measured gauge-wheel load for corn and cotton ranged from 0.1 to 0.4 kN (Tables 4.20 and 4.21). Assuming normality, approximately 68% of corn and cotton gauge-wheel load measurements ranged between 0.2 to 0.8 kN. Similarly, 95% of corn and cotton gauge-wheel load measurements ranged between 0.4 to 1.6 kN. In-field variability in measured gauge-wheel load was fairly consistent among treatment combinations. Results indicated strong in-field variability of measured gauge-wheel load, and additional analysis was required to characterize site-specific gauge-wheel load response and relationship to measured seeding depth.

Table 4.20: In-field standard deviation in measured gauge-wheel load [kN] for corn by row-unit depth, row-unit downforce, field, and growing season.

Row-Unit Depth [cm]	Row-Unit Downforce	Field A		Field A	
		– 2014 –	– 2015 –	– 2014 –	– 2015 –
2.5	**No**	0.1	0.1	0.1	0.1
	Medium	0.3	0.2	0.3	0.3
	Heavy	0.4	0.2	0.4	0.3
5.1	**No**	0.2	0.1	0.1	0.1
	Medium	0.3	0.2	0.2	0.3
	Heavy	0.4	0.2	0.3	0.2
7.6	**No**	0.2	0.1	0.2	0.1
	Medium	0.2	0.2	0.1	0.2
	Heavy	0.4	0.2	0.2	0.2

Table 4.21: In-field standard deviation in measured gauge-wheel load [kN] for cotton by row-unit depth, row-unit downforce, field, and growing season.

Row-Unit Depth [cm]	Row-Unit Downforce	Field A		Field B	
		– 2014 –	– 2015 –	– 2014 –	– 2015 –
2.5	No	0.1	0.2	0.1	0.1
	Medium	0.2	0.2	0.2	0.2
	Heavy	0.4	0.2	0.3	0.3
5.1	No	0.1	0.1	0.1	0.1
	Medium	0.3	0.2	0.3	0.3
	Heavy	0.3	0.2	0.3	0.3
7.6	No	0.1	0.1	0.2	0.1
	Medium	0.3	0.2	0.2	0.3
	Heavy	0.3	0.2	0.3	0.2

4.6 Discussion

Corn and cotton measured seeding depth was significantly affected by changing soil conditions between fields and growing seasons, and field calibration of row-unit depth and downforce adjustments is essential to ensure accurate seeding depth performance. Deeper row-unit depth must be considered in clayier and wetter soils to achieve desired seeding depth due to increased soil resistance to furrow opening. Increasing row-unit downforce significantly increased corn and cotton measured seeding depth, and heavier downforce should be associated with shallower row-unit depth to maintain accurate seeding depth. Increasing row-unit downforce from no to heavy setting on selected planter generated a 0.2 to 1.1 cm increase in measured seeding depth. Measured seeding depth and gauge-wheel load also strongly varied within individual field trials suggesting the existence of substantial spatial effects within fields. Finally, measured gauge-wheel load increased with increasing row-unit downforce, and reduced with increasing row-unit depth. Therefore, in soil conditions that are particularly sensitive to soil compaction (e.g. clayier and wetter soils), seeding depth should be adjusted by allowing deeper row-unit depths and lighter row-unit downforce.

4.7 Summary

This chapter discussed field-scale planting response to row-unit depth and downforce adjustments and changing soil conditions between fields and growing season. A summary of results is presented in Figure 4.9. Corn and cotton measured seeding depth increased with increasing row-unit depth and downforce, and row-unit downforce adjustment affected measured seeding depth by as much as 1.1 cm. Corn and cotton measured seeding depth was significantly affected by the different soil conditions between fields and growing seasons, and field calibration of row-unit depth and downforce planter settings is required to ensure accurate planter performance. Deeper row-unit depths are required in clayier and wetter soil conditions to achieve the desired seeding depth due to higher soil resistance to furrow opening. Heavier row-unit downforce limited furrow closure at typical cotton seeding depths due to better contact between the soil and planter components. Measured gauge-wheel load increased with increasing row-unit downforce, and decreased with increasing row-unit depth. Gauge-wheel load response to row-unit downforce reduced with increasing row-unit depth due to a redistribution of row-unit weight toward planter components actively involved with furrow opening and closing. Finally, measured seeding depth and measured gauge-wheel load strongly varied within individual field trials, establishing the need to investigate site-specific planting response to field spatial variability. Results and discussion enhanced understanding of field-scale planting response to row-unit depth and downforce adjustments with changing field conditions.

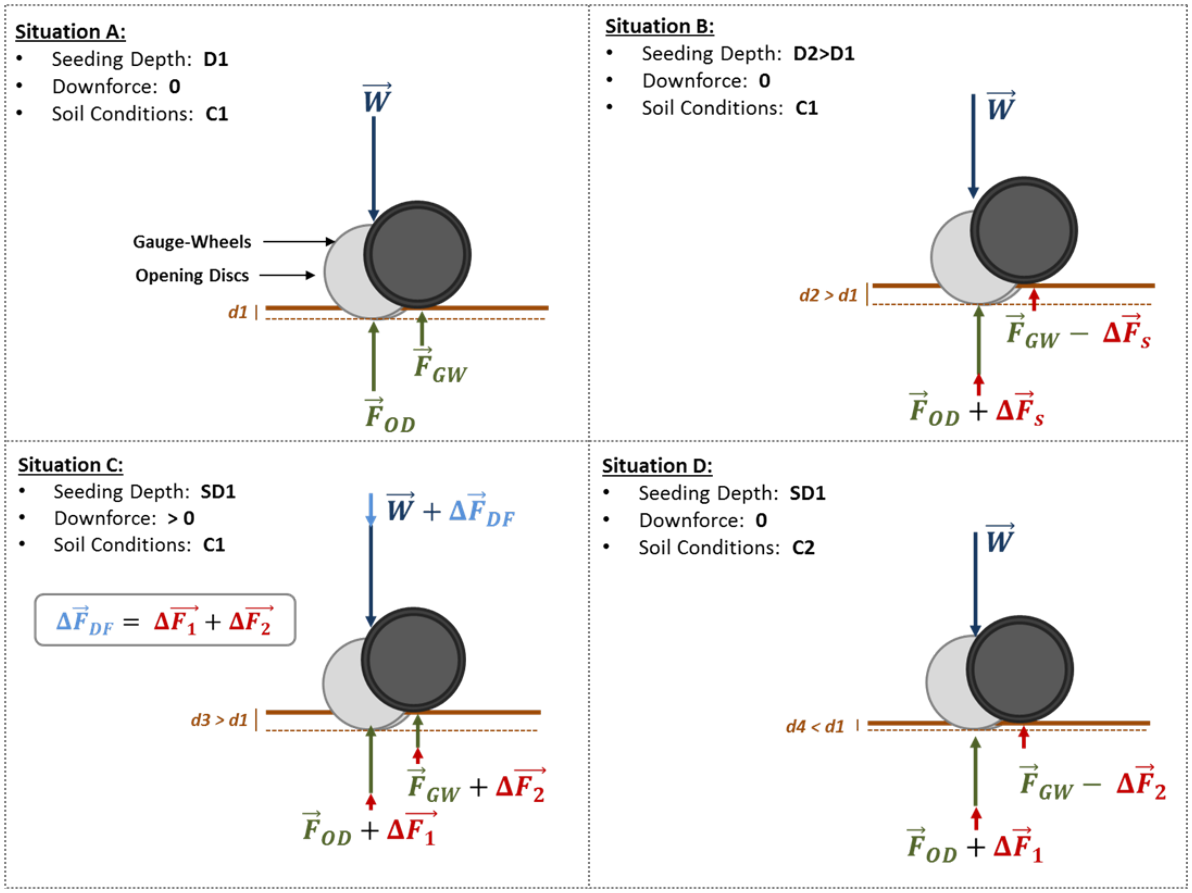

Figure 4.9: Illustration of how row-unit depth and downforce adjustments and soil conditions influence seeding depth.

C1 soil conditions providing less soil resistance to furrow opening than C2 soil conditions. $\vec{W}$**:** *row-unit weight*, $\Delta\vec{F}_{\mathbf{DF}}$**:** *applied downforce*, $\vec{F}_{\mathbf{OD}}$**:** *soil reaction force applied onto the opening discs*, and $\vec{F}_{\mathbf{GW}}$**:***soil reaction force applied onto the planter gauge-wheels.* Soil reaction forces applied onto the coulter and closing wheels were neglected in comparison to soil reaction forces applied onto the opening discs and planter gauge-wheels.

Chapter 5

Site-Specific Seeding Depth Variability

Chapter 5 evaluates site-specific seeding depth variability within individual corn and cotton trials. Results presented address objective 1 of this research. Seeding depth data collected at individual sampling sites were used to identify spatial variability within individual corn and cotton trials. Standardized soil electrical-conductivity (EC), standardized soil water content, and measured gauge-wheel load data were used to describe field spatial variablity. Analyses of covariance (ANCOVA) as well as ordinary least square (OLS) and geographically weighted (GW) regressions were computed to model in-field seeding depth relationship to row-unit depth, row-unit downforce, and selected field variables. This chapter is divided into 3 sections characterizing site-specific seeding depth variability with a discussion of the results. Complementary results to Chapter 5 are presented in appendix B.2.

5.1 Identification of Site-Specific Seeding Depth Variability

Summary of corn and cotton seeding depth response to row-unit depth and downforce adjustments by field and growing season is presented in Tables 5.1 and 5.2. Positive spatial auto-correlation – clustering – was identified among model residuals within all corn trials and within the 2015-A cotton trial (Tables 5.3 and 5.4). No spatial auto-correlation was identified among model residuals within the 2014-A, 2014-B, and 2015-B cotton trials. Therefore, significant site-specific seeding depth variability was identified within all corn trials and within the 2015-A cotton trial whereas field-scale treatment effects accounted for all explainable sources of variation in measured seeding depth within the 2014-A, 2014-B, and 2015-B cotton trials. Increased site-specific seeding depth variability identified within

Table 5.1: Analysis of covariance conducted to model field-scale corn seeding depth response to row-unit depth and downforce adjustments by field and growing season.

Optimized Linear Regression Model Equation:

$$MD = I + Y_i + F_j + (Y:F)_{ij} + SD + DF + SD:DF + Y_i:SD + F_j:SD + Y_i:DF + (Y:F)_{ij}:SD + Y_i:SD:DF + \epsilon_{ij}$$

Overall Model Statistics:	
Adjusted R^2 :	76.7%
F-Statistic :	267.6
Model p-value :	< 0.001

Residuals [cm]:

Min	**1Q**	**Median**	**3Q**	**Max**
-2.9	-0.4	0.0	0.4	2.0

Regression Coefficients:

Model Parameters	**Estimate**	**SE**	**t-value**
Intercept	1.34	0.16	8.25 ***
$\mathbf{Y_{2015}}$	2.39	0.23	10.41 ***
$\mathbf{F_B}$	0.70	0.17	4.18 ***
$\mathbf{(Y:F)_{2015,B}}$	-1.64	0.24	-6.95 ***
SD	0.58	0.03	19.50 ***
DF	0.57	0.11	4.97 ***
SD:DF	-0.02	0.02	-0.97
$\mathbf{Y_{2015}}$**:SD**	-0.25	0.04	-5.87 ***
$\mathbf{F_B}$**:SD**	0.06	0.03	2.09 *
$\mathbf{Y_{2015}}$**:DF**	0.06	0.16	0.38
$\mathbf{(Y:F)_{2015,B}}$**:SD**	0.22	0.04	5.04 ***
$\mathbf{Y_{2015}}$**:SD:DF**	-0.07	0.03	-2.44 *

*Significance: ***: P = 0.001; **: P = 0.01; *: P = 0.05; .: P = 0.1*

Derived Linear Equations for Individual Field Trials:

Season	**Field**	**Model Equation**
2014	**A**	MD = 1.35 + 0.58 · SD + 0.57 · DF – 0.02 · SD · DF
2014	**B**	MD = 2.05 + 0.65 · SD + 0.57 · DF – 0.02 · SD · DF
2015	**A**	MD = 3.74 + 0.34 · SD + 0.63 · DF – 0.09 · SD · DF
2015	**B**	MD = 4.44 + 0.62 · SD + 0.63 · DF – 0.09 · SD · DF

*With: **MD**: Measured Seeding Depth [cm]; **I**: Model Intercept; $\boldsymbol{Y_i}$, $\boldsymbol{F_j}$: Growing Season and Field effects categorical variables; $\boldsymbol{i} \ni \{2014, 2015\}$, $\boldsymbol{j} \ni \{A, B\}$; **SD, DF**: Row-Unit Depth [cm] and Downforce [kN] – continuous variables; $\boldsymbol{\epsilon_{ij}}$: Random Error [cm]; ":" denotes interaction between main effects.*

Table 5.2: Analysis of covariance conducted to model field-scale cotton seeding depth response to row-unit depth and downforce adjustments by field and growing season.

Optimized Linear Regression Model Equation:

$$MD = I + Y_i + F_j + (Y:F)_{ij} + SD + DF + Y_i:SD + F_j:SD + Y_i:DF + (Y:F)_{ij}:SD + \epsilon_{ij}$$

Overall Model Statistics:

Adjusted R^2 :	58.9%
F-Statistic :	77.6
Model p-value :	< 0.001

Residuals [cm]:

Min	1Q	Median	3Q	Max
-0.9	-0.2	0.0	0.2	1.3

Regression Coefficients:

Model Parameters	Estimate	SE	t-value
Intercept	0.82	0.09	9.15 ***
Y_{2015}	-0.07	0.12	-0.55
F_B	0.08	0.11	0.71
SD	0.32	0.05	6.68 ***
DF	0.09	0.03	2.68 **
$(Y:F)_{2015,B}$	0.17	0.15	1.13
Y_{2015}:SD	0.35	0.06	5.44 ***
F_B:SD	0.09	0.06	1.53
Y_{2015}:DF	0.13	0.05	2.85 **
$(Y:F)_{2015,B}$:SD	-0.34	0.09	-3.91 ***

*Significance: ***: P = 0.001; **: P = 0.01; *: P = 0.05; .: P = 0.1*

Derived Linear Equations for Individual Field Trials:

Season	Field	——— Model Equation ———
2014	**A**	MPD = 0.82 + 0.32 · SD + 0.09 · DF
2014	**B**	MPD = 0.89 + 0.41 · SD + 0.09 · DF
2015	**A**	MPD = 0.75 + 0.66 · SD + 0.22 · DF
2015	**B**	MPD = 0.99 + 0.42 · SD + 0.22 · DF

*With: **MD**: Measured Seeding Depth [cm]; **I**: Model Intercept; $\boldsymbol{Y_i}$, $\boldsymbol{F_j}$: Growing Season and Field effects categorical variables; $\boldsymbol{i} \ni \{2014, 2015\}$, $\boldsymbol{j} \ni \{A, B\}$; **SD, DF**: Row-Unit Depth [cm] and Downforce [kN] – continuous variables; $\boldsymbol{\epsilon_{ij}}$: Random Error [cm]; **":"** denotes interaction between main effects.*

corn versus cotton trials resulted from stronger soil-planter interactions as corn was planted deeper than cotton. Significant site-specific seeding depth variability identified within the 2015-A cotton trial was explained by the higher percentage of cotton seeds that failed to be placed within the soil furrow in this particular trial (Table 4.7). Indeed, germination of those seeds was limited by available soil water on the soil surface whereas seeding depth was exclusively measured on emerged cotton seedlings. Further analysis of data was computed for corn only.

Table 5.3: Evaluation of spatial auto-correlations among residuals from ANCOVA models characterizing site-specific seeding depth variability within individual corn trials.

Season	Field	Global Moran's I	Spatial Auto-Correlation
2014	**A**	0.23 ***	Clustered
2014	**B**	0.14 ***	Clustered
2015	**A**	0.33 ***	Clustered
2015	**B**	0.11 ***	Clustered

*** *: Significant at P = 0.01.*

Table 5.4: Evaluation of spatial auto-correlations among residuals from ANCOVA models characterizing site-specific seeding depth variability within individual cotton trials.

Season	Field	Global Moran's I	Spatial Auto-Correlation
2014	**A**	-0.02	Random
2014	**B**	0.02	Random
2015	**A**	0.22 ***	Clustered
2015	**B**	0.12	Random

*** *: Significant at P = 0.01.*

5.2 Explanation of Site-Specific Seeding Depth Variability

5.2.1 Seeding Depth Relationship to Soil EC and Soil Water Content

Corn seeding depth was not significantly correlated to standardized soil water content data. Corn seeding depth was significantly correlated to standardized soil EC data (Table 5.5), and site-specific seeding depth relationship to standardized soil EC explained 8.5%, 5.5%, 28.8%, and 4.3% of seeding depth variability within the 2014-A, 2014-B, 2015-A, and

2015-B corn trials, respectively. No spatial auto-correlation was identified among new model residuals (Table 5.6), and seeding depth relationship to standardized soil EC explained all site-specific seeding depth variability identified within individual corn trials in section 5.1. For 2014-A, a 1 $mS.m^{-1}$ increase in soil EC was correlated to a 0.05 cm reduction in corn seeding depth throughout the trial. Seeding depth relationship to standardized soil EC was not uniform across the other corn trials, and 1 $mS.m^{-1}$ increase in soil EC was correlated to seeding depth variations ranging from -0.29 cm to 0.48 cm. Such result was consistent with information published in literature as several studies demonstrated non-linear soil EC relationship to crop production parameters (Grisso et al., 2009). In-field seeding depth relationship to standardized soil EC within individual corn trials are illustrated in 5.1 to 5.4. In-field changes in soil EC were correlated to in-field seeding depth variations of 1.0 cm, 0.3 cm, 1.6 cm, and 0.4 cm within the 2014-A, 2014-B, 2015-A, and 2015-B corn trials, respectively. Stronger seeding depth relationship to standardized soil EC was observed in field A due to greater spatial variability.

Table 5.5: Corn seeding depth relationship to row-unit depth, row-unit downforce, and standardized soil EC by field and growing season.

Season	Field	Model Equation
2014	**A**	$MD = 1.35 + 0.58 \cdot SD + 0.57 \cdot DF - 0.02 \cdot SD \cdot DF - \mathbf{0.05} \cdot \mathbf{EC}$
2014	**B**	$MD = 2.05 + 0.65 \cdot SD + 0.57 \cdot DF - 0.02 \cdot SD \cdot DF + \gamma_{XY} \cdot \mathbf{EC}$
2015	**A**	$MD = 3.74 + 0.34 \cdot SD + 0.63 \cdot DF - 0.09 \cdot SD \cdot DF + \gamma_{XY} \cdot \mathbf{EC}$
2015	**B**	$MD = 4.44 + 0.62 \cdot SD + 0.63 \cdot DF - 0.09 \cdot SD \cdot DF + \gamma_{XY} \cdot \mathbf{EC}$

MD: Measured Seeding Depth [cm]; **SD, DF:** Row-Unit Depth [cm] and Downforce [kN]; **EC:** Standardized Soil EC [$mS.m^{-1}$]; γ_{XY}**:** Local Regression Coefficient for Standardized Soil EC [$cm/mS.m^{-1}$].

Table 5.6: Evaluation of spatial auto-correlations among residuals from regression models characterizing seeding depth relationship to standardized soil EC within individual corn trials.

Season	Field	Global Moran's I	Spatial Auto-Correlation
2014	**A**	0.11	Random
2014	**B**	0.04	Random
2015	**A**	-0.04	Random
2015	**B**	0.07	Random

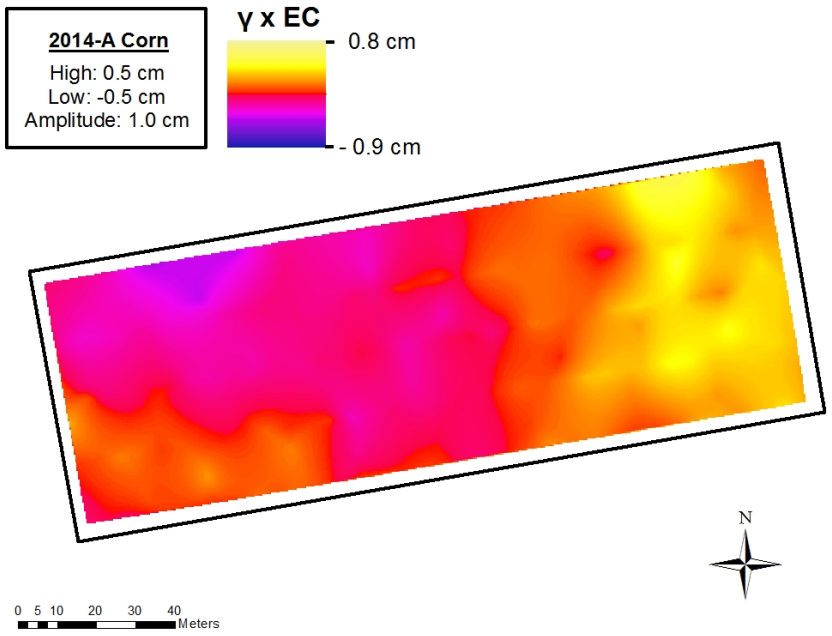

Figure 5.1: Site-specific seeding depth relationship to standardized soil EC within the 2014-A corn trial.

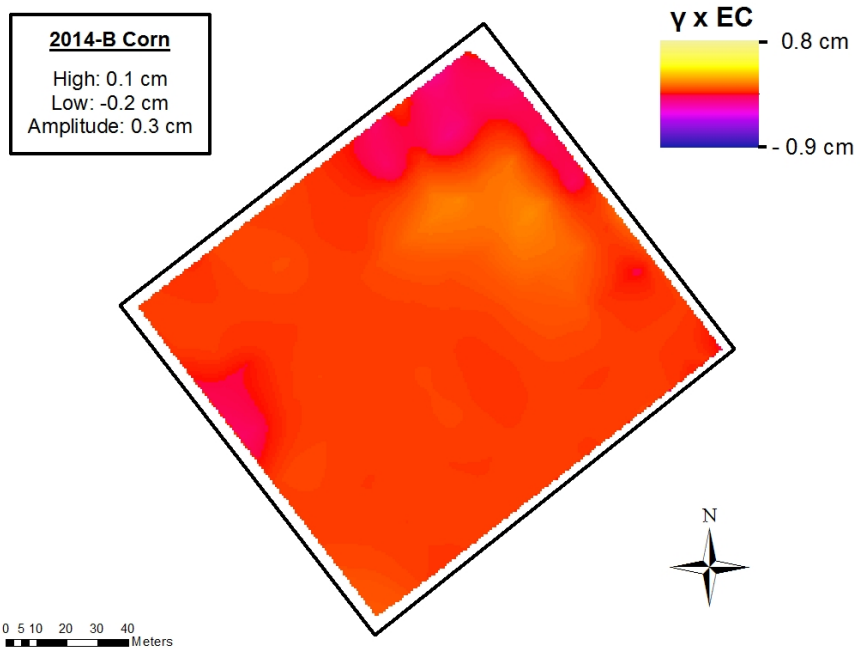

Figure 5.2: Site-specific seeding depth relationship to standardized soil EC within the 2014-B corn trial.

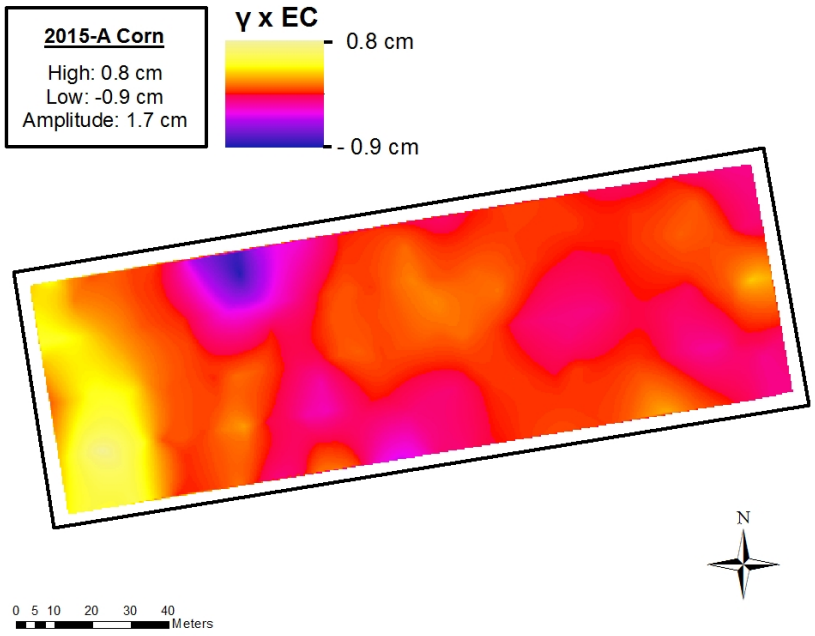

Figure 5.3: Site-specific seeding depth relationship to standardized soil EC within the 2015-A corn trial.

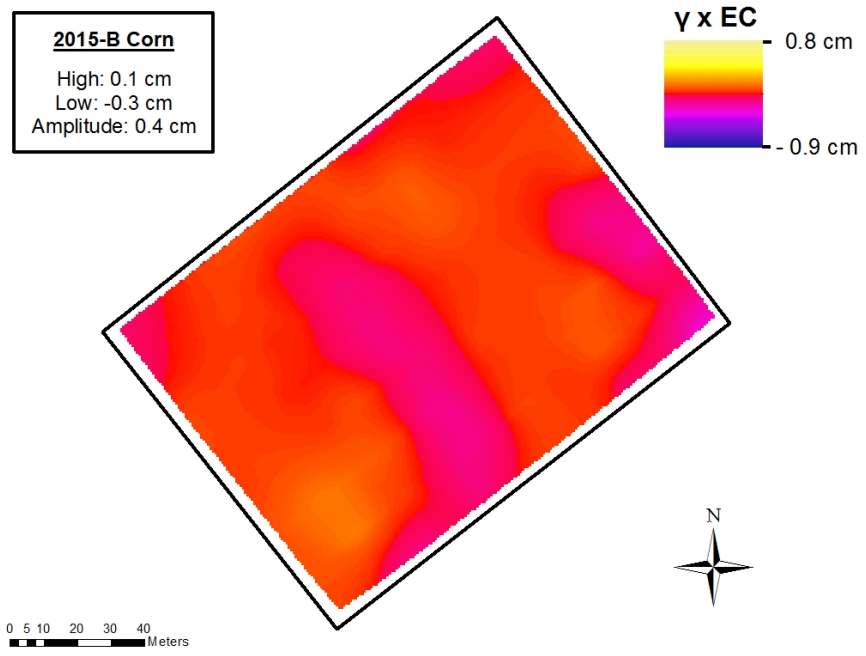

Figure 5.4: Site-specific seeding depth relationship to standardized soil EC within the 2015-A corn trial.

5.2.2 Seeding Depth Relationship to Measured Gauge-Wheel Load

Gauge-wheel has previously been used in literature to describe seeding depth variability within fields (Hanna et al., 2010). Computed regression models generated p-values less than 0.05 and explained 2% to 6% of seeding depth variability within individual corn trials (Table 5.7). No spatial auto-correlation was identified among new model residuals within the 2014-B and 2015-B corn trials (Table 5.8), and seeding depth relationship to measured gauge-wheel load explained all site-specific seeding depth variability identified in section 5.1 for field B. Positive spatial auto-correlation – clustering – persisted within the 2014-A and 2015-A corn trials, and seeding depth relationship to measured gauge-wheel load did not explain all site-specific seeding depth variability identified in section 5.1 for field A. Field A exhibited stronger spatial variability than field B, and results suggested that gauge-wheel load data did not provide sufficient information to describe spatial variability in more heterogeneous field conditions. Seeding depth relationship to measured gauge-wheel load varied with row-unit depth since affecting row-unit geometry.

Table 5.7: Corn seeding depth relationship to row-unit depth, row-unit downforce, and measured gauge-wheel load by field and growing season.

Season	Field	Model Equation
2014	**A**	$MD = 1.35 + 0.58 \cdot SD + 0.57 \cdot DF - 0.02 \cdot SD \cdot DF + \gamma_{SD} \cdot \mathbf{GWL}$
2014	**B**	$MD = 2.05 + 0.65 \cdot SD + 0.57 \cdot DF - 0.02 \cdot SD \cdot DF + \gamma_{SD} \cdot \mathbf{GWL}$
2015	**A**	$MD = 3.74 + 0.34 \cdot SD + 0.63 \cdot DF - 0.09 \cdot SD \cdot DF + \gamma_{SD} \cdot \mathbf{GWL}$
2015	**B**	$MD = 4.44 + 0.62 \cdot SD + 0.63 \cdot DF - 0.09 \cdot SD \cdot DF + \gamma_{SD} \cdot \mathbf{GWL}$

MD: Measured Seeding Depth [cm]; **SD, DF:** Row-Unit Depth [cm] and Downforce [kN]; **GWL:** Measured Gauge-Wheel Load [kN]; γ_{XY}**:** Regression Coefficient for Measured Gauge-Wheel Load – varies with row-unit depth [cm/kN].

Table 5.8: Evaluation of spatial auto-correlations among regression model residuals characterizing seeding depth response to measured gauge-wheel load within individual corn trials.

Season	Field	Global Moran's I	Spatial Auto-Correlation
2014	**A**	0.14^{**}	Clustered
2014	**B**	0.01	Random
2015	**A**	0.22^{***}	Clustered
2015	**B**	0.07	Random

** *: Significant at P = 0.05* *** *: Significant at P = 0.01*

5.3 Discussion

Significant site-specific seeding depth variability was measured for corn. Therefore, opportunities exist to improve seeding depth consistency of standard row-crop planters. No site-specific seeding depth variability was determined within 3 of 4 cotton trials. Corn seeding depth was not significantly correlated to soil water content, and soil water content data could not be used in this study to describe site-specific seeding depth variability. Corn seeding depth was significantly affected by soil EC, and soil EC data explained all spatial effects identified within individual corn trials. Corn seeding depth was also significantly correlated to measured gauge-wheel load, and gauge-wheel load data explained all spatial effects identified within field B but not within field A because of stronger spatial variability in this field. This demonstrated the possibility of using real-time gauge-wheel load monitoring to manage planter settings adjustments during the planting operation. However, benefits from developing a technology with such capabilities could be limited to more uniform field situations.

5.4 Summary

This chapter discussed corn and cotton site-specific seeding depth variability. Significant site-specific seeding depth variability was measured within individual corn trials, outlining opportunities to improve standard row-crop planters seeding depth performance. Stronger site-specific seeding depth variability was observed within individual corn versus cotton trials. Corn seeding depth was not significantly correlated to standardized soil water content data in this study. Corn seeding depth was significantly correlated to standardized soil EC data, and seeding depth relationship to soil EC explained 4.3% to 28.8% of total seeding depth variability within individual corn trials. In-field changes in soil EC were correlated to in-field seeding depth variations of 0.3 to 1.6 cm. Stronger seeding depth relationship to standardized soil EC was observed in field A due to greater spatial variability. Corn seeding

depth was also significantly correlated to measured gauge-wheel load at planting. Seeding depth relationship to measured gauge-wheel load explained 2% to 6% of seeding depth variability within individual corn trials. Results provided in this chapter established baseline models used in Chapter 7 to outline implementation of prescription-based and real-time planting technologies to improve seed placement at planting.

Chapter 6

Corn Emergence and Yield Response to Seeding Depth, Gauge-Wheel Load and Varying Field Conditions in the Southeast US

Chapter 6 investigates corn emergence and yield response to measured seeding depth, gauge-wheel load, and varying soil conditions between fields and growing seasons. Results and discussion address objective 2. Emergence data were analyzed separately for 2014 and 2015 growing seasons since exhibiting different responses to treatment combinations. Corn emergence was evaluated on the following criteria: final live population, emergence timeliness, uniformity of emergence, and seedling vigor. Yield data were analyzed across growing seasons. Results and discussion are presented into 6 individual sections. Complementary results to Chapter 6 are presented in appendix B.3.

6.1 Final Corn Population

The 2014 final corn population was significantly affected by field, row-unit depth, and row-unit downforce (Table 6.1). The 2015 final corn population was significantly affected by field, row-unit depth, row-unit downforce, and the two-way interaction between field and row-unit depth (Table 6.2). Final corn population was higher in 2015 than in 2014. Therefore, warmer soil temperatures observed during the 2015 planting season provided better soil conditions for corn emergence and similar response to soil temperature has been described in literature (Alessi and Power, 1971; Scheider and Gupta, 1985). Weather conditions during the 2014 planting season did not enable to achieve the expected 95% corn emergence rate. Final corn population was higher in field B than in field A and lower clay content in field B also provided better soil conditions for corn emergence by limiting soil crusting after rainfall

and promoting better drainage in lower areas of the field. Such response to soil texture was consistent with results published in literature (Elmore et al., 2015). Medium row-unit downforce maximized final corn population at the 2.5 and 5.1 cm row-unit depth during the 2014 planting season. No row-unit downforce maximized final corn population at the 2.5 and 5.1 cm row-unit depth during the 2015 planting season. Final corn population response to measured seeding depth and gauge-wheel laod was non-linear (Tables 6.3 and 6.4). Achieved seeding depths of 3.8 and 4.4 cm maximized final corn population at 89.5% and 93.8% within the 2014-A and 2014-B field trials, respectively (Figure 6.1). Achieved seeding depth of 4.0 cm maximized final corn population at 94.3% and 96.9% within 2015-A and 2015-B field trials (Figure 6.2). Deviations from these optimum seeding depths (ΔDepth [cm]) decreased final corn population by -1.6$\cdot\Delta$Depth^2 [%] in 2014, and -0.4$\cdot\Delta$Depth^2 [%] in 2015. At the optimum seeding depths, gauge-wheel loads of 1.3 kN, 1.9 kN, and 1.1 kN increased final corn population by an additional 2.3%, 1.1%, and 0.9% within the 2014-A, 2014-B, and 2015-B field trials, respectively. Deviations from these gauge-wheel loads (ΔGWL [kN]) decreased final corn population by -15.2 $\cdot$ ΔGWL^2 [%] in 2014-A, -1.5 $\cdot$ ΔGWL^2 [%] in 2014-B, and -1.7 $\cdot$ ΔGWL^2 [%] in 2015-B. Final corn population was not significantly affected by gauge-wheel load in 2015-A. Stronger seeding depth and gauge-wheel load effects in 2014 versus 2015 demonstrated greater final population response to row-crop planter performance in least favorable soil conditions for corn establishment.

Table 6.1: Mixed-effect analysis of variance conducted for corn final population data during the 2014 growing season.

Mixed-Effect Model Equation:

$$FP = \mu + F_j + SD_k + DF_l + (F:SD)_{jk} + (F:DF)_{jl} + (SD:DF)_{kl} + (F:SD:DF)_{jkl} + \tau_r + \epsilon_{jkl}$$

Scaled Residuals [%]:

Min	1Q	Median	3Q	Max
-2.5	-0.2	0.0	0.3	2.7

Random Effects:

Groups	Variance [cm^2]	Std. Dev. [%]
Whole Plot Error	0.03	0.20
Sub Plot Error	22.99	4.79

Fixed Effects - ANOVA Table:

Model Parameters	Df	Sum Sq.	Mean Sq.	F-Value	Sum Sq. [%]
F	1	212.32	212.32	9.23 *	10.3
SD	2	1373.20	686.60	29.86 ***	66.5
DF	2	140.90	70.45	3.06 .	6.8
F:SD	2	4.19	2.10	0.09	0.2
F:DF	2	106.69	53.34	2.32	5.2
SD:DF	4	93.70	23.43	1.02	4.5
F:SD:DF	4	134.94	33.73	1.47	6.5

*Significance: ***: P = 0.001; **: P = 0.01; *: P = 0.05; .: P = 0.1*

Estimated Means:

Row-Unit Depth	Row-Unit Downforce	Field A		Field B	
		Plants.Acre^{-1}	% Seeding Rate	Plants.Acre^{-1}	% Seeding Rate
2.5 cm	**No**	23,520	89.2% ^{abcd}	24,670	93.5% ^{ab}
	Medium	24,030	91.1% ^{abc}	25,100	95.2% ^{a}
	Heavy	23,470	89.0% ^{abcd}	24,780	94.0% ^{ab}
5.1 cm	**No**	23,390	88.7% ^{abcd}	23,830	90.4% ^{abcd}
	Medium	23,590	89.5% ^{abcd}	24,570	93.2% ^{abc}
	Heavy	22,470	85.2% ^{abcd}	23,760	90.1% ^{abcd}
7.6 cm	**No**	21,870	82.9% ^{cd}	22,360	84.8% ^{abcd}
	Medium	22,010	83.5% ^{bcd}	20,910	79.3% ^{de}
	Heavy	18,860	71.5% ^{e}	22,070	83.7% ^{bcd}

$^{a,\ldots,l}$ *: Least significant difference between treatments at a 95% confidence interval.*

With: ***FP****: Final Corn Population;* $\boldsymbol{\mu}$*: Model Intercept;* $\boldsymbol{F_j}$*,* $\boldsymbol{SD_k}$*,* $\boldsymbol{DF_l}$*: Field, Row-Unit Depth, and Row-Unit Downforce main effects;* $\boldsymbol{j} \ni \{A, B\}$*,* $\boldsymbol{k} \ni \{2.5, 5.1, 7.6\}$*,* $\boldsymbol{l} \ni \{No, Medium, Heavy\}$*;* $\boldsymbol{\tau_r}$*:* ***Random Effect*** *– defined as a replication within a field;* $\boldsymbol{r} \in \{1, 2, ..., 7\}$*;* $\boldsymbol{\epsilon_{ijkl}}$*:* ***Random Error****; ":" denotes interaction between two or more main effects.*

Table 6.2: Mixed-effect analysis of variance conducted for corn final population data during the 2015 growing season.

Mixed-Effect Model Equation:

$$FP = \mu + F_j + SD_k + DF_l + (F:SD)_{jk} + (F:DF)_{jl} + (SD:DF)_{kl} + (F:SD:DF)_{jkl} + \tau_r + \epsilon_{jkl}$$

Scaled Residuals [%]:

Min	1Q	Median	3Q	Max
-2.6	-0.4	0.0	0.6	2.2

Random Effects:

Groups	Variance [cm^2]	Std. Dev. [%]
Whole Plot Error	0.24	0.50
Sub Plot Error	4.94	2.22

Fixed Effects - ANOVA Table:

Model Parameters	Df	Sum Sq.	Mean Sq.	F-Value	Sum Sq. [%]
F	1	37.93	37.93	7.68 **	10.5
SD	2	141.61	70.0	14.34 ***	39.1
DF	2	30.57	30.28	6.13 **	16.7
F:SD	2	66.66	33.33	6.75 **	18.4
F:DF	2	5.24	2.62	0.53	1.4
SD:DF	4	15.65	3.94	0.79	4.3
F:SD:DF	4	34.71	8.68	1.76	9.6

*Significance: ***: P = 0.001; **: P = 0.01; *: P = 0.05; .: P = 0.1*

Estimated Means:

Row-Unit Depth	Row-Unit Downforce	Field A		Field B	
		Plants.Acre^{-1}	% Seeding Rate	Plants.Acre^{-1}	% Seeding Rate
2.5 cm	**No**	25,220	95.7% ^{abcd}	25,710	97.5% ^{a}
	Medium	25,100	95.2% ^{abcd}	25,620	97.2% ^{abc}
	Heavy	24,910	94.5% ^{abcd}	25,450	96.5% ^{abc}
5.1 cm	**No**	24,950	94.6% ^{abcd}	25,660	97.3% ^{ab}
	Medium	24,330	92.3% ^{cde}	25,480	96.6%^{abc}
	Heavy	24,130	91.5% ^{de}	25,420	96.4% ^{abcd}
7.6 cm	**No**	24,660	93.5% ^{abcd}	25,130	95.3% ^{abcd}
	Medium	24,370	92.4% ^{bde}	24,230	91.9% ^{cde}
	Heavy	24,340	92.3% ^{cde}	23,130	87.7% ^{e}

$^{a,...,l}$ *: Least significant difference between treatments at a 95% confidence interval.*

With: ***FP****: Final Corn Population;* $\boldsymbol{\mu}$*: Model Intercept;* $\boldsymbol{F_j}$*,* $\boldsymbol{SD_k}$*,* $\boldsymbol{DF_l}$*: Field, Row-Unit Depth, and Row-Unit Downforce main effects;* $\boldsymbol{j} \ni \{A, B\}$*,* $\boldsymbol{k} \ni \{2.5, 5.1, 7.6\}$*,* $\boldsymbol{l} \ni \{No, Medium, Heavy\}$*;* $\boldsymbol{\tau_r}$*:* ***Random Effect*** *– defined as a replication within a field;* $\boldsymbol{r} \in \{1, 2, ..., 7\}$*;* $\boldsymbol{\epsilon_{ijkl}}$*:* ***Random Error****; ":" denotes interaction between two or more main effects.*

Table 6.3: Analysis of covariance (ANCOVA) conducted to model 2014 field-scale final corn population response to measured seeding depth and gauge-wheel load.

Optimized ANCOVA Model Equation:

$$FP = I + F_j + F_j : MD + F_j : (MD)^2 + (F : SD)_{jk} : GWL + (F : SD)_{jk} : GWL^2 + \epsilon_{ij}$$

Overall Model Statistics:

Adjusted R^2 :	55.7%
Model p-value :	< 0.001

Residuals [%]:

Min	1Q	Median	3Q	Max
-10.9	-2.0	0.4	2.3	10.3

Regression Coefficients:

Model Parameters	Estimate	SE	t-value
Intercept	66.24	14.99	4.43 ***
F_B	-4.57	26.26	-0.17
F_A:MD	12.26	6.77	1.81 .
F_B:MD	14.32	8.00	1.79 .
F_A:MD^2	-1.63	0.72	-2.28 *
F_B:MD^2	-1.61	0.71	-2.26 *
$(F:SD)_{A,2.5}$:GWL	12.40	11.66	1.06
$(F:SD)_{B,2.5}$:GWL	2.83	16.40	0.17
$(F:SD)_{A,5.1}$:GWL	4.64	17.08	0.27
$(F:SD)_{B,5.1}$:GWL	15.79	22.74	0.69
$(F:SD)_{A,7.6}$:GWL	-23.98	20.45	-1.17
$(F:SD)_{B,7.6}$:GWL	-253.31	112.56	-2.25 *
$(F:SD)_{A,2.5}$:GWL^2	-15.22	14.94	-1.02
$(F:SD)_{B,2.5}$:GWL^2	-1.52	25.99	-0.06
$(F:SD)_{A,5.1}$:GWL^2	-2.35	28.12	-0.08
$(F:SD)_{B,5.1}$:GWL^2	-33.63	63.43	-0.53
$(F:SD)_{A,7.6}$:GWL^2	21.51	51.99	0.41
$(F:SD)_{B,7.6}$:GWL^2	-3168.20	1177.90	-2.69 **

*Significance: ***: P = 0.001; **: P = 0.01; *: P = 0.05; .: P = 0.1*

Derived Linear Equations for Field A and B:

Field	Model Equation
A	$FP = 66.4 + 12.3 \cdot MD - 1.6 \cdot MD^2 + \alpha_{SD} \cdot GWL + \beta_{SD} \cdot GWL^2$
B	$FP = 61.8 + 14.3 \cdot MD - 1.6 \cdot MD^2 + \alpha_{SD} \cdot GWL + \beta_{SD} \cdot GWL^2$

*With: **FP**: Final Corn Population [%]; **I**: Model Intercept; $\boldsymbol{F_j}$, $\boldsymbol{SD_k}$: Field and Row-Unit Depth effects – categorical variables; $\boldsymbol{j} \ni \{A, B\}$, $\boldsymbol{k} \ni \{2.5, 5.1, 7.6\}$; **MD, GWL**: Corn Seeding Depth [kN], Difference between measured gauge-wheel and gauge-wheel load at 0.0 kN row-unit downforce at selected row-unit depth – continuous variables; $\boldsymbol{\epsilon_{ij}}$: **Random Error** [cm]; **":"** denotes interaction between main effects.*

Table 6.4: Analysis of covariance (ANCOVA) conducted to model 2015 field-scale final corn population response to measured seeding depth and gauge-wheel load.

Optimized ANCOVA Model Equation:

$$MD = I + F_j + MD + (MD)^2 + (F:SD)_{jk}:GWL + (F:SD)_{jk}:GWL^2 + \epsilon_{ij}$$

Overall Model Statistics:

Adjusted R^2 :	42.9%
Model p-value :	< 0.001

Residuals [%]:

Min	1Q	Median	3Q	Max
-7.5	-0.4	0.3	1.0	4.2

Regression Coefficients:

Model Parameters	Estimate	SE	t-value
Intercept	89.36	10.22	8.65 ***
F_B	2.50	0.77	3.24 **
MD	2.90	3.62	0.80
MD^2	-0.36	0.32	-1.15
$(F:SD)_{A,2.5}$:GWL	-0.15	5.09	-0.03
$(F:SD)_{B,2.5}$:GWL	0.60	5.04	0.12
$(F:SD)_{A,5.1}$:GWL	-2.73	5.46	-0.50
$(F:SD)_{B,5.1}$:GWL	3.57	5.83	0.61
$(F:SD)_{A,7.6}$:GWL	0.85	6.32	0.13
$(F:SD)_{B,7.6}$:GWL	-8.67	8.90	-0.98
$(F:SD)_{A,2.5}$:GWL^2	0.03	4.2	0.01
$(F:SD)_{B,2.5}$:GWL^2	-1.68	4.76	-0.35
$(F:SD)_{A,5.1}$:GWL^2	-0.06	6.30	-0.01
$(F:SD)_{B,5.1}$:GWL^2	-3.20	5.94	-0.54
$(F:SD)_{A,7.6}$:GWL^2	-5.44	9.40	-0.58
$(F:SD)_{B,7.6}$:GWL^2	-2.33	13.37	-0.17

*Significance: *** : P = 0.001; ** : P = 0.01; * : P = 0.05; .: P = 0.1*

Derived Linear Equations for Field A and B:

Field	Model Equation
A	$FP = 88.5 + 2.9 \cdot MD - 0.4 \cdot MD^2 + \alpha_{SD} \cdot GWL + \beta_{SD} \cdot GWL^2$
B	$FP = 91.0 + 2.9 \cdot MD - 0.4 \cdot MD^2 + \alpha_{SD} \cdot GWL + \beta_{SD} \cdot GWL^2$

*With: **FP**: Final Corn Population [%]; **I**: Model Intercept; $\boldsymbol{F_j}$, $\boldsymbol{SD_k}$: Field and Row-Unit Depth effects – categorical variables; $\boldsymbol{j} \ni \{A, B\}$, $\boldsymbol{k} \ni \{2.5, 5.1, 7.6\}$; **MD, GWL**: Corn Seeding Depth [kN], Difference between measured gauge-wheel and gauge-wheel load at 0.0 kN row-unit downforce at selected row-unit depth – continuous variables; $\boldsymbol{\epsilon_{ij}}$: **Random Error** [cm]; **":"** denotes interaction between main effects.*

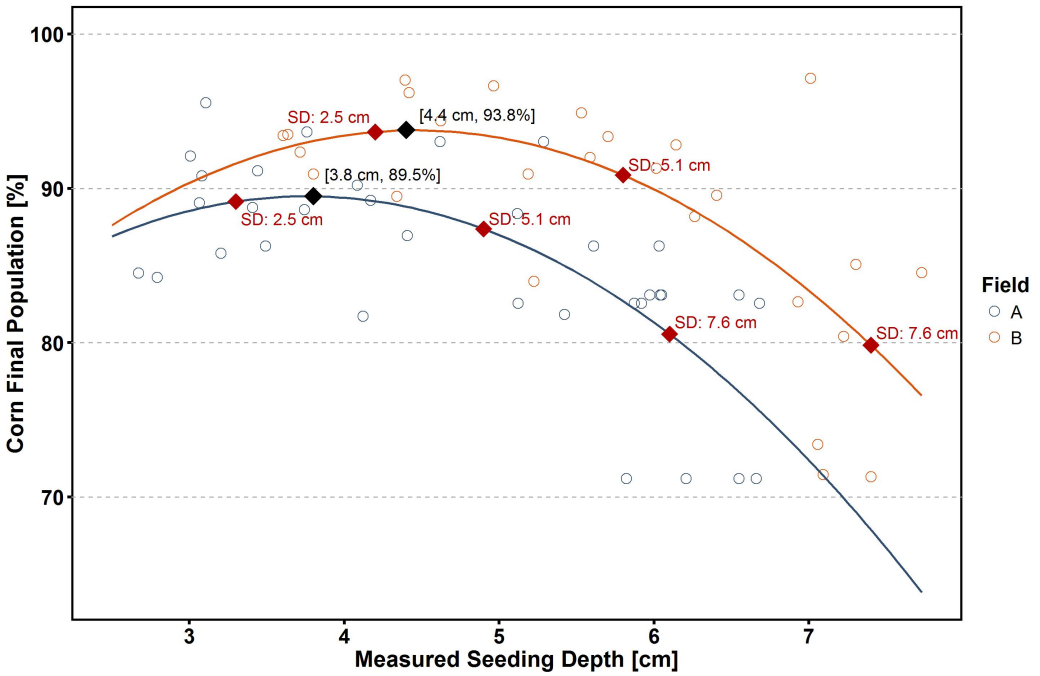

Figure 6.1: Determination of optimum seeding depth to maximize final population of corn within individual 2014 field trials – SD: row-unit depth adjustment.

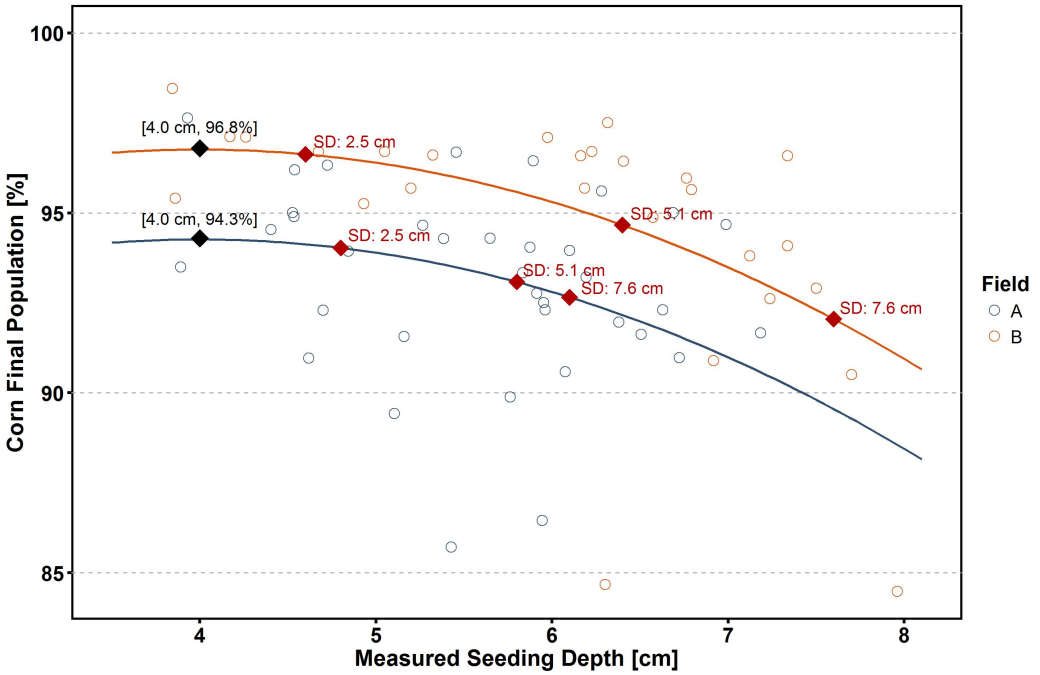

Figure 6.2: Determination of optimum seeding depth to maximize final population of corn within individual 2014 field trials – SD: row-unit depth adjustment.

6.2 Emergence Timeliness

In 2015, full emergence was achieved in less than 6 days which corresponded to the initial date for data collection due to poor weather conditions. Hence, 2015 data did not enable accurate determination of the corn emergence window. Therefore, results presented in this section focus on 2014 data only. In 2014, corn emergence began on day 11 for 16 out of 18 treatment combinations (Table 6.5), and the beginning of emergence was consistent across field, row-unit depth, and row-unit downforce. Later emergence was explained by cooler and wetter soil conditions than during the 2015 growing season, which was consitent with results found in literature (Hesketh and Warrington, 1989). The 2014 emergence duration was significantly affected by field, row-unit depth, and row-unit downforce (Table 6.6). The 2014 emergence duration was 1 to 2 days longer in field A than in field B as clayier soils in field a crusted after rainfall, generating excessive soil resistance to seedling emergence and more delayed emergence. Emergence duration linearly increased with increasing seeding depth (Table 6.7), and deeper seeding depths were characterized by poorer emergence timeliness. Emergence duration response to gauge-wheel load was non-linear, and 1.3 kN gauge-wheel load minimized emergence duration in both 2014-A and 2014-B field trials. Deviations from this optimum gauge-wheel load (ΔGWL [kN]) increased emergence duration by $10.2 \cdot \Delta GWL^2$ [days] in 2014-A, and by $4.4 \cdot \Delta GWL^2$ [days] in 2014-B.

Table 6.5: Corn emergence window for the 2014 growing season.

Seeding Depth	Row-unit Downforce	Field A [DAP - DAP]	Field B [DAP - DAP]
2.5 cm	**No**	11 - 16	11 - 14
	Medium	11 - 16	11 - 14
	Heavy	11 - 17	11 - 15
5.1 cm	**No**	11 - 18	11 - 17
	Medium	11 - 21	11 - 18
	Heavy	11 - 21	11 - 20
7.6 cm	**No**	11 - 22	11 - 20
	Medium	12 - 23	11 - 21
	Heavy	12 - 22	11 - 23

DAP: Days After Planting

Table 6.6: Mixed-effect analysis of variance conducted for 2014 corn emergence duration data.

Mixed-Effect Model Equation:

$$ED = \mu + F_j + SD_k + DF_l + (F:SD)_{jk} + (F:DF)_{jl} + (SD:DF)_{kl} + (F:SD:DF)_{jkl} + \tau_r + \epsilon_{jkl}$$

Scaled Residuals [days]:

Min	1Q	Median	3Q	Max
-2.0	-0.5	0.0	0.7	1.4

Random Effects:

Groups	Variance [cm^2]	Std. Dev. [%]
Whole Plot Error	0.49	0.70
Sub Plot Error	1.05	1.02

Fixed Effects - ANOVA Table:

Model Parameters	Df	Sum Sq.	Mean Sq.	F-Value	Sum Sq. [%]
F	1	7.36	7.36	7.01 *	1.9
SD	2	348.80	174.40	166.18 ***	88.0
DF	2	19.65	9.83	9.36 ***	5.0
F:SD	2	2.46	1.23	1.17	0.6
F:DF	2	6.08	3.04	2.90 .	1.5
SD:DF	4	6.26	1.57	1.49	1.6
F:SD:DF	4	5.58	1.39	1.33	1.4

*Significance: ***: P = 0.001; **: P = 0.01; *: P = 0.05; .: P = 0.1*

Estimated Means:

Row-Unit Depth	Row-unit Downforce	Field A [days]	Field B [days]
2.5 cm	**No**	5 ef	3 f
	Medium	5 ef	3 f
	Heavy	6 def	4 f
5.1 cm	**No**	7 bcde	6 cdef
	Medium	10 ab	7 bcde
	Heavy	10 ab	9 abc
7.6 cm	**No**	11 ab	9 abc
	Medium	11 a	10 ab
	Heavy	10 ab	12 a

$^{a,\ldots,f}$ *: Least significant difference between treatments at a 95% confidence interval.*

With: ***ED****: Corn Emergence Duration;* $\boldsymbol{\mu}$*: Model Intercept;* $\boldsymbol{F_j}$*,* $\boldsymbol{SD_k}$*,* $\boldsymbol{DF_l}$*: Field, Row-Unit Depth, and Row-Unit Downforce main effects;* $\boldsymbol{j} \ni \{A, B\}$*,* $\boldsymbol{k} \ni \{2.5, 5.1, 7.6\}$*,* $\boldsymbol{l} \ni \{No, Medium, Heavy\}$*;* $\boldsymbol{\tau_r}$*:* ***Random Effect*** *– defined as a replication within a field;* $\boldsymbol{r} \in \{1, 2, ..., 7\}$*;* $\boldsymbol{\epsilon_{ijkl}}$*:* ***Random Error****; ":" denotes interaction between two or more main effects.*

Table 6.7: Analysis of covariance (ANCOVA) conducted to model 2014 field-scale corn emergence duration response to measured seeding depth and gauge-wheel load.

Optimized ANCOVA Model Equation:

$$ED = I + F_j + F_j : MD + (F : SD)_{jk} : GWL + (F : SD)_{jk} : GWL^2 + \epsilon_{ij}$$

Overall Model Statistics:

Adjusted R^2 :	95.87%
Model p-value :	< 0.001

Residuals [days]:

Min	1Q	Median	3Q	Max
-3.3	-0.6	0.1	0.6	2.4

Regression Coefficients:

Model Parameters	Estimate	SE	t-value
Intercept	0.25	0.87	-0.09
F_B	-4.77	1.47	-3.25 **
F_A:MD	1.74	0.18	9.89 ***
F_B:MD	1.99	0.20	9.77 ***
$(F:SD)_{A,2.5}$:GWL	-8.79	2.94	-2.98 **
$(F:SD)_{B,2.5}$:GWL	-4.70	4.14	-1.13
$(F:SD)_{A,5.1}$:GWL	7.71	4.31	1.79 .
$(F:SD)_{B,5.1}$:GWL	4.99	5.75	0.87
$(F:SD)_{A,7.6}$:GWL	-10.46	5.16	-2.02 *
$(F:SD)_{B,7.6}$:GWL	-3.60	28.43	-0.13
$(F:SD)_{A,2.5}$:GWL^2	10.22	3.77	2.71 **
$(F:SD)_{B,2.5}$:GWL^2	4.43	6.57	0.67
$(F:SD)_{A,5.1}$:GWL^2	-13.90	7.10	-1.96 .
$(F:SD)_{B,5.1}$:GWL^2	-14.38	16.02	-0.90
$(F:SD)_{A,7.6}$:GWL^2	18.11	13.13	1.38
$(F:SD)_{B,7.6}$:GWL^2	-150.68	297.56	-0.51

*Significance: ***: P = 0.001; **: P = 0.01; *: P = 0.05; .: P = 0.1*

Derived Linear Equations for Field A and B:

Field	Model Equation
A	$ED = -0.1 + 1.7 \cdot MD + \alpha_{SD} \cdot GWL + \beta_{SD} \cdot GWL^2$
B	$ED = -4.9 + 2.0 \cdot MD + \alpha_{SD} \cdot GWL + \beta_{SD} \cdot GWL^2$

*With: **ED**: Corn Emergence Duration [days]; **I**: Model Intercept; $\boldsymbol{F_j}$, $\boldsymbol{SD_k}$: Field and Row-Unit Depth effects – categorical variables; $\boldsymbol{j} \ni \{A, B\}$, $\boldsymbol{k} \ni \{2.5, 5.1, 7.6\}$; **MD, GWL**: Corn Seeding Depth [kN], Difference between measured gauge-wheel and gauge-wheel load at 0.0 kN row-unit downforce at selected row-unit depth – continuous variables; $\boldsymbol{\epsilon_{ij}}$: **Random Error** [cm]; **":"** denotes interaction between main effects.*

6.3 Uniformity of Emergence

Uniformity of corn emergence was measured using standardized Gibb's index with more uniform stands characterized by higher index values. The uniformity of 2014 corn emergence was significantly affected by field, row-unit depth, row-unit downforce, and the two-way interaction between field and row-unit depth (Table 6.8). The uniformity of 2015 corn emergence was significantly affected by row-unit depth and row-unit downforce (Table 6.9). The 2014 corn emergence was significantly more uniform in field B than in field A as reduced clay content in field B promoted shorter emergence duration and therefore more synchronized early seedling development (section 5.2). Gibb's index linearly decreased with increasing seeding depth (Tables 6.10 and 6.11), and deeper seeding depths were characterized by less uniform stand establishment. Gibb's index response to gauge-wheel load was non-linear, and most uniform stands were achieved at 1.3, 1.6, 1.6, and 1.2 kN gauge-wheel load within the 2014-A, 2014-B, 2015-A, and 2015-B field trials, respectively. Deviations from these optimum gauge-wheel loads (ΔGWL [kN]) decreased Gibb's index by $-0.9 \cdot \Delta GWL^2$ in 2014-A, $-0.1 \cdot \Delta GWL^2$ in 2014-B, $-0.3 \cdot \Delta GWL^2$ in 2015-A, and $-0.2 \cdot \Delta GWL^2$ in 2015-B.

Table 6.8: Mixed-effect analysis of variance conducted for uniformity of corn emergence during the 2014 growing season.

Mixed-Effect Model Equation:

$$GI = \mu + F_j + SD_k + DF_l + (F:SD)_{jk} + (F:DF)_{jl} + (SD:DF)_{kl} + (F:SD:DF)_{jkl} + \tau_r + \epsilon_{jkl}$$

Scaled Residuals:

Min	1Q	Median	3Q	Max
-2.0	-0.6	0.0	0.6	1.9

Random Effects:

Groups	Variance [cm^2]	Std. Dev. [%]
Whole Plot Error	0.00	0.05
Sub Plot Error	0.01	0.11

Fixed Effects - ANOVA Table:

Model Parameters	Df	Sum Sq.	Mean Sq.	F-Value	Sum Sq. [%]
F	1	0.31	0.31	24.55 **	10.8
SD	2	1.98	0.99	78.84 ***	69.5
DF	2	0.21	0.11	8.49 ***	7.5
F:SD	2	0.24	0.12	9.68 ***	8.5
F:DF	2	0.01	0.00	0.43	0.4
SD:DF	4	0.04	0.01	0.74	1.3
F:SD:DF	4	0.06	0.01	1.14	2.0

*Significance: ***: P = 0.001; **: P = 0.01; *: P = 0.05; .: P = 0.1*

Estimated Means:

Row-Unit Depth	Row-unit Downforce	Field A [days]	Field B [days]
2.5 cm	**No**	0.84 abc	0.95 a
	Medium	0.77 abcd	0.94 ab
	Heavy	0.70 abcd	0.94 a
5.1 cm	**No**	0.36 f	0.84 abc
	Medium	0.28 f	0.68 abcde
	Heavy	0.27 f	0.64 cde
7.6 cm	**No**	0.45 ef	0.66 bcde
	Medium	0.36 f	0.54 def
	Heavy	0.34 f	0.35 f

a,...,f *: Least significant difference between treatments at a 95% confidence interval.*

With: $\boldsymbol{GI}$*: Gibb's Index;* $\boldsymbol{\mu}$*: Model Intercept;* $\boldsymbol{F_j}$*,* $\boldsymbol{SD_k}$*,* $\boldsymbol{DF_l}$*: Field, Row-Unit Depth, and Row-Unit Downforce main effects;* $\boldsymbol{j} \ni \{A, B\}$*,* $\boldsymbol{k} \ni \{2.5, 5.1, 7.6\}$*,* $\boldsymbol{l} \ni \{No, Medium, Heavy\}$*;* $\boldsymbol{\tau_r}$*:* ***Random Effect*** *– defined as a replication within a field;* $\boldsymbol{r} \in \{1, 2, ..., 7\}$*;* $\boldsymbol{\epsilon_{ijkl}}$*:* ***Random Error;*** *":" denotes interaction between two or more main effects.*

Table 6.9: Mixed-effect analysis of variance conducted for uniformity of corn emergence during the 2015 growing season.

Mixed-Effect Model Equation:

$$GI = \mu + F_j + SD_k + DF_l + (F:SD)_{jk} + (F:DF)_{jl} + (SD:DF)_{kl} + (F:SD:DF)_{jkl} + \tau_r + \epsilon_{jkl}$$

Scaled Residuals:

Min	1Q	Median	3Q	Max
-2.4	-0.4	0.0	0.6	1.6

Random Effects:

Groups	Variance [cm^2]	Std. Dev. [%]
Whole Plot Error	0.00	0.00
Sub Plot Error	0.01	0.10

Fixed Effects - ANOVA Table:

Model Parameters	Df	Sum Sq.	Mean Sq.	F-Value	Sum Sq. [%]
F	1	0.02	0.02	2.19	1.5
SD	2	1.06	0.5	55.61 ***	74.7
DF	2	0.25	0.12	13.15 ***	17.7
F:SD	2	0.00	0.00	0.28	0.4
F:DF	2	0.00	0.00	0.24	0.3
SD:DF	4	0.07	0.02	1.81	4.9
F:SD:DF	4	0.01	0.00	0.22	0.6

Significance: ***: *P = 0.001;* **: *P = 0.01;* *: *P = 0.05;* .: *P = 0.1*

Estimated Means:

Row-Unit Depth	Row-unit Downforce	Field A [days]	Field B [days]
2.5 cm	**No**	0.62 a	0.63 a
	Medium	0.56 ab	0.62 a
	Heavy	0.54 abc	0.50 abcd
5.1 cm	**No**	0.56 ab	0.56 abc
	Medium	0.32 de	0.38 bcde
	Heavy	0.29 e	0.36 bcde
7.6 cm	**No**	0.30 de	0.34 cde
	Medium	0.21 e	0.27 e
	Heavy	0.18 e	0.24 e

a,...,e *: Least significant difference between treatments at a 95% confidence interval.*

With: ***GI****: Gibb's Index;* $\boldsymbol{\mu}$*: Model Intercept;* $\boldsymbol{F_j}$, $\boldsymbol{SD_k}$, $\boldsymbol{DF_l}$*: Field, Row-Unit Depth, and Row-Unit Downforce main effects;* $\boldsymbol{j} \ni \{A, B\}$, $\boldsymbol{k} \ni \{2.5, 5.1, 7.6\}$, $\boldsymbol{l} \ni \{No, Medium, Heavy\}$; $\boldsymbol{\tau_r}$*:* ***Random Effect*** *– defined as a replication within a field;* $\boldsymbol{r} \in \{1, 2, ..., 7\}$; $\boldsymbol{\epsilon_{ijkl}}$*:* ***Random Error****;* ***":"*** *denotes interaction between two or more main effects.*

Table 6.10: Analysis of covariance (ANCOVA) conducted to model field-scale measured seeding depth and gauge-wheel load effects on uniformity of 2014 corn emergence.

Optimized ANCOVA Model Equation:

$$GI = I + F_j + F_j : MD + (F : SD)_{jk} : GWL + (F : SD)_{jk} : GWL^2 + \epsilon_{ij}$$

Overall Model Statistics:

Adjusted R^2 :	67.99%
Model p-value :	< 0.001

Residuals:

Min	1Q	Median	3Q	Max
-0.4	-0.1	0.0	0.1	0.2

Regression Coefficients:

Model Parameters	Estimate	SE	t-value
Intercept	1.08	0.10	10.82 ***
F_B	0.40	0.16	2.45 *
F_A:MD	-0.13	0.02	-6.16 ***
F_B:MD	-0.13	0.02	-6.06 ***
$(F:SD)_{A,2.5}$:GWL	0.79	0.35	2.23 *
$(F:SD)_{B,2.5}$:GWL	0.21	0.50	0.41
$(F:SD)_{A,5.1}$:GWL	-1.07	0.52	-2.06 *
$(F:SD)_{B,5.1}$:GWL	-1.16	0.69	-1.67
$(F:SD)_{A,7.6}$:GWL	0.22	0.62	0.35
$(F:SD)_{B,7.6}$:GWL	-1.11	1.42	-0.78
$(F:SD)_{A,2.5}$:GWL^2	-0.90	0.46	-1.97 .
$(F:SD)_{B,2.5}$:GWL^2	-0.13	0.79	-0.17
$(F:SD)_{A,5.1}$:GWL^2	1.44	0.85	1.69 .
$(F:SD)_{B,5.1}$:GWL^2	3.59	1.93	1.86 .
$(F:SD)_{A,7.6}$:GWL^2	-0.17	1.59	-0.11
$(F:SD)_{B,7.6}$:GWL^2	-1.58	16.01	-0.85

*Significance: ***: P = 0.001; **: P = 0.01; *: P = 0.05; .: P = 0.1*

Derived Linear Equations for Field A and B:

Field	Model Equation
A	GI = 1.1 – 0.1·MPD + α_{SD}·GWL + β_{SD}·GWL^2
B	GI = 1.5 – 0.1·MPD + α_{SD}·GWL + β_{SD}·GWL^2

*With: **GI**: Gibb's Index; **I**: Model Intercept; $\boldsymbol{F_j}$, $\boldsymbol{SD_k}$: Field and Row-Unit Depth effects – categorical variables; $\boldsymbol{j} \ni \{A, B\}$, $\boldsymbol{k} \ni \{2.5, 5.1, 7.6\}$; **MD, GWL**: Corn Seeding Depth [kN], Difference between measured gauge-wheel and gauge-wheel load at 0.0 kN row-unit downforce at selected row-unit depth – continuous variables; $\boldsymbol{\epsilon}_{ij}$: **Random Error** [cm]; ":" denotes interaction between main effects.*

Table 6.11: Analysis of covariance (ANCOVA) conducted to model field-scale measured seeding depth and gauge-wheel load effects on uniformity of 2015 corn emergence.

Optimized ANCOVA Model Equation:

$$GI = I + F_j + F_j : MD + (F : SD)_{jk} : GWL + (F : SD)_{jk} : GWL^2 + \epsilon_{ij}$$

Overall Model Statistics:

Adjusted R^2 :	72.3%
Model p-value :	< 0.001

Residuals:

Min	1Q	Median	3Q	Max
-0.2	-0.1	0.0	0.1	0.2

Regression Coefficients:

Model Parameters	Estimate	SE	t-value
Intercept	0.99	0.16	5.76 ***
F_B	0.10	0.22	0.48
F_A:MD	-0.10	0.03	-3.35 **
F_B:MD	-0.10	0.02	-4.26 ***
$(F:SD)_{A,2.5}$:GWL	0.38	0.27	1.41 *
$(F:SD)_{B,2.5}$:GWL	0.11	0.27	0.41
$(F:SD)_{A,5.1}$:GWL	-0.37	0.29	-1.26
$(F:SD)_{B,5.1}$:GWL	-0.10	0.31	-0.33
$(F:SD)_{A,7.6}$:GWL	-0.26	0.33	-0.78
$(F:SD)_{B,7.6}$:GWL	-0.44	0.47	-0.95
$(F:SD)_{A,2.5}$:GWL^2	-0.28	0.24	-1.18
$(F:SD)_{B,2.5}$:GWL^2	0.16	0.25	0.63
$(F:SD)_{A,5.1}$:GWL^2	0.28	0.33	0.85
$(F:SD)_{B,5.1}$:GWL^2	-0.01	0.31	-0.03
$(F:SD)_{A,7.6}$:GWL^2	-0.15	0.50	-0.29
$(F:SD)_{B,7.6}$:GWL^2	0.37	0.70	0.53

*Significance: ***: P = 0.001; **: P = 0.01; *: P = 0.05; .: P = 0.1*

Derived Linear Equations for Field A and B:

Field	Model Equation
A	GI = 0.9 – 0.1·MD + α_{SD}·GWL + β_{SD}·GWL^2
B	GI = 1.0 – 0.1·MD + α_{SD}·GWL + β_{SD}·GWL^2

*With: **GI**: Gibb's Index; **I**: Model Intercept; $\boldsymbol{F_j}$, $\boldsymbol{SD_k}$: Field and Row-Unit Depth effects – categorical variables; $\boldsymbol{j} \ni \{A, B\}$, $\boldsymbol{k} \ni \{2.5, 5.1, 7.6\}$; **MD, GWL**: Corn Seeding Depth [kN], Difference between measured gauge-wheel and gauge-wheel load at 0.0 kN row-unit downforce at selected row-unit depth – continuous variables; $\boldsymbol{\epsilon_{ij}}$: **Random Error**[cm]; **":"** denotes interaction between main effects.*

6.4 Seedling Vigor

Seedling vigor was evaluated through computation of Emergence Rate Index (ERI), with higher corn vigor characterized by higher ERI values. Computation of ERI required accurate determination of emergence window, and results presented in this section focus on 2014 data only. The 2014 seedling vigor was significantly affected by field, row-unit depth, and row-unit downforce (Table 6.12) and results were comparable to the results described by Hanna et al. (2010). Seedling vigor was higher in field B than in field A, and the lower clay content in field B reduced soil resistance to seedling emergence providing an improved environment for early seedling development. ERI linearly decreased with increasing seeding depth, and deeper seeding depths were characterized by smaller seedling vigor (Table 6.13). ERI response to gauge-wheel load was non-linear, and higher seedling vigors were observed at measured gauge-wheel loads of 1.4 kN and 1.7 kN within 2014-A and 2014-B corn trials, respectively. Deviations from these optimum gauge-wheel loads (ΔGWL [kN]) reduced ERI by $-2.7 \cdot \Delta GWL^2$ in 2014-A, and by $-0.9 \cdot \Delta GWL^2$ in 2014-B.

Table 6.12: Mixed-effect analysis of variance conducted for Emergence Rate Index (ERI) data computed to quantify corn seedling vigor during the 2014 growing season.

Mixed-Effect Model Equation:

$$ERI = \mu + F_j + SD_k + DF_l + (F:SD)_{jk} + (F:DF)_{jl} + (SD:DF)_{kl} + (F:SD:DF)_{jkl} + \tau_r + \epsilon_{jkl}$$

Scaled Residuals:

Min	1Q	Median	3Q	Max
-2.1	-0.4	0.1	0.5	2.2

Random Effects:

Groups	Variance [cm^2]	Std. Dev. [%]
Whole Plot Error	0.03	0.17
Sub Plot Error	0.23	0.48

Fixed Effects - ANOVA Table:

Model Parameters	Df	Sum Sq.	Mean Sq.	F-Value	Sum Sq. [%]
F	1	8.92	8.92	39.03 ***	9.2
SD	2	79.10	39.55	172.99 ***	81.7
DF	2	4.77	2.38	10.42 ***	4.9
F:SD	2	0.27	0.13	0.59	0.3
F:DF	2	0.08	0.04	0.17	0.1
SD:DF	4	2.92	0.73	3.19 *	3.0
F:SD:DF	4	0.70	0.17	0.77	0.7

*Significance: ***: P = 0.001; **: P = 0.01; *: P = 0.05; .: P = 0.1*

Estimated Means:

Row-Unit Depth	Row-unit Downforce	Field A [days]	Field B [days]
2.5 cm	**No**	6.7 abc	7.5 ab
	Medium	6.4 bcd	7.6 a
	Heavy	6.6 abc	7.6 a
5.1 cm	**No**	6.0 cde	6.6 abc
	Medium	5.3 ef	6.4 abcd
	Heavy	5.1 efg	5.8 de
7.6 cm	**No**	4.5 fg	5.4 def
	Medium	4.2 gh	4.6 fg
	Heavy	3.3 h	4.0 gh

a,...,h *: Least significant difference between treatments at a 95% confidence interval.*

With: ***ERI****: Emergence Rate Index;* $\boldsymbol{\mu}$*: Model Intercept;* $\boldsymbol{F_j}$*,* $\boldsymbol{SD_k}$*,* $\boldsymbol{DF_l}$*: Field, Row-Unit Depth, and Row-Unit Downforce main effects;* $\boldsymbol{j} \ni \{A, B\}$*,* $\boldsymbol{k} \ni \{2.5, 5.1, 7.6\}$*,* $\boldsymbol{l} \ni \{No, Medium, Heavy\}$*;* $\boldsymbol{\tau_r}$*:* ***Random Effect*** *– defined as a replication within a field;* $\boldsymbol{r} \in \{1, 2, ..., 7\}$*;* $\boldsymbol{\epsilon_{ijkl}}$*:* ***Random Error****; ":" denotes interaction between two or more main effects.*

Table 6.13: Analysis of covariance (ANCOVA) conducted to model field-scale measured seeding depth and gauge-wheel load effects on corn seedling vigor during the 2014 growing season.

Optimized ANCOVA Model Equation:

$$ERI = I + F_j + F_j : MD + (F : SD)_{jk} : GWL + (F : SD)_{jk} : GWL^2 + \epsilon_{ij}$$

Overall Model Statistics:

Adjusted R^2 :	75.6%
Model p-value :	< 0.001

Residuals:

Min	1Q	Median	3Q	Max
-1.7	-0.3	0.0	0.4	1.2

Regression Coefficients:

Model Parameters	Estimate	SE	t-value
Intercept	8.96	0.43	21.08 ***
F_B	2.19	0.73	2.99 **
F_A:MD	-0.79	0.09	-9.03 ***
F_B:MD	-0.89	0.10	-8.74
$(F:SD)_{A,2.5}$:GWL	2.49	1.59	1.59
$(F:SD)_{B,2.5}$:GWL	1.71	2.24	0.76
$(F:SD)_{A,5.1}$:GWL	0.03	2.33	-0.01
$(F:SD)_{B,5.1}$:GWL	-0.23	3.11	-0.07
$(F:SD)_{A,7.6}$:GWL	-1.46	2.79	-0.52
$(F:SD)_{B,7.6}$:GWL	-8.64	15.37	-0.56
$(F:SD)_{A,2.5}$:GWL^2	-2.72	2.04	-1.33
$(F:SD)_{B,2.5}$:GWL^2	-090	3.55	-0.25
$(F:SD)_{A,5.1}$:GWL^2	1.87	3.84	0.49
$(F:SD)_{B,5.1}$:GWL^2	4.15	8.66	0.48
$(F:SD)_{A,7.6}$:GWL^2	0.22	7.10	0.03
$(F:SD)_{B,7.6}$:GWL^2	-103.00	160.90	-0.64

*Significance: ***: P = 0.001; **: P = 0.01; *: P = 0.05; .: P = 0.1*

Derived Linear Equations for Field A and B:

Field	Model Equation
A	ERI = 9.1 – 0.8·MPD + α_{SD}·GWL + β_{SD}·GWL^2
B	ERI = 11.3 – 0.9·MPD + α_{SD}·GWL + β_{SD}·GWL^2

*With: **ERI**: Emergence Rate Index; **I**: Model Intercept; $\boldsymbol{F_j}$, $\boldsymbol{SD_k}$: Field and Row-Unit Depth effects – categorical variables; $\boldsymbol{j} \ni \{A, B\}$, $\boldsymbol{k} \ni \{2.5, 5.1, 7.6\}$; **MD, GWL**: Corn Seeding Depth [kN], Difference between measured gauge-wheel and gauge-wheel load at 0.0 kN row-unit downforce at selected row-unit depth – continuous variables; $\boldsymbol{\epsilon_{ij}}$: **Random Error** [cm]; **":"** denotes interaction between main effects.*

6.5 Final Yields

Corn final yields were significantly affected by growing season, field, row-unit depth, row-unit downforce, and the following interaction effects: growing season x field, growing season x row-unit depth, and row-unit depth x row-unit downforce (Tables 6.14 and 6.15). Final corn yields were significantly higher in 2015 and in field B, than in 2014 and in field A due to more favorable climate throughout the 2015 growing season and more favorable soil conditions in field B. Highest differences in yield across treatments was 6,210 kg ha^{-1} (12,930 kg ha^{-1} in 2015-B at 5.1 cm row-unit depth - 6,210 kg ha^{-1} in 2014-A at 7.6 cm row-unit depth). Corn final yield response to measured seeding depth was non-linear (Table 6.16, Figure 6.3). Seeding depths of 3.9 cm, 4.9 cm, and 5.8 cm maximized final corn yield at 9,751 kg.ha^{-1}, 9,268 kg.ha^{-1}, and 12,666 kg.ha^{-1} within the 2014-B, 2015-A, and 2015-B field trials. Deviations from these optimum seeding depths (ΔDepth [cm]) decreased corn final yields by -129·$\Delta Depth^2$ [kg ha^{-1}] in 2014-B, -198·$\Delta Depth^2$ [kg ha^{-1}] in 2015-A, and -103·$\Delta Depth^2$ [kg ha^{-1}] in 2015-B. In 2014-A, corn final yield decreased with increasing seeding depth. Optimum seedings depths for yields were deeper than optimum seeding depths for final corn population hence suggesting that seeding depth also impacted corn response to climate conditions throughout the growing season. Corn final yield was not significantly affected by gauge-wheel load. Computation of Spearman's correlations to evaluate relationships between corn final yield and corn emergence metrics indicated that corn final yields were negatively correlated to emergence duration and positively correlated to corn final population, uniformity of emergence, and seedling vigor (Table 6.17). Therefore, improved crop establishment resulted in higher corn yields at harvest.

Table 6.14: Mean corn yield by row-unit depth, row-unit downforce, field, and growing season.

Estimated Means:

Row-Unit Depth	Row-Unit Downforce	— Season 2014 —		— Season 2015 —	
		Field A	**Field B**	**Field A**	**Field B**
2.5 cm	**No**	9,100 ^{fghij}	9,580 ^{defghi}	8,430 ^{fghijk}	12,300 ^{abc}
	Medium	9,260 ^{fghij}	9,940 ^{bcdefg}	9,950 ^{cdef}	12,550 ^{ab}
	Heavy	9,130 ^{fghij}	9,880 ^{cdefgh}	9,540 ^{efghi}	12,870 ^{a}
5.1 cm	**No**	8,800 ^{fghij}	9,600 ^{defghij}	9,980 ^{cdef}	12,930 ^{a}
	Medium	8,190 ^{fghijk}	8,950 ^{fghij}	9,560 ^{defghi}	12,910 ^{a}
	Heavy	7,390 ^{ijk}	9,230 ^{efghij}	8,520 ^{fghi}	12,850 ^{a}
7.6 cm	**No**	7,590 ^{ghijk}	8,750 ^{fghij}	9,600 ^{defghi}	12,320 ^{abc}
	Medium	7,090 ^{jk}	8,160 ^{fghijk}	8,130 ^{fghijk}	12,030 ^{abcd}
	Heavy	6,210 ^{k}	7,260 ^{hijk}	7,560 ^{ghijk}	11,820 ^{abcde}

$^{a,\ldots,k}$ *: Least significant difference between treatments at a 95% confidence interval.*

Table 6.15: Mixed-effect analysis of variance conducted for corn final yield data.

Mixed-Effect Model Equation:

$$FY = \mu + Y_i + F_j + SD_k + DF_l + (Y:F)_{i,j} + (Y:SD)_{ik} + (F:SD)_{jk} + (Y:DF)_{il} + (F:DF)_{jl} + (SD:DF)_{kl} + (Y:F:SD)_{ijk} + (Y:F:DF)_{ijk} + (Y:SD:DF)_{ikl} + (F:SD:DF)_{jkl} + (Y:F:SD:DF)_{jkl} + \tau_r + \epsilon_{jkl}$$

Scaled Residuals [kg ha^{-1}]:

Min	1Q	Median	3Q	Max
-3.1	-0.5	0.0	0.5	2.4

Random Effects:

Groups	Variance [kg^2 ha^{-2}]	Std. Dev. [kg ha^{-1}]
Whole Plot Error	744017	862.6
Sub Plot Error	491322	700.9

Fixed Effects - ANOVA Table:

Model Parameters	Df	Sum Sq.	Mean Sq.	F-Value	Sum Sq. [%]
Y	1	10245788	10245788	20.85 **	9.9
F	1	10355112	10355112	21.08 ***	10.0
SD	2	40497673	20248837	41.21 ***	39.2
DF	2	6682871	3341435	6.80 **	6.5
Y:F	1	3370079	3370079	6.86 *	3.3
Y:SD	2	9243549	4621775	9.41 ***	8.9
F:SD	2	1056304	528152	1.07	1.0
Y:DF	2	569310	284655	0.58	0.6
F:DF	2	2239453	1119726	2.2	2.2
SD:DF	4	13229648	3307412	6.73 ***	12..8
Y:F:SD	2	60388	30194	0.06	0.1
Y:F:DF	2	200701	100351	0.20	0.2
Y:SD:DF	4	1177434	294358	0.60	1.1
F:SD:DF	4	2219282	554820	1.13	2.1
Y:F:SD:DF	4	2139343	534836	1.09	2.1

Significance: ****: P = 0.001;* ***: P = 0.01;* **: P = 0.05; .: P = 0.1*

With: $\boldsymbol{FY}$*: Final Corn Yield;* $\boldsymbol{\mu}$*: Model Intercept;* $\boldsymbol{F_j}$*,* $\boldsymbol{SD_k}$*,* $\boldsymbol{DF_l}$*: Field, Row-Unit Depth, and Row-Unit Downforce main effects;* $\boldsymbol{j} \ni \{A, B\}$*,* $\boldsymbol{k} \ni \{2.5, 5.1, 7.6\}$*,* $\boldsymbol{l} \ni \{No, Medium, Heavy\}$*;* $\boldsymbol{\tau_r}$*:* ***Random Effect*** *– defined as a replication within a field;* $\boldsymbol{r} \in \{1, 2, ..., 7\}$*;* $\boldsymbol{\epsilon_{ijkl}}$*:* ***Random Error****; ":" denotes interaction between two or more main effects.*

Table 6.16: Analysis of covariance (ANCOVA) conducted to model field-scale corn final yield response to measured seeding depth and gauge-wheel load.

Optimized ANCOVA Model Equation:

$$FY = I + (Y:F)_{ij} + (Y:F)_{ij}:MD + (Y:F)_{ij}:(MD)^2 + (F:SD)_{jk}:GWL + (F:SD)_{jk}:GWL^2 + \epsilon_{ij}$$

Overall Model Statistics:

Adjusted R^2 :	69.2%
Model p-value :	< 0.001

Residuals [kg ha^{-1}]:

Min	1Q	Median	3Q	Max
-2749.2	-538.6	80.0	582.4	2620.1

Regression Coefficients:

Model Parameters	Estimate	SE	t-value
Intercept	10186.99	3182.49	3.22 **
Y_{2015}	-5727.79	7875.44	-0.73
F_B	-2451.31	4940.39	-0.496
$(Y:F)_{2015,B}$	7143.80	10199.45	0.70
$(Y:F)_{2014,A}$:MD	-225.83	1432.58	-0.16
$(Y:F)_{2014,B}$:MD	1005.30	1353.71	0.4
$(Y:F)_{2015,A}$:MD	1940.77	2651.59	0.73
$(Y:F)_{2015,B}$:MD	1193.13	1857.50	064
$F_{2014,A}$:MD^2	-40.32	151.38	-0.2
$F_{2014,B}$:MD^2	-129.46	116.30	-1.11
$F_{2015,A}$:MD^2	-198.46	240.13	-0.83
$F_{2015,B}$:MD^2	-103.13	158.70	-0.65

*Significance: ***: P = 0.001; **: P = 0.01; *: P = 0.05; .: P = 0.1*

Derived Linear Equations by Field and Growing Season:

Season	Field	Model Equation
2014	**A**	MFY = 10,250 – 226·MPD – 40·MPD^2
	B	MFY = 7,799 + 1,005·MPD – 129·MPD^2
2015	**A**	MFY = 4523 + 1,941·MPD – 198·MPD^2
	B	MFY = 9,215 + 1,193·MPD – 103·MPD^2

*With: **FP**: Final Corn Population [%]; **I**: Model Intercept; $\boldsymbol{F_j}$, $\boldsymbol{SD_k}$: Field and Row-Unit Depth effects – categorical variables; $\boldsymbol{j} \ni \{A, B\}$, $\boldsymbol{k} \ni \{2.5, 5.1, 7.6\}$; **MD, GWL**: Corn Seeding Depth [kN], Difference between measured gauge-wheel and gauge-wheel load at 0.0 kN row-unit downforce at selected row-unit depth – continuous variables; $\boldsymbol{\epsilon}_{ij}$: **Random Error** [cm]; **":"** denotes interaction between main effects.*

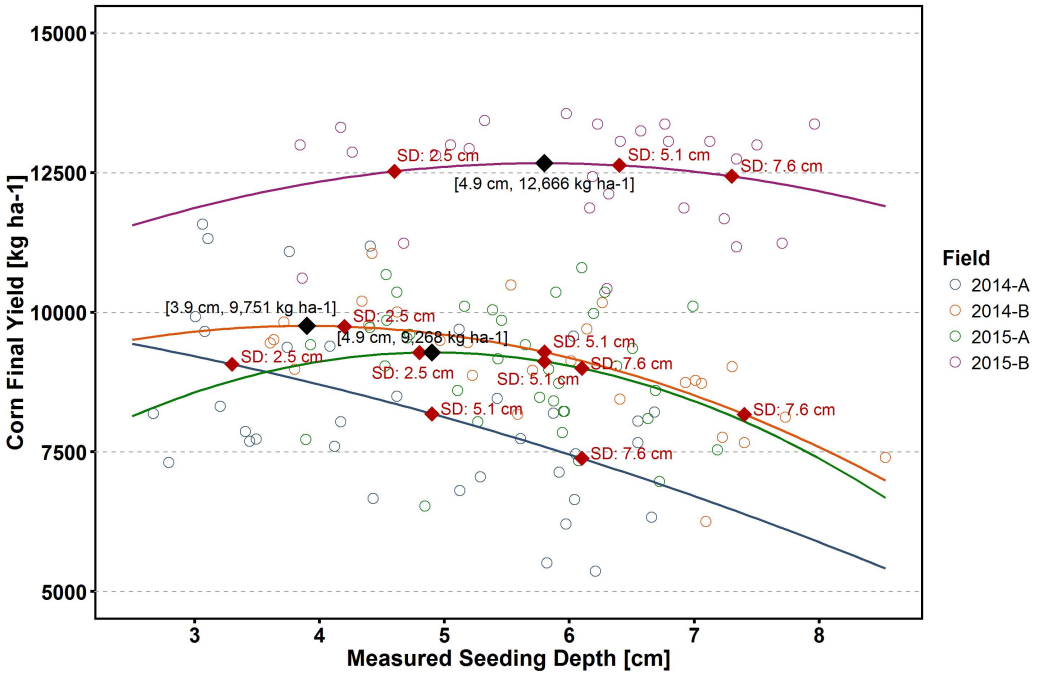

Figure 6.3: Determination of optimum seeding depth to maximize final yield of corn within individual field trials – SD: row-unit depth adjustment.

Table 6.17: Spearman's correlations to characterize relationships between corn final yields and corn emergence metrics within all field trials.

	Growing Season	Final Population	Emergence Duration	ERI	Uniformity
Final Yields	**2014**	0.64	-0.74	0.80	0.73
	2015	0.51	-	-	0.34

6.6 Discussion

Corn emergence and yields were primarily affected by varying conditions between fields and growing seasons. Environmental conditions constituted the first limiting factor for crop establishment and growth, and maximum crop yield potential requires planting during proper time window to place individual seeds within optimum soil conditions for germination and emergence. All corn emergence metrics were significantly affected by measured seeding depth and gauge-wheel load, and crop establishment was significantly affected by row-crop planter performance. Stronger seeding depth and gauge-wheel load effects were observed within least favorable soil conditions for emergence, and optimum planter performance is even more desirable when planting within poor soil conditions for corn establishment. Seeding depths of 3.8, 4.4 and 4.0 cm maximized final plant population for 2014-A, 2014-B, 2015-A/B. Deeper seeding depths resulted in poorer emergence timeliness, less uniform emergence, and reduced seedling vigor. Gauge-wheel load of 1.3, 1.3 to 1.9, and 1.1 to 1.2 kN optimized corn emergence for 2014-A, 2014-B, and 2015-B. Gauge-wheel load had little impact on corn emergence for 2015-A. Improved corn emergence correlated with higher corn final yields indicating the importance of improving emergence to maximize crop yield potential. Finals yields were also significantly affected by measured seeding depth, and seeding depths of 3.9 cm, 4.9 cm, and 5.8 cm maximized crop yields within the 2014-A, 2015-A, and 2015-B corn trials. Optimum seeding depths for yields were deeper than optimum seeding depths for final corn population within individual corn trial. Results suggested that seeding depth also impacted crop response to climate conditions within the growing season. Such effects must be accounted for when selecting a target seeding depth that maximizes crop yield potential.

6.7 Summary

Corn emergence and yield response was influenced by measured seeding depth, gauge-wheel load, and varying soils conditions between fields and growing seasons. Corn emergence

and yields were primarily affected by varying conditions between fields and growing season with warmer soil conditions promoting quicker emergence, more uniform stand establishment, and thereby higher final corn populations. Soils with more clays provided worse soil conditions for corn establishment and growth due to soil crusting after rainfall and poorer drainage in lower areas of the field. Corn emergence metrics were significantly impacted by measured seeding depth and gauge-wheel load, with stronger seeding depth and gauge-wheel load effects observed within the least favorable field conditions for corn establishment. Maximum final corn populations were achieved at 3.8 cm, 4.4, and 4.0 cm seeding depths in 2014-A, 2014-B, 2015-A, and 2015-B corn trials. Deeper seeding depths resulted in poor emergence timeliness, less uniform emergence, and reduced seedling vigor. Gauge-wheel load of 1.3 kN, 1.3 to 1.9 kN, and 1.1 to 1.2 kN optimized corn emergence within the 2014-A, 2014-B, and 2015-B corn trials. Better corn emergence correlated with higher corn final yields. Final yields were significantly affected by measured seeding depth, and seeding depths of 3.9 cm, 4.9 cm, and 5.8 cm maximized crop yields within the 2014-A, 2015-A, and 2015-B corn trials.

Chapter 7

Implementation of Prescription-Based Implied Technologies to Manage In-Field Seeding Depth Variability in the Southeast US.

Chapter 7 examines development and implementation of prescription-based and real-time planting technologies to manage in-field seeding depth variability in the Southeast US. Results address objective 3. Prescription-based and real-time seeding depth management strategies were discussed separately. Data analysis was conducted for corn only. Results presented in section 5.2.1 demonstrated significant correlations between corn seeding depth and standardized soil EC data. Regression models presented in section 5.2.1 and characterizing seeding depth relationship to standardized soil EC within individual corn trials were used to discuss prescription-based seeding depth management at planting. Similarly, results presented in section 5.2.2 demonstrated significant correlations between corn seeding depth and measured gauge-wheel load at planting. Regression models presented in section 5.2.2 and characterizing seeding depth relationship to measured gauge-wheel load within individual corn trials were used to discuss real-time seeding depth management at planting. This chapter is divided into 3 sections outlining prescription-based and real-time seeding depth management with a discussion of the results.

7.1 Prescription-Based Seeding Depth Management

This approach to prescription-driven planter setup presumed the ability to alter row-unit depth and downforce adjustments in response to position within a field. A prescription map detailing changes for a set of management zones, based on soil EC, would be developed based on results similar to those presented in Chapter 5. Specifically, the model in equation

7.1 predicted seeding depth based on a set of five parameters. Those parameters were summarized for individual corn trials in Table 5.5. Three of the parameters were specific to a chosen row-unit depth ($\alpha_{F,S}$) and row-unit downforce ($\beta_{F,S}$), plus their interaction ($\lambda_{F,S}$) and would be fixed for a given field, F, and season, S. A fourth was an intercept ($I_{F,S}$), also fixed for a specific field and season. The last parameter, γ, was the change in seeding depth that could be associated to changes in soil EC across the field. The prescription planter setup map, therefore, was based on this effect and knowledge of EC in the field.

$$ESD = I_{F,S} + \alpha_{F,S} \cdot SD + \beta_{F,S} \cdot DF + \lambda_{F,S} \cdot SD \cdot DF + \gamma \cdot EC \tag{7.1}$$

Generating the prescription maps require the following steps.

1. Setting an allowable tolerance in seeding depth variation, τ.
2. Developing a set of zones for a given field such that the mean $\gamma \cdot EC$ within a zone corresponded to the field global average $\gamma \cdot EC$ parameter plus (or minus) an integer multiple of τ.
3. Determining proper row-unit depth and downforce adjustments to achieve targeted depths within individual management zones using equation 7.1.

The following sections detail this procedure.

7.1.1 Allowable Seeding Depth Variability

Bowen (1966) determined that seeding depth should be maintained within a range of ± 0.3 cm relative to a target for optimum crop establishment. For this study, prescription maps were created such that seeding depth variability associated with spatial changes in soil EC within individual management zones was $\tau = \pm 0.2$ cm. The lower limit was chosen to be a good compromise between tight tolerance on seeding depth and limiting the number of zones within a field.

7.1.2 Management Zones Delineation

The associated change in seeding depth expected from $\gamma \cdot EC$ variation was mapped in Figures 5.1 through 5.4 for individual corn trials, and these were the basis of the prescription maps developed for this study. The range in $\gamma \cdot EC$ identified for a field divided by τ and rounded to the nearest integer set the number of management zones for a given field. For instance, results presented in Figure 5.1 indicated that $\gamma \cdot EC$ within the 2014-A corn trial ranged from -0.5 to 0.5 cm and the 2014-A corn trial was divided into (0.5 - (-0.5)) / 0.2 = 5 management zones. Results presented in Figures 5.1 through 5.4 were classified based on the computed number of management zones. Areas of uniform $\gamma \cdot EC$ were drawn by hand based on the classified maps. These areas became the management zones for site-specific row-unit depth and downforce modification. The zones were shown in Figures 7.1-7.4. Individual zones were associated to a global $\gamma \cdot EC$ value computed as the average between the minimum and maximum $\gamma \cdot EC$ values within a zone.

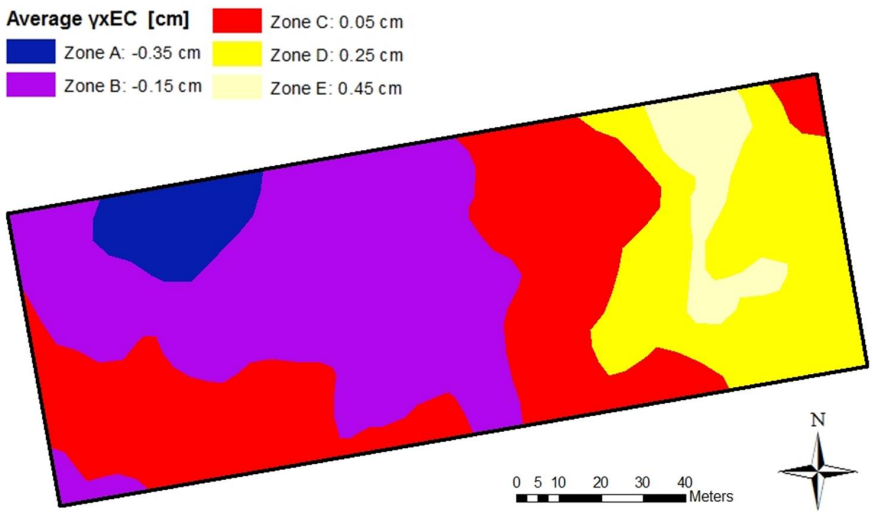

Figure 7.1: Management zones delineated for site-specific row-unit depth and downforce modifications within the 2014-A corn trial.

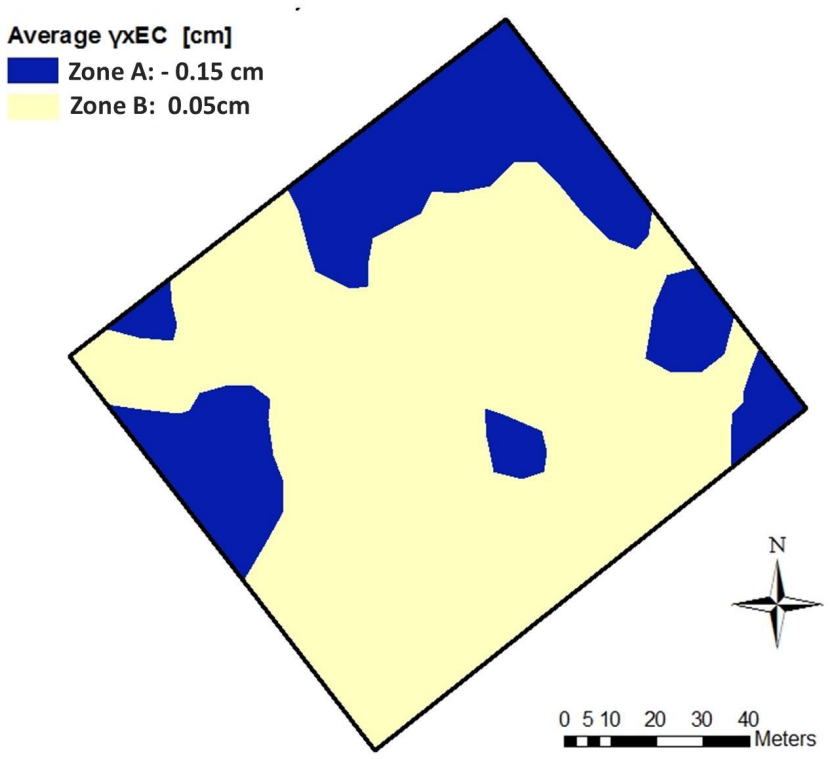

Figure 7.2: Management zones delineated for site-specific row-unit depth and downforce modifications within the 2014-B corn trial

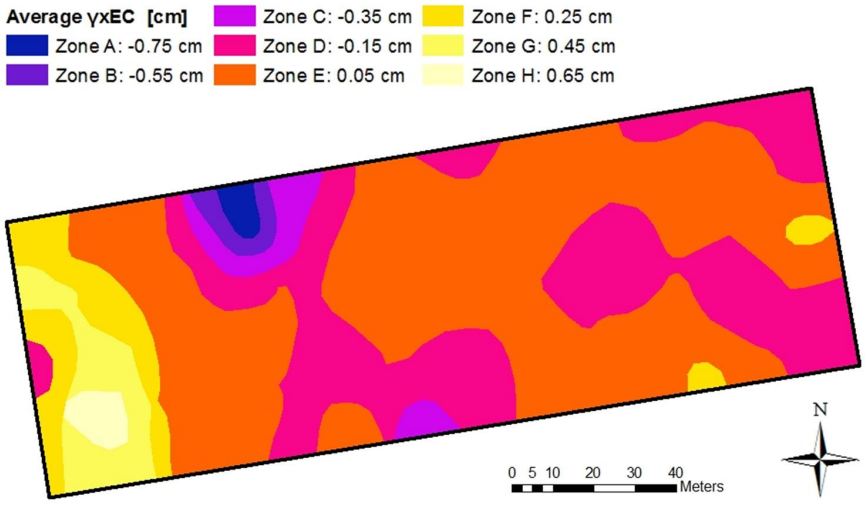

Figure 7.3: Management zones delineated for site-specific row-unit depth and downforce modifications within the 2015-A corn trial.

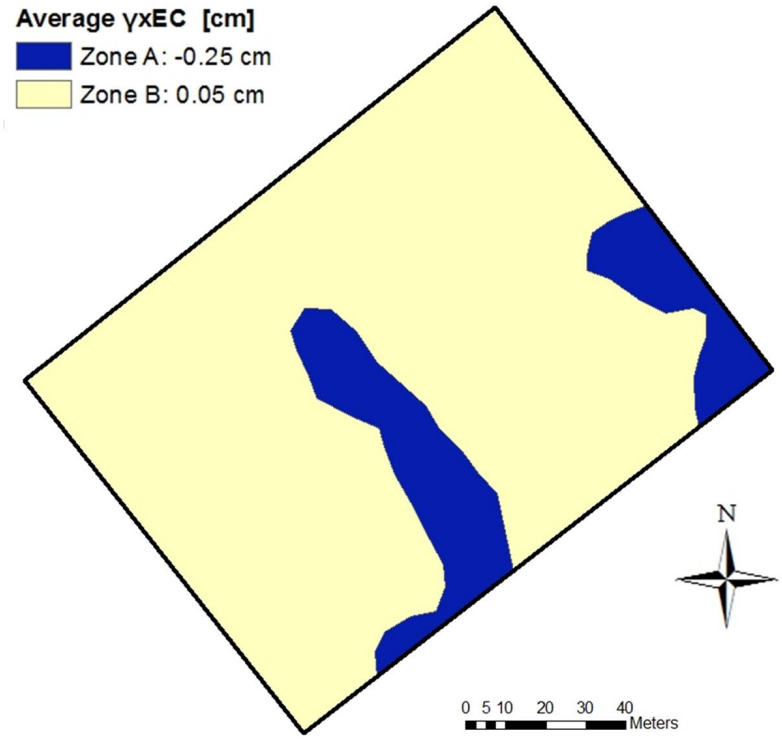

Figure 7.4: Management zones delineated for site-specific row-unit depth and downforce modifications within the 2015-B corn trial

7.1.3 Determination of Proper Depth and Downforce Settings

Let TD_A and TD_B represent the targeted seeding depths in any management zones A and B, respectively. Equations 7.2 and 7.3 define all row-unit depth and downforce combinations permitting to achieve TD_A and TD_B in management zone A and B, respectively. Targeted seeding depth can be constant throughout the field or vary from management zone to management zone.

For instance, if corn was planted within the 2014-B corn trial in zone A at a targeted seeding depth of 5.1 cm, all row-unit depth and downforce combinations permitting to achieve the targeted 5.1 cm depth were defined by equation 7.4. Similarly, if corn was planted within the 2014-B corn trial in zone B at a targeted depth of 5.1 cm, all row-unit depth and downforce combinations permitting to achieve the targeted 5.1 cm depth were defined by

equation 7.5. Comparison of results provided by equations 7.2 and 7.3 is presented in Figure 7.5.

Several row-unit depth by downforce combinations can be selected to achieve any targeted depth within each management zone. Proper row-unit depth and downforce within individual management zone should be selected from all possible combinations depending on soil texture and soil conditions at planting. For instance, results presented in chapter 4 demonstrated that planting in clayier soils would require lighter row-unit downforce and deeper row-unit depth adjustments than planting in less clayey soils to minimize soil compaction below the gauge-wheels and provide better soil conditions within the seedbed for crop emergence. For instance, the 5.1 cm targeted depth in 2014-B could be achieved using 4.1 cm row-unit depth and 1.1 kN row-unit downforce in zone A, and using 3.7 cm row-unit depth and 1.2 kN row-unit downforce in zone B. Those values could be used to complete the prescription map for the 2014-B field trial.

$$SD = \frac{TD_A - I_{F,S} - (\gamma \cdot EC)_A - \beta_{F,S} \cdot DF}{\alpha_{F,S} + \lambda_{F,S} \cdot DF} \tag{7.2}$$

$$SD = \frac{TD_A - I_{F,S} - (\gamma \cdot EC)_A - \beta_{F,S} \cdot DF}{\alpha_{F,S} + \lambda_{F,S} \cdot DF} \tag{7.3}$$

$$SD = \frac{5.1 - 2.05 + 0.15 - 0.57 \cdot DF}{0.65 - 0.02 \cdot DF} = \frac{3.2 - 0.57 \cdot DF}{0.65 - 0.02 \cdot DF} \tag{7.4}$$

$$SD = \frac{5.1 - 2.05 - 0.05 - 0.57 \cdot DF}{0.65 - 0.02 \cdot DF} = \frac{3.0 - 0.57 \cdot DF}{0.65 - 0.02 \cdot DF} \tag{7.5}$$

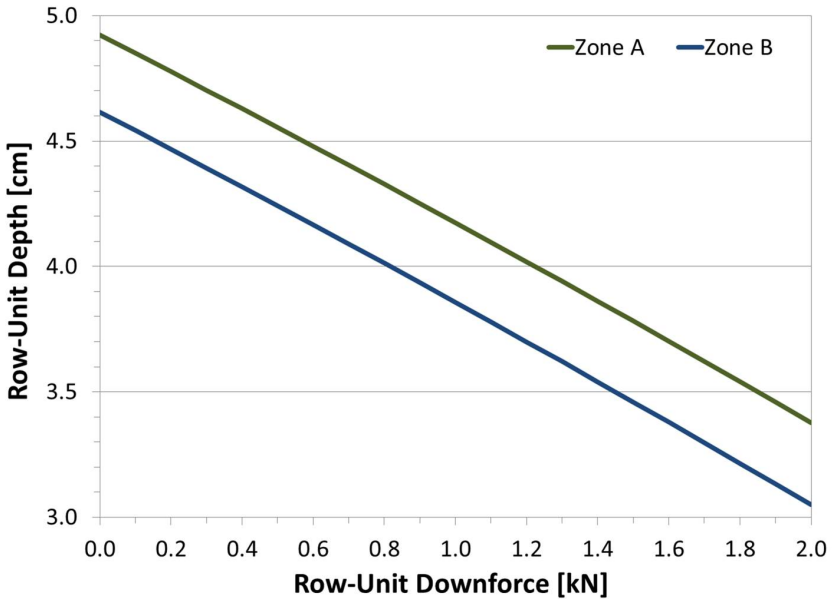

Figure 7.5: Row-unit depth and downforce combinations permitting to achieve 5.1 cm targeted depth within the 2014-B corn trial in zones A and B.

7.1.4 Evaluation of Benefits

Data analysis was conducted to estimate yield benefits which could have been achieved if the computed prescription maps had been used within individual field trials. Results presented in section 6.5 identified 3.9, 4.9, and 5.8 cm as optimum seeding depths within the 2014-B, 2015-A, and 2015-B corn trials to maximize corn yields at harvest. Deviations from these optimum seeding depth decreased corn final yields by -129·ΔDepth^2 [kg ha^{-1}] in 2014-B, -198·ΔDepth^2 [kg ha^{-1}] in 2015-A, and -103·ΔDepth^2 [kg ha^{-1}] in 2015-B. Yield loss associated with site-specific seeding depth variability identified within individual field trials was estimated using equation 7.6. Results demonstrated that accounting for site-specific variability using computed prescription maps would have permitted to increase crop yields by 1.0 kg ha^{-1} in 2014-B, 10 kg ha^{-1} in 2015-A, and 1.1 kg ha^{-1} in 2015-B. Computed results assumed proper row-unit depth and downforce adjustments to achieve optimum seeding depth at reference soil conditions within individual field trials. Benefits of using the computed

prescription maps would be higher if accounting for a biaised selection of row-unit depth and downforce planter settings adjustments.

$$\Delta Y_{F,S} = \frac{\sum_{Z \text{in} F,S} L_{F,S} \cdot A_{Z \text{in} F,S} \cdot (\gamma_Z \cdot EC_Z)^2}{A_{F,S}} \tag{7.6}$$

$\mathbf{\Delta Y_{F,S}}$: Yield loss due to site specific variability within selected corn trial [kg ha]; **Z in F,S**: management zone within selected corn trial; $\mathbf{L_{F,S}}$: model parameter provided in section 6.5 [kg ha^{-1}] – -129 in 2014-B, -198 in 2015-A, and -103 in 2015-B; $\mathbf{A_{Z \text{ in } F,S}}$: Percentage of trial area represented by zone Z [%]; $\boldsymbol{\gamma_Z \cdot EC_Z}$: parameter defined for individual management zone in figures 7.1 through 7.4; and $\mathbf{A_{F,S}}$: total trial area [ha].

7.2 Real-Time Seeding Depth Management

This approach to real-time planter setup presumed the ability to alter row-unit depth and downforce adjustments in response to real-time gauge-wheel load monitoring. The procedure for real-time row-unit depth and downforce adjustments, based on real-time measurements of gauge-wheel load at planting, would be similar to the procedure described in section 7.1 for prescription-based seeding depth management. Specifically, the model in equation 7.7 predicted seeding depth for any given gauge-weel load based on a set of five parameters. Those parameters were summarized for individual corn trials in Table 5.7. Three parameters were specific to a chosen row-unit depth ($\alpha_{F,S}$) and row-unit downforce ($\beta_{F,S}$), plus their interaction ($\lambda_{F,S}$) and would be fixed for a given field, F and season S. A fourth was an intercept ($I_{F,S}$), also fixed for a specific field and season. The last parameter, γ was the change in seeding depth that could be associated to changes in gauge-wheel load across the field. γ would be fixed for a given row-unit depth SD. Real-time depth and downforce adjustments would be performed based on this effect and on-the-go measurements of gauge-wheel load in the field. Therefore, real-time depth and downforce adjustments would require developing

an algorithm to manage changing gauge-wheel load into planter settings adjustments. The following section details this procedure.

$$ESD = I_{F,S} + \alpha_{F,S} \cdot SD + \beta_{F,S} \cdot DF + \lambda_{F,S} \cdot SD \cdot DF + \gamma_{SD} \cdot GWL \tag{7.7}$$

7.2.1 Real-Time Adjustments of Row-Unit Depth and Downforce Settings

Let TD represent the targeted seeding depth in a given field. Equation 7.8 define all row-unit depth and downforce combinations permitting to achieve TD at measured gauge-wheel load equal to GWL. For instance, if corn was planted within the 2014-B field trial at a targeted seeding depth of 5.1 cm and measured gauge-wheel load was equal to 1.2 kN, equation 7.8 would become equation 7.9 after replacing the equation parameters by their numerical values. As for prescription-based seeding depth management, row-unit depth and downforce adjustments should be selected from all possible depth and downforce combinations satisfying equation 7.8 depending on local soil conditions to optimize crop emergence. Row-unit depth and downforce combinations permitting to achieve TD vary with in-field variations in gauge-wheel load. γSD varies with row-unit depth adjustment due to changes in row-unit geometry.

$$SD = \frac{TD - I_{F,S} - \gamma_{SD} \cdot GWL - \beta_{F,S} \cdot DF}{\alpha_{F,S} + \lambda_{F,S} \cdot DF} \tag{7.8}$$

$$SD = \frac{5.1 - 2.05 - \gamma_{SD} \cdot 1.2 - 0.57 \cdot DF}{0.65 - 0.02 \cdot DF} \tag{7.9}$$

7.2.2 Computation of Local Gauge-Wheel Load Predictions

The performance of real-time technologies to manage site-specific seeding depth variability at planting woud depend on the system ability to perform in-field row-unit depth and downforce adjustments with proper timeliness, and therefore on the duration – or lag

– between the moment when gauge-wheel load is measured and the moment when row-unit depth and downforce settings are adjusted. One possibility to optimize the performance of such real-time system would consist in computing local gauge-wheel load predictions within the field. ARIMA models were computed to describe auto-correlations among gauge-wheel load data (Table 7.1) within individual corn trials. Results demonstrated the existence of 3 to 4 seconds spatial dependency among gauge-wheel load data therefore indicating that it is possible to compute local gauge-wheel load predictions within a field. Residual root mean square errors for ARIMA models were equal to 0.28 kN, 0.21 kN, 0.20 kN, and 0.22 kN within the 2014-A, 2014-B, 2015-A, and 2015-B corn trials.

Table 7.1: ARIMA models describing spatial auto-correlations among gauge-wheel load data within individual field trials.

Season	Field	Model Equation
2014	**A**	$y_t = 1.02 \cdot y_{t-1} + 0.20 \cdot y_{t-2} - 0.74 \cdot y_{t-3} + 0.11 \cdot y_{t-4} - 0.68 \cdot e_{t-1} - 0.35 \cdot e_{t-2} + 0.52 \cdot e_{t-3} + e_t$
2014	**B**	$y_t = 0.30 \cdot y_{t-1} + 0.23 \cdot y_{t-2} - 0.25 \cdot y_{t-3} + 0.33 \cdot y_{t-4} + 0.21 \cdot e_{t-1} - 0.16 \cdot e_{t-2} + 0.12 \cdot e_{t-3} - 0.24 \cdot e_{t-4} + e_t$
2015	**A**	$y_t = -1.00 \cdot y_{t-1} - 0.65 \cdot y_{t-2} + 0.13 \cdot y_{t-3} + 1.06 \cdot e_{t-1} + 0.74 \cdot e_{t-2} + e_t$
2015	**B**	$y_t = 1.40 \cdot y_{t-1} - 1.08 \cdot y_{t-2} - 0.98 \cdot y_{t-3} - 0.98 \cdot e_{t-1} + 0.51 \cdot e_{t-2} + e_t$

$\mathbf{y_t}$**:** Measured Gauge-Wheel Load at time t [kN]; $\mathbf{y_{t-1,\ t-2,\ t-3,\ t-4}}$**:** Lagged Gauge-Wheel Loads [kN] (lag: 1 s); $\mathbf{e_{t-1,\ t-2,\ t-3,\ t-4}}$**:** Lagged Errors [kN]; $\mathbf{e_t}$: Random Noise.

7.3 Discussion

Real-time planting technologies could permit to adjust row-unit depth and downforce settings at a more local scale than prescription based planting technologies therefore permitting a more precise management of seeding depth variability within fields. However, successful implementation of real-time planting technologies requires a thorough understanding of site-specific seeding depth response to measured gauge-wheel load in encountered soil conditions throughout the field to provide proper planter settings adjustments. Proper modeling of site-specific seeding depth response to measured gauge-wheel load and one's ability to

compute local gauge-wheel load predictions within a field would determine the performance and benefits of any real-time system to manage site-specific seeding variability at planting.

7.4 Summary

This chapter discussed development and implementation of prescription-based and real-time planting technologies to manage in-field seeding variability in Southeast US. Results presented in section 5.2.1 served to establish a set of prescription maps used to discuss prescription-based seeding depth management within fields. Regression models characterizing seeding depth response to row-unit depth and downforce adjustments and in-field soil EC were used to describe row-unit depth and downforce adjustments between management zones. Computed ARIMA models demonstrated the possibility of calculating local gauge-wheel load predictions for real-time planting applications, and regression models established in section 5.2.2 served to describe real-time row-unit depth and downforce adjustments based on real-time gauge-wheel load measurements at planting. Measured gauge-wheel load data exhibited 3 to 4 seconds temporal dependency. Even if most of the row-unit depth and downforce adjustments could be provided by dynamic downforce systems, optimum row-crop planter performance requires simultaneous seeding detph by downforce changes to maximize crop yield potential at planting.

Chapter 8

Conclusions

8.1 Research Conclusions

The following conclusions were drawn from this research:

1. Corn and cotton seeding depth increased with increasing row-unit depth and downforce. Row-unit downforce adjustments affected measured seeding depth by as much as 1.1 cm. Corn and cotton seeding depth was significantly affected by changing soil conditions between fields and growing season. Shallower seeding depths were achieved in clayier and wetter soil conditions which provided stronger soil resistance to furrow opening. Heavier row-unit downforce limited furrow closure at typical cotton seeding depths. Measured gauge-wheel load increased with increasing row-unit downforce, and reduced with increasing row-unit depth. Measured seeding depth and measured gauge-wheel load strongly varied within fields. Significant site-specific seeding depth variability was identified within individual corn trials, and within 1 of 4 cotton trials. Corn seeding depth did not significantly correlate with in-field changes in soil water content. Corn seeding depth significantly correlated with in-field changes in soil EC. Seeding depth relationship to soil EC explained all site-specific seeding depth variability observed within individual corn trials and characterized in-field changes in seeding depth ranging from 0.3 to 1.6 cm across individual corn trials. Corn seeding depth also significantly correlated to measured gauge-wheel load at planting. Gauge-wheel load effects explained all site-specific seeding depth variability observed in 1 of 2 fields.

2. Corn emergence and yields were primarily affected by changing conditions between fields and growing seasons. Warmer soil temperatures promoted quicker emergence,

more uniform stand establishment, and higher final plant population. Clayier soils provided poor soil conditions for corn establishment and growth. Corn emergence metrics were significantly affected by measured seeding depth and gauge-wheel load. Improved corn emergence correlated with higher corn final yields. Optimum seeding depths and gauge-wheel loads were identified to maximize the quality of crop establishment and final yields within individual corn trials.

3. Prescription maps were generated to maintain seeding depth variability associated with spatial changes in soil EC within individual management zones within $\tau = \pm 0.2cm$. Spatial dependency was identified among gauge-wheel load data demonstrating the possibility of computing local gauge-wheel load predictions for real-time planting applications. Regression models computed to characterize seeding depth response to row-unit depth and downforce adjustments and changing soil conditions within fields were used to discuss prescription-based and real-time row-unit depth and downforce adjustments to manage seeding variability at planting. Most of the seeding depth adjustments could be provided through dynamic downforce systems, but optimum row-crop planter performance requires concurrent row-unit depth by downforce changes.

8.2 Practical Implications

The optimum goal at planting is to place individual seeds within proper soil conditions for immediate germination and emergence to maximize crop yield potential at the start of the growing season. Even if the concept and capabilities are years away, development and implementation of new and soon to be released planting technologies increases the scope of possiblities to optimize modern row-crop planters seeding depth performance. Thus, after developing dynamic downforce systems to manage in-field seeding depth variability, companies are now working on precision technologies that will enable in-fields adjustments of both row-unit depth and downforce planter adjustments. In-field adjustments of row-unit depth and downforce settings could be based on the use of prescription maps for seeding depth or

real-time monitoring of row-unit performance. Soil EC was identified as a potential parameter to use to optimize management zone determination for prescription-based applications. Soil water content data could also be used as covariate to characterize field spatial variability providing sufficient data resolution. Real-time gauge-wheel load monitoring could be considered to adjust row-unit depth and downforce settings on-the-go providing proper data resolution and adequate field conditions. Development of planting technologies with such site-specific capabilities could contribute to increase crop yields by a much as 10% to 15% in some field areas. Success could require increasing planter instrumentation, and changing row-unit design to support the new technology. New technology should also provide operators with proper feedback to ensure adequate seeding depth performance. Successful implementation of such technologies will require the development of robust models characterizing seeding depth and crop response to row-unit depth and downforce adjustments and changing soil conditions within fields. Finally, advances with Precision planting technologies improves our understanding of row-crop planters performance in response to their environment which enables to get one step closer to the true concept of Precision Agriculture.

8.3 Future Research

Methods used in this research provided quantifiable results as related to characterizing seeding depth and crop response to row-unit depth and downforce adjustments in different field conditions. Results demonstrated that seeding depth performance of standard row-crop planter was significantly affected by changing soil conditions within fields, and standards should be developed to characterize seeding depth variability within actual field situations and its impact on crop establishment. Establishment of such standards would provide researchers, producers, manufacturers, and consultants with valuable data to evaluate and understand existing seeding depth variabillity within current field situations. These standards would also make producers aware of the importance of optimizing seeding depth performance to maximize field productivity.

Results presented in this study provided relevant examples to discuss implementation of prescription-based and real-time planting technologies to manage in-field seeding depth variability. However, results were limited to two fields, two growing seasons, and available data, and future research would consider accounting for a wider diversity of soils and climate conditions to build more robust models and better understand seeding depth and crop response to field spatial variability. Moreover, field spatial variability was measured considering only two soil properties, and future research could also include the use of data from the field as well as remote sensing and aerial imagery to investigate how other soil parameters can be used to predict site-specific seeding depth response. Furthermore, real-time gauge-wheel load measurements only were available to monitor row-unit behavior at planting, and future research would consider increasing planter instrumentation. Additional measurements would include applied downforce at the downforce system, and vertical forces exerted onto the soil furrow openers. Future research would also consider expanding results to other management strategies including no-till versus strip-till versus conventional tillage, as well as irrigated crop versus non-irrigated crops.

Additionally, measured seeding depth data were collected at low resolution which constituted one of the major limitations of this study. Hence, future research could consider measuring seeding depth at higher sampling resolution (along a planter pass for instance) to better characterize seeding depth response to gauge-wheel load operation and field spatial variability. Future research could also consider collecting more data during the growing season to better understand seeding depth impact on crop growth and resistance to unfavorable environmental conditions.

References

Abendroth, L., & Elmore, R. (2006). *What Row Spacing is Best?* (Tech. Rep.). Iowa State University Agronomy Extension. Retrieved from `http://www.agronext.iastate.edu/corn/production/management/planting/row.html`

Alessi, J., & Power, J. F. (1971). Corn Emergence in Relation to Soil Temperature and Seeding Depth. *Agronomy Journal*, *63*(5), 717-719.

Auernhammer, H. (2001). Precision Farming - the Environmental Challenge. *Computers and Electronics in Agriculture*, *30*(1), 31-43.

Auernhammer, H., & Schueller, J. K. (1999). Precision Farming. *CIGR Handbook of Agricultural Engineering*, *3*, 598-616.

Bates, D., Mächler, M., Bolker, B., & Walker, S. (2015). Fitting Linear Mixed-Effects Models Using lme4. *Journal of Statistical Software*, *67*(1), 1-48.

Bowen, H. D. (1966). Measurement of Edaphic Factors for Determining Planter Specifications. *Transactions of the ASAE*, *9*(5), 725-0735.

Bridges, R. (2016). *Soil-Planter Interaction Force Distribution as Affected by Planting Depth Setting and Planter Configuration.* (Unpublished master's thesis). Auburn University.

Burce, M. E., Kataoka, T., Okamoto, H., & Shibata, Y. (2009). Active Seed Depth Control for No-Tillage System. In *Proceedings of the 2009 ASABE Annual International Meeting.* St. Joseph MI: ASABE.

Butzen, S. (2003). *Corn Seeding Rate Considerations.* (Tech. Rep.). DuPont Pioneer. Retrieved from `https://www.pioneer.com/home/site/us/agronomy/library/corn-seeding-rate-considerations/`

Carter, P. R., Nafzinger, E. D., & Lauer, J. G. (1990). *Uneven Emergence in Corn.* (Tech. Rep.). University of Illinois at Urbana-Champaign: Cooperation Extension Service for

North Central Regional Extension Service.

Chung, Y., Rabe-Hesketh, S., Dorie, V., Gelman, A., & Liu, J. (2013). A Nondegenerate Penalized Likelihood Estimator for Variance Parameters in Multilevel Models. *Psychometrika*, *78*(4), 685-709.

Dawn. (2014). *Closing Wheels.* Retrieved from http://www.dawnequipment.com/

Dekalb. (2015). *Populations and Variable Rate Seeding for Corn* (Tech. Rep.). Montsanto Technology LLC. Retrieved from http://www.aganytime.com/Corn/Pages/Article.aspx?name=Populations_and_Variable_Rate_Seeding_for_Corn&fields=article&article=485

Deltapine. (2012). *Variety by Seeding Rate by pGr in Cotton* (Tech. Rep.). Montsanto Technology LLC. Retrieved from http://www.monsanto.com/products/documents/learning-center-research/2012/slc-dp-variety-by-seeding-rate-by-pgr-in-cotton.pdf

Deltapine. (2015). *Optimum Planting Conditions and Seed Placement for Cotton.* (Tech. Rep.). Montsanto Technology LLC. Retrieved from http://www.aganytime.com/Documents/ArticlePDFs/Optimum%20Planting%20Conditions%20and%20Seed%20Placement%20for%20Cotton.pdf

Dickey, E. C., & Jasa, P. J. (1983). G83-684 Row-Crop Planters: Equipment Adjustments and Performance in Conservation Tillage. *Historical Materials from University of Nebraska-Lincoln Extension*, 692.

Elmore, R., Daugherty, R. B., & Mueller, N. (2015). *Growing Degree Units and Corn Emergence.* (Tech. Rep.). University of Nebraska-Lincoln.

Evans, L. T., & Fischer, R. A. (1999). Yield Potential: Its Definition, Measurement, and Significance. *Crop Sciences*, *36*(6), 1544-1551.

Fernandez-Cornejo, J. (2004). *The Seed Industry in U.S. Agriculture. An Exploration of Data and Information on Crop Seed Markets, Regulation, Industry Structure, and Research and Development.* (Tech. Rep.). USDA.

Grisso, R., Alley, M., Holshouser, D., & Thomasson, W. (2009). *Precision Farming Tools: Soil Electrical Conductivity.* (Tech. Rep.). Virginia Cooperative Extension.

Hanna, H. M., Steward, B. L., & Aldinger, L. (2010). Soil Loading Effects of Planter Depth-Gauge Wheels on Early Corn Growth. *Applied Engineering in Agriculture.*, *26*(4), 551-556.

Heraud, J. A., & Lange, A. F. (2009). Agricultural Automatic Vehicle Guidance from Horses to GPS: How We Got Here, and Where We Are Going. In *Agricultural Equipment Technology Conference* (Vol. 33, p. 1-67). St. Joseph MI: ASABE.

Hesketh, J. D., & Warrington, I. J. (1989). Corn Growth Response to Temperature: Rate and Duration of Leaf Emergence. *Agronomy Journal*, *81*(4), 696-701.

Hest, D. (2011). *Variable-Rate Seeding has Variable Payoff* (Tech. Rep.). Farm Industry News. Retrieved from `http://farmindustrynews.com/variable-rate/variable-rate-seeding-has-variable-payoff?page=1`

Hiemstra, P., Pebesma, E., Twenh"ofel, C., & Heuvelink, G. (2008). Real-Time Automatic Interpolation of Ambient Gamma Dose Rates from the Dutch Radioactivity Monitoring Network. *Computers and Geosciences*.

Holekamp, E. R., Hudspeth, E. B., & Ray, L. L. (1966). Relation of Soil Temperature Prior to Planting to Emergence of Cottonseed. *Transactions of the ASAE*, *9*(2), 203-0205.

Hudspeth, E. B., & Wanjura, D. F. (1970). A Planter for Precision Depth and Placement of Cottonseed. *Transactions of the ASAE*, *13*(2), 153-154.

Hunter, J. R., & Erickson, A. E. (1952). Relation of Seed Germination to Soil Moisture Tension. *Agronomy Journal*, *44*(3), 107-109.

Hyndman, R. J., & Khandakar, Y. (2008). Automatic Time Series Forecasting: the Forecast Package for R. *Journal of Statistical Software*, *26*(3), 1-22.

Jeschke, M., Carter, P., Bax, P., & Schon, R. (2012). *Putting Variable-Rate Seeding to Work on Your Farm.* (Tech. Rep.). DuPont Pioneer, Crop Insights. Retrieved from `https://www.pioneer.com/home/site/us/agronomy/library/variable-rate-seeding/`

John Deere. (2004). *1700 Integral 6RW MaxEmerge Plus John Deere Planter Manual, Section: 90 - General Attachments: Heavy-Duty Downforce Springs.* Retrieved from http://manuals.deere.com/omview/OMA70299_19/OMA70299_19.htm

Karayel, D., & Ozmerzi, A. (2008). Evaluation of Three Depth-Control Component on Seed Placement Accuracy and Emergence for a Precision Planter. *Applied Engineering in Agriculture*, *24*(3), 271-276.

Knappenberger, T., & Köller, K. (2011). Spatial Assesment of the Correlation of Seeding Depth with Emergence and Yield of Corn. *Precision Agriculture*, *13*(2), 163-180.

Kocher, M. F., M, C. J., Smith, J. A., & Kachman, S. D. (2011). Corn Seed Spacing Uniformity as Affected by Seed Tube Condition. *Applied Engineering in Agriculture*, *27*(2), 177-183.

Kush, G. S. (1999). Green Revolution: Preparing for the 21st Century. *Genome*, *42*(4), 646-655.

Luck, J. D., Zandonadi, R. S., & Shearer, S. A. (2011). A Case Study to Evaluate Field Shape Factors for Estimating Overlap Errors with Manual and Automatic Section Control. *Transactions of the ASABE*, *54*(4), 1237-1243.

Martin, D. L., & Thraikill, D. J. (1993). Moisture and Humidity Requirements for Germination of Surface Seeded Corn. *Applied Engineering in Agriculture*, *9*(1), 43-48.

Martin, K. L., Hodgen, P. J., Freeman, K. W., Melchiori, R., Arnall, D. B., Teal, R. K., ... Raun, W. R. (2005). Plant-to-Plant Variability in Crop Production. *Agronomy Journal*, *97*(6), 1603-1611.

Miller, E. A., Rascon, J., Koller, A., Porter, W. M., Taylor, R. K., Raun, W. R., & Kochenower, R. (2012). Evaluation of Corn Seed Vacuum Metering Systems. In *Proceedings of the 2012 ASABE Annual International Meeting.* St. Joseph MI: ASABE.

Morrison, J. E. (1988). Interactive Planter Depth Control and Pneumatic Downpressure System. *Transactions of the ASAE*, *31*(1), 14-18.

Morrison, J. E. (1989). Factors Affecting Plant Establishment with a No-Tillage Planter

Opener. *Applied Engineering in Agriculture*, *5*(3), 316-318.

Morrison, L. (2010). *Tips for More Accurate Planting Tools and Practices. Corn and Soybean Digest.*

Morrison Jr, J. E., & Gerik, T. J. (1983). Planter Depth-Control Predictions and Projected Effects on Crop Emergence [Tillage]. *Paper-American Society of Agricultural Engineers*.

Mullenix, D., Fulton, J., Broadbeck, C., Winstead, A., & Norwood, S. (2008). *Overview of Automatic Section Control Technology.* (Tech. Rep.). Department of Biosystems Engineering, Auburn University.

Murray, J. R., Tulberg, J. N., & Basnet, B. B. (2006). *Planters and their Components: Types, Attributes, Functional Requirements, Classification and Description.* (No. 121). ACIAR Monograph.

Nafziger, E. D., Carter, P. R., & Graham, E. E. (1991). Response of Corn to Uneven Emergence. *Crop Science*, *31*(3), 811-815.

NDSU. (2010). *Producers May Want to Consider Section and Row Control for Planters.* Retrieved from `https://www.ag.ndsu.edu/news/newsreleases/2010/may-24-2010/producers-may-want-to-consider-section-and-row-control-for-planters/`

Piepho, H. P., Büchse, A., & K, E. (2003). A Hitchhiker's Guide to Mixed Models for Randomized Experiments. *Journal of Agronomy and Crop Science*, *189*(5), 310-322.

Pioneer. (2014). *Row-Width in Corn Grain Production.* (Tech. Rep.). DuPont Pioneer, Agronomy Sciences Research Summary.

Price, R. R. (2011). A General Method to Illustrate the Different Field Efficiency Gains of Guidance Systems. In *Proceedings of the 2011 ASABE Annual International Meeting.* St. Joseph MI: ASABE.

R Core Team. (2016). *R: A Language and Environment for Statistical Computing.* Retrieved from `http://www.R-project.org/`

Rene-Laforest, F., Adamchuck, V., Mastorakos, M., Dhawale, N., & Su, Y. (2014). Variable

Depth Planting of Corn. In *Proceedings of the 2014 ASABE Annual International Meeting.* St. Joseph MI: ASABE.

Runge, M., Fulton, J., Griffin, T., Virk, S., & Brooke, A. (2014). *Automatic Section Control Technology for Row-Crop Planters* (Tech. Rep.). Alabama Cooperative Extension System.

Schneider, E. C., & Gupta, S. C. (1985). Corn Emergence as Influenced by Soil Temperature, Matric Potential, and Aggregate Size Distribution. *Soil Science Society of America Journal.*, *49*(2), 415-422.

Schnitkey, G. (2015). *Corn: How Much Seed Cost has Increased Since 1994.* (Tech. Rep.). University of Illinois. Retrieved from `http://agfax.com/2015/11/18/corn-much-seed-cost-increased-since-1994/`

Scott, J. (2015). *10 Tips for High-Speed Planting. Successful Farming at AGRICULTURE.COM.* Retrieved from `http://www.agriculture.com/machinery/farm-implements/planters/10-tips-f-highspeed-plting_231-ar47375`

Searle, C. L., Kocher, M. F., Smith, J. A., & Blankenship, E. E. (2008). Field Slope Effects on Uniformity of Corn Seed Spacing for Three Precision Planter Metering Systems. *Applied Engineering in Agriculture*, *24*(5), 581-586.

Srivastava, A. K., Goering, C. E., Rohrbach, R. P., & Buckmaster, D. R. (2006). Crop Planting. In *Engineering Principles of Agricultural Machines* (2nd ed., p. 231-265). St. Joseph, MI: ASABE.

Staggenborg, S. A., Taylor, R. K., & Maddux, L. D. (2004). Effect of Planter Speed and Seed Firmers on Corn Stand Establishment. *Applied Engineering in Agriculture*, *20*(5), 573-580.

Sutherland, A. (2012). *Degree-Day Heat Unit Calculator* (Tech. Rep.). Mesonet.

Terra, J. A., Shaw, J. N., Reeves, D. W., Raper, R. L., Van Santen, E., & Mask, P. L. (2004). Soil Carbon Relationships with Terrain Attributes, Electrical Conductivity, and a Soil Survey in a Coastal Plain Landscape. *Soil Science*, *169*(12), 819-831.

Terra, J. A., Shaw, J. N., Reeves, D. W., Raper, R. L., Van Santen, E., Schwab, E. B., & Mask, P. L. (2006). Soil Management and Landscape Variability Affects Field-Scale Cotton Productivity. *Soil Science Society of America*, *70*(1), 98-107.

Thomison, P., Jeschke, M., & Butzen, S. (2013). *Planting Depth Effects on Corn Stand and Grain Yields.* (Tech. Rep.). DuPont Pioneer, Field Facts. Retrieved from `https://www.pioneer.com/home/site/us/agronomy/library/planting-depth-and-stand-yields/`

USDA. (2006). *Increasing Production Costs.* Retrieved from `http://www.usda.gov/documents/INCREASING_PRODUCTION_COSTS.pdf`

USDA. (2016). *Population Projections.* Retrieved from `http://www.ers.usda.gov/data-products/international-macroeconomic-data-set.aspx`

Wanjura, D. F. (1982). Reduced Cotton Productivity from Delayed Emergence. *Transactions of the ASAE*, *25*(6), 1536-1539.

Weatherly, E. T., & Bowers, C. G. (1997). Automatic Depth Control of a Seed Planter based on Soil Drying Front Sensing. *Transactions of the ASAE*, *40*(2), 295-305.

White, M. L., Shaw, J. N., Raper, R. L., rodekohr, D., & Wood, C. W. (2012). A Multivariate Approach for High Resolution Soil Survey Development. *Soil Science*, *177*(5), 345-354.

Winstead, A., Fulton, J., & Mullenix, D. (2010). *Considerations for Adopting and Implementing Precision Ag Technologies* (Tech. Rep.). Alabama Cooperative Extension System.

Yao, A. Y., & Shaw, R. H. (1964). Effect of Plant Population and Planting Pattern of Corn on Water Use and Yield. *Agronomy Journal*, *56*(2), 147-152.

Yazgi, A., & Degirmencioglu, A. (2007). Optimization of the Seed Spacing Uniformity Performance of a Vacuum-Type Precision Seeder using Response Surface Methodology. *Biosystems Engineering*, *97*(3), 347-356.

Zhang, J., Wang, W. M., Dong, Q. X., & Hou, J. L. (2006). Effect of Different Planting Density on Cotton Canopy Structure, Canopy Photosynthesis, and Yield Formation.

In *Proceedings of the 2006 ASABE Annual International Meeting.* St. Joseph MI: ASABE.

Appendices

Appendix A

Suppplementary Information for Individual Field Trials

A.1 Tillage - Planting Date - Seed Variety

Table A.1: Supplementary information provided for individual field trials conducted in this study – strip-tillage date, planting date, seed variety.

Crop	Year	Field	Strip-Tillage	Planting Date	Variety
Corn	2014	A	04/11/2014	04/13/2014	P2088 R
		B	04/12/2014		
Corn	2015	A	04/09/2015	04/09/2015	P2089 YHR
		B	04/08/2015		
Cotton	2014	A	04/11/2014	05/08/2014	PHY375 WRF
		B	04/12/2014		
Cotton	2015	A	05/06/2015	05/08/2015	PHY375 WRF
		B	04/08/2015		

A.2 Plots and Sampling Layouts

---------- Field A ----------

Rep. 1	Plot	*6 Rows Buffer*	101	102	103	104	105	106	107	108	109
	Seed Depth		2.5 cm	7.6 cm	5.1 cm	2.5 cm	2.5 cm	5.1 cm	5.1 cm	7.6 cm	7.6 cm
	Spring Setting		Heavy	Heavy	No	No	Medium	Medium	Heavy	Medium	No

Rep. 2	Plot	201	202	203	204	205	206	207	208	209
	Seed Depth	2.5 cm	2.5 cm	5.1 cm	2.5 cm	5.1 cm	7.6 cm	7.6 cm	5.1 cm	7.6 cm
	Spring Setting	No	Heavy	Heavy	Medium	No	Medium	No	Medium	Heavy

Rep. 3	Plot	301	302	303	304	305	306	307	308	309
	Seed Depth	5.1 cm	2.5 cm	5.1 cm	2.5 cm	5.1 cm	7.6 cm	2.5 cm	7.6 cm	7.6 cm
	Spring Setting	Heavy	Medium	Medium	No	No	Medium	Heavy	No	Heavy

Rep. 4	Plot	401	402	403	404	405	406	407	408	409
	Seed Depth	5.1 cm	5.1 cm	7.6 cm	7.6 cm	7.6 cm	2.5 cm	2.5 cm	2.5 cm	5.1 cm
	Spring Setting	Medium	No	No	Medium	Heavy	Heavy	Medium	No	Heavy

---------- Field B ----------

Rep. 1	Plot	*6 Rows Buffer*	101	102	103	104	105	106	107	108	109
	Seed Depth		5.1 cm	7.6 cm	5.1 cm	2.5 cm	2.5 cm	5.1 cm	7.6 cm	2.5 cm	7.6 cm
	Spring Setting		Medium	Heavy	No	Heavy	No	Heavy	Medium	Medium	No

Rep. 2	Plot	201	202	203	204	205	206	207	208	209
	Seed Depth	2.5 cm	5.1 cm	5.1 cm	7.6 cm	7.6 cm	2.5 cm	5.1 cm	7.6 cm	2.5 cm
	Spring Setting	No	Medium	Heavy	Medium	No	Medium	No	Heavy	Heavy

Rep. 3	Plot	301	302	303	304	305	306	307	308	309
	Seed Depth	7.6 cm	7.6 cm	2.5 cm	5.1 cm	5.1 cm	2.5 cm	7.6 cm	5.1 cm	2.5 cm
	Spring Setting	No	Heavy	Medium	No	Medium	Heavy	Medium	Heavy	No

Figure A.1: Plot layouts for 2014-A and 2014-B corn trials.

---------- Field A ----------

Rep. 1	Plot	*6 Rows Buffer*	101	102	103	104	105	106	107	108	109
	Seed Depth		7.6 cm	2.5 cm	5.1 cm	7.6 cm	2.5 cm	7.6 cm	5.1 cm	5.1 cm	2.5 cm
	Spring Setting		Medium	No	Medium	Heavy	Heavy	No	Heavy	No	Medium

Rep. 2	Plot	201	202	203	204	205	206	207	208	209
	Seed Depth	7.6 cm	7.6 cm	5.1 cm	5.1 cm	2.5 cm	2.5 cm	5.1 cm	7.6 cm	2.5 cm
	Spring Setting	Heavy	Medium	Heavy	Medium	Heavy	Medium	No	No	No

Rep. 3	Plot	301	302	303	304	305	306	307	308	309
	Seed Depth	7.6 cm	2.5 cm	7.6 cm	5.1 cm	2.5 cm	7.6 cm	5.1 cm	2.5 cm	5.1 cm
	Spring Setting	Heavy	Heavy	No	No	Medium	Medium	Medium	No	Heavy

Rep. 4	Plot	401	402	403	404	405	406	407	408	409
	Seed Depth	2.5 cm	2.5 cm	7.6 cm	7.6 cm	5.1 cm	5.1 cm	5.1 cm	7.6 cm	2.5 cm
	Spring Setting	No	Heavy	Heavy	Medium	Heavy	No	Medium	No	Medium

---------- Field B ----------

Rep. 1	Plot	*6 Rows Buffer*	101	102	103	104	105	106	107	108	109
	Seed Depth		2.5 cm	7.6 cm	2.5 cm	5.1 cm	7.6 cm	7.6 cm	5.1 cm	2.5 cm	5.1 cm
	Spring Setting		No	Heavy	Medium	No	No	Medium	Medium	Heavy	Heavy

Rep. 2	Plot	201	202	203	204	205	206	207	208	209
	Seed Depth	7.6 cm	5.1 cm	5.1 cm	7.6 cm	2.5 cm	2.5 cm	5.1 cm	2.5 cm	7.6 cm
	Spring Setting	Medium	No	Medium	Heavy	Medium	No	Heavy	Heavy	No

Rep. 3	Plot	301	302	303	304	305	306	307	308	309
	Seed Depth	7.6 cm	5.1 cm	2.5 cm	5.1 cm	5.1 cm	7.6 cm	2.5 cm	7.6 cm	2.5 cm
	Spring Setting	Heavy	Medium	Heavy	Heavy	No	Medium	No	No	Medium

Figure A.2: Plot layouts for 2015-A and 2015-B corn trials.

---------- Field A ----------

Rep. 1	Plot	*6 Rows Buffer*	101	102	103	104	105	106	107	108	109
	Seed Depth		0.6 cm	1.3 cm	2.5 cm	2.5 cm	0.6 cm	2.5 cm	0.6 cm	1.3 cm	1.3 cm
	Spring Setting		Heavy	No	Medium	Heavy	No	No	Medium	Medium	Heavy

Rep. 2	Plot	201	202	203	204	205	206	207	208	209
	Seed Depth	2.5 cm	1.3 cm	2.5 cm	0.6 cm	0.6 cm	2.5 cm	1.3 cm	0.6 cm	1.3 cm
	Spring Setting	No	No	Medium	No	Medium	Heavy	Medium	Heavy	Heavy

Rep. 3	Plot	301	302	303	304	305	306	307	308	309
	Seed Depth	0.6 cm	1.3 cm	2.5 cm	0.6 cm	2.5 cm	0.6 cm	1.3 cm	1.3 cm	2.5 cm
	Spring Setting	Medium	Medium	Medium	Heavy	No	No	Heavy	No	Heavy

Rep. 4	Plot	401	402	403	404	405	406	407	408	409
	Seed Depth	2.5 cm	1.3 cm	1.3 cm	0.6 cm	0.6 cm	2.5 cm	2.5 cm	1.3 cm	0.6 cm
	Spring Setting	Medium	No	Medium	Medium	Heavy	No	Heavy	Heavy	No

---------- Field B ----------

Rep. 1	Plot	*6 Rows Buffer*	101	102	103	104	105	106	107	108	109
	Seed Depth		2.5 cm	1.3 cm	1.3 cm	0.6 cm	0.6 cm	2.5 cm	0.6 cm	1.3 cm	2.5 cm
	Spring Setting		No	No	Medium	Heavy	Medium	Medium	No	Heavy	Heavy

Rep. 2	Plot	201	202	203	204	205	206	207	208	209
	Seed Depth	1.3 cm	0.6 cm	1.3 cm	0.6 cm	2.5 cm	2.5 cm	0.6 cm	2.5 cm	1.3 cm
	Spring Setting	Heavy	Heavy	Medium	Medium	Medium	Heavy	No	No	No

Rep. 3	Plot	301	302	303	304	305	306	307	308	309
	Seed Depth	2.5 cm	0.6 cm	0.6 cm	2.5 cm	0.6 cm	2.5 cm	1.3 cm	1.3 cm	1.3 cm
	Spring Setting	Medium	No	Medium	Heavy	Heavy	No	Medium	No	Heavy

Figure A.3: Plot layouts for 2015-A and 20015-B cotton trials.

---------- Field A ----------

Rep. 1	Plot	*6 Rows Buffer*	101	102	103	104	105	106	107	108	109
	Seed Depth		1.3 cm	2.5 cm	1.3 cm	2.5 cm	0.6 cm	2.5 cm	1.3 cm	0.6 cm	0.6 cm
	Spring Setting		Medium	Medium	No	No	Medium	Heavy	Heavy	No	Heavy

Rep. 2	Plot	201	202	203	204	205	206	207	208	209
	Seed Depth	0.6 cm	0.6 cm	2.5 cm	1.3 cm	1.3 cm	1.3 cm	2.5 cm	2.5 cm	0.6 cm
	Spring Setting	Heavy	No	Medium	Heavy	Medium	No	No	Heavy	Medium

Rep. 3	Plot	301	302	303	304	305	306	307	308	309
	Seed Depth	0.6 cm	2.5 cm	1.3 cm	1.3 cm	2.5 cm	1.3 cm	0.6 cm	2.5 cm	0.6 cm
	Spring Setting	Medium	Heavy	No	Medium	No	Heavy	Heavy	Medium	No

Rep. 4	Plot	401	402	403	404	405	406	407	408	409
	Seed Depth	1.3 cm	2.5 cm	2.5 cm	0.6 cm	2.5 cm	1.3 cm	0.6 cm	1.3 cm	0.6 cm
	Spring Setting	Medium	Medium	No	No	Heavy	No	Heavy	Heavy	Medium

---------- Field B ----------

Rep. 1	Plot	*6 Rows Buffer*	101	102	103	104	105	106	107	108	109
	Seed Depth		1.3 cm	1.3 cm	0.6 cm	0.6 cm	0.6 cm	1.3 cm	2.5 cm	2.5 cm	2.5 cm
	Spring Setting		No	Heavy	No	Heavy	Medium	Medium	Medium	Heavy	No

Rep. 2	Plot	201	202	203	204	205	206	207	208	209
	Seed Depth	0.6 cm	2.5 cm	2.5 cm	0.6 cm	1.3 cm	1.3 cm	0.6 cm	2.5 cm	1.3 cm
	Spring Setting	Medium	Heavy	No	Heavy	No	Medium	No	Medium	Heavy

Rep. 3	Plot	301	302	303	304	305	306	307	308	309
	Seed Depth	2.5 cm	0.6 cm	2.5 cm	1.3 cm	1.3 cm	2.5 cm	0.6 cm	0.6 cm	1.3 cm
	Spring Setting	No	Medium	Medium	Medium	Heavy	Heavy	No	Heavy	No

Figure A.4: Plot layouts for 2014-A and 2014-B cotton trials.

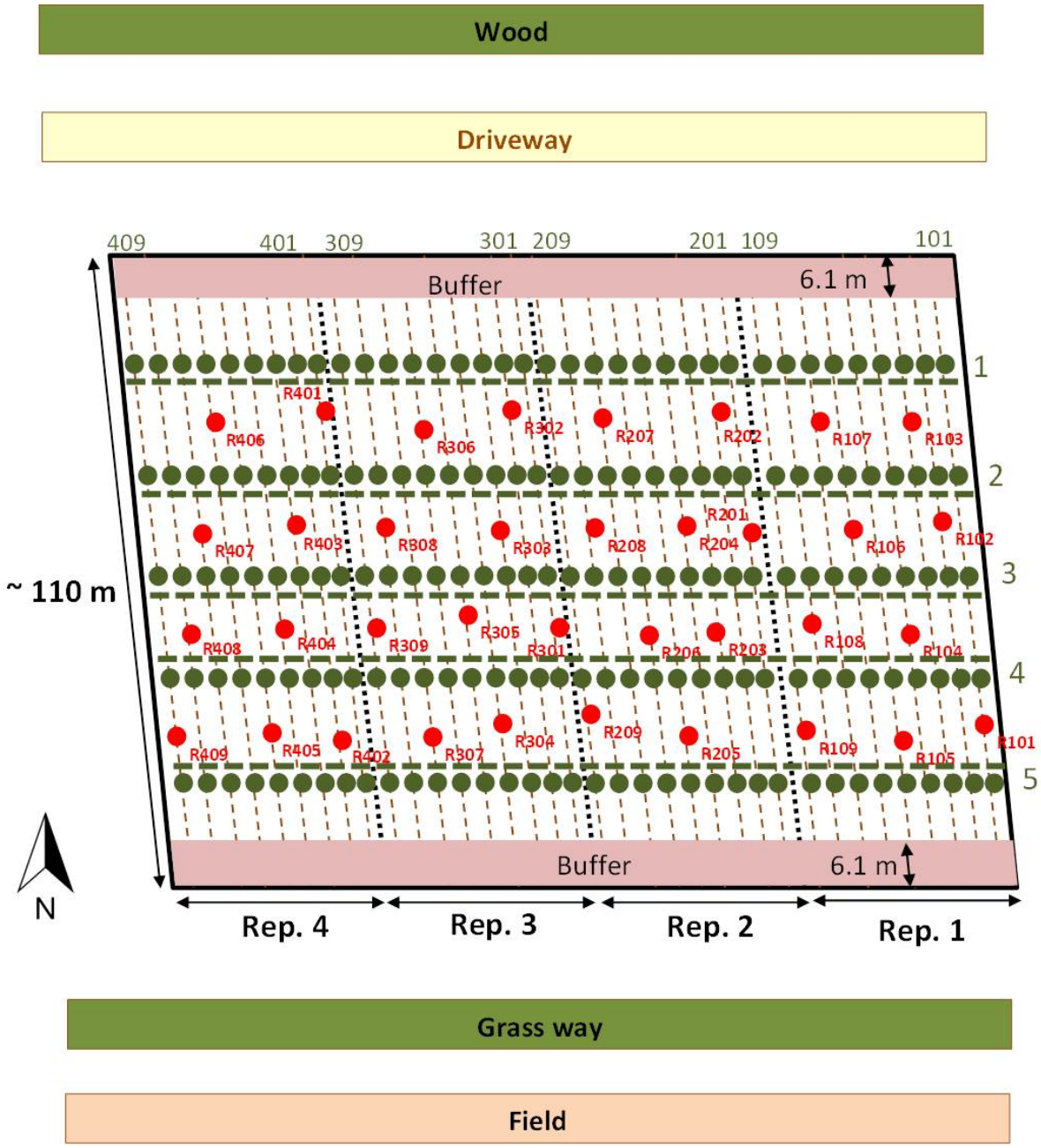

Figure A.5: Sampling sites layout for 2014-A corn trial.

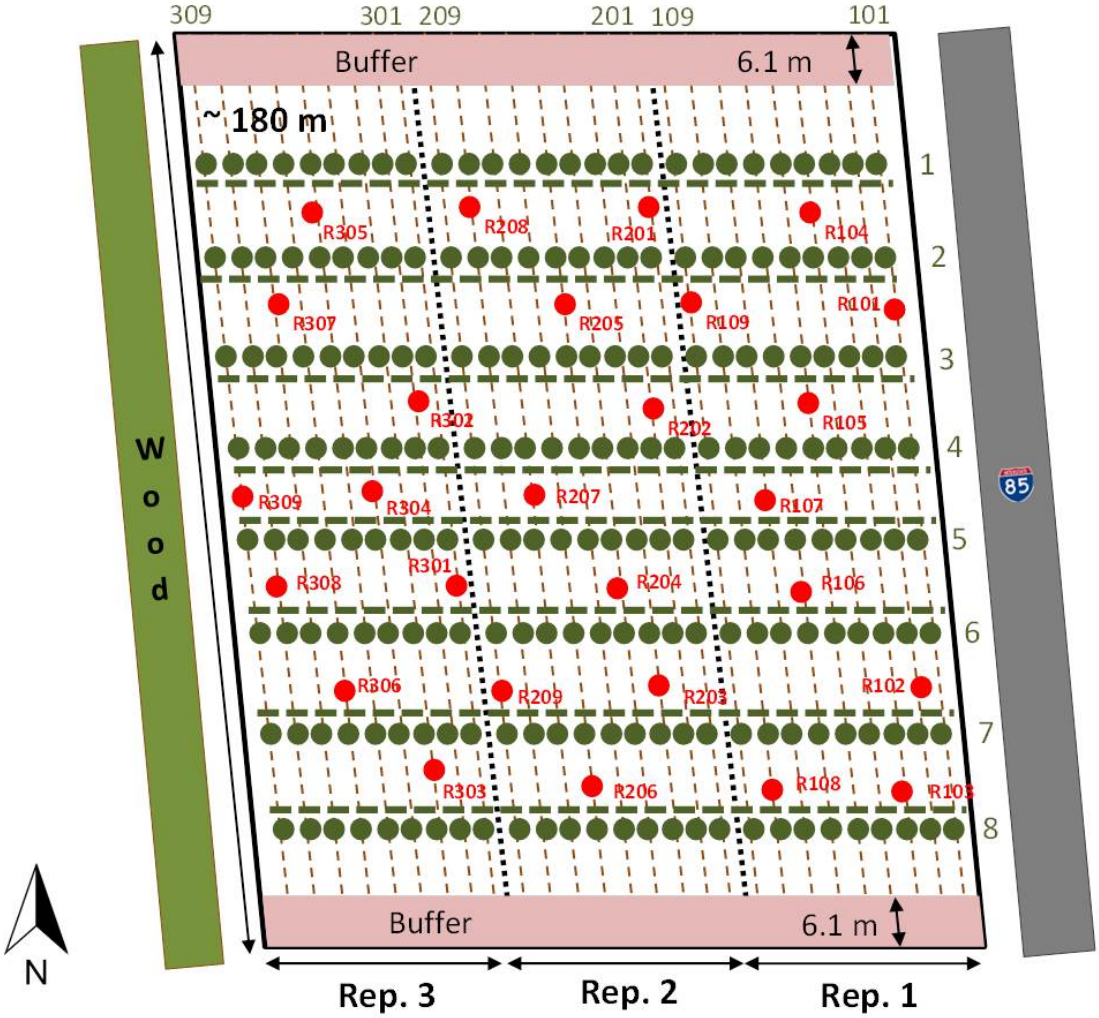

Figure A.6: Sampling sites layout for 2014-B corn trial.

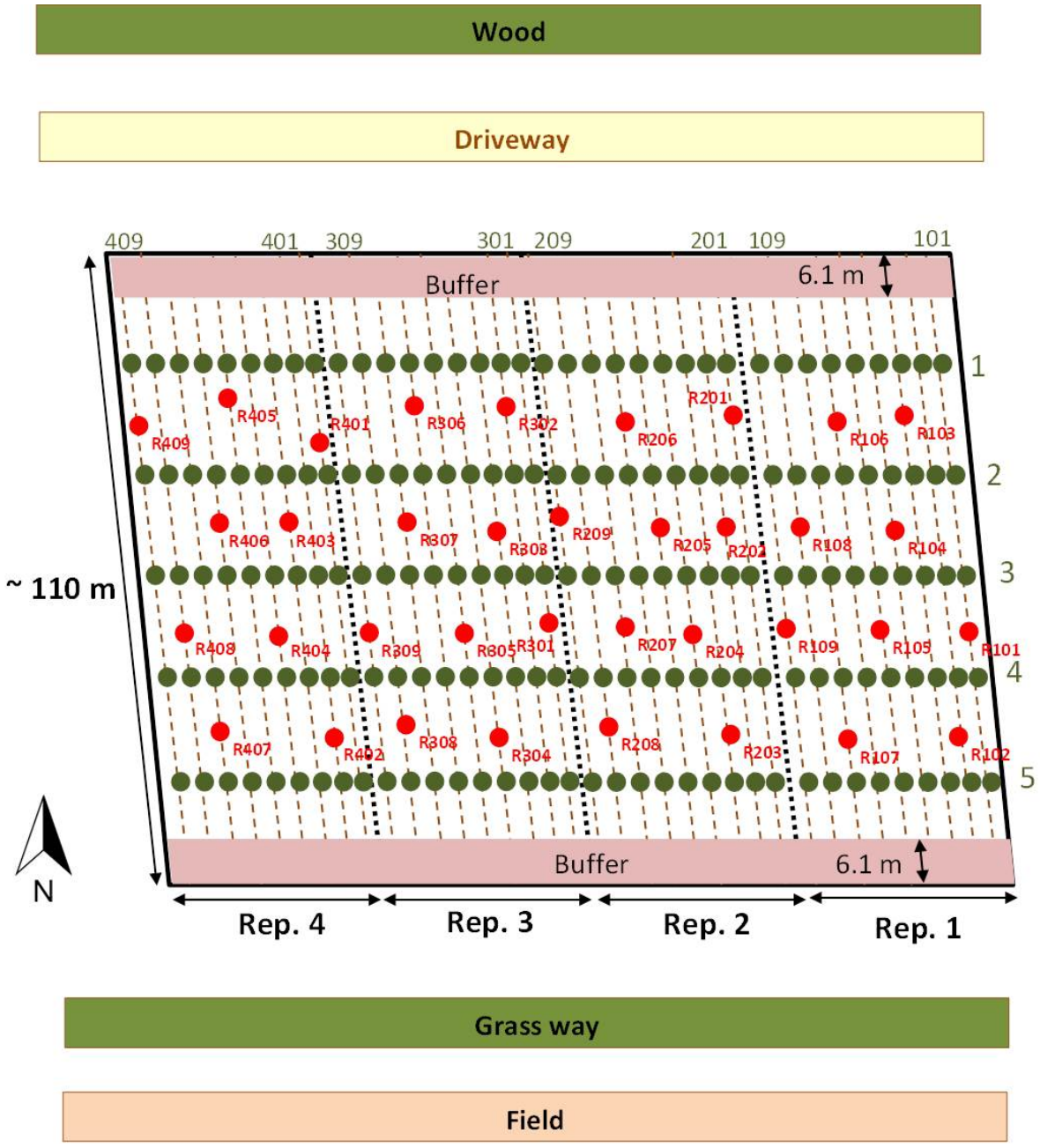

Figure A.7: Sampling sites layout for 2014-A cotton trial.

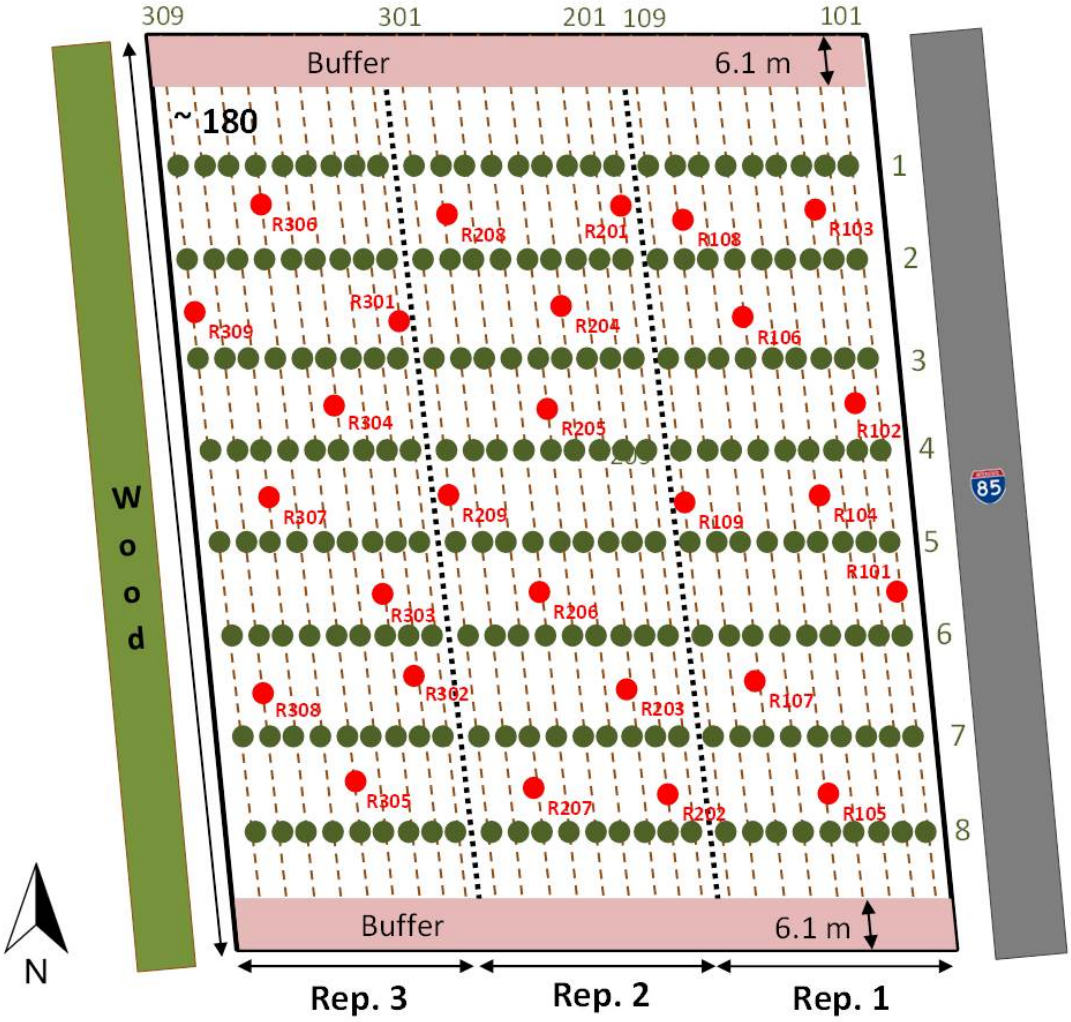

Figure A.8: Sampling sites layout for 2014-B cotton trial.

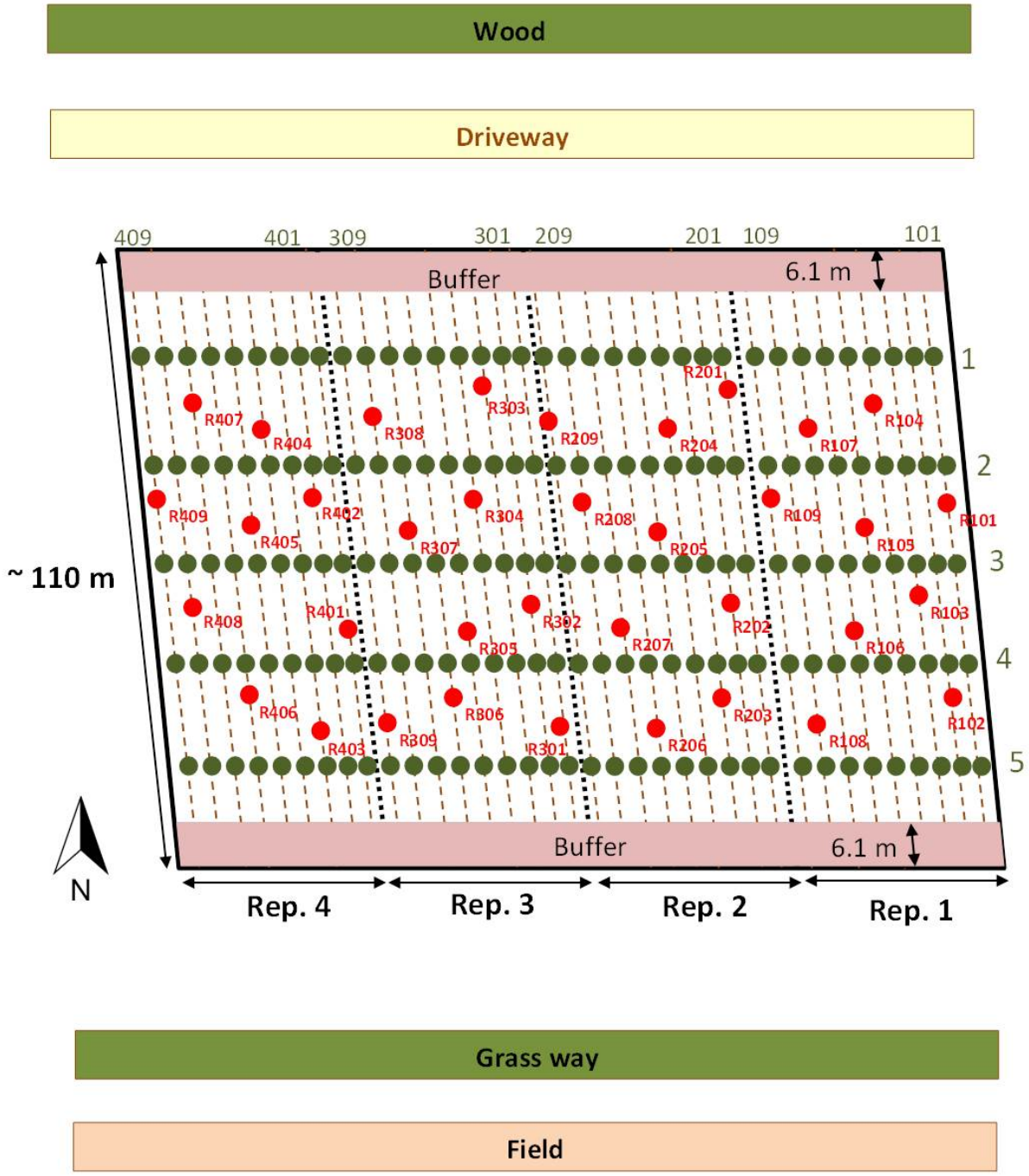

Figure A.9: Sampling sites layout for 2015-A corn trial.

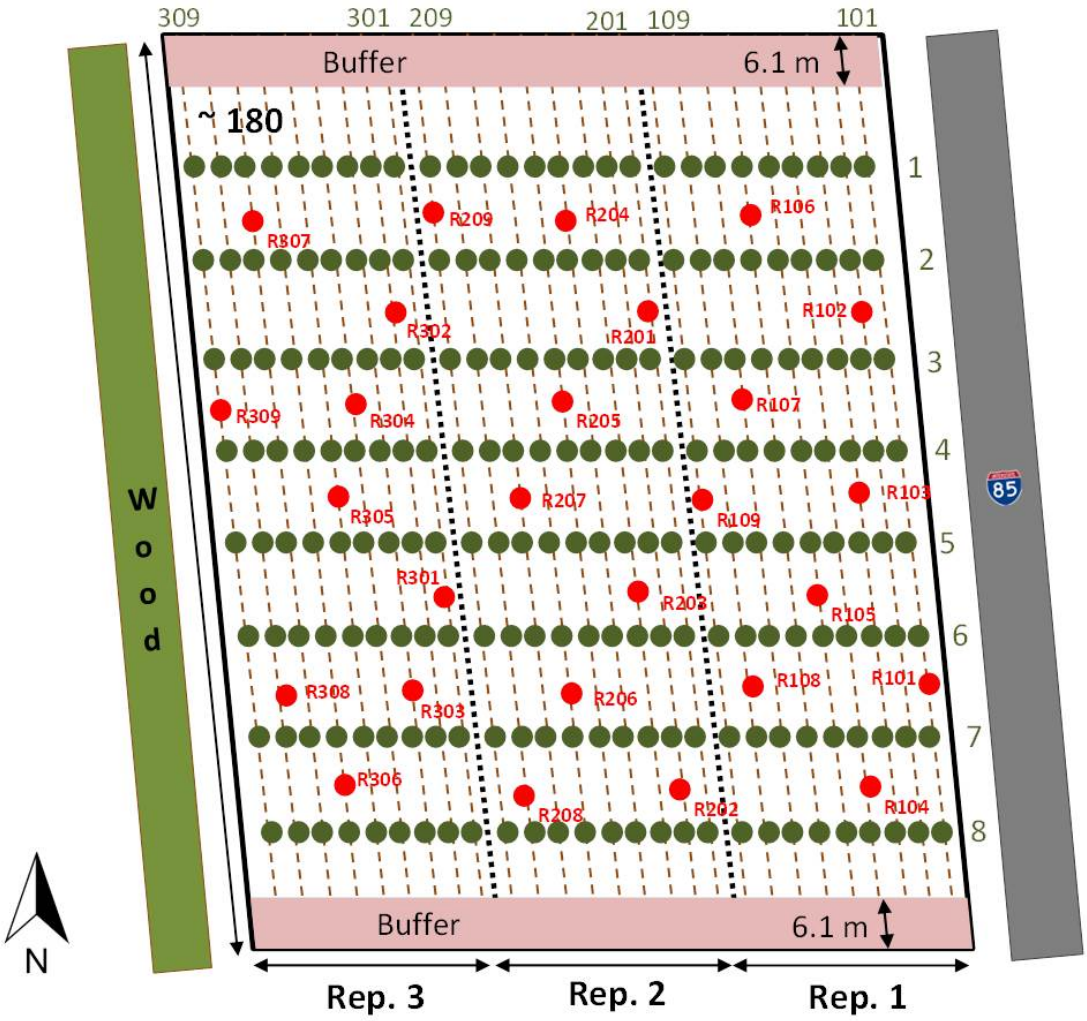

Figure A.10: Sampling sites layout for 2015-B corn trial.

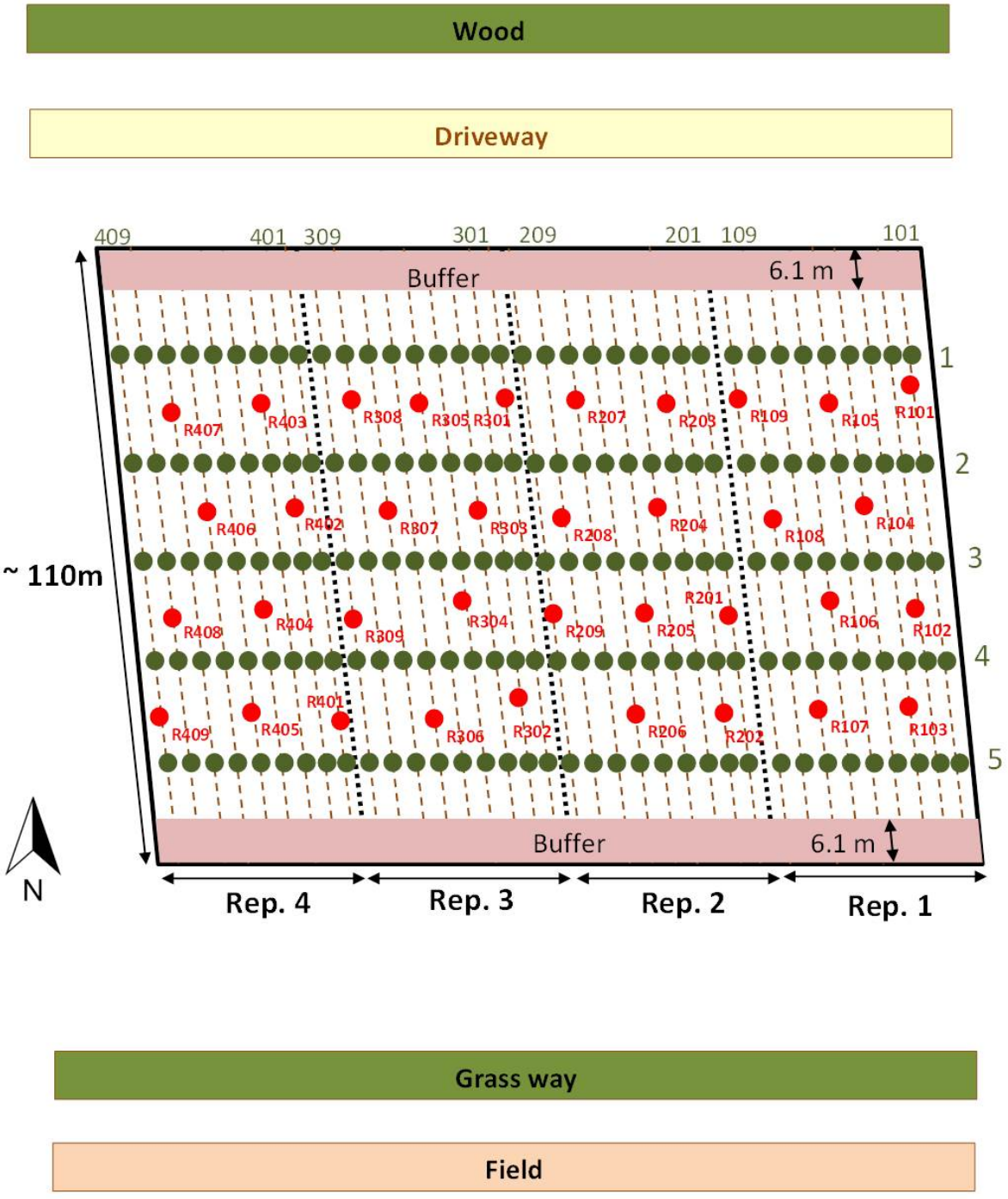

Figure A.11: Sampling sites layout for 2015-A cotton trial.

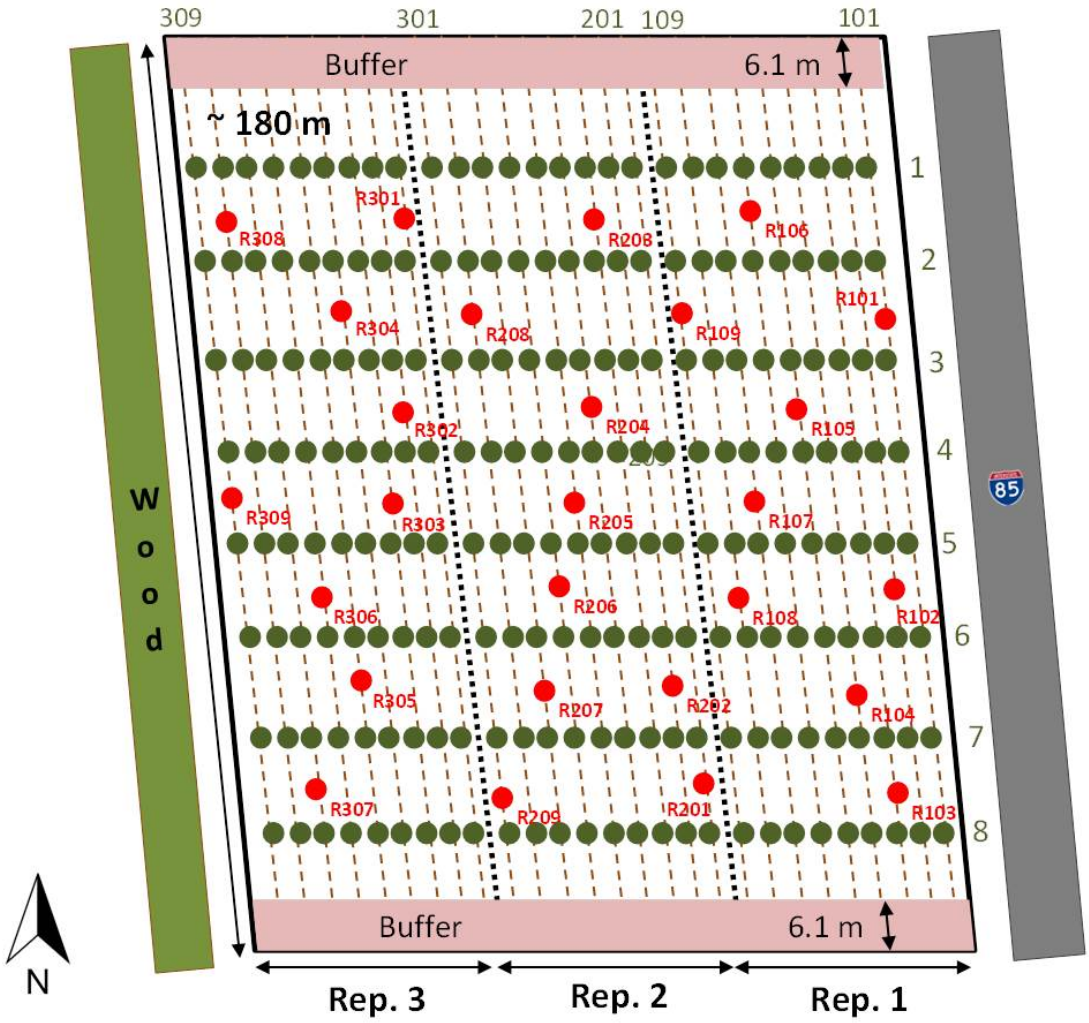

Figure A.12: Sampling sites layout for 2015-B cotton trial.

A.3 Additional Field Trial

- **Trial Location:** Tennessee Valley Research Center, 2014 growing season, corn only.
- **Soil Type:** Decatur Silty Clay Loam (Fine, kaolinitic, thermic Rhodic Paleuduts).
- **Planter:** 4-row John Deere Planter with MaxEmerge Plus Row-Unit, 76-cm (30-in) row spacing.
- **Experimental Design**:
  - 3 row-unit depths: 2.5, 5.1, and 7.6 cm,
  - 3 row-unit downforce: No, Medium, Heavy.
- **Field Management Strategy:** no-tillage, irrigated corn, 84,015 seeds ha^{-1}.

Table A.2: Mean seeding depth of corn and seeding depth standard deviation by row-unit depth and downforce within the 2014 field trial conducted at the Tennessee Valley Research Center.

Row-Unit Depth	Row-Unit Downforce	Mean Seeding Depth [cm]	Seeding Depth Std. Dev [cm]
2.5 cm	**No**	2.7	0.3
	Medium	3.0	0.3
	Heavy	3.2	0.4
5.1 cm	**No**	3.5	0.5
	Medium	4.3	0.2
	Heavy	4.5	0.4
7.6 cm	**No**	4.2	0.4
	Medium	4.8	0.3
	Heavy	5.9	0.5

Appendix B

Statistical Results

B.1 Complement to Chapter 4

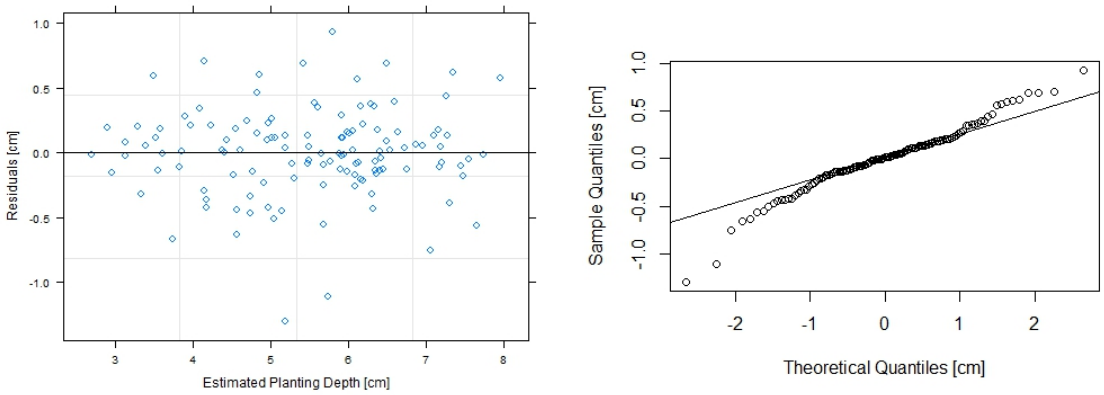

(a) (b)

Figure B.1: (a) Residual plot and (b) Quantile-Quantile plot used to validate the assumptions of linear mixed-effect analysis conducted for measured planting depth of corn.

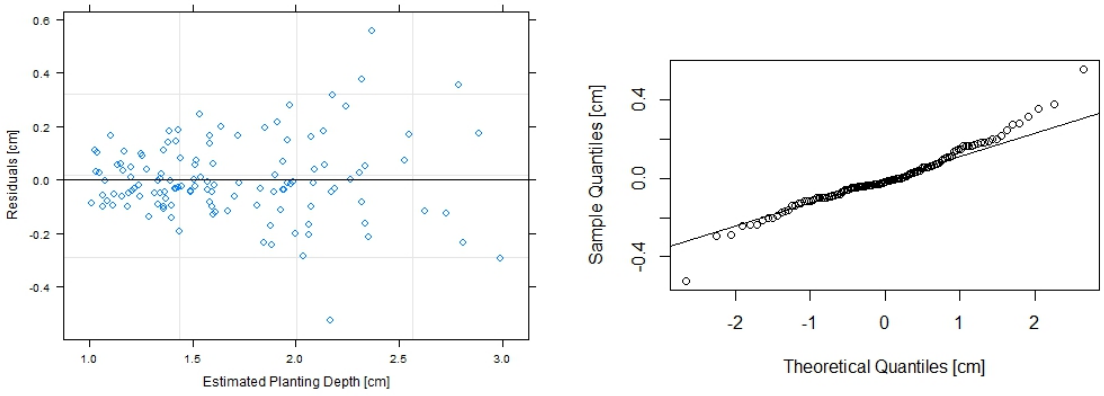

(a) (b)

Figure B.2: (a) Residual plot and (b) Quantile-Quantile plot used to validate the assumptions of linear mixed-effect analysis conducted for measured planting depth of cotton.

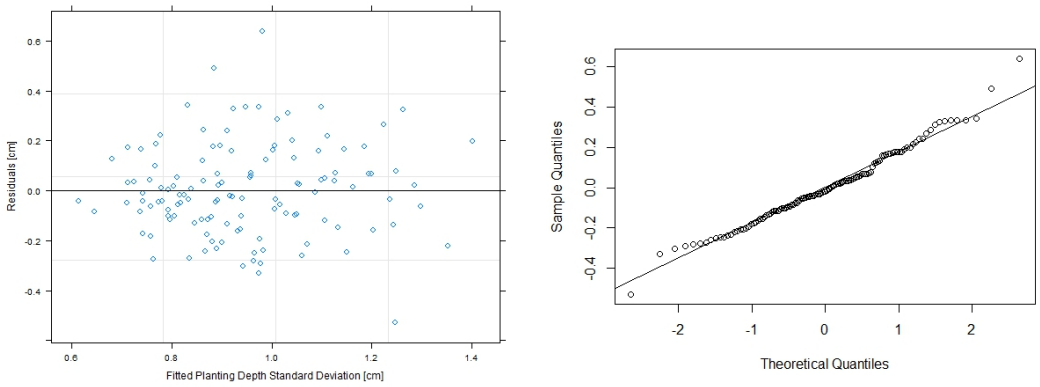

(a) (b)

Figure B.3: (a) Residual plot and (b) Quantile-Quantile plot used to validate the assumptions of linear mixed-effect analysis conducted for corn planting depth standard deviation at a given location.

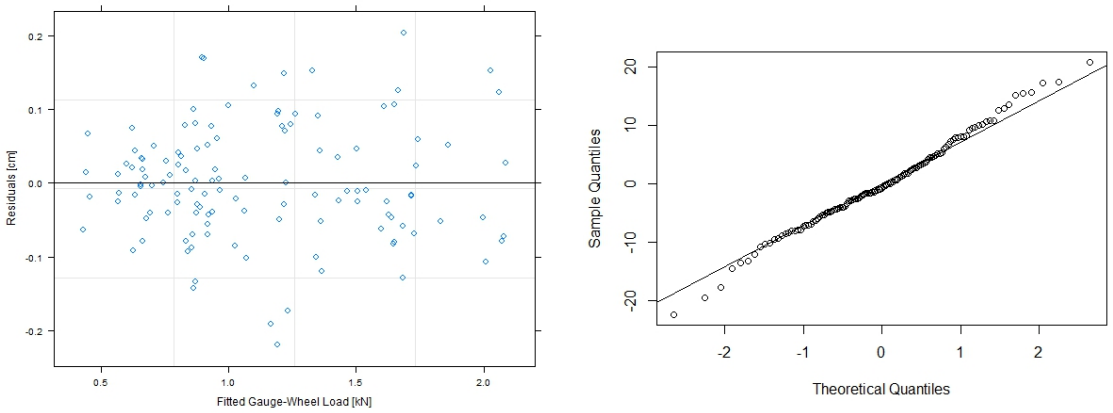

(a) (b)

Figure B.4: (a) Residual plot and (b) Quantile-Quantile plot used to validate the assumptions of linear mixed-effect analysis conducted on measured gauge-wheel load data for corn.

Table B.1: Mean corn planting depth standard deviation at a given sampling site by seeding depth, row-unit downforce, field and growing season.

Seeding Depth	Row-Unit Downforce	Field	Depth Std. Deviation [cm]		Field	Depth Std. Deviation [cm]	
			– 2014 –	– 2015 –		– 2014 –	– 2015 –
2.5 cm	**No**	**A**	0.7 ^{cd}	1.2 ^{abc}	**B**	0.8 ^{bcd}	0.9 ^{abcd}
	Medium		0.9 ^{abcd}	0.9 ^{abcd}		0.6 ^{d}	1.2 ^{abc}
	Heavy		0.9 ^{abcd}	1.0 ^{abcd}		0.7 ^{cd}	1.0 ^{abcd}
5.1 cm	**No**		0.9 ^{abcd}	0.8 ^{cd}		0.8 ^{bcd}	1.0 ^{abcd}
	Medium		0.8 ^{cd}	0.9 ^{abcd}		0.7 ^{cd}	1.0 ^{abcd}
	Heavy		0.9 ^{abcd}	1.0 ^{abcd}		0.8 ^{cd}	1.0 ^{abcd}
7.6 cm	**No**		1.0 ^{abcd}	1.1 ^{abcd}		0.8 ^{cd}	0.9 ^{abcd}
	Medium		1.1 ^{abcd}	1.0 ^{abcd}		0.9 ^{abcd}	1.3 ^{a}
	Heavy		1.1 ^{abcd}	1.3 ^{ab}		0.9 ^{abcd}	1.2 ^{abc}

$^{a,\ldots,d}$ *: Least significant difference between treatments at a 95% confidence interval.*

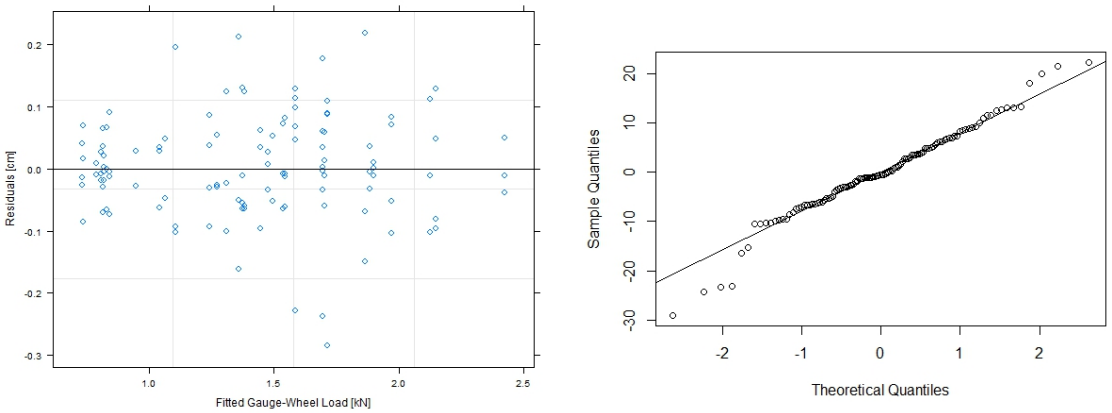

(a) (b)

Figure B.5: (a) Residual plot and (b) Quantile-Quantile plot used to validate the assumptions of linear mixed-effect analysis conducted on measured gauge-wheel load data for cotton.

Table B.2: Mean measured gauge-wheel load for corn by seeding depth, row-unit downforce, field and growing season.

Seeding Depth	Row-Unit Downforce	Field	Gauge-Wheel Load [kN]		Field	Gauge-Wheel Load [kN]	
			– 2014 –	– 2015 –		– 2014 –	– 2015 –
2.5 cm	**No**	**A**	0.9 ^{klm}	0.9 ^{klm}	**B**	1.0 ^{klm}	0.9 ^{klmn}
	Medium		1.5 ^{def}	1.7 ^{cde}		1.2 ^{hij}	1.6 ^{cde}
	Heavy		1.7 ^{cd}	2.1 ^{a}		1.6 ^{cde}	2.0 ^{ab}
5.1 cm	**No**		0.8 ^{mnopq}	0.8 ^{mnopqr}		0.9 ^{lmnop}	0.8 ^{lmnopq}
	Medium		1.1 ^{ijk}	1.4 ^{fgh}		1.0 ^{jkl}	1.2 ^{ghi}
	Heavy		1.4 ^{efg}	1.7 ^{c}		1.2 ^{hij}	1.8 ^{bc}
7.6 cm	**No**		0.6 ^{rs}	0.5 ^{s}		0.7 ^{pqr}	0.7 ^{opqr}
	Medium		0.6 ^{qr}	0.9 ^{mno}		0.6 ^{pqr}	0.9 ^{klmno}
	Heavy		0.9 ^{lmn}	1.2 ^{hij}		0.7 ^{nopqr}	1.3 ^{fgh}

$^{a,\ldots,q}$ *: Least significant difference between treatments at a 95% confidence interval.*

Table B.3: Mean measured gauge-wheel load for cotton by seeding depth, row-unit downforce, field and growing season.

Seeding Depth	Row-Unit Downforce	Field	Gauge-Wheel Load [kN]		Field	Gauge-Wheel Load [kN]	
			– 2014 –	– 2015 –		– 2014 –	– 2015 –
2.5 cm	**No**	**A**	0.9 ^{opqr}	1.0 ^{nop}	**B**	0.8 ^{pqr}	1.1 ^{mnopq}
	Medium		1.5 ^{ghijk}	1.7 ^{ef}		1.4 ^{hijkl}	1.9 ^{cde}
	Heavy		1.7 ^{ef}	2.1 ^{b}		1.9 ^{de}	2.4 ^{a}
5.1 cm	**No**		0.8 ^{pqr}	0.8 ^{pqr}		0.7 ^{r}	0.8 ^{pqr}
	Medium		1.3 ^{jklm}	1.5 ^{fghi}		1.1 ^{mno}	1.5 ^{fghij}
	Heavy		1.5 ^{fghijk}	2.0 ^{bcd}		1.7 ^{ef}	2.1 ^{bc}
7.6 cm	**No**		0.8 ^{qr}	0.8 ^{r}		1.4 ^{hijkl}	0.7 ^{r}
	Medium		1.2 ^{lmn}	1.4 ^{ijkl}		1.3 ^{klm}	1.4 ^{ijkl}
	Heavy		1.6 ^{fgh}	1.7 ^{efg}		1.6 ^{fghi}	1.9 ^{de}

$^{a,\ldots,r}$ *: Least significant difference between treatments at a 95% confidence interval.*

B.2 Complement to Chapter 5

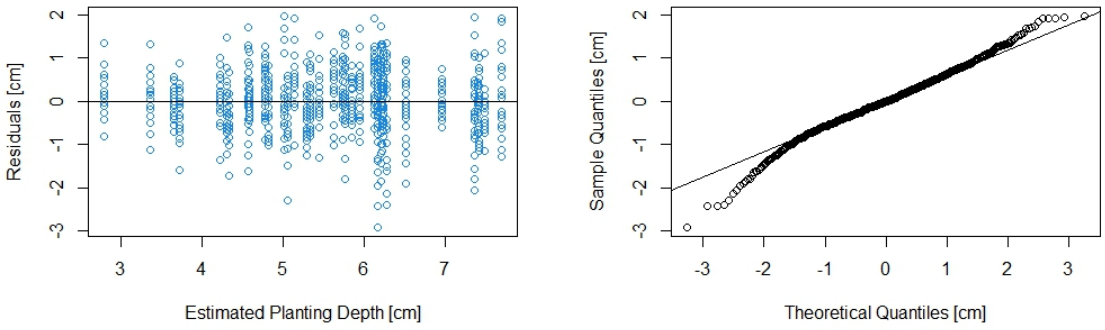

(a) (b)

Figure B.6: (a) Residual plot and (b) Residuals Quantile-Quantile plot for linear regression analysis conducted to evaluate corn planting depth response to row-unit depth and downforce adjustments by field and growing season.

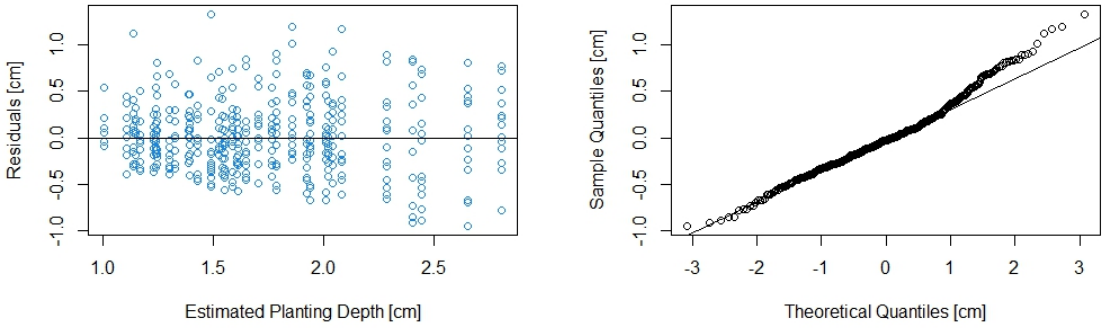

(a) (b)

Figure B.7: (a) Residual plot and (b) Residuals Quantile-Quantile plot for linear regression analysis conducted to evaluate cotton planting depth response to row-unit depth and downforce adjustments by field and growing season.

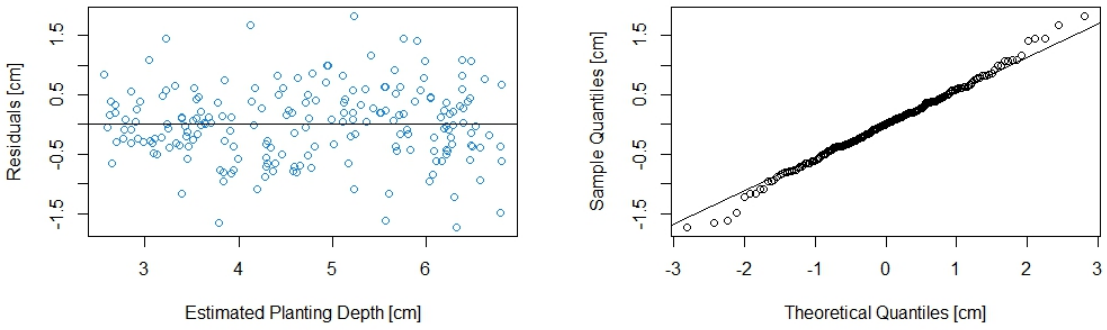

(a) (b)

Figure B.8: (a) Residual plot and (b) Residuals Quantile-Quantile plot for Ordinary Least Square Regression conducted to evaluate planting depth response to planter seeding depth, row-unit downforce, and standardized soil EC within the 2014-A corn trial.

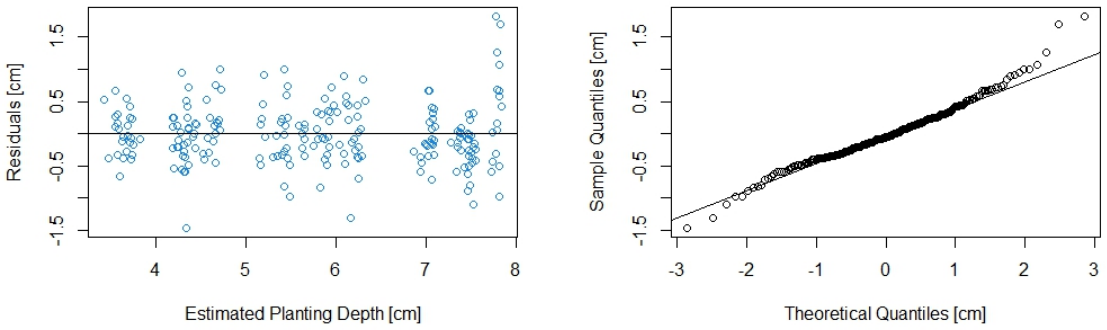

(a) (b)

Figure B.9: (a) Residual plot and (b) Residuals Quantile-Quantile plot for Geographically Weighted Regression conducted to evaluate planting depth response to planter seeding depth, row-unit downforce, and standardized soil EC within the 2014-B corn trial.

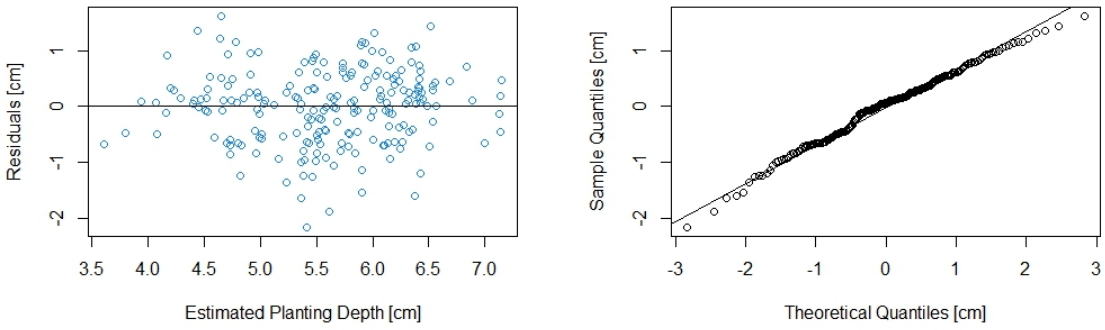

(a) (b)

Figure B.10: (a) Residual plot and (b) Residuals Quantile-Quantile plot for Geographically Weighted Regression conducted to evaluate planting depth response to planter seeding depth, row-unit downforce, and standardized soil EC within the 2015-A corn trial.

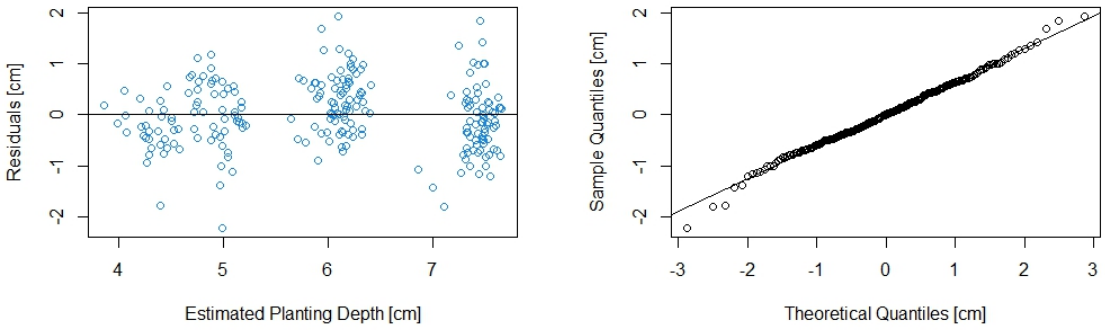

(a) (b)

Figure B.11: (a) Residual plot and (b) Residuals Quantile-Quantile plot for Geographically Weighted Regression conducted to evaluate planting depth response to planter seeding depth, row-unit downforce, and standardized soil EC within the 2015-B corn trial.

Table B.4: Corn planting depth response to measured gauge-wheel load by planter seeding depth, field, and growing season.

		Regression Coefficient γ_{SD} [cm.kN^{-1}]		
Season	**Field**	**SD = 2.5 cm**	**SD = 5.1 cm**	**SD = 7.6 cm**
2014	**A**	– 0.28	0.44	0.00
	B	0.15	0.32	1.10
2015	**A**	– 0.25	0.24	0.00
	B	0.21	0.04	0.00

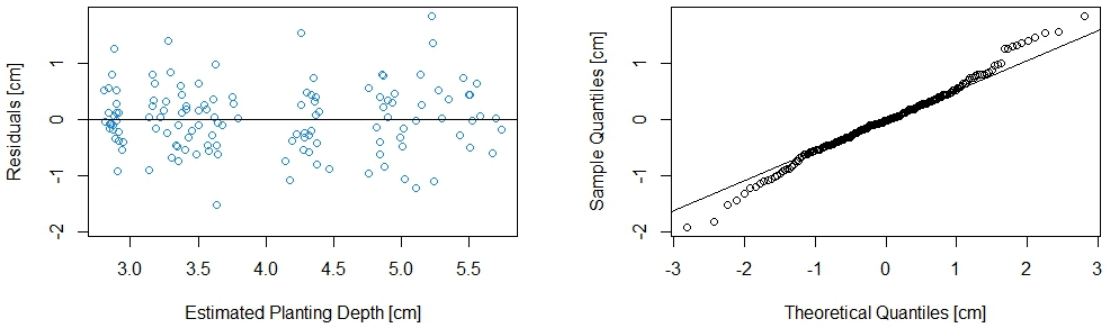

(a) (b)

Figure B.12: (a) Residual plot and (b) Residuals Quantile-Quantile plot for linear regression conducted to evaluate planting depth response to planter seeding depth, row-unit downforce, and measured gauge-wheel load within the 2014-A corn trial.

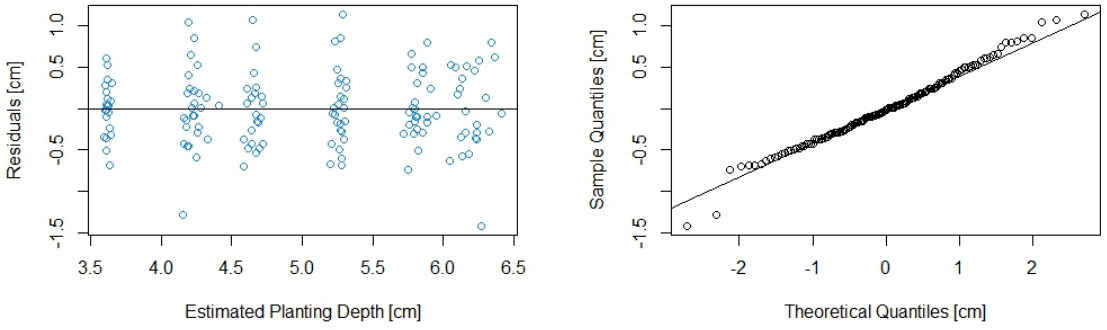

(a) (b)

Figure B.13: (a) Residual plot and (b) Residuals Quantile-Quantile plot for linear regression conducted to evaluate planting depth response to planter seeding depth, row-unit downforce, and measured gauge-wheel load within the 2014-B corn trial.

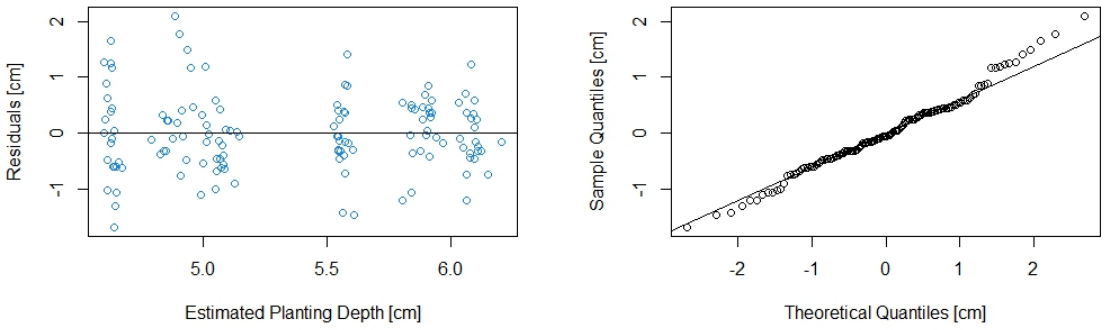

(a) (b)

Figure B.14: (a) Residual plot and (b) Residuals Quantile-Quantile plot for linear regression conducted to evaluate planting depth response to planter seeding depth, row-unit downforce, and measured gauge-wheel load within the 2015-A corn trial.

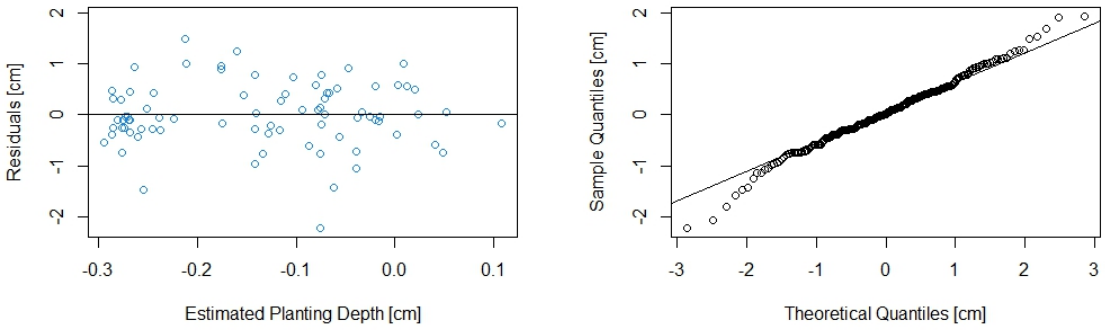

(a) (b)

Figure B.15: (a) Residual plot and (b) Residuals Quantile-Quantile plot for linear regression conducted to evaluate planting depth response to planter seeding depth, row-unit downforce, and measured gauge-wheel load within the 2015-B corn trial.

B.3 Complement to Chapter 6

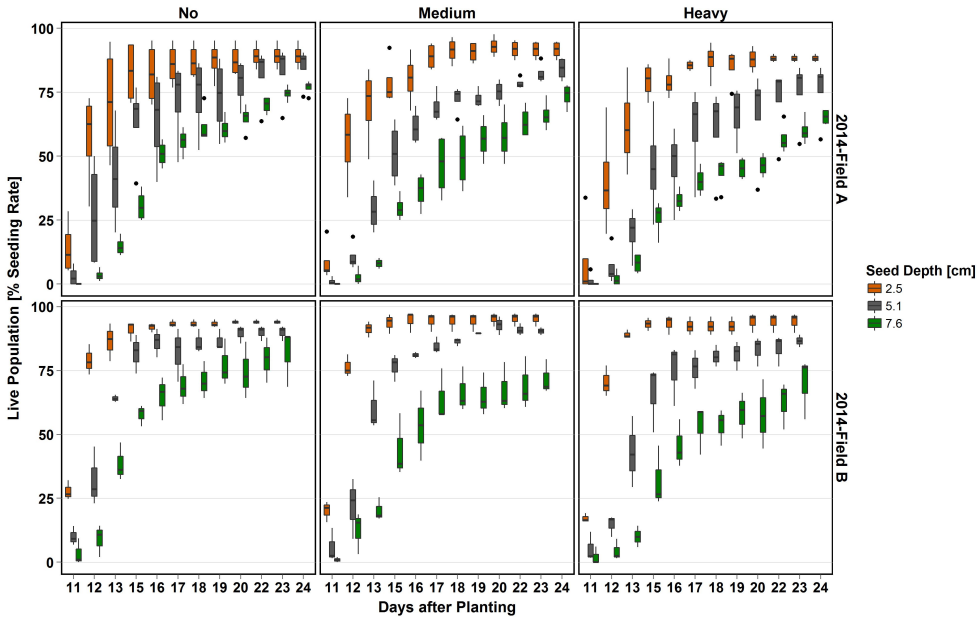

Figure B.16: Corn daily live population by field, seeding depth, and row-unit downforce during 2014 growing season (summary of row data).

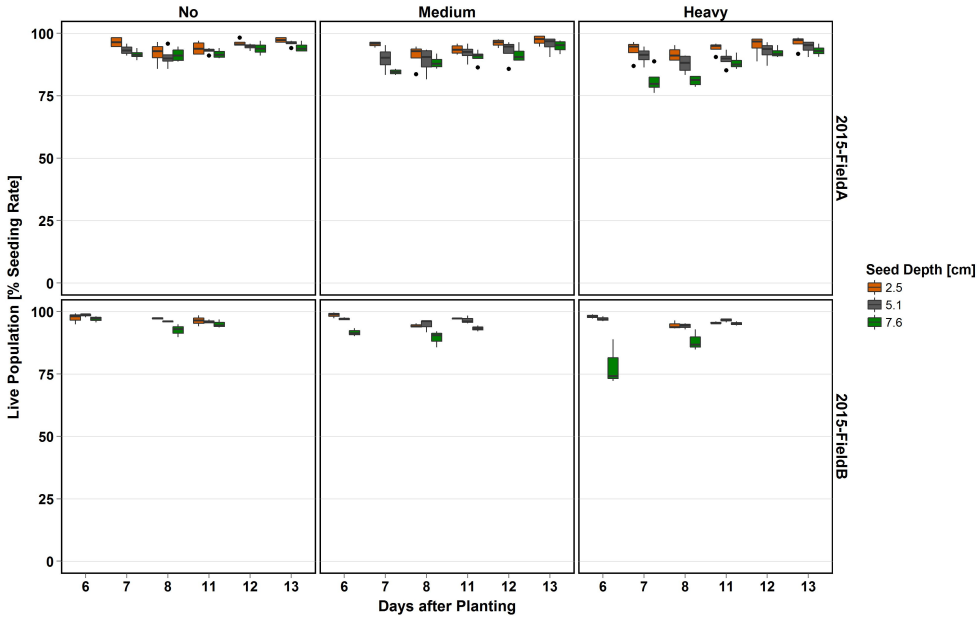

Figure B.17: Corn daily live population by field, seeding depth, and row-unit downforce during 2015 growing season (summary of row data).

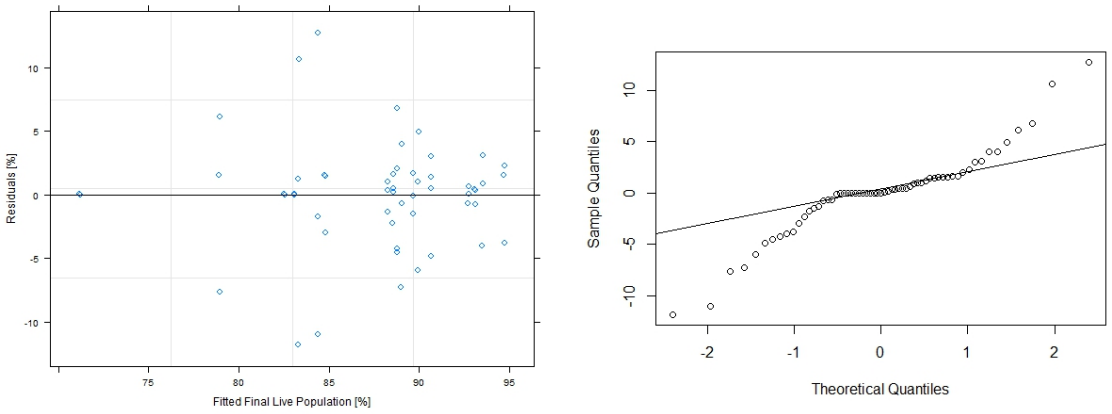

(a) (b)

Figure B.18: (a) Residual plot and (b) Quantile-Quantile plot computed to validate the assumptions of linear mixed-effect analysis conducted for final maize population during 2014 growing season.

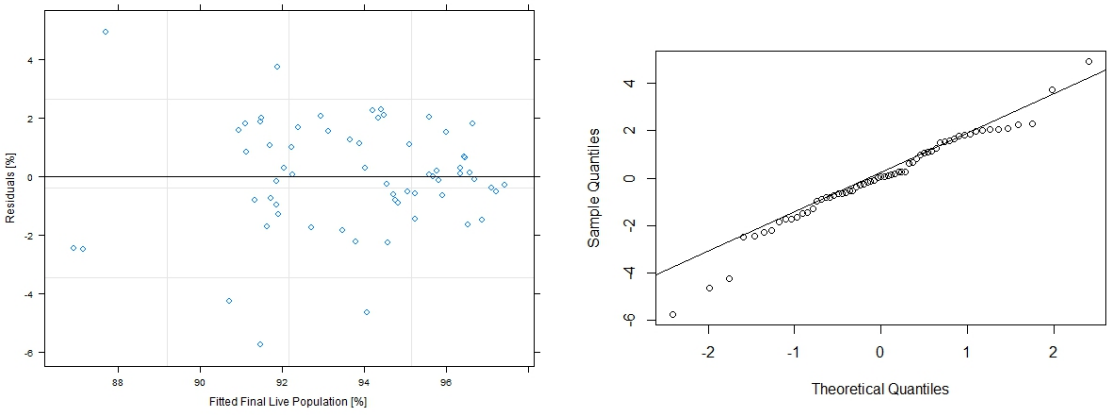

(a) (b)

Figure B.19: (a) Residual plot and (b) Quantile-Quantile plot computed to validate the assumptions of linear mixed-effect analysis conducted for final maize population during 2015 growing season.

Table B.5: Final maize population by seeding depth, row-unit downforce, and field during 2014 growing season.

Seeding Depth	Row-Unit Downforce	Field	Final Population		Field	Final Population	
			Plants.Acre^{-1}	% Seeding Rate		Plants.Acre^{-1}	% Seeding Rate
2.5 cm	**No**	**A**	23,520	89.2% ^{abcd}	**B**	24,670	93.5% ^{ab}
	Medium		24,030	91.1% ^{abc}		25,100	95.2% ^{a}
	Heavy		23,470	89.0% ^{abcd}		24,780	94.0% ^{ab}
5.1 cm	**No**		23,390	88.7% ^{abcd}		23,830	90.4% ^{abcd}
	Medium		23,590	89.5% ^{abcd}		24,570	93.2% ^{abc}
	Heavy		22,470	85.2% ^{abcd}		23,760	90.1% ^{abcd}
7.6 cm	**No**		21,870	82.9% ^{cd}		22,360	84.8% ^{abcd}
	Medium		22,010	83.5% ^{bcd}		20,910	79.3% ^{de}
	Heavy		18,860	71.5% ^{e}		22,070	83.7% ^{bcd}

$^{a,\ldots,l}$ *: Least significant difference between treatments at a 95% confidence interval.*

Table B.6: Final maize population by seeding depth, row-unit downforce, and field during 2015 growing season.

Seeding Depth	Row-Unit Downforce	Field	Final Population		Field	Final Population	
			Plants.Acre^{-1}	% Seeding Rate		Plants.Acre^{-1}	% Seeding Rate
2.5 cm	**No**	**A**	25,220	95.7% ^{abcd}	**B**	25,710	97.5% ^{a}
	Medium		25,100	95.2% ^{abcd}		25,620	97.2% ^{abc}
	Heavy		24,910	94.5% ^{abcd}		25,450	96.5% ^{abc}
5.1 cm	**No**		24,950	94.6% ^{abcd}		25,660	97.3% ^{ab}
	Medium		24,330	92.3% ^{cde}		25,480	96.6%^{abc}
	Heavy		24,130	91.5% ^{de}		25,420	96.4% ^{abcd}
7.6 cm	**No**		24,660	93.5% ^{abcd}		25,130	95.3% ^{abcd}
	Medium		24,370	92.4% ^{bde}		24,230	91.9% ^{cde}
	Heavy		24,340	92.3% ^{cde}		23,130	87.7% ^{e}

$^{a,\ldots,l}$ *: Least significant difference between treatments at a 95% confidence interval.*

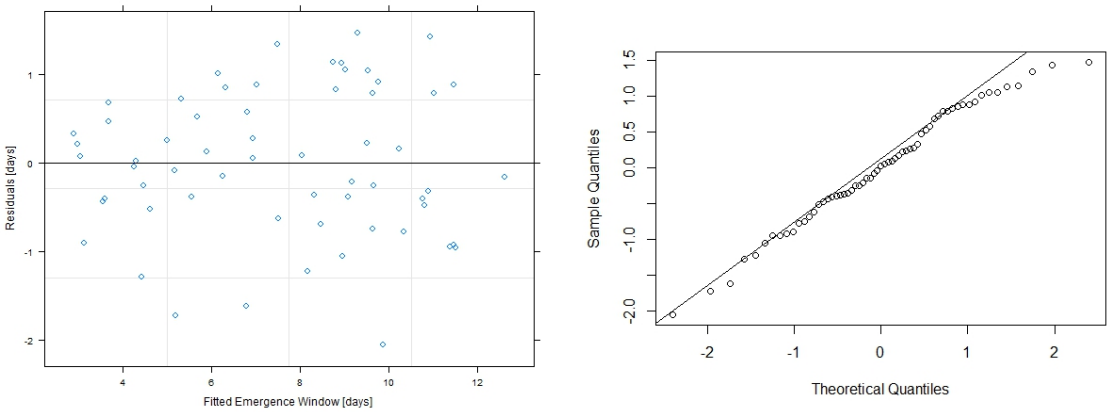

(a) (b)

Figure B.20: (a) Residual plot and (b) Quantile-Quantile plot computed to validate the assumptions of linear mixed-effect analysis conducted for maize emergence duration within 2014 field trials.

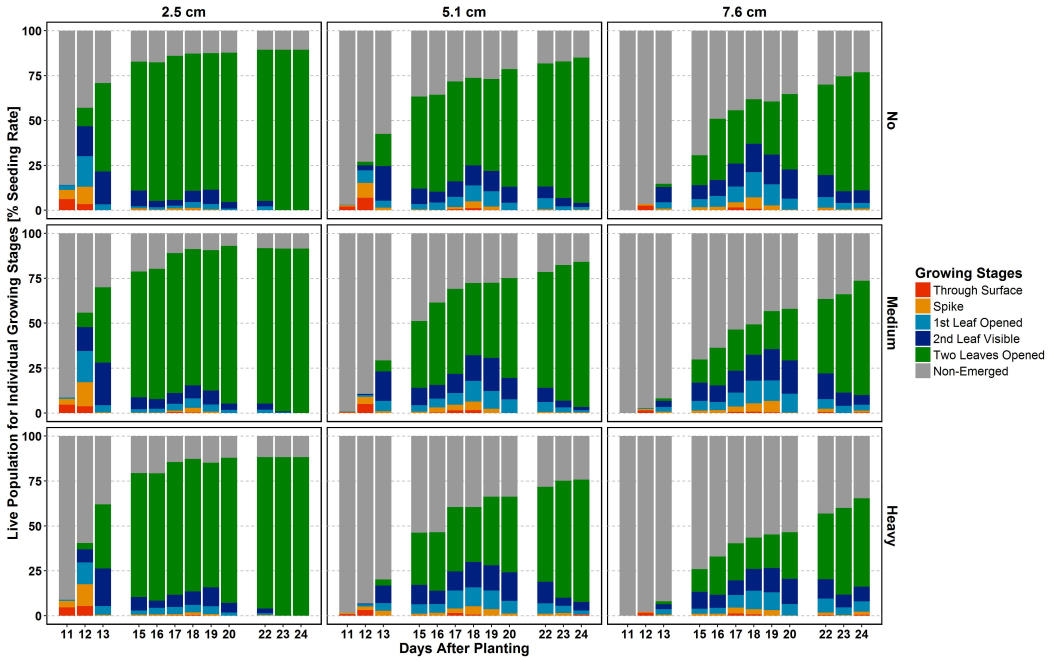

Figure B.21: Uniformity of seedling growth by seeding depth and row-unit downforce within the 2014-A field trial (summary of row data).

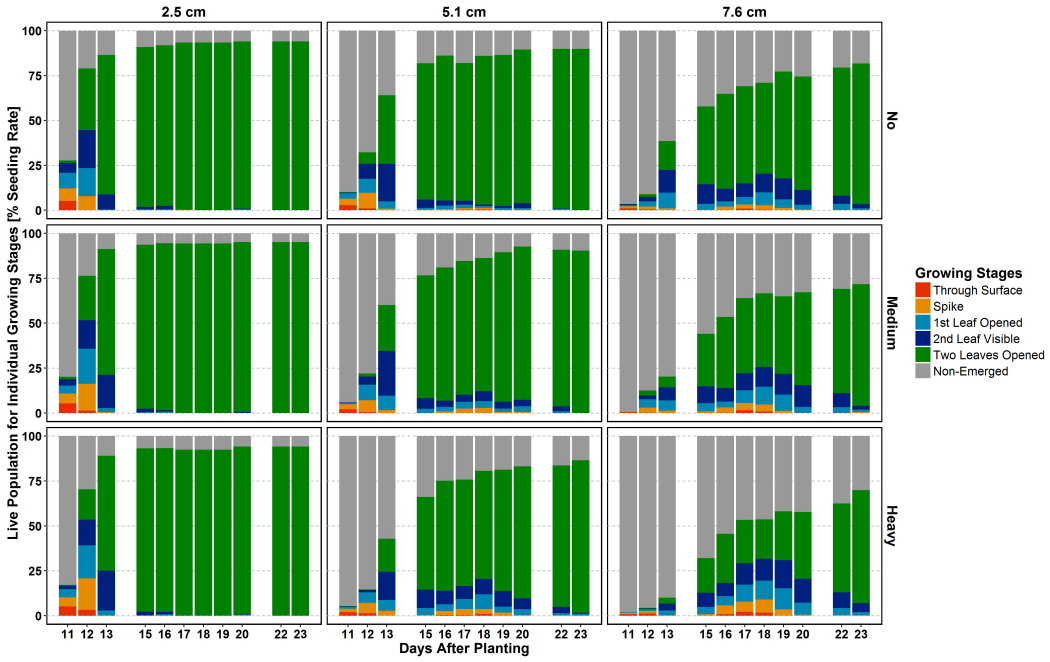

Figure B.22: Uniformity of seedling growth by seeding depth and row-unit downforce within the 2014-B field trial (summary of row data).

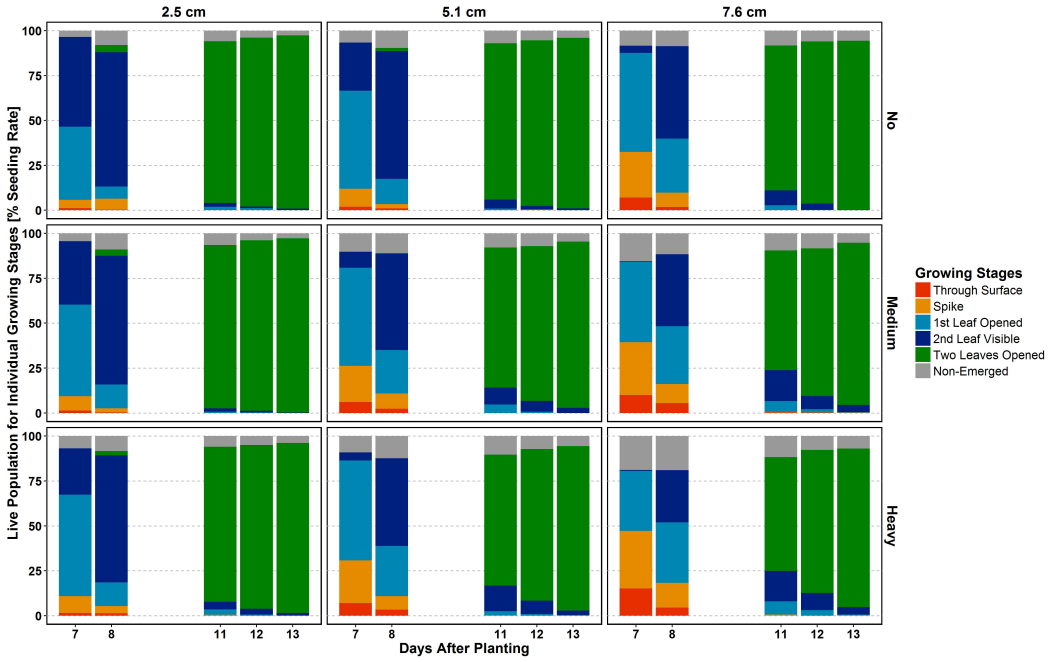

Figure B.23: Uniformity of maize seedlings growth by seeding depth and row-unit downforce within 2015-A field trial.

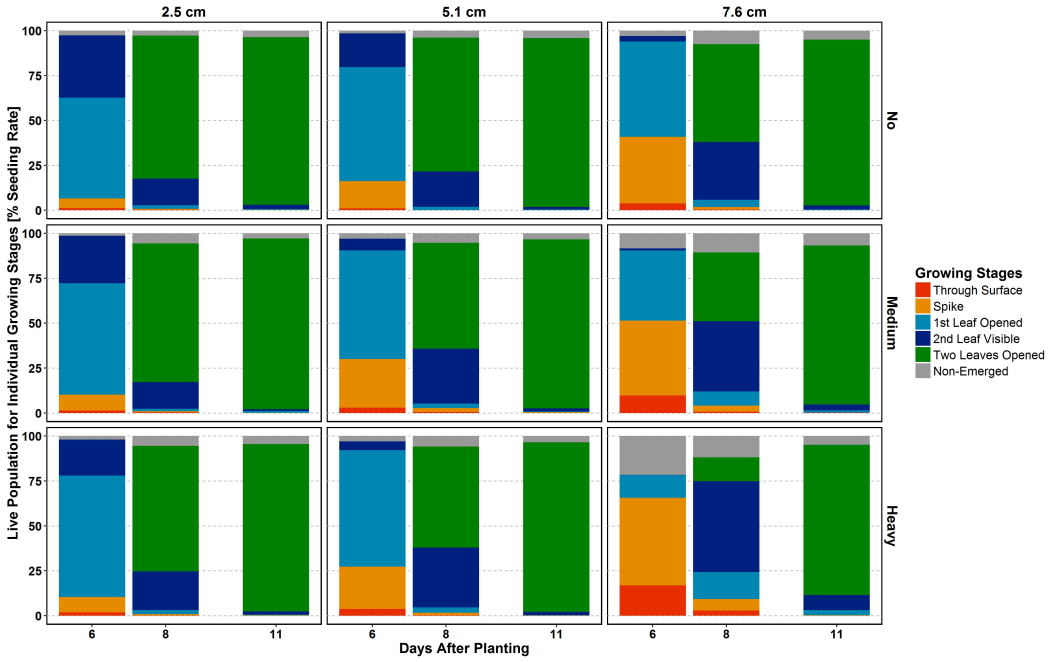

Figure B.24: Uniformity of maize seedlings growth by seeding depth and row-unit downforce within 2015-B field trial (summary of row data).

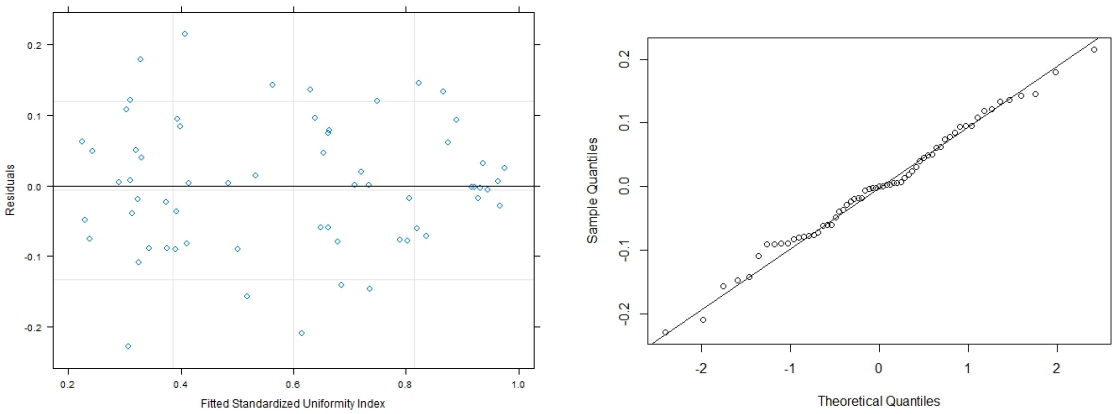

(a) (b)

Figure B.25: (a) Residual plot and (b) Quantile-Quantile plot computed to validate the assumptions of linear mixed-effect analysis conducted to characterize 2014 maize emergence uniformity.

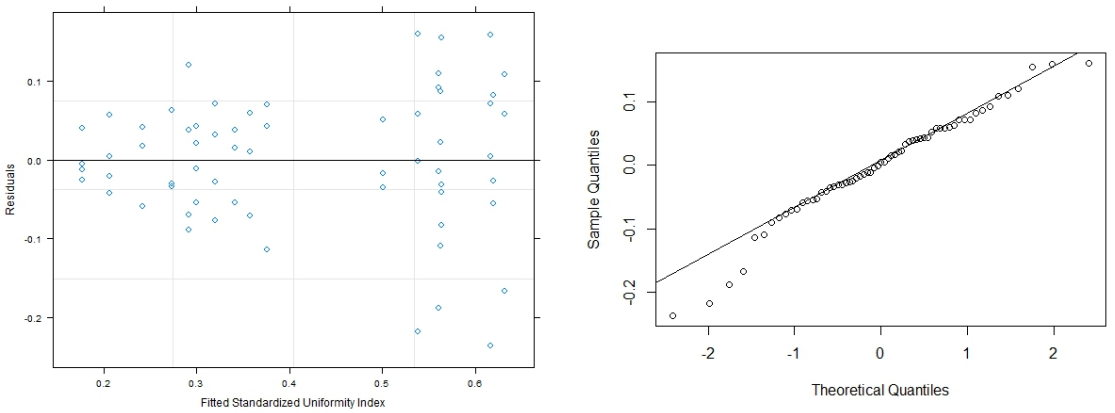

(a) (b)

Figure B.26: (a) Residual plot and (b) Quantile-Quantile plot computed to validate the assumptions of linear mixed-effect analysis conducted to characterize 2015 maize emergence uniformity.

Table B.7: Gibb's Index to describe 2014 maize emergence uniformity by seeding depth, row-unit downforce, and field (summary of row data).

Seeding Depth	Row-Unit Downforce	Field	Gibb's Index	Field	Gibb's Index
	No		0.84 ^{abc}		0.95 ^{a}
2.5 cm	**Medium**		0.77 ^{abcd}		0.94 ^{ab}
	Heavy		0.70 ^{abcd}		0.94 ^{a}
	No		0.36 ^{f}		0.84 ^{abc}
5.1 cm	**Medium**	**A**	0.28 ^{f}	**B**	0.68 ^{abcde}
	Heavy		0.27 ^{f}		0.64 ^{cde}
	No		0.45 ^{ef}		0.66 ^{bcde}
7.6 cm	**Medium**		0.36 ^{f}		0.54 ^{def}
	Heavy		0.34 ^{f}		0.35 ^{f}

$^{a,\ldots,f}$ *: Least significant difference between treatments at a 95% confidence interval.*

Table B.8: Gibb's Index to describe 2015 maize emergence uniformity by seeding depth, row-unit downforce, and field (summary of row data).

Seeding Depth	Row-Unit Downforce	Field	Gibb's Index	Field	Gibb's Index
	No		0.62 ^{a}		0.63 ^{a}
2.5 cm	**Medium**		0.56 ^{ab}		0.62 ^{a}
	Heavy		0.54 ^{abc}		0.50 ^{abcd}
	No		0.56 ^{ab}		0.56 ^{abc}
5.1 cm	**Medium**	**A**	0.32 ^{de}	**B**	0.38 ^{bcde}
	Heavy		0.29 ^{e}		0.36 ^{bcde}
	No		0.30 ^{de}		0.34 ^{cde}
7.6 cm	**Medium**		0.21 ^{e}		0.27 ^{e}
	Heavy		0.18 ^{e}		0.24 ^{e}

$^{a,\ldots,e}$ *: Least significant difference between treatments at a 95% confidence interval.*

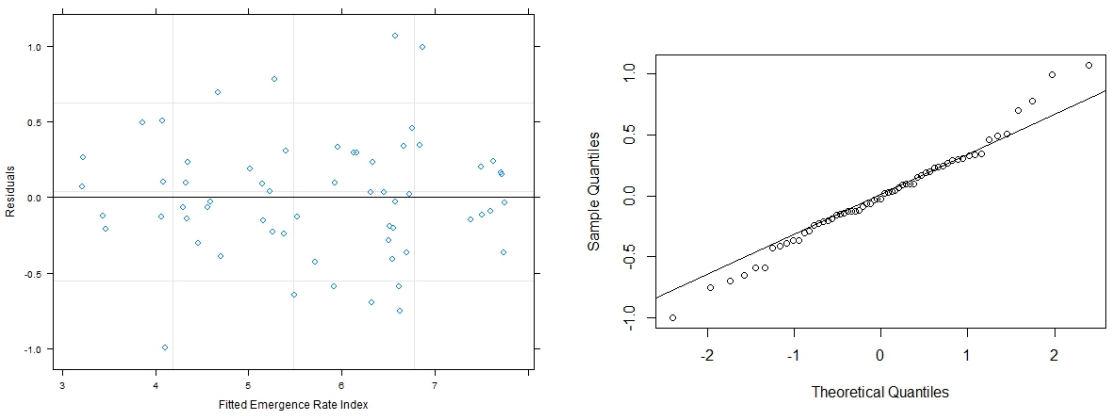

(a) (b)

Figure B.27: (a) Residual plot and (b) Quantile-Quantile plot computed to validate the assumptions of linear mixed-effect analysis conducted for Emergence Rate Index to describe 2014 maize seedling vigor.

Table B.9: Emergence Rate Index (ERI) to describe 2014 maize seedling vigor by seeding depth, row-unit downforce, and field.

Seeding Depth	**Row-Unit Downforce**	**Field**	**ERI [%.day^{-1}]**	**Field**	**ERI [%.day^{-1}]**
	No		6.7 ^{abc}		7.5 ^{ab}
2.5 cm	**Medium**		6.4 ^{bcd}		7.6 ^{a}
	Heavy		6.6 ^{abc}		7.6 ^{a}
	No		6.0 ^{cde}		6.6 ^{abc}
5.1 cm	**Medium**	**A**	5.3 ^{ef}	**B**	6.4 ^{abcd}
	Heavy		5.1 ^{efg}		5.8 ^{de}
	No		4.5 ^{fg}		5.4 ^{def}
7.6 cm	**Medium**		4.2 ^{gh}		4.6 ^{fg}
	Heavy		3.3 ^{h}		4.0 ^{gh}

$^{a,\ldots,h}$ *: Least significant difference between treatments at a 95% confidence interval.*

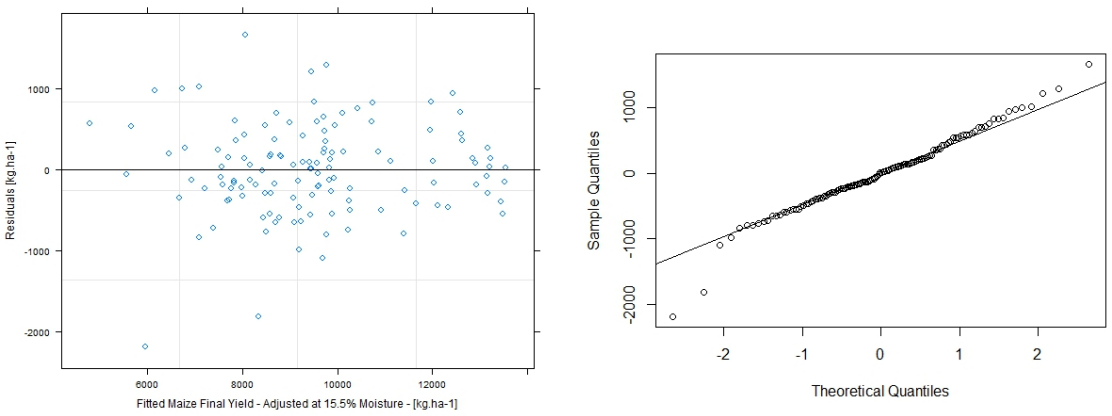

(a) (b)

Figure B.28: (a) Residual plot and (b) Quantile-Quantile plot computed to validate the assumptions of linear mixed-effect analysis conducted for final maize yield.

Table B.10: Maize final yield by seeding depth, row-unit downforce, field, and growing season.

Seeding Depth	Row-Unit Downforce	Growing Season	Final Yield [kg.ha^{-1}]		Growing Season	Final Yield [kg.ha^{-1}]	
			Field A	Field B		Field A	Field B
2.5 cm	**No**	**2014**	9100 ^{fghij}	9580 ^{defghi}	**2015**	8430 ^{fghijk}	12300 ^{abc}
	Medium		9260 ^{fghij}	9940 ^{bcdefg}		9950 ^{cdef}	12550 ^{ab}
	Heavy		9130 ^{fghij}	9880 ^{cdefgh}		9540 ^{efghi}	12870 ^{a}
5.1 cm	**No**		8800 ^{fghij}	9600 ^{defghij}		9980 ^{cdef}	12930 ^{a}
	Medium		8190 ^{fghijk}	8950 ^{fghij}		9560 ^{defghi}	12910 ^{a}
	Heavy		7390 ^{ijk}	9230 ^{efghij}		8520 ^{fghi}	12850 ^{a}
7.6 cm	**No**		7590 ^{ghijk}	8750 ^{fghij}		9600 ^{defghi}	12320 ^{abc}
	Medium		7090 ^{jk}	8160 ^{fghijk}		8130 ^{fghijk}	12030 ^{abcd}
	Heavy		6210 ^{k}	7260 ^{hijk}		7560 ^{ghijk}	11820 ^{abcde}

$^{a,\ldots,k}$ *: Least significant difference between treatments at a 95% confidence interval.*

B.4 Complement to Chapter 7

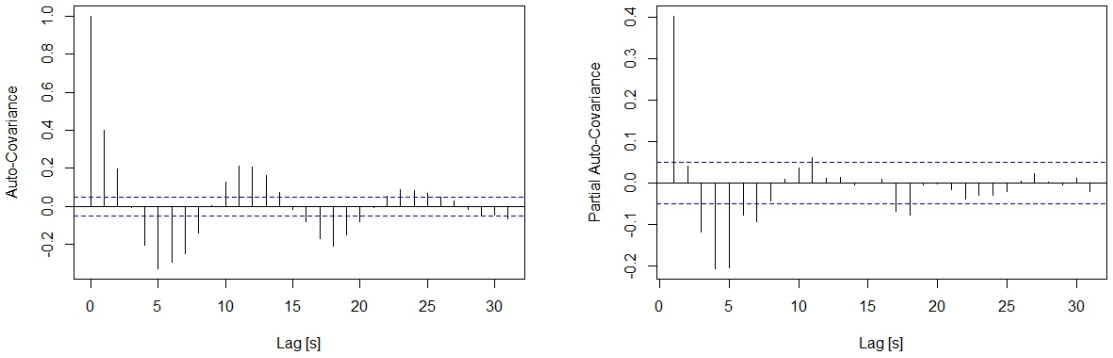

(a) (b)

Figure B.29: Estimation of (a) auto-covariance and (b) partial auto-covariance for smoothed gauge-wheel load data in 2014-A corn trial.

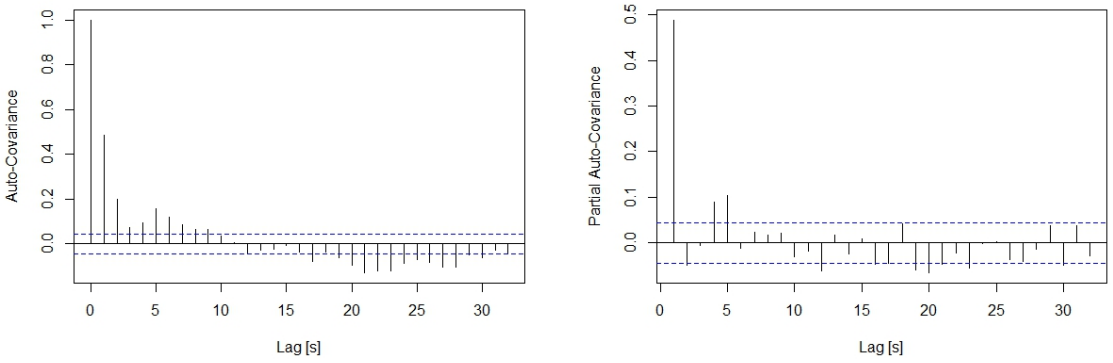

(a) (b)

Figure B.30: Estimation of (a) auto-covariance and (b) partial auto-covariance for smoothed gauge-wheel load data in 2014-B corn trial.

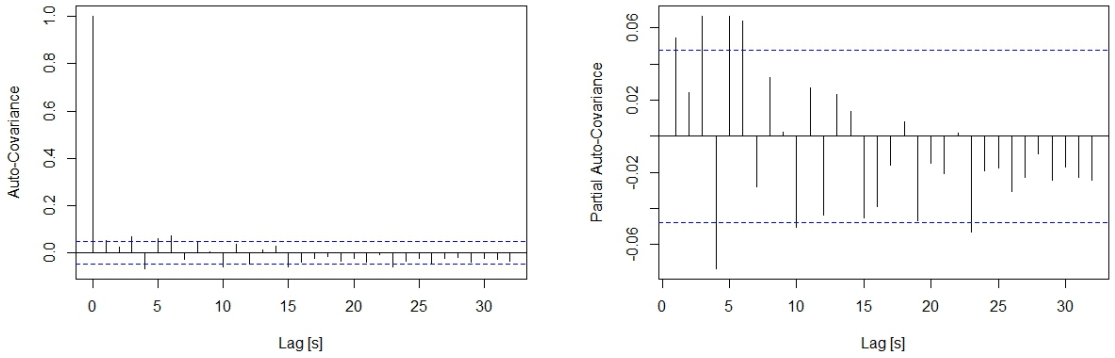

(a) (b)

Figure B.31: Estimation of (a) auto-covariance and (b) partial auto-covariance for smoothed gauge-wheel load data in 2015-A corn trial.

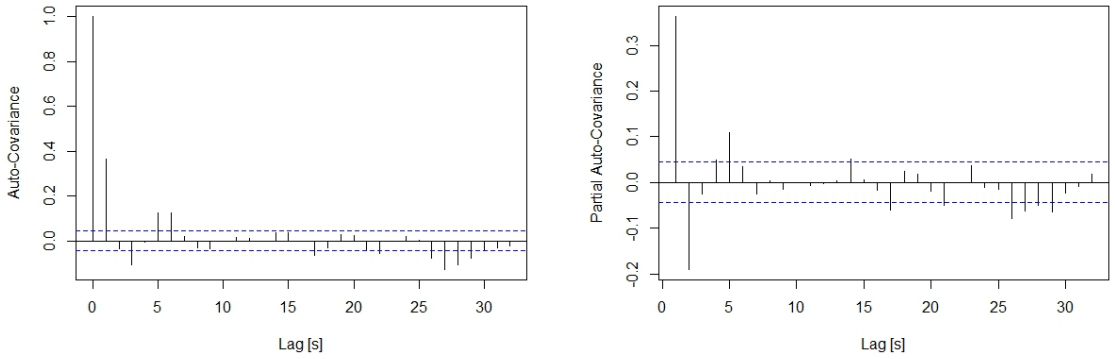

(a) (b)

Figure B.32: Estimation of (a) auto-covariance and (b) partial auto-covariance for smoothed gauge-wheel load data in 2015-B corn trial.

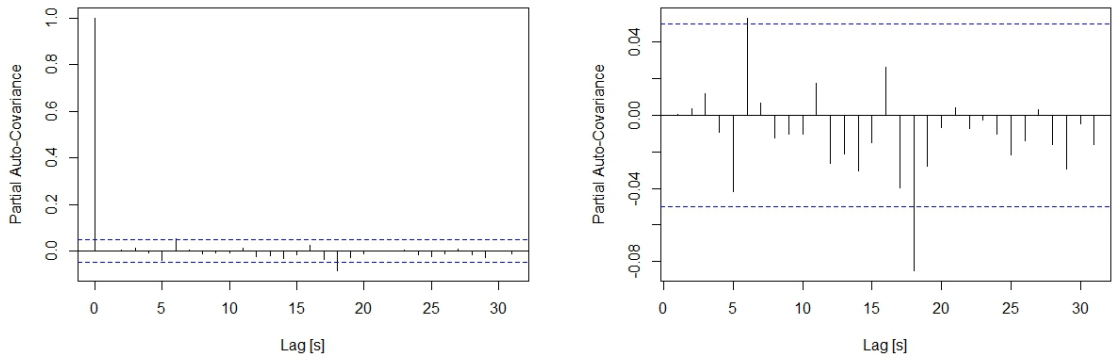

(a) (b)

Figure B.33: Estimation of (a) auto-covariance and (b) partial auto-covariance among residuals from ARIMA model established to compute local gauge-wheel load predictions within the 2014-A corn trials.

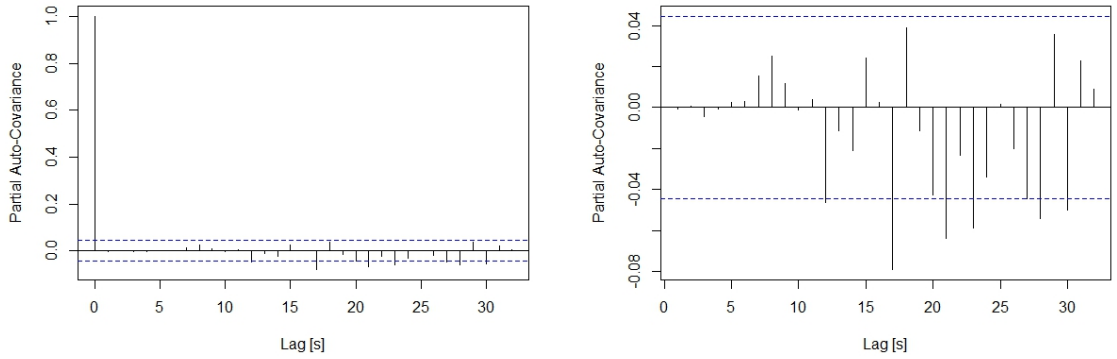

(a) (b)

Figure B.34: Estimation of (a) auto-covariance and (b) partial auto-covariance among residuals from ARIMA model established to compute local gauge-wheel load predictions within the 2014-B corn trials.

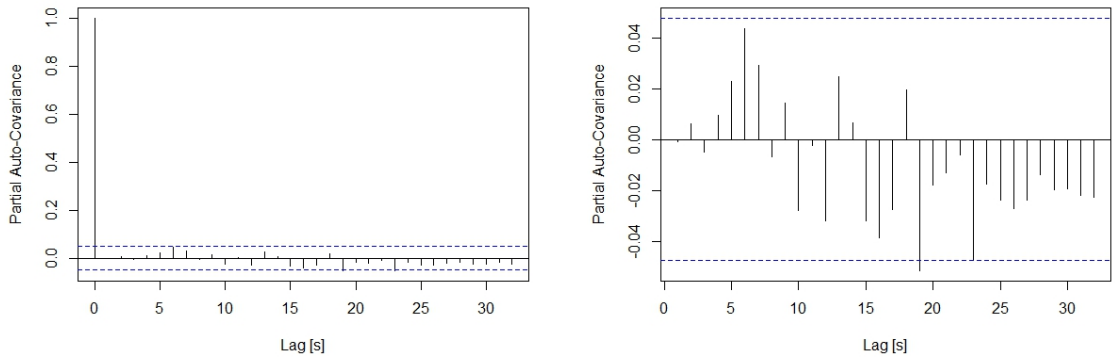

(a) (b)

Figure B.35: Estimation of (a) auto-covariance and (b) partial auto-covariance among residuals from ARIMA model established to compute local gauge-wheel load predictions within the 2015-A corn trials.

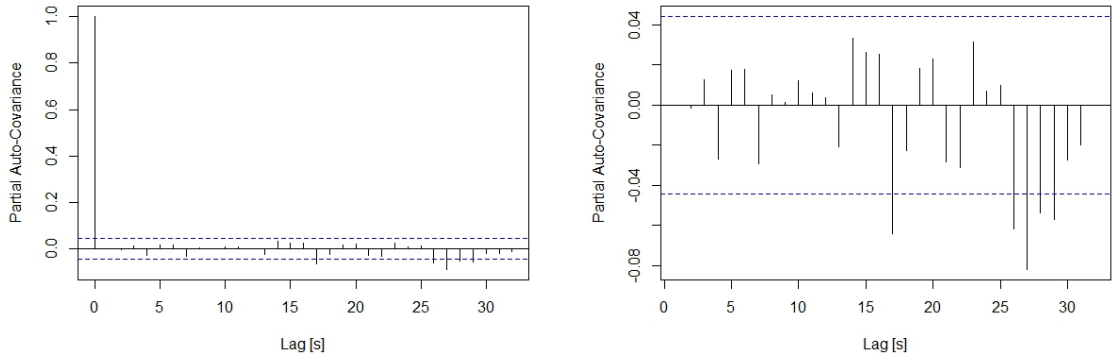

(a) (b)

Figure B.36: Estimation of (a) auto-covariance and (b) partial auto-covariance among residuals from ARIMA model established to compute local gauge-wheel load predictions within the 2015-B corn trials.

Appendix C

Experimental Equipment Specifications

C.1 John Deere Model 8130 Tractor

Power:	
Engine [kW]	167.8
PTO [kW]	134.2
Engine:	
Manufacturer	John Deere
Fuel	Diesel
Cylinders	6
Displacement [L]	9.0
Rated Engine Speed [RPM]	2100
Coolant Capacity [L]	40.0
Oil Capacity [L]	24.1L
Hydraulic Flow Rate [LPM]	166.5
Transmission:	
Type	Full Power Shift
Dimensions:	
Wheelbased [mm]	3020
Electrical:	
Display	Precision Planting Seed Sense
Display (contd)	Trimble Field IQ

C.2 John Deere Model 1700 Integral MaxEmerge® Plus Planter

General:	
Manufacturer	John Deere
Number of Rows	6
Row Spacing [cm]	91
Fold Configuration	Non-Folding Rigid
Attachement	Tractor Mounted Three-Point Hitch
Row-Units:	
Depth Gauging	2 - semi-pneumatic wheels, 4 12 x 16 in
Adjustment	T-Handle, 1/4 to 4-in depth in 14-in increment
Hoppers Capacity [m^3]	0.06
Row-Unit Downforce	Adjustable Heavy Duty, 4 Settings: 0, 0.5, 1.1, 1.8 kN
Drive System	1-motor hydraulic variable-rate drive
Seed Transmission	Mechanical Rear-Mounted

C.3 Veris 3100

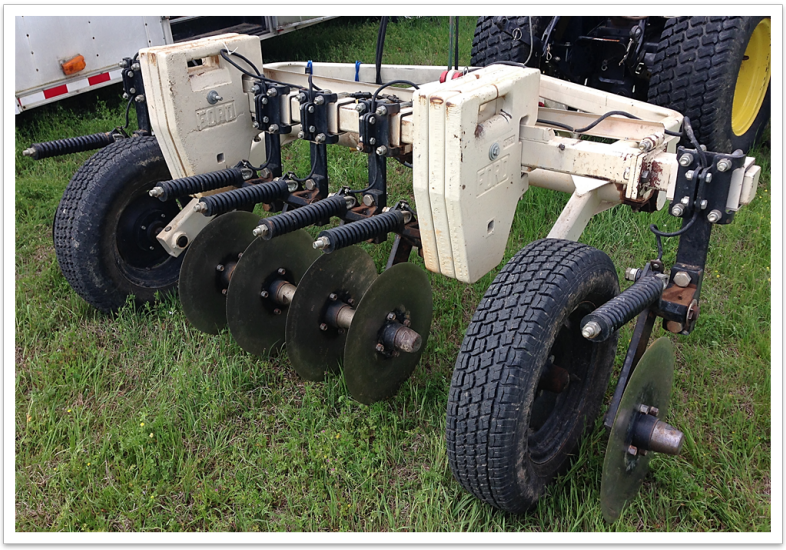

General:	
Manufacturer	Veris® Technologies
Implement Dimensions [cm]	Width: 235, Length: 244, Height: 89
Weight [kg]	544
Maximum Field Speed ($km.h^{-1}$	25
Coulter-Electrode Blade:	
Diameter [cm]	43
Thickness [mm]	4
Sensor Data-Logger:	
Microprocessor	80 pin PIC
Logging Rate [Hz]	1
Power	10-15 V - DC

C.4 Field Scout TDE 300 Soil Moisture Meter

General:	
Manufacturer	Spectrum® Technologies, Inc
Measurement:	
Principle	Time-Domain Measurement Methods
Units	Percent Volumetric Water Content
Resolution	0.1% Volumetric Water Content
Accuracy	+/- 0.3% Volumetric Water Content
Range	0% to Saturation
Data Logger:	
Number of Measurements	2,320 without GPS
	1,160 with GPS / DGPS

C.5 Trimble GeoXH Handheld

System:	
Manufacturer	Trimble
Processor	416 MHz Intel X-Scale Processor
Memory	512 MB onboard plus removable SD memory
Softawe	Microsoft ActiveSync®
	TerraSync
GPS:	
Accuracy	H-Star technology fir 30 cm post-processed accuracy
	Submeter accuracy in real-time
	RTCM real-time correction support
	EVERESTTM multipath rejection technology Software

C.6 DICKEY-John Grain Moisture Meter

General:

Manufacturer	Ag Star services, Inc
Validated Grain Temperature	5°C to 45°C
Humidity	5% to 95%

Appendix D

Instrumentation and Data Acquisition

D.1 National Instrument NI USB-6225 Data Acquisition Module

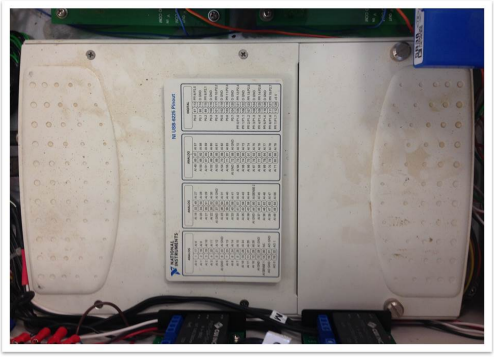

General:	
Manufacturer	National Instrument
Measurement Type	Quadrature Encoder Voltage
Form Factor, Operating System	USB, Windows
Analog Input:	
Single-Ended Channels	80
Differential Channels	40
Resolution	16 bits
Maximum Voltage Range	Range: -10 V to 10 V
	Accuracy [μV]: 3100, Sensitivity [μV]: 97.6
Minimum Voltage Range	Range: -200 mV to 200 mV
	Accuracy [μV]: 112, Sensitivity [μV]: 5.2
Analog Output:	
Number of Channels, Resolution	2, 16 bits
Maximum Voltage Range	Range: -10 V to 10 V
	Accuracy [μV]: 3230
Digital I/O:	
Bidirectional Channels	24
Maximum Voltage Range	0 V to 5 V

D.2 Analog Device 5B38 Signal Conditioning Module

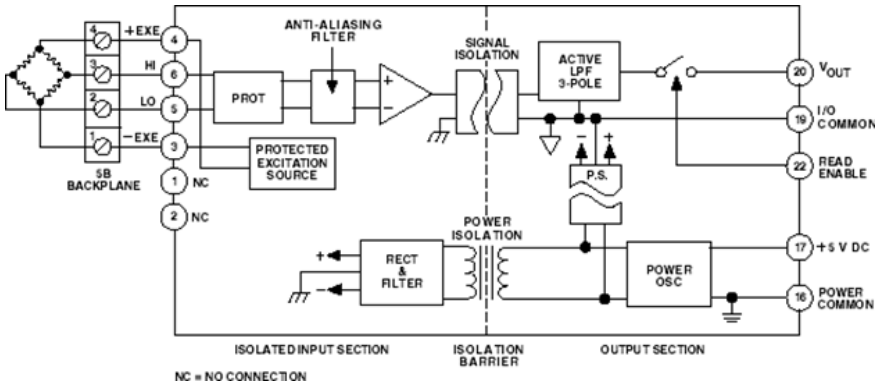

Manufacturer	Analog Devices, Inc©
Features	Accepts Strain Gage Input
	Provides Bridge Excitation
	10 kHz BW
	+/- 5 V Output
Calibrated Accuracy	+/- 0.05 %
Size	2.25” x 2.25” x 0.60 ”

D.3 CUI PYB20-Q24-D12-U DC-DC Converter

Manufacturer	CUI Inc©
Input Voltage [Vdc]	Typ: 48, Range: 18 75
Output Voltage [Vdc]	5
Output Current [mA]	Min: 150, Max: 3000
Output Power [W]	Max: 15
Ripple and Noise [mVp-p]	Max: 100
Efficiency [%]	Typ: 89

D.4 CUI PYB15-Q24-S5-U DC-DC Converter

Manufacturer	CUI Inc©
Input Voltage [Vdc]	Typ: 24, Range: 9 36
Output Voltage [Vdc]	+/- 12
Output Current [mA]	Min: +/-42, Max: +/- 834
Output Power [W]	Max: 20
Ripple and Noise [mVp-p]	Max: 100
Efficiency [%]	Typ: 88

D.5 Vishay Precision Transducers Model No 3810

Manufacturer	Vishay, Precision Group
Model	3810
Capacity [kg]	544
Full Scale Output [$mV.V^{-1}$]	1.355
Zero Balance [$mV.V^{-1}$]	+/- 0.10
Rated Excitation [Vdc]	10
Max Excitation [Vdc]	15
Input Resistance [Ω]	350 to 410
Output Resistance [Ω]	350 to 380
Insulation Resistance	$>$ 2000 MΩ at 50 V DC
Safe Overload [kg]	1360

D.6 Automation Direct TRD-GK3600-RZD Heavy Duty Encoder

General:	
Manufacturer	Automation Direct
Power Supply:	
Operating Voltage [Vdc]	Nominal: 10-30, Range: 9.7-30.9
Current Consumption	at less than 16 Vdc: 50 mA max
	at 16 Vdc or more: 70 mA max
Output Waveform:	
Output Signal	Quadrature + Home Position
Duty Ratio	50% +/- 25%
Maximum Frequency Response [kHz]	100
Operating Speed	(Max Response Frequency / Resolution) * 60
Output:	
Output Type	Totem-Pole
Maximum Current: Outflow: H [mA]	30
Voltage H - L [V]	(Power Source Voltage - 4V) min - 2 max
Mechanical Specifications:	
Starting Torque [N.m]	0.1 max at 20°c
Max Allowable Shaft Load [N]	Radial: 100, Axial: 50
Max Allowable Speed [rpm]	5,000

D.7 LabVIEW Program

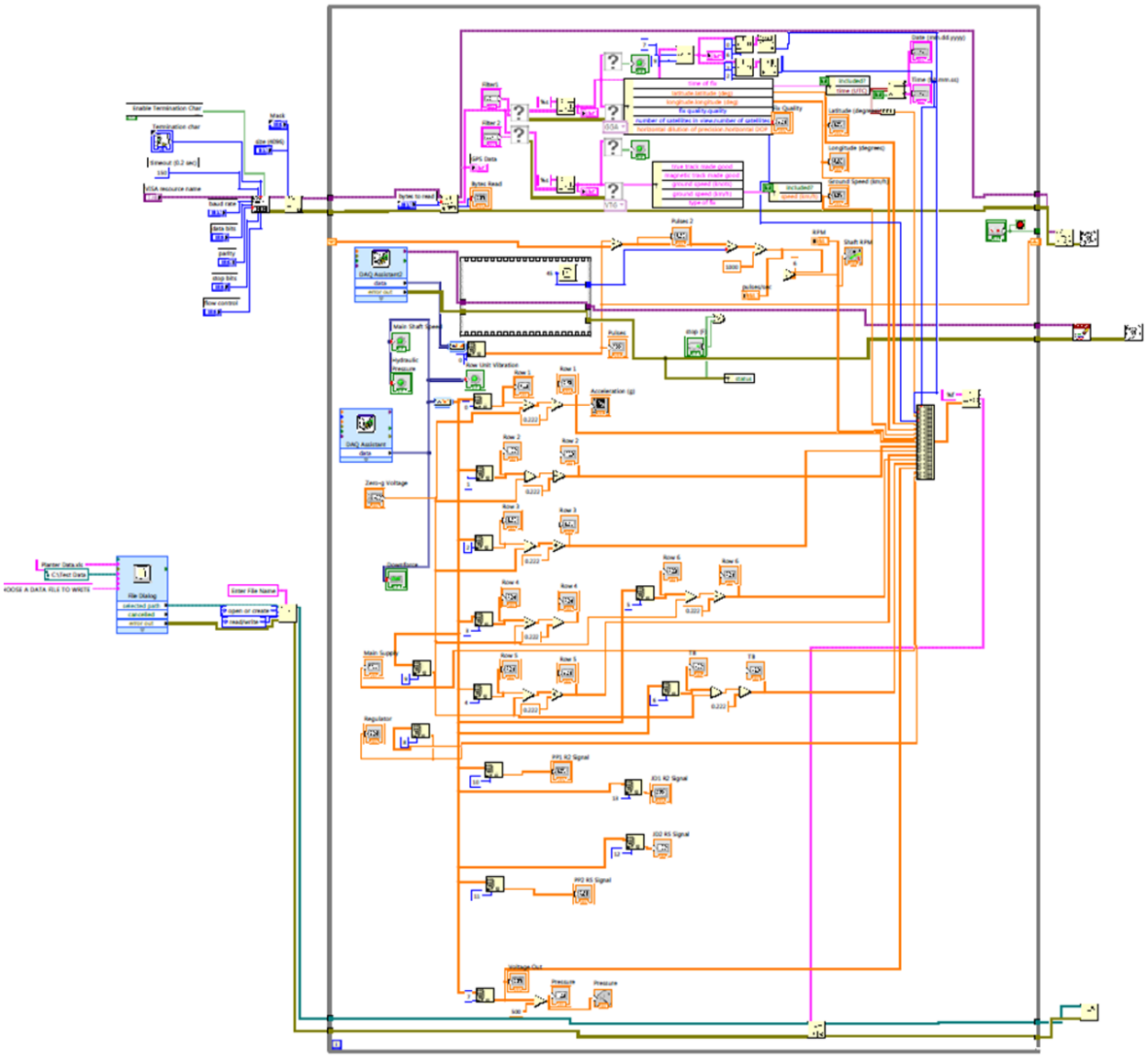

Figure D.1: LabVIEW program used to collect data with the data acquisition system.

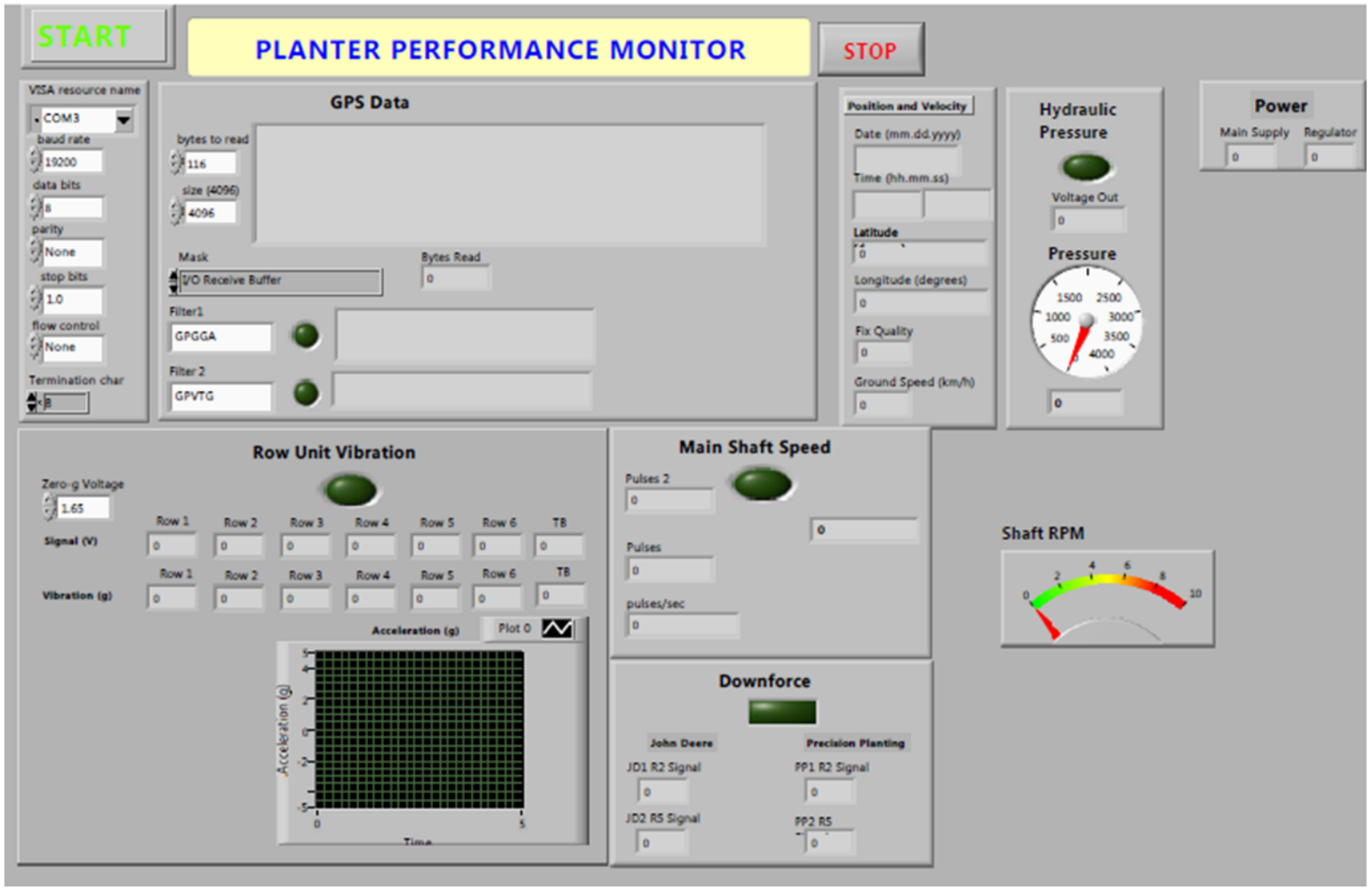

Figure D.2: User interface for LabVIEW program.

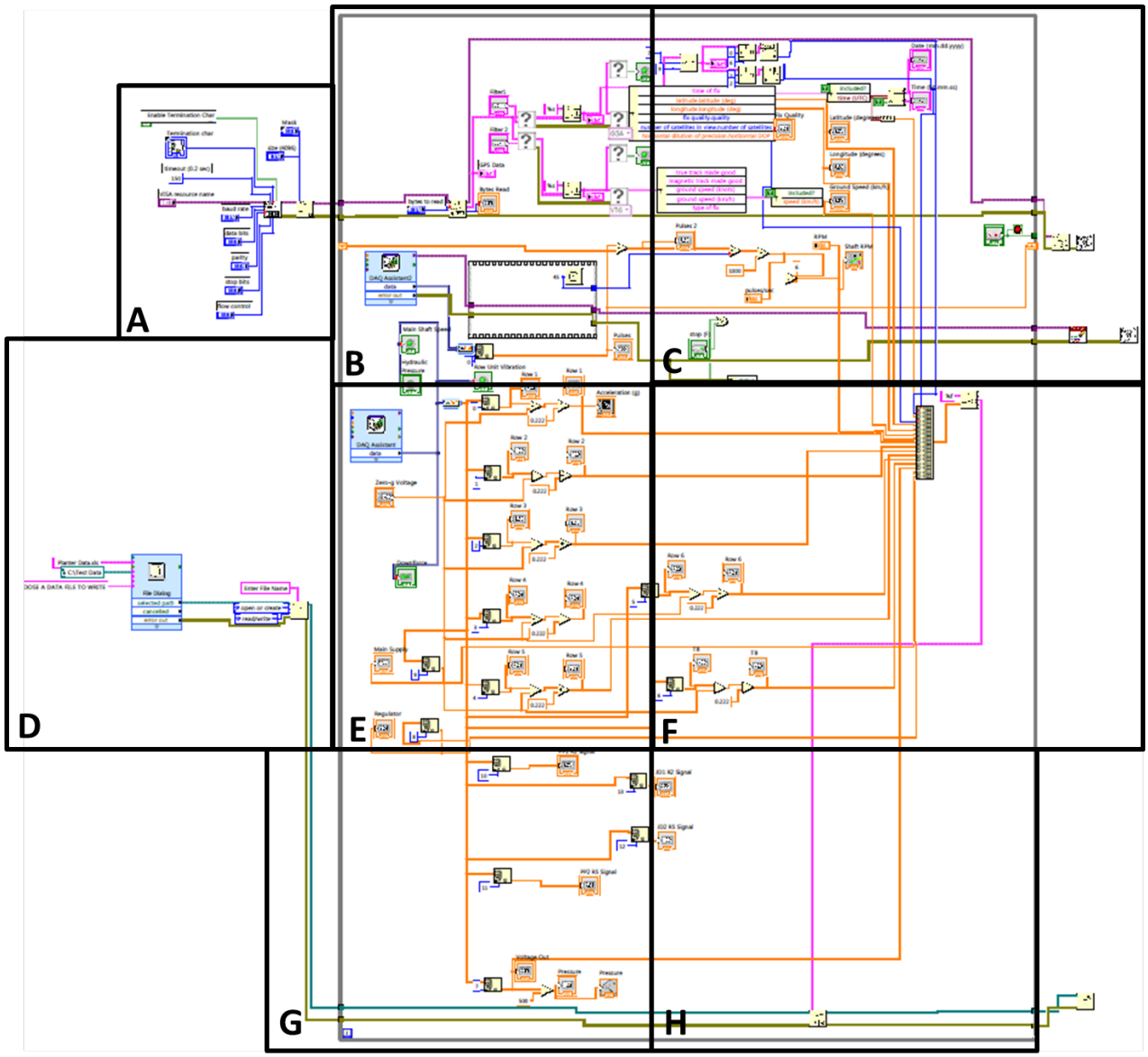
A
B
C
D
E
F
G
H

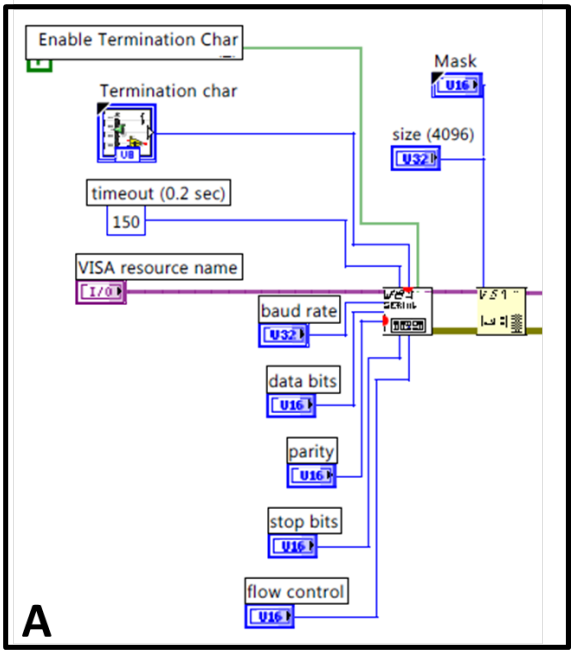
Enable Termination Char
Mask
U16
Termination char
U8
size (4096)
U32
timeout (0.2 sec)
150
VISA resource name
I/O
baud rate
U32
data bits
U16
parity
U16
stop bits
U16
flow control
U16
A

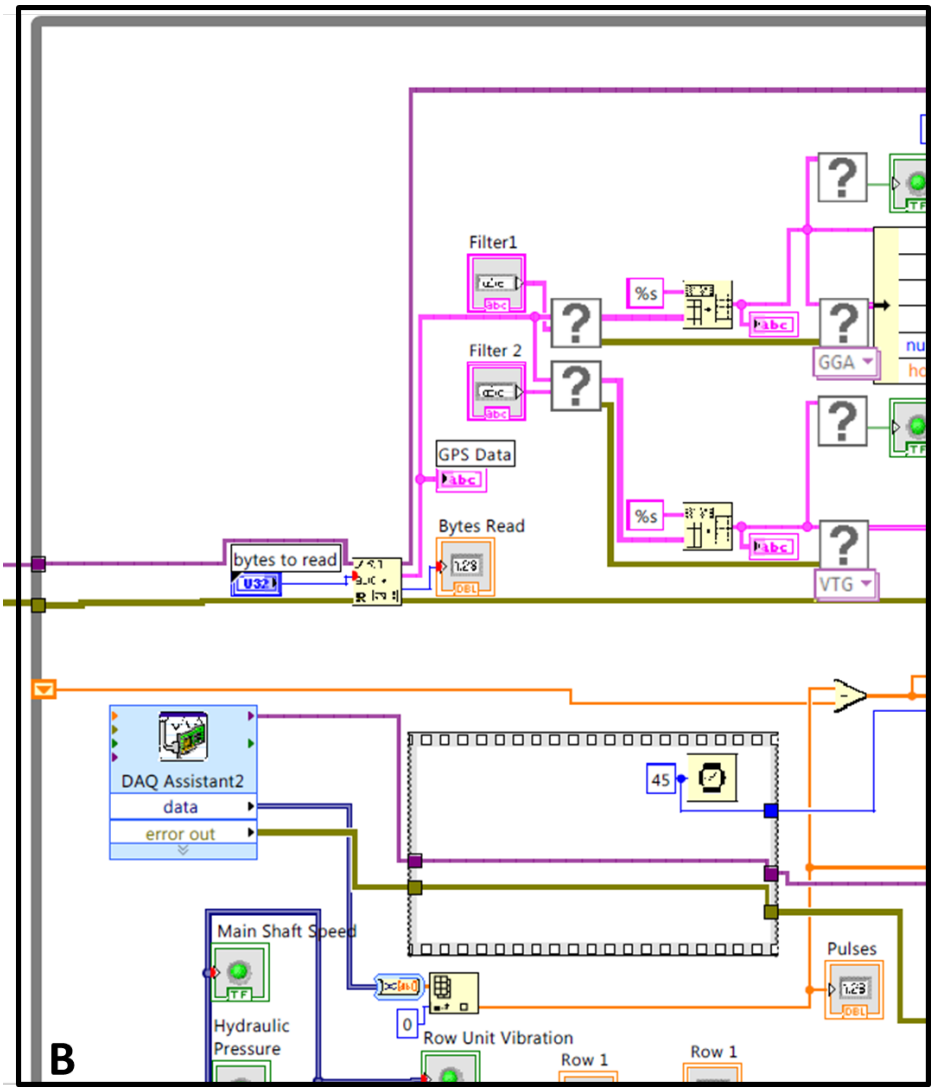
Filter1
Filter 2
%s
%s
GGA
VTG
GPS Data
Bytes Read
bytes to read
DAQ Assistant2
data
error out
45
Main Shaft Speed
Hydraulic
Pressure
0
Row Unit Vibration
Row 1
Row 1
Pulses
B

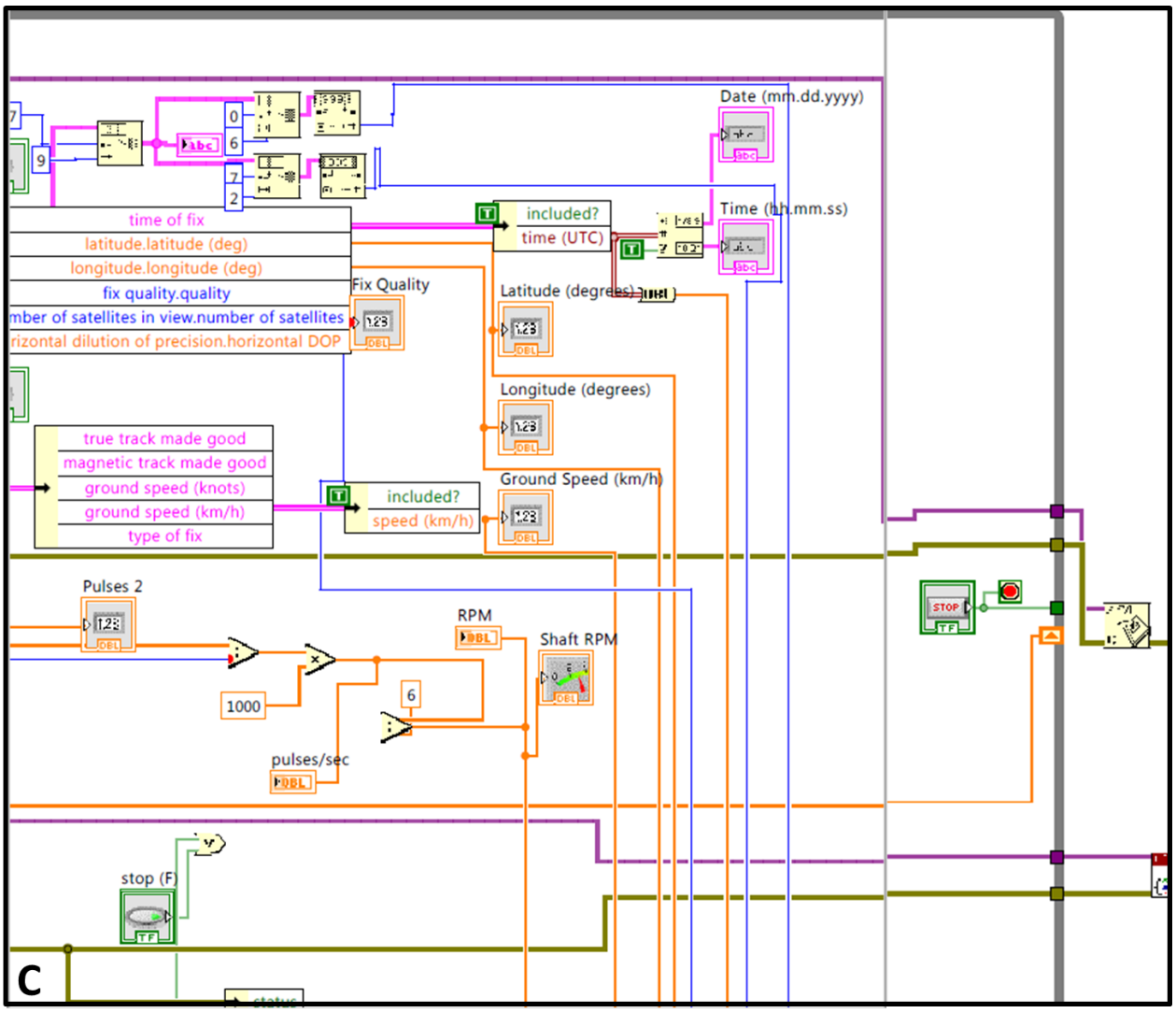
Date (mm.dd.yyyy)
Time (hh.mm.ss)
included?
time (UTC)
time of fix
latitude.latitude (deg)
longitude.longitude (deg)
fix quality.quality
mber of satellites in view.number of satellites
rizontal dilution of precision.horizontal DOP
Fix Quality
Latitude (degrees)
Longitude (degrees)
Ground Speed (km/h)
true track made good
magnetic track made good
ground speed (knots)
ground speed (km/h)
type of fix
included?
speed (km/h)
Pulses 2
RPM
Shaft RPM
1000
6
pulses/sec
stop (F)
STOP
C

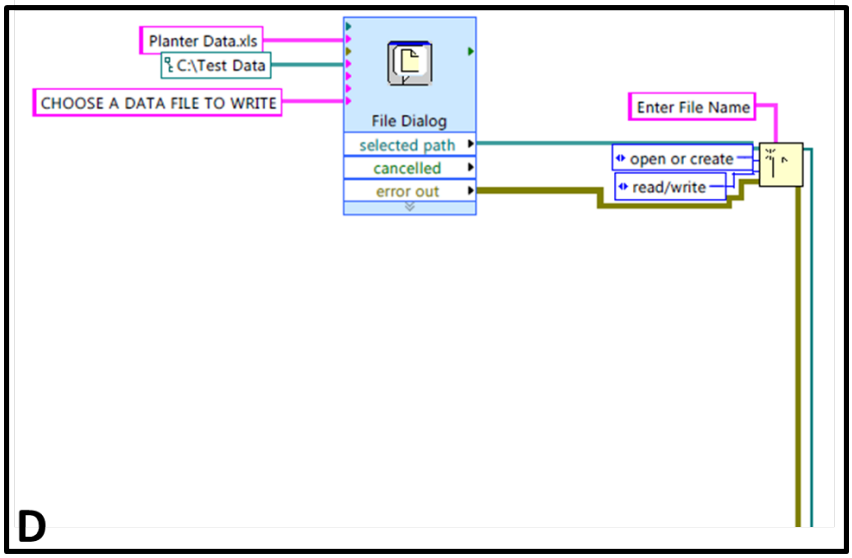
Planter Data.xls
C:\Test Data
CHOOSE A DATA FILE TO WRITE
File Dialog
selected path
cancelled
error out
Enter File Name
open or create
read/write
D

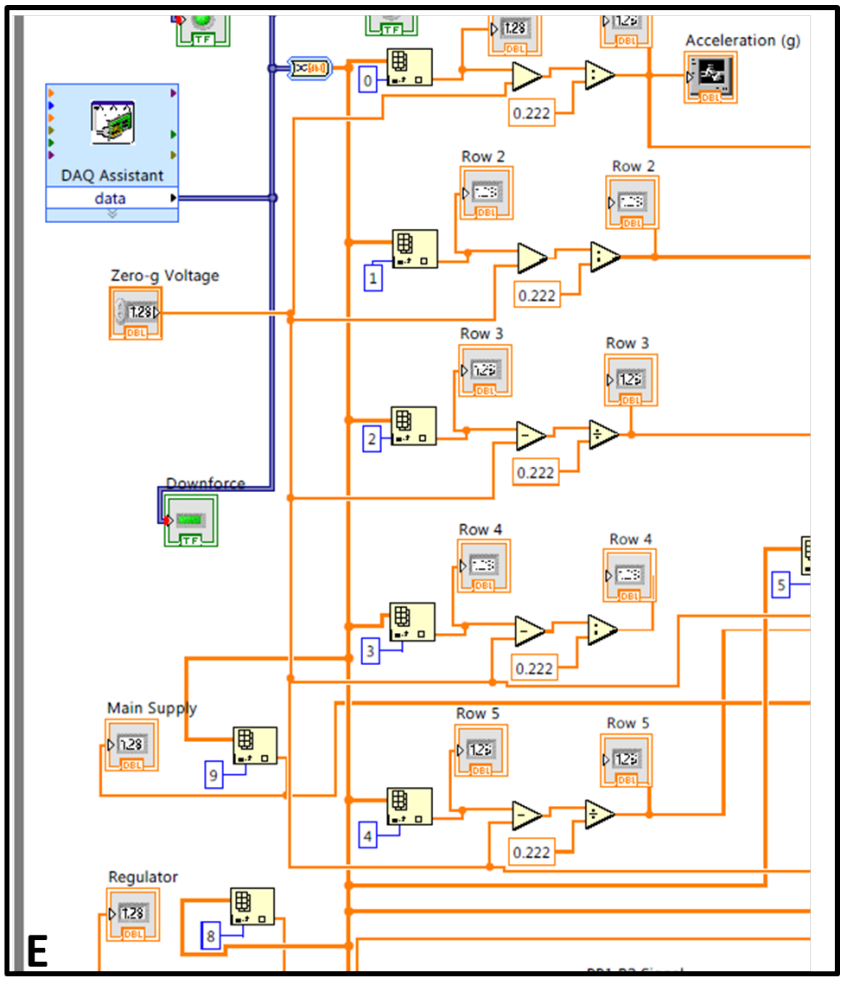
DAQ Assistant
data
Acceleration (g)
Zero-g Voltage
Downforce
Main Supply
Regulator
Row 2
Row 3
Row 4
Row 5
0.222
E

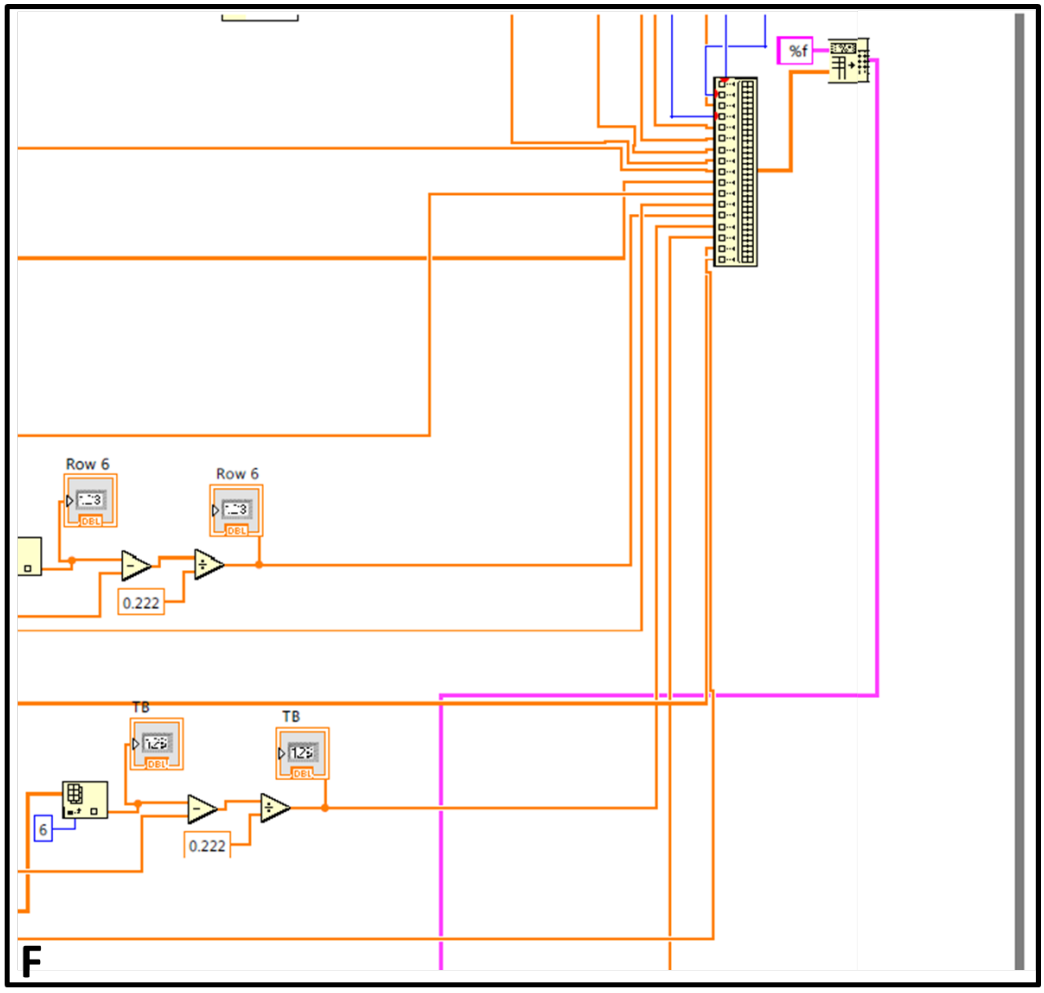
%f
Row 6
Row 6
0.222
TB
TB
6
0.222
F

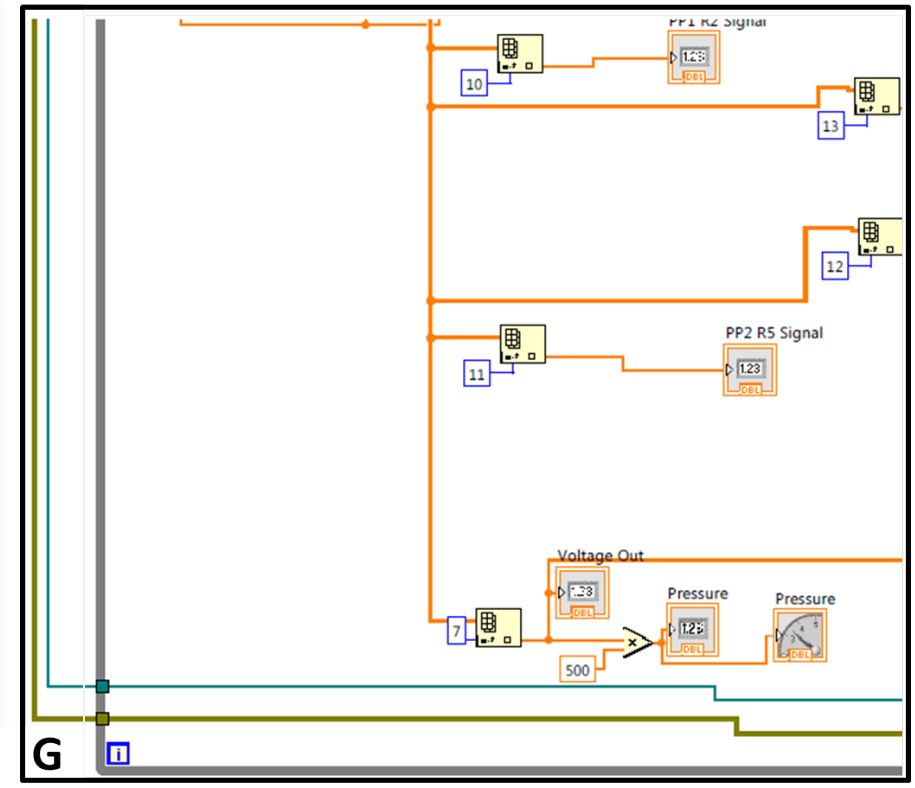
10
13
12
11
PP2 R5 Signal
Voltage Out
Pressure
Pressure
7
500
G
i

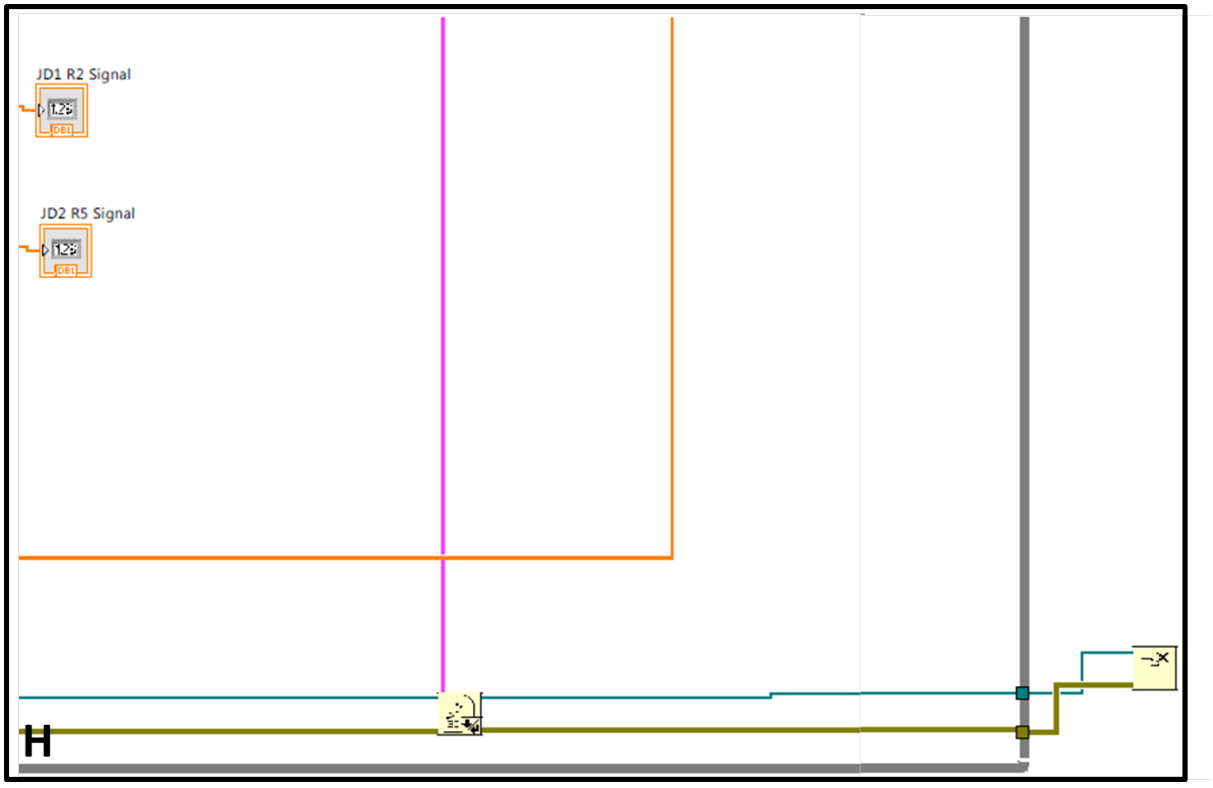
JD1 R2 Signal
JD2 R5 Signal
H